

# The Biological Potentials of Olive Oil By-products: Valorization Through Recovery and Utilization of Bioactive Metabolites

ロジャース, ムワカルクワ

<https://hdl.handle.net/2324/4110554>

---

出版情報 : 九州大学, 2020, 博士 (農学), 課程博士  
バージョン :  
権利関係 :

The Biological Potentials of Olive Oil By-products: Valorization  
Through Recovery and Utilization of Bioactive Metabolites

**Rogers Mwakalukwa**

A Thesis submitted in fulfillment of the requirement for the Degree of  
Doctor of Philosophy in the Field of Natural Product Chemistry and  
Metabolomics

Graduate School of Bioresource and Bioenvironmental Sciences  
Kyushu University  
August 2020



## FRONTISPIECE



The paint that portrays the Greek goddess, Athena (*on the right*) taking part in a secret ritual in front of the olive tree together Cecrops, who is depicted as half human and half snake (*on the left*). The olive tree for the ancient Greeks was a symbol of the Olympic ideals of Peace, Wisdom, and Victory; and it was protected by law by the state (14<sup>th</sup> – 13<sup>th</sup> Century BC).

Source: <http://hellenicgroves.gr/olive-oil-history>

## DECLARATION AND COPYRIGHT

I, Rogers Mwakalukwa, declare that this thesis is my own original work and that it has not been presented and will not be presented to any other university for a similar or any other degree award.

Signature: \_\_\_\_\_

Date: \_\_\_\_\_

This thesis is a copyright material protected under national and international enactments, in that behalf, on intellectual property. It may not be reproduced by any means, in full or part, except for short extracts in fair dealing, for research or private study, critical scholarly review or discourse with acknowledgment, without the written permission of the administration of the Graduate School of Bioresource and Bioenvironmental Sciences, on behalf of both the author and Kyushu University.

## ACKNOWLEDGMENTS

First of all, I would like to express my deepest gratitude to my supervisor, Associate Prof. Kuniyoshi Shimizu, whose guidance throughout the study made a major contribution to this work. Again, special thanks go out to him for his continuous, tireless support in social and other non-academic issues during my stay in Japan (April 2017 to 2020). I would like to record my warm appreciation to my advisor, Prof. Atsushi Kume<sup>1</sup> for his guidance and imparting his knowledge to me in one way or another during this study.

I am also highly indebted to many people/ organizations who/ which have contributed in one way or another to the accomplishment of this study. Just to mention a few of them; Prof. Tomofumi Miyamoto<sup>2</sup>, Dr. Yasuharu Niwa<sup>1</sup>, Dr. Yhiya Amen<sup>1,3</sup>, Dr. Ahmed Ashour<sup>1,3</sup>, Dr. Sonam Tamrakar<sup>1, 4</sup>, Dr. Naomichi Takemoto<sup>1</sup>, and Dr. Maki Nagata<sup>1</sup> – for devoting their valuable time to help with some technical issues, when needed, and for reviewing the manuscripts before submission to the respective journals. Organizations; Research Support Center, Research Center for Human Disease Modeling, Graduate School of Medical Sciences, Kyushu University for some technical assistance; Japanese government scholarship through MEXT (monbukagakusho) for providing a full scholarship for my PhD studies here in Japan; JICA-JST through Science and Technology Research Partnership for Sustainable Development (SATREPS 2) Project: “Valorization of Bioresources in Semi-Arid and Arid land for Regional Development for New Industry”, for financial aid to some laboratory work, making the execution of this study possible.

The completion of this work could not have been possible without the cooperation and moral support I got from ALL Shinrinken laboratory members during my study period in Japan. Both researchers and students, as well as supporting staff members, especially Ms. Kayoko Yoshihara, who has constantly been devoting her time to help in several university regulatory matters, are highly acknowledged. I would also like to thank my employer, Muhimbili University of Health and Allied Sciences (MUHAS) for excusing me from duties during the period of PhD study.

My special thanks are due to my '*senpai*' Dr. Moein Farahnakh and Dr. Dedi Satria, together with Dr. Yhiya Amen, who were not only my colleagues but also my brothers. Their kind support to me materially, academically, and socially throughout my study in one way or another. Dr. Asuka Kishikawa, whom we worked together in the Olive project in Shinrinken laboratory before she left. Her kind assistance before she left is highly acknowledged. I would also like to pass my appreciation to Dr. Wang Dong Mei for her kind assistance in analytical chemistry, especially LC/QTOF-MS quantification.

Last but not least, Dr. Lwitiko Mwakalukwa, Ms. Glory Mwakibuti, Ms. Anne Mwambela, Ms. Julieth Kileo, Amani Mwakalukwa, and the rest of my family members and friends are highly acknowledged for their moral support and above all, the blessings of our almighty God.

<sup>1</sup> Department of Agro-Environmental Sciences, Graduate School of Bioresource and Bioenvironmental Science, Kyushu University, Japan

<sup>2</sup> Graduate School of Pharmaceutical Sciences, Kyushu University, Japan

<sup>3</sup> Department of Pharmacognosy, Faculty of Pharmacy, Mansoura University, Egypt

<sup>4</sup> Nepal Plant Diseases and Agro Associates

<sup>5</sup> Faculty of Science, Kyushu University

<sup>6</sup> Evaluation Center of materials, properties and function, IMCE, Kyushu University



## ABSTRACT

The global increase in demand for olive oil leads to an increase in its production. As olive oil production increases, so does the amount of olive oil by-products (OOBPs), which cause environmental problems. Thus, new ways to utilize them are needed. In this thesis, the biological importance and chemical characteristics of the by-products (OMW, leaves) were assessed to address the possible ways to utilize them. Seventeen (17) metabolites were isolated, two of them being novel, from OMW following bioassay-guided fractionation, and screened for their anti-allergic activity in RBL-2H3 cells (10 metabolites); and anti-diabetic activity (7 metabolites). Anti-allergic active metabolites reduced intracellular  $Ca^{2+}$  levels by decreasing the expression of calcium channel proteins, suggesting that they act mainly as ‘mast cell stabilizers’ to reduce the release of allergic mediators. While, the anti-diabetic active metabolites inhibited  $\alpha$ -glucosidase enzyme either in uncompetitive, non-competitive, or in partial-mixed fashion to reduce postprandial hyperglycemia. To understand the contribution of each of the isolated metabolites to the respective biological activity, their individual “total activities” were established. For the first time, it was found that two isolated anti-diabetic metabolites (both triterpenes), oleanolic acid, and maslinic acid had the highest contribution to the activity, while for anti-allergic, it was the phenolic compounds; luteolin and hydroxytyrosol acetate. This was because not only were they active but also they were the major metabolites in OMW following quantitation by HPLC/ ultra-high performance liquid chromatography coupled with quadrupole time-of-flight mass spectrometry (LC/QTOF-MS).

To address the identification of as many possible metabolites, olive leaves (different cultivars) were studied. Firstly, their acetylcholinesterase (AChE) inhibitory rates were tested, then six cultivars (three most active and three least active ones) were chosen for further studies. Since cultivars are always easily confused due to their extremely similar morphology and metabolites, a novel high-resolution mass spectrometry (HRMS)-based metabolomics approach that is capable of identifying both triterpenoids and phenolic compounds simultaneously, as well as for screening specific biomarkers for cultivars was developed by LC/QTOF-MS employing the all-ion fragmentation (AIF) acquisition mode in data mining. Firstly, the metabolic profiles were analyzed to detect all components as molecular features, MFs. Then, to get final metabolites with high quality, all components were compared among the cultivars and were filtered with Mass Profiler Professional (MPP) software – whereby a total of 66 MFs were detected, of which 29 MFs have been tentatively identified (6 MFs as triterpenoids and 23 MFs as phenolic compounds). For screening specific biomarkers, the extracted ion chromatograms (EICs) were compared and the MFs which were found in significantly higher abundance in a specific cultivar were considered as specific for that cultivar. As an example, the specific biomarkers for Lucca and Cipressino cultivars are MF #39 ( $m/z$  515.0805, RT=6.63 min) and MF #13 ( $m/z$  137.0246, RT=8.06 min), respectively. However, verification of the selected biomarkers is ongoing. The novel developed AIF-based workflow can thus be employed in the selection of the specific biomarkers, and the identification of active metabolites in closely related herbs.

## TABLE OF CONTENTS

FRONTISPIECE.....	iii
DECLARATION AND COPYRIGHT .....	iv
ACKNOWLEDGMENTS .....	v
ABSTRACT .....	viii
TABLE OF CONTENTS .....	x
LIST OF TABLES .....	xv
LIST OF FIGURES.....	xvii
LIST OF APPENDICES.....	xix
LIST OF ABBREVIATIONS .....	xxii
DEFINITION OF KEY TERMS .....	xxv
<b>CHAPTER 1: INTRODUCTION .....</b>	<b>27</b>
Part I: Background.....	28
1.1.1. The Olive Tree, Olive Oil, and The Olive Oil By-products.....	28
1.1.2. The Sustainable Management of OOBPs.....	31
1.1.3. Recovery and Reuse of the Components from OOBPs.....	34
1.1.4. Phytochemical Review of OOBPs.....	34
1.1.5. Aims of the Thesis .....	45
<b>CHAPTER 2: Mast Cell Stabilizing Effect of the Isolated Compounds from Olive Mill Waste Following Allergic Sensitization.....</b>	<b>48</b>
Part I: INTRODUCTION – TYPE 1 ALLERGY .....	49
2.1.1. Allergic reaction and hypersensitivity .....	49

2.1.2. Pathophysiology of FcεRI-mediated mast cell degranulation .....	50
2.1.3. The Role of Calcium Channel Proteins (SOC) in Degranulation .....	51
2.1.4. Research Gap and Way-forward.....	53
Part II: EXPERIMENTAL.....	55
2.2.1. Materials and Sample .....	55
2.2.2. Cell lines, Chemicals, and reagents.....	55
2.2.3. Methods.....	56
2.2.3.1. HPLC Analysis of the OMW Ethanolic Extract.....	56
2.2.3.2. Fractionation and Isolation Procedure .....	57
2.2.3.3. Procedure for the Identification of the Isolated compounds .....	63
2.2.3.4. Cytotoxicity Assay .....	64
2.2.3.5. β-hexosaminidase release (degranulation) Assay .....	65
2.2.3.6. β-hexosaminidase Enzymatic Inhibition Assay .....	67
2.2.3.7. Intracellular Ca <sup>2+</sup> Levels Analysis by Fluorescence Technique .....	69
2.2.3.8. qRT-PCR Analysis of the Calcium Channel Proteins .....	70
2.2.4. Statistical analysis .....	71
Part III: RESULTS AND DISCUSSION.....	72
2.3.1. Chemical Properties of EtOH Extract of OMW .....	72
2.3.2. Identification of the Isolated Compounds.....	75
2.3.3. Effect of the Isolated Compounds on RBL-2H3 cells' degranulation .	87
2.3.4. Effect of the Isolated Compounds on Free Intracellular Ca <sup>2+</sup> Concentration, and on the Expression of Ca <sup>2+</sup> Channel Proteins .....	98

<b>CHAPTER 3: Postprandial Hyperglycemia Lowering Effect of the Isolated Compounds from Olive Mill Wastes – An Inhibitory Activity and Kinetics Studies on <math>\alpha</math>-Glucosidase and <math>\alpha</math>-Amylase Enzymes</b> .....	110
Part I: INTRODUCTION – DIABETES .....	111
3.1.1. Diabetes Mellitus .....	111
3.1.2. Research Gap and Way-forward.....	113
Part II: EXPERIMENTAL.....	115
3.2.1. Material and Sample .....	115
3.2.2. Chemicals and Reagents.....	115
3.2.3. Methods.....	116
3.2.3.1. Chemical Profiling of OMW Extract by UPLC/qTOF-MS .....	116
3.2.3.2. Procedure for Extraction and Isolation .....	118
3.2.3.3. Identification of the Isolated compounds .....	121
3.2.3.4. Assay for $\alpha$ -glucosidase inhibitory activity .....	122
3.2.3.5. Assay for $\alpha$ -amylase inhibitory activity .....	122
3.2.3.6. Analysis of $\alpha$ -Glucosidase Enzyme Inhibitory Kinetics .....	123
3.2.4. Data Analysis.....	124
Part III: RESULTS AND DISCUSSION .....	125
3.3.1. The Structure of the Identified Isolated compounds.....	125
3.3.2. Chemical Profile of the Extract by UPLC/QTOF-MS.....	132
3.3.3. Inhibitory Effect of the Isolated Compounds on $\alpha$ -Glucosidase and $\alpha$ -Amylase Enzymes.....	135

3.3.4. Effect of the Active Isolated Compounds Enzyme Kinetics .....	143
Part IV: CONCLUSION.....	152
<b>CHAPTER 4: Anti-Alzheimer’s activity of olive leaves cultivars: Cultivar-specific metabolic profiling of olive leaves by LCMS based non-targeted metabolomics for determining AChE inhibitor metabolites .....</b>	<b>155</b>
Part I: INTRODUCTION – ALZHEIMER’S DISEASE.....	156
4.1.1. Dementia and AD .....	156
4.1.2. Olives and Treatment of AD: Research Gap and Way Forward .....	159
4.1.3. Metabolomics approach.....	159
Part II: EXPERIMENTAL.....	162
4.2.1. Materials and Sample .....	162
4.2.2. Chemicals and reagents .....	162
4.2.3. Methods.....	163
4.2.3.1. Procedure for Extraction of Olive Leaves Cultivars .....	163
4.2.3.2. Assay for AChE inhibitory activity .....	165
4.2.3.3. Sample Preparation for Untargeted LCMS-Based Metabolomics. ....	165
4.2.3.4. UPLC/QTOF-MS Analysis of the Olive Leaves Cultivar .....	166
4.2.4. Data Processing and Statistical Analysis.....	168
Part III: RESULTS AND DISCUSSION.....	171
4.3.1. Anti-AChE Activity of Olive Leaves Cultivars .....	171
4.3.2. Validation of the UPLC/QTOF-MS Analytical Method.....	173
4.3.3. Metabolite Profiling (MP) .....	176

4.3.4. Data Mining and Pre-treatment.....	176
4.3.5. Identification of the Cultivar Biomarkers .....	182
4.3.6. Multivariate Analysis .....	186
Part IV: CONCLUSION .....	192
<b>CHAPTER 5: CONCLUSION AND RECOMMENDATION .....</b>	<b>194</b>
APPENDICES .....	198
REFERENCES.....	228

## LIST OF TABLES

Table 1: Physicochemical Characteristics of Olive Mill Wastes.....	30
Table 2: The Major Biophenols in OOBPs (OMW and olive leaves) and Their Reported Activities .....	37
Table 3: Chemical structure of main phenolic compounds found in by-products of olive oil production.....	42
Table 4: <sup>1</sup> H and <sup>13</sup> C NMR data for compound <b>5</b> and hemialdehydic decarboxymethylated oleuropein aglycone (HDOA).....	79
Table 5: <sup>13</sup> C NMR data for the isolated triterpene compounds <b>2</b> , <b>3</b> , <b>4</b> , and <b>6</b> .....	85
Table 6: <sup>13</sup> C NMR data for 1-acetoxypinoresinol <b>9</b> .....	86
Table 7: The anti-allergic activity (IC <sub>50</sub> ) and cytotoxicity (CC <sub>50</sub> ) of isolated compounds from OMW .....	94
Table 8: The enzyme inhibitory effect, anti-allergic activity (IC <sub>50</sub> ) and the total activities of the active isolated compounds from OMW .....	95
Table 9: <sup>1</sup> H and <sup>13</sup> C NMR data for compound <b>5</b> and hydroxytyrosol .....	127
Table 10: <sup>13</sup> C NMR data for the isolated triterpene compounds <b>1</b> and <b>2</b> (Oleanolic acid <b>1</b> and Maslinic acid <b>2</b> ) .....	131
Table 11: Characterization of the isolated compounds (and (+)-pinoresinol) from the OMW extract by UPLC/QTOF-MS.....	134
Table 12: IC <sub>50</sub> values for $\alpha$ -glucosidase inhibitory activity of <i>n</i> -hexane, methanol extracts, and acarbose .....	137



Table 13: IC <sub>50</sub> values for $\alpha$ -glucosidase inhibitory activity of the MeOH fractions following LLE .....	138
Table 14: The enzymatic inhibitory activity (IC <sub>50</sub> ), the total amount in dry weight and the total activity of the isolated compounds from OMW.....	141
Table 15: The average sizes of the sampled leaves cultivars .....	164
Table 16: The variability of retention times (RT), impulse <i>m/z</i> and peak areas in 10 sets of data obtained via acquisition of QC specimen .....	175
Table 17: The overview of final MFs obtained in negative ion mode .....	180
Table 18: The overview classification results obtained by the PLS-DA model ....	190

## LIST OF FIGURES

Figure 1: Proposed Methods and Processes for the Valorization of OOBPs.....	33
Figure 2: A scheme of RBL-2H3 cells' degranulation pathway.....	52
Figure 3: A summary of the bioassay-guided fractionation of OMW ethanolic extract .....	60
Figure 4: A summary of the bioassay-guided fractionation of the active fraction, Fr. 6 .....	61
Figure 5: Purification and isolation of compounds from the active sub-fractions of the active fraction, Fr. 6.....	2
Figure 6: A schematic presentation of protocols for RBL-2H3 cells' degranulation assay using A23187 (A), and $\beta$ -hexosaminidase inhibitory activity (B) .....	68
Figure 7: HPLC chromatogram of the EtOH extract of OMW and the chemical structures of oleuropein and hydroxytyrosol.....	74
Figure 8: The chemical structures of the isolated compounds from OMW .....	80
Figure 9: Inhibitory effects of tested phytosterol (1) and triterpenic compounds on RBL-2H3 cells' degranulation .....	90
Figure 10: Inhibitory effects of tested polyphenolic compounds on RBL-2H3 cells' degranulation, and on $\beta$ -hexosaminidase enzymatic activity.....	92
Figure 11: Effects of isolated Polyphenols on Ag-stimulated intracellular $Ca^{2+}$ elevation in RBL-2H3 cells .....	101
Figure 12: Effect of polyphenolic compounds on the expression of RBL-2H3 cells' calcium channel proteins.....	105

Figure 13: Extraction and LLE protocol of OMW as guided by $\alpha$ -glucosidase inhibitory activity. ....	119
Figure 14: The chemical structures of the isolated compounds from OMW. ....	128
Figure 15: The chromatograms of OMW total extract.....	133
Figure 16: $\alpha$ -glucosidase inhibitory activity of <i>n</i> -hexane, methanol extracts, and acarbose.....	136
Figure 17: Inhibitory effects of the isolated compounds on the enzymatic activity of $\alpha$ -glucosidase and $\alpha$ -amylase enzymes .....	139
Figure 18: Kinetic analysis of $\alpha$ -glucosidase inhibition. ....	145
Figure 19: Physiology of the cholinergic synapse.....	158
Figure 20: AChE inhibitory activity of Olive leaves cultivars .....	176
Figure 21: Combined TCC obtained from the six olive leaves cultivars.....	176
Figure 22: The aligned metabolites and mass-retention curve in 18 samples.....	179
Figure 23: EIC of possible markers to discriminate the cultivars .....	185
Figure 24: 3D PCA scores plot of olive leaves cultivars .....	189
Figure 25: 3D PLS-DA scores plot of olive leaves cultivars.....	191

## LIST OF APPENDICES

Appendix i: Tentative identification of the olive leaves cultivar markers .....	198
Appendix ii: <sup>1</sup> H-NMR (whole region) for the novel compound, new HDOA.....	201
Appendix iii: <sup>1</sup> H-NMR (δH 4.5 to 2.5 ppm) for the novel compound, new HDOA.	202
Appendix iv: <sup>1</sup> H-NMR (δH 2.3 to 1.0 ppm) for the novel compound, new HDOA.	203
Appendix v: <sup>13</sup> C-NMR (whole spectra) for the novel compound, new HDOA .....	204
Appendix vi: <sup>13</sup> C-NMR (δH 65.0 to 150.0 ppm) for the novel compound, new HDOA .....	205
Appendix vii: HSQC-NMR (whole spectra) for the novel compound, new HDOA	206
Appendix viii: HSQC-NMR (δH 7.0 to 3.5 ppm) for the novel compound, new HDOA.....	207
Appendix ix: HSQC-NMR (δH 3.5 to 1.0 ppm) for the novel compound, new HDOA .....	208
Appendix x: HMBC-NMR (whole spectra) for the novel compound, new HDOA .	209
Appendix xi: HMBC-NMR (δH 9.5 to 6.5 ppm) for the novel compound, new HDOA .....	210
Appendix xii: HMBC-NMR (δH 4.4 to 1.7 ppm) for the novel compound, new HDOA .....	211
Appendix xiii: HMBC-NMR (δH 9.0 to 3.5 ppm) for the novel compound, new HDOA.....	212
Appendix xiv: HMBC-NMR (δH 3.7HDO to 1.0 ppm) for the novel compound, new HDOA.....	213

Appendix xv: LR-FAB-MS of the novel compound, new HDOA.....	214
Appendix xvi: <sup>1</sup> H-NMR (whole region) for the novel compound, 3,4- dihydroxyphenyl-2-methoxyethanol.....	215
Appendix xvii: <sup>1</sup> H-NMR (region δH 7.0 to 5.0 ppm) for the novel compound, 3,4- dihydroxyphenyl-2-methoxyethanol.....	216
Appendix xviii: <sup>1</sup> H-NMR (region δH 4.5 to 3.5 ppm) for the novel compound, 3,4- dihydroxyphenyl-2-methoxyethanol.....	217
Appendix xix: <sup>1</sup> H-NMR (region δH 3.0 to 0.5 ppm) for the novel compound, 3,4- dihydroxyphenyl-2-methoxyethanol.....	218
Appendix xx: <sup>1</sup> H-NMR (H-1' and H-2') for the novel compound, 3,4- dihydroxyphenyl-2-methoxyethanol.....	219
Appendix xxi: <sup>13</sup> C-NMR (whole region) for the novel compound, 3,4- dihydroxyphenyl-2-methoxyethanol.....	220
Appendix xxii: HSQC-NMR (whole region) for the novel compound, 3,4- dihydroxyphenyl-2-methoxyethanol.....	221
Appendix xxiii: HSQC-NMR (region δH 7.0 to 2.0 ppm) for the novel compound, 3,4-dihydroxyphenyl-2-methoxyethanol.....	222
Appendix xxiv: HSQC-NMR (region δH 2.0 to 0.0 ppm) for the novel compound, 3,4-dihydroxyphenyl-2-methoxyethanol.....	223
Appendix xxv: HMBC-NMR (whole region) for the novel compound, 3,4- dihydroxyphenyl-2-methoxyethanol.....	224

Appendix xxvi: HMBC-NMR (region $\delta$ H 7.0 to 2.0 ppm) for the novel compound 5 - 3,4-dihydroxyphenyl-2-methoxyethanol.....	225
Appendix xxvii: HMBC-NMR (region $\delta$ H 2.0 to 0.0 ppm) for the novel compound, 3,4-dihydroxyphenyl-2-methoxyethanol.....	226
Appendix xxviii: HR-ESI-MS of the novel compound, 3,4-dihydroxyphenyl-2- methoxyethanol .....	227

## LIST OF ABBREVIATIONS

AChE	Acetylcholinesterase
AD	Alzheimer's disease
A23187	Calcium Ionophore (Calcimycin)
BGF	Bioassay-guided fractionation
BPSD	Behavioral and Psychological Symptoms of Dementia
CD <sub>3</sub> OD	Deuterated methanol
CRAC	Calcium release-activated calcium channels
DAD	Diode-array detector
DAG	Diacylglycerol
DCM	Dichloromethane
DMSO	Dimethyl sulfoxide
DMSO- <i>d</i> <sub>6</sub>	Deuterated dimethyl sulfoxide
DNP-BSA	Albumin from Bovine Serum, 2,4-Dinitrophenylated
ELSD	Evaporative Light Scattering Detector
EMEM	Eagle's minimal essential medium
ESI	Electrospray Ionization
FBS	Fetal bovine serum
GAE	Gallic acid equivalent
GDP	Gross Domestic Product
HDOA	Hemialdehydic decarboxymethylated oleuropein aglycone
HMBC	Heteronuclear multiple bond correlation

HPLC	High-performance liquid chromatography
HR-ESI-MS	High-resolution electrospray ionization mass spectrometry
HR-FAB-MS	High-resolution fast atom bombardment mass spectrometry
HSQC	Heteronuclear single quantum coherence
IP <sub>3</sub>	Inositol-1,4,5-trisphosphate
JICA	Japan International Cooperation Agency
JST	Japan Science and Technology Agency
LC/QTOF-MS	Liquid chromatography quadrupole-time-of-flight mass spectrometry
LCMS	Liquid chromatography-mass spectrometry
LLE	Liquid-liquid extraction
MP	Metabolic profiling
MEXT	Ministry of Education, Culture, Sports, Science, and Technology – Japan
MPLC	Medium pressure liquid chromatography
MTT	3-(4,5-Dimethylthiazol-2-yl)-2,5-Diphenyltetrazolium Bromide
NCD	Non-communicable diseases
NMR	Nuclear magnetic resonance
ODS	Octa-decyl silyl
OMW	Olive Mill Wastes
OOBPs	Olive oil by-products



PBS	Phosphate buffered saline
PCA	Principal component analysis
PIP <sub>2</sub>	Phosphatidylinositol-4,5-bisphosphate
PLC	Phospholipase C
PLS-DA	Partial least square
RT-PCR	Real-time polymerase chain reaction
TLC	Thin-layer chromatography
VOO	Virgin Olive Oil
WHO	World Health Organization

## DEFINITION OF KEY TERMS

### **Olive oil by-products (OOBPs)**

These includes olive tree residues produced during all processes involved in the production of virgin olive oil (VOO), covering a wide range of activities from day 1 of tree plantation, to tree maintenance and fruit harvesting, to the final process of oil extraction <sup>1</sup>. The following are the OOBPs:

- i. Leaves and twigs whose diameter is less than 3 cm – these are obtained by tree pruning and separation of big branches, usually it is done monthly in the farm. Leaves are also obtained after the washing and cleaning of olive fruits in the factory.
- ii. Liquid residue – it is obtained by centrifugation or by sedimentation after pressing of olive tree fruits during oil extraction in the factory. Liquid residue has been known with different names such as, olive mill wastewaters; vegetation waters; alpechins; etc.
- iii. Solid residues – these are exclusively obtained during oil extraction from industrial production. They include olive oil cakes and olive pulp.

In some literature, by-products obtained 'during' oil extraction process, such as olive mill wastewaters or alpechins, olive oil cakes, leaves obtained after washing - are called olive oil wastes (OOW) <sup>2</sup>. Therefore, OOBPs is more inclusive and broader.

### **Olive mill wastes (OMW)**

OMW refers to the dried mixture of the liquid residue (olive mill wastewaters) and solid residue (olive cake, pulp) produced during oil extraction. Since it is dried, OMW is solid in physical appearance!

### **Olive leaves**

For the purpose of this thesis, it refers to those obtained monthly during tree pruning in the farm. We exclude those obtained after the washing and cleaning of olive fruits in the factory.

**CHAPTER 1**  
**INTRODUCTION**

## **Part I: Background**

### **1.1.1. The Olive Tree, Olive Oil, and The Olive Oil By-products**

The olive tree (*Olea europaea* L, family Oleaceae) has been used for medicinal and dietary purposes since ancient times, recorded as far back as 7000 BC<sup>3</sup>. It is famous for its fruits, called 'olives', which are commercially important as the prime source of olive oil<sup>4</sup> – the major product widely used<sup>5</sup>. Each olive tree yields between 15 and 40 kg of olives annually. It is estimated that global olive oil production for the year 2002 was about 2.5 million tons produced from approximately 750 million productive olive trees, the majority of which are in the Mediterranean region – which accounts for 97% of the total olive oil production. Outside the Mediterranean basin, olives are cultivated in the Middle East, the USA, Argentina, and Australia<sup>6</sup>.

Olive oil production tends to increase over the last decades as a valuable source of antioxidants and essential fatty acids in the human diet and constitutes one of the most important dietary trends worldwide<sup>4</sup>. Due to rising awareness about the beneficial effects of optimal nutrition and functional foods among today's health-conscious societies, the worldwide consumption of olives and olive products has increased significantly, especially in high-income countries such as the USA, Europe, Japan, Canada, and Australia, resulting in the development of many olive-based products<sup>7,8</sup>.

Since olive oil is increasingly gaining interest in the food industry – as it provides the body with additional benefits as compared to traditional oils, as a result, a huge

amount of olive oil by-products (OOBPs) are generated during the production process(es) from plantation to oil extraction, these include olive mill wastes (OMW) and leaves<sup>9,10</sup>. Conventionally, these by-products have been regarded as 'wastes', and they can lead to serious damages if they remained untreated<sup>4</sup>. For instance, OMW may have a great impact on environments because of their high organic loads (**Table 1**), especially the phenolic compounds which are not easily biodegradable<sup>11</sup>. This leads into phytotoxicity and they have a terrestrial bactericidal effect.

It is worth noting that it is this rapid increase in the demand for olive oil worldwide, which leads to a growing problem in the environmental pollution posed by, especially, OMW. Now, the olive oil industry is facing a serious challenge to find an environmentally sound and economically viable solution in handling OOBPs, especially OMW<sup>11</sup>. One of the most promising ways is through the recovery of bioactive metabolites, which can be utilized in different fields<sup>12</sup>.

**Table 1: Physicochemical Characteristics of Olive Mill Wastes**

<b>Parameter</b>	<b>Unit</b>	<b>Range of Value</b>
pH	–	4.8 – 5.7
Conductivity	dS/M	5 – 81
Biodegradability	–	0.1 – 0.26
Dry residue	g/L	11.5 – 90.7
Organic loads		
Lipids	g/L	7
Phenolic compounds	g/L	0.8– 8.9
Sugar	g/L	1.3– 4.3
Total Nitrogen	g/L	0.06 – 0.9

*Source of data:* <sup>13,14</sup>

### 1.1.2. The Sustainable Management of OOBPs

The high organic loads including, organo-halogenated pollutants, fatty acids, and phenolic compounds (**Table 1**), make OMW the most environmental pollutant (toxic to both terrestrial and aquatic organisms; plants, bacterial and fungi) <sup>4,10</sup>. Therefore, these by-products need to be managed to minimize the environmental effects induced by their disposal <sup>15</sup>. Their management often aims at the treatment approach which involves the destruction of organic matter and phenolic compounds, and hence the reduction of chemical oxygen demand and phytotoxicity, respectively. However, these treatments are difficult and expensive as it has high territorial scattering and the presence of nonbiodegradable organic compounds like long-chain fatty acids and phenols <sup>13</sup>.

Since the management through treatment is difficult and expensive, other management approaches that are cheaper and more environmentally friendly should be placed in use. In an attempt to categorize the proposed cheaper and environmentally friendly methods, two categories can be denoted:

1. Waste reduction via olive production systems conversion (i.e., to use the system that produces relatively small amounts of wastewaters).
2. Recovery or recycling of components from OMW (involves the isolation of bioactive compounds/ fractions with a certain biological activity).

The first approach is now widely placed in use. However, the increased production of virgin olive oil (VOO) has led to increased production of OOBPs exceeding that



the olive industry can manage <sup>13,15</sup>. As a result, research suggests that the best management process must integrate different methodologies such as combining both treatments, recycling, waste reduction via olive production systems conversion, and energy-producing processes. Such integrative management could lead to the achievement of several purposes altogether as summarized in **Figure 1**. Therefore this concept makes the treatment process cost-effective and results in an environmentally friendly VOO production process <sup>16</sup>.

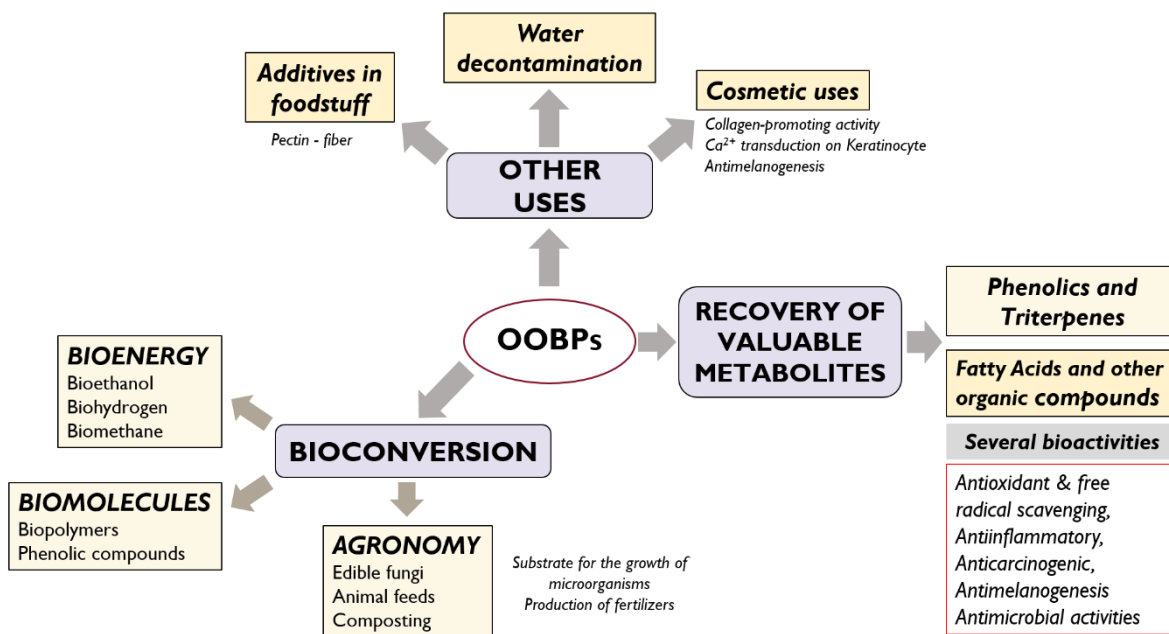


Figure 1: Proposed Methods and Processes for the Valorization of OOBPs

### **1.1.3. Recovery and Reuse of the Components from OOBPs (OMW and Leaves)**

The valorization of the by-products is a challenging opportunity for the sustainable and competitive development of several industrial sectors, including the biorefinery of olive oil by-products (OOBPs): leaves and olive mill waste (OMW). We have seen why the management of OMW, in particular, has received much attention over recent years – high organic loads thus limiting its biological treatment, non-biodegradability, and environmental hazardous <sup>10</sup>. It is now known that during the olive oil production, almost all phenolic content of the olive fruit (~98%) remains in the by-products OMW. Therefore, apart from being a serious environmental problem, OMW can also represent an inexpensive source of highly- and potentially valuable molecules for recovery and reuse purposes <sup>12</sup>.

The approach of recovery and reuse appears to be the new and best frontier in the valorization of the olive oil by-products. This thesis has explored the biological potential of the recovered molecules (metabolites) and reuse them in the treatment/prevention of several disease conditions. Moreover, the analytical chemical techniques such as characterization of the extracts for their phenolic (and triterpenoid) content were performed.

### **1.1.4. Phytochemical Review of OOBPs**

Many research works have been done concerning the phytochemistry of the OOBPs. Today, OMW and olive leaves are considered as an inexpensive source of highly valuable metabolites, mainly those belonging to the family of biophenols. Oleuropein,

a secoiridoid group member and its hydrolysis derivative; hydroxytyrosol are the most studied olive biophenols <sup>17</sup>. In general, even though the phenolic compounds are known to be the major contributors to the toxicity of OMW <sup>10</sup>, they are endowed with several biological activities such as antioxidant properties <sup>18–20</sup>. This has led to the proposal of the production of biologically active compounds such as phenolic antioxidants from OMW constitutes as a viable alternative for valorizing this problematic waste <sup>18</sup>.

Following a long-time recognition of the antioxidant activity of OMW and the association of oxidative stress such as ROS with many diseases, it was logical to consider OMW as a potential source of biophenolic antioxidants. In this section, the olive biophenol metabolites, with their biological properties have been reviewed.

### **Phenolic Content**

The phenolic profiles of olive fruit and the corresponding oil (VOO), leaves, and OMW obtained either from the industry or by the laboratory-scale press has been compared in previous works <sup>12,18,21–25</sup>. In general, the chromatogram profiles of the fruit showed similarity to that of the OMW where secoiridoid glycosides were present in high concentration. In contrast, many studies found out that secoiridoid derivative, hydroxytyrosol was found in higher amounts in the OMW than in the VOO and olive leaves <sup>12,21</sup>. This poor correlation between the phenolic content of the fruits and that of the OMW has been ascribed to several factors involved during extraction – the effects of processing <sup>13,26</sup>. However, it is worth mentioning that OMW has been

proven to be richer in biophenols as compared to oil, fruits, or olive leaves <sup>12</sup>. **Table 2 and 3** below shows some of the biophenols reported in OOBPs and their reported biological activities and their chemical structures.

**Table 2: The Major Biophenols in OOBPs (OMW and olive leaves) and Their Reported Activities**

<b>Biophenol</b>	<b>Bioactivity</b>	<b>Remark(s)</b>
Oleuropein <sup>21</sup>	Antioxidant	From olive cake extract <sup>27</sup> . In vivo and in vitro activity <sup>28,29</sup> . Free radical scavenging activity <sup>30,31</sup> .
	Cardioprotective	Inhibition of LDL oxidation and platelets aggregation <sup>32,33</sup> . Fatty acid composition of rat heart <sup>34,35</sup> . Enhances nitric oxide production
	Antiulcer	Prevents ethanol-induced gastric ulcers <sup>36</sup> .
	Hypoglycemic	Reduces blood sugar in rats – normal and diabetic <sup>37,38</sup> .
	Antihypertensive	Vasodilator <sup>39</sup> .
	Anti-inflammatory	Prostaglandin sparing and analgesic effect <sup>40</sup> . Inhibition of 5-lipoxygenase <sup>41</sup> .
	Antimicrobial	Antibacterial <sup>42</sup> . Antimycoplasmal <sup>43</sup> . Antifungal effects <sup>44</sup> . Anti-HIV activity of olive leaf extract <sup>45</sup> .
	Endocrinal activity	Thyroid stimulation <sup>46,47</sup> .
	Neuroprotective	Neuroprotective following spinal cord injury in rats <sup>48</sup> .

<b>Biophenol</b>	<b>Bioactivity</b>	<b>Remark(s)</b>
		Neuroprotective against cognitive dysfunction in hippocampal CA1 area in rats <sup>49</sup>
		In vitro and epidemiological <sup>32</sup> .
Hydroxytyrosol 18,21,50–52	Antioxidant	Isolated from OMWW, antioxidant in rats, and liver cells <sup>53,54</sup> .
		Protects human erythrocytes against oxidative damage <sup>55</sup> .
	Cardioprotective	scavenges and reduces superoxide anion production in human promonocyte cells <sup>56,57</sup> .
	Chemopreventive	Protective against oxidative stress in kidney cells <sup>58</sup> .
		Cancer chemoprevention through G1 cell cycle arrest and apoptosis <sup>59</sup> .
		Induces cytochrome C-dependent apoptosis <sup>60</sup> .
		Inhibition of the proliferation of tumor cells <sup>59</sup> .
	Antimicrobial	Antibacterial <sup>42</sup> .
		Antimycoplasmal <sup>43</sup> .
		Antiviral <sup>61</sup> .
	Anti-inflammatory	Prostaglandin sparing <sup>40</sup> .
		Inhibition of leukocytes leukotriene B4 <sup>62</sup> .
		Impairs Cytokine and Chemokine Production in Macrophages <sup>63</sup> .
		inhibition of 5-lipoxygenase <sup>41</sup> .
	Skin lighting property	topical and bath preparation <sup>52</sup> .

<b>Biophenol</b>	<b>Bioactivity</b>	<b>Remark(s)</b>
	Age-related dementia (Alzheimer's disease)	Restores proper insulin signaling in an astrocytic model of Alzheimer's disease <sup>64</sup> Improves cognitive function in Rats <sup>65</sup> .
Tyrosol <sup>27,50</sup>	Antioxidant	Restored intracellular antioxidant defense <sup>66</sup> . DPPH scavenging <sup>67</sup> Protect against oxidized LDL <sup>68</sup> .
	Chemopreventive	Protective against oxidative stress in kidney cells <sup>58</sup> .
	Anti-inflammatory	Inhibition of 5-lipoxygenase (less active than HT) <sup>41</sup> .
Caffeic acid <sup>19,69</sup>	Antioxidant	Stabilized oxidative stress <sup>70</sup>
	Anti-inflammatory	Inhibition of 5-lipoxygenase (less active than HT and tyrosol) <sup>41</sup> .
	Chemoprotective	Inhibits DNA oxidation (less active than hydroxytyrosol but more efficient than tyrosol in prostate cells <sup>71</sup> .
	Antimicrobial	Antibacterial <sup>72</sup> . Antifungal <sup>72</sup> .
Verbascoside <sup>73</sup>	Antioxidant	Isolated from OMWW <sup>73</sup> . Food antioxidants <sup>73</sup> . Antioxidant in Rats by TEAC assay <sup>51</sup> .
	Chemoprevention	Protects the human keratinocyte against solar UV <sup>74</sup> .
	Antiplatelet	Inhibits ADP and arachidonic acid-induced platelet aggregation <sup>75</sup> .

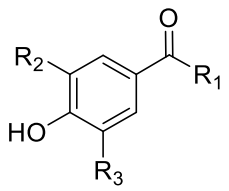
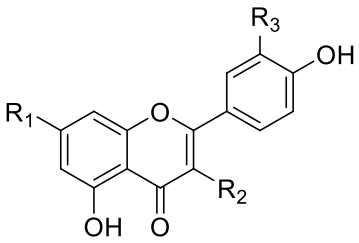
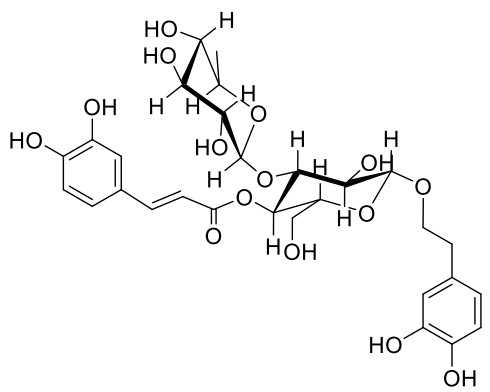


<b>Biophenol</b>	<b>Bioactivity</b>	<b>Remark(s)</b>
	Antihypertensive	Angiotensin-converting enzyme (ACE) inhibitor <sup>76</sup> .
	Anti-inflammatory	Multiple mechanisms <sup>77</sup> .
Rutin <sup>78</sup>	Antioxidant	In vitro antioxidant <sup>79</sup> .
	Anti-inflammatory	Intestinal anti-inflammatory effects in the CD4+ CD62L+ T cell transfer model of colitis <sup>80</sup> .  Anti-inflammatory on rat paw oedema, and on neutrophils chemotaxis and degranulation <sup>81</sup> .
	Antihyperglycemic	Antihyperglycemic in Streptozotocin-Induced Diabetic Wistar Rats <sup>82</sup> .
	Chemopreventive	Attenuates intestinal toxicity induced by Methotrexate <sup>83</sup> .
<i>p</i> -coumaric acid <sup>69</sup>	Antioxidant	Scavenges the reactive oxygen species (ROS) in Rats <sup>84</sup> .  Minimizes the oxidation of LDL in Rats <sup>84</sup> .  Protects the rat heart from the oxidative stress of doxorubicin <sup>85</sup> .  Antioxidant in multiple in vitro cell-free systems; DPPH, ORAC, SOSA, & ABTS <sup>86</sup> .
	Antimicrobial	Inhibits the <i>Listeria monocytogenes</i> RecA protein function <sup>87</sup> .  General antimicrobial <sup>88</sup> .
	Chemopreventive	Chemopreventive via induction of Nrf2 in colon cancer <sup>89</sup> .  Anticancer against HCT-15 colon cancer cells

<b>Biophenol</b>	<b>Bioactivity</b>	<b>Remark(s)</b>
Vanillic acid 21,69	Antioxidant	Protective effects on lipid peroxidation in cardiotoxic Rats <sup>90</sup> .  Antioxidant in multiple in vitro cell-free systems; DPPH, ORAC, OxHLIA, ABTS <sup>91</sup> .
	Antimetabolic syndromes	Reduced risks in high fat-induced diabetic hypertensive Rats <sup>92</sup> .
	Antimicrobial	Antibacterial <sup>45</sup> .  Antifungal <sup>45</sup> .

**Table 3: Chemical structure of main phenolic compounds found in by-products of olive oil production**

Class (Group)	Chemical Structure	Compound		
Secoiridoids		<b>Oleuropein:</b> R <sub>1</sub> =OH, R <sub>2</sub> =CH <sub>3</sub> , R <sub>3</sub> =Glucose  <b>3,4-DHPEA-EA:</b> R <sub>1</sub> =OH, R <sub>2</sub> =CH <sub>3</sub> , R <sub>3</sub> =H  <b>Ligstroside:</b> R <sub>1</sub> =H, R <sub>2</sub> =CH <sub>3</sub> , R <sub>3</sub> = Glucose		
		Phenylalcohols		<b>Hydroxytyrosol:</b> R <sub>1</sub> =OH, R <sub>2</sub> =H  <b>Tyrosol:</b> R <sub>1</sub> =H, R <sub>2</sub> =H  <b>Hydroxytyrosol glucoside:</b> R <sub>1</sub> =OH, R <sub>2</sub> =Glucose
			<b>3,4-DHPEA-EA:</b> R <sub>1</sub> =OH  <b>p-HPEA-EA:</b> R <sub>1</sub> =H	
Phenolic acids/ aldehyde		<b>Caffeic acid:</b> R <sub>1</sub> =OH; R <sub>2</sub> =H  <b>p-Coumaric acid:</b> R <sub>1</sub> =H; R <sub>2</sub> =H  <b>Ferulic acid:</b> R <sub>1</sub> =H; R <sub>2</sub> =OCH <sub>3</sub>		

Class (Group)	Chemical Structure	Compound
		<p><b>Gallic acid:</b> R<sub>1</sub>=OH; R<sub>2</sub>=OH; R<sub>3</sub>=OH</p> <p><b>Vanillic acid:</b> R<sub>1</sub>=OH; R<sub>2</sub>=OCH<sub>3</sub>; R<sub>3</sub>=H</p> <p><b>Protocatechuic acid:</b> R<sub>1</sub>=OH; R<sub>2</sub>=OH; R<sub>3</sub>=H</p> <p><b>Vanillin:</b> R<sub>1</sub>=H; R<sub>2</sub>=OCH<sub>3</sub>; R<sub>3</sub>=H</p>
Flavonoids		<p><b>Rutin:</b> R<sub>1</sub>=OH; R<sub>2</sub>=O-rutinose; R<sub>3</sub>=OH</p> <p><b>Luteolin:</b> R<sub>1</sub>=OH; R<sub>2</sub>=H; R<sub>3</sub>=OH</p> <p><b>Luteolin-7-O-glucoside:</b> R<sub>1</sub>=OH; R<sub>2</sub>=O-glucose; R<sub>3</sub>=OH</p> <p><b>Apigenin:</b> R<sub>1</sub>=OH; R<sub>2</sub>=H; R<sub>3</sub>=H</p> <p><b>Apigenin-7-O-glucoside:</b> R<sub>1</sub>=OH; R<sub>2</sub>=O-glucose; R<sub>3</sub>=H</p>
Phenylethanoid glycoside		<p><b>Verbascoside</b></p>

Class (Group)	Chemical Structure	Compound
Lignans		<p><b>Pinoresinol</b>, <math>R_1=H</math></p> <p><b>1-acetoxypinoresinol</b>, <math>R_1=Ac</math></p>

3,4-DHPEA-EA: oleuropein aglycon mono-aldehyde; 3,4-DHPEA-EDA: oleuropein-aglycone di-aldehyde; *p*-HPEA-EDA: ligstroside-aglycone di-aldehyde

## 1.1.5. Aims of the Thesis

### 1.1.5.1. Why OOBPs?

The presence of phenolic compounds along with other minor ones, the pentacyclic triterpenes, makes VOO useful not only as traditional food but also as folk medicine. Today, it is known that during the olive oil extraction, almost all the phenolic content of the olive fruit (~98%) remains in the OMW, a major OOBP<sup>93</sup>. Among many other compounds are oleuropein and hydroxytyrosol – which are the well-known active phenolic compounds of the olives<sup>17,94</sup>. Several other metabolites have been isolated from OOBPs and a variety of biological activities have been explored as seen in the phytochemistry review section (**Table 2**).

Thus, besides being a serious environmental problem, the OOBPs represent a precious resource of useful compounds for recovery and valorization purposes for use in different industrial sectors<sup>10,13,22,95,96</sup>. However, it is still not effectively applied and are only described in the scientific literature. Scientific evidence about the bio-functional aspects of the natural product must lead us to utilize that natural source as a sustainable resource.. However, the knowledge about the functionality of the extracts of OOBPs including OMW and its active compounds is still limited.

Therefore, the main purpose of this thesis was to investigate the biological importance and chemical characteristics of the by-products (OMW, leaves) in an effort to address the possible ways to utilize; a focus on non-communicable diseases (NCDs).

#### **1.1.5.2. Why OOBPs and non-communicable diseases (NCDs)?**

Non-communicable diseases (NCDs), also known as chronic diseases, are a result of multiple factors including/ a combination of genetic, physiological, environmental, and behavioral factors. The main types of NCDs are cardiovascular diseases (like heart attacks and stroke), cancers, diabetes, and chronic respiratory diseases (such as chronic obstructive pulmonary disease, COPD, and asthma). Other major NCDs are such as allergic reactions – notably became prevalent due to global climate changes, among many other factors <sup>97,98</sup>. Recently, NCDs disproportionately affect people in low- and middle-income countries where more than three quarters (75%) of global NCD deaths – 32 million – occur <sup>99</sup>.

According to WHO factsheet about NCDs, the following are the major shocking and alarming facts about NCDs prevalence worldwide: one, they are the number killer in the world – killing 41 million people each year, equivalent to 71% of all deaths globally. Two, 15 million people who are dying annually from an NCD are between the ages of 30 and 69 years – over 85% of these "premature" deaths occur in low- and middle-income countries. Diabetes kills 1.6 million people annually <sup>100</sup>, and Alzheimer's kills about 1.5 million people in 2010 <sup>101</sup>. These numbers are expected to rise with time. For instance; in 2014 diabetes affected 422 million adults and it is expected to affect more than 592 million people by 2035 <sup>100,102</sup>, and for AD, 44.4 million patients in 2013, with that number estimated to increase to 135 million by 2050 <sup>103</sup>.

Now, NCDs are considered a global burden because they present with the major socio-economic problem; high medical costs and a high requirement for care <sup>103</sup>. The cost of dealing with NCD can be exemplified with AD patients, whereby the total annual societal cost per patient with AD goes as high as \$56,000 in the USA <sup>104</sup>. Taking into consideration the burden of cost and their debilitating effects on patients, NCDs raises the urgency for the need to put more emphasis on research and development of medicines and functional foods from which will be cheap and effective, and eventually helping to reduce this burden. Luckily, there is a very close link between NCDs and the increase in ROS. It means that the antioxidant property of olive phenolic compounds could be of paramount importance in fighting against NCDs <sup>105–109</sup>.

To address that issue, the biological potential of OOBPs was explored on three major NCDs – allergy, diabetes, and Alzheimer’s disease (AD).



## **CHAPTER 2**

**Mast Cell Stabilizing Effect of the Isolated Compounds from Olive Mill Waste**

**Following Allergic Sensitization**

## **Part I: INTRODUCTION – TYPE 1 ALLERGY**

### **2.1.1. Allergic reaction and hypersensitivity**

An allergy refers to a hypersensitivity disorder in which the immune system abnormally reacts to non-infectious environmental substances, usually considered harmless, named allergens <sup>110,111</sup>. These include pollen, food, dust mites, cosmetics, mold spores, and animal hairs. An allergic reaction can be rapid in onset and chronic, comprising a range of disorders associated with reduced quality of life, such as eczema, allergic rhinitis or atopic dermatitis, and life-threatening reactions, such as severe asthma episodes and anaphylaxis <sup>112</sup>. Worldwide, a high prevalence of allergic diseases has been reported in all age groups <sup>113</sup> and reported to increase during the last two decades <sup>114–116</sup>. Several changes in environmental factors, including sensitizers such as indoor and outdoor allergens, air pollution and rise of ambient temperature – which may induce early springs with increased airborne pollen, and various infections, may contribute to the rise of the problem <sup>97,98,110</sup>.

The commonest form of allergic reaction is called ‘type 1 allergy’ and it is commonly triggered by immunoglobulin E (IgE). Basophils and mast cells play important roles in both immediate- and late-phase reactions of this type of allergy by releasing histamines or other cytokines after being mediated by IgE <sup>117,118</sup> – a process called degranulation. The release of allergic and inflammatory mediators from the cytoplasmic granules is stimulated by the aggregation of high-affinity IgE receptors, known as Fc-receptor I (FcεRI), on mast cells. When FcεRI is stimulated, it triggers the formation of microtubules that leads to the translocation of granules from the

cytoplasm to the plasma membrane, where they release the mediators and granule – plasma membrane fusion is known to be calcium-dependent <sup>119–121</sup>.

### **2.1.2. Pathophysiology of FcεRI-mediated mast cell degranulation**

Pathophysiologically, when antigen-specific IgEs bound to the Fcε receptor I (FcεRI) receptor on basophils or mast cells, cross-linking of IgE with newly absorbed allergens leads to a cascade of events activates phosphoinositide-specific phospholipase C. Phospholipase C breaks down phosphatidylinositol-4,5-bisphosphate to generate inositol-1,4,5-trisphosphate (IP3) and diacylglycerol. IP3 binds its receptor that is located on the surface of the endoplasmic reticulum (ER) which is the main internal Ca<sup>2+</sup> store, and activates the release of Ca<sup>2+</sup> from ER into the cytoplasm - the event known as 'store depletion'. The process of store depletion, in turn, activates store-operated calcium (SOC) channels in the plasma membrane to recruit the influx of Ca<sup>2+</sup> from the extracellular spaces. That leads to an elevation of intracellular free Ca<sup>2+</sup> levels, which in turn plays an essential role in degranulation process <sup>122–125</sup>.

The major degranulation marker of immediate allergic reactions is histamine, which is released from the secretory granules of basophils or mast cells. For *in vitro* studies, the same marker (histamine) or the enzyme β-hexosaminidase are used. β-hexosaminidase is also stored in the secretory granules and is released simultaneously with histamine when the cells are immunologically activated <sup>124</sup>. This is why β-hexosaminidase is now commonly used as a degranulation marker and it

has been used for the evaluation of anti-allergic activity of compounds in this study. The compound is considered to have anti-allergic activity if it can inhibit degranulation and produce a significant reduction in  $\beta$ -hexosaminidase release.

### **2.1.3. The Role of Calcium Channel Proteins (SOC) in Degranulation**

The main mode of influx of  $\text{Ca}^{2+}$  from extracellular spaces into mast cells is through SOC. The best characterized SOC channels in mast cells, and other lymphocytes, are known as 'calcium release-activated calcium' (CRAC) channels <sup>126</sup>. The CRAC channels are characterized by being highly  $\text{Ca}^{2+}$ -selective, low-conductance channels <sup>125</sup>. Based on RNA-mediated high-throughput screens, it is known that STIM1 (stromal interaction molecule 1) is the ER- $\text{Ca}^{2+}$ -sensor, and Orai1 (calcium release-activated calcium modulator 1, CRACM1) is a pore-forming subunit of CRAC channels <sup>127,128</sup>. Moreover, transient receptor potential channel 1 (TRPC1) has also been reported to increase intracellular  $\text{Ca}^{2+}$  concentrations <sup>125</sup>. All STIM1, Orai1, and TRPC1 are important in the make of CRAC channels.

During degranulation, there is an overall increase in the cytosolic/ intracellular  $\text{Ca}^{2+}$  concentrations. Usually, a specific requirement for CRAC channel-mediated  $\text{Ca}^{2+}$  influx has been evaluated derived from, mainly, Orai1- and STIM1-knockout mice <sup>129</sup>.

**Figure 2** summarizes the whole process of the pathophysiology of allergy causation.

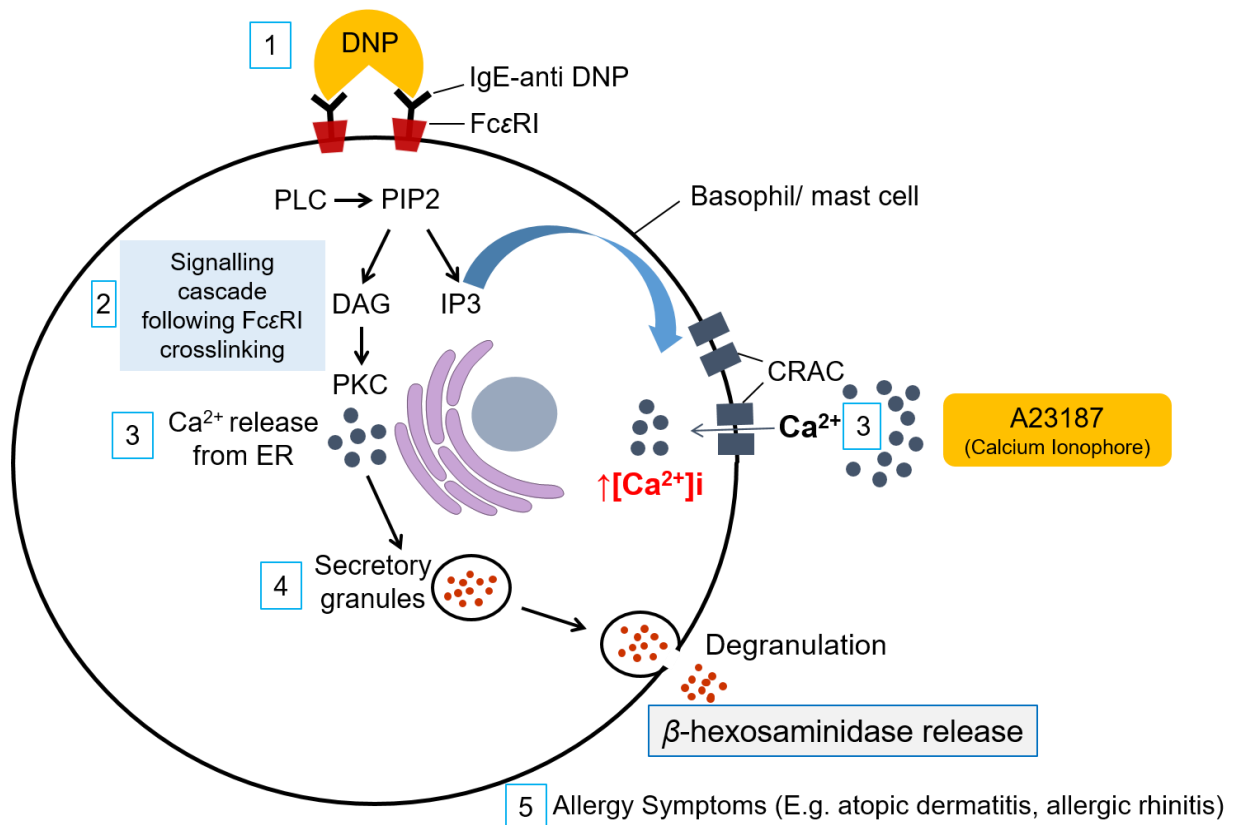


Figure 2: A scheme of RBL-2H3 cells' degranulation pathway. DNP antigen activates signal transduction pathways via IgE-antiDNP/FcεRI receptor complex, in which, phosphoinositide-specific PLC breaks down PIP<sub>2</sub> to generate IP<sub>3</sub> and DAG. IP<sub>3</sub> binds to its receptor located on the surface of ER, and activates the release of Ca<sup>2+</sup> – an event known as 'store depletion'. This, in turn, activates 'calcium release-activated calcium' (CRAC) channels in the cell membrane to recruit Ca<sup>2+</sup>. The overall result is the increase of [Ca<sup>2+</sup>]<sub>i</sub> through both IgE-anti DNP/FcεRI pathway, or calcium ionophore (A23187) stimulation – both play an essential role in degranulation. (Note: Under resting conditions, the intracellular Ca<sup>2+</sup> levels in the cytoplasm [Ca<sup>2+</sup>]<sub>i</sub> is about 100 nM, while in the extracellular it ranges from 1–2 mM, and that in the major intracellular storage compartment, endoplasmic reticulum (ER), ranges 0.1–1.0 mM.

PLC - phospholipase C; PIP<sub>2</sub> - phosphatidylinositol-4,5-bisphosphate; IP<sub>3</sub> - inositol-1,4,5-trisphosphate; DAG - diacylglycerol)

#### 2.1.4. Research Gap and Way-forward

Interest in anti-allergic activity by OMW grew immediately following results from previous research about biological activities of ethanolic and water extract of each part of the olive tree (*Olea europaea* L.); leaves, fruit pulp, seeds, and OMW – in which it was found that the degranulation of a basophilic model, i.e., rat basophil leukemia (RBL-2H3), was mostly reduced by the ethanol extract of OMW whereas the ethanol extract of fruit pulp or that of seeds showed a very low reduction in degranulation, i.e. weak anti-allergic activity <sup>22</sup>.

Following the interesting anti-allergic activity of the OMW ethanolic extract, fractionation was done to isolate the active compounds. As a result, six pentacyclic triterpenoids were isolated and reported for their anti-allergic activity and only one had good anti-allergic activity; strong degranulation reduction in RBL-2H3 cells <sup>96</sup>. The rest of the isolated compounds (five triterpenes) were not anti-allergic active, and almost all of them were cytotoxic at higher concentrations <sup>130</sup>. Considering higher activity of the OMW ethanolic extract and low amount of the active compound, it was 'novel' isolated for the first time in nature, these results leave us with one major question, "*what other compounds/ metabolites contributes to the higher anti-allergic activity of the OMW extract?*"

Moreover, no study had clarified the anti-allergic mechanisms by the OMW compounds. In this chapter, these two research gaps noticed from OMW were addressed so that to attract more industrial attention to these 'wastes' by creating

the agricultural demand through valorization – recovery of bioactive compounds. In summary, the anti-allergic activity of the OMW and its isolated compounds were screened to close the existing research gap on anti-allergic activity. Furthermore, the ability of the isolated active compounds to reduce intracellular  $\text{Ca}^{2+}$  levels and their effect on the expression of calcium channel proteins (CRAC) in RBL-2H3 cells was also investigated. These sets of experiments assisted the possible characterization of the mechanisms by which they reduce degranulation (anti-allergic action).

## Part II: EXPERIMENTAL

### 2.2.1 Materials and Sample

Fresh OMW sample was collected from an olive farm in Nakagawa (Kyushu, Japan) in October 2014. The freeze-dried OMW (1.92 Kg) was extracted by maceration (by shaking at 200 rpm) with 19.2 L of EtOH at room temperature for 72 h. The extract was evaporated under reduced pressure at 40 °C to obtain 360.1 g residue (extraction yield was 18.8%).

### 2.2.2. Cell lines, Chemicals, and reagents

The cell line of rat basophilic leukemia (RBL-2H3) was purchased from Riken Bioresource Center (Tokyo, Japan) and was maintained in 10% FBS (Thermo Fisher Science, Gibco BRL, Tokyo, Japan) in Eagle's minimal essential medium (EMEM) (Nissui, Tokyo, Japan) with Penicillin (100 U/ml) and streptomycin (100 µg/ml) in an incubator at 37 °C in a humidified and atmosphere of 5.0% CO<sub>2</sub>. A calcium ionophore (A23187), monoclonal anti-Dinitrophenyl antibody produced in mouse (anti-DNP IgE), dinitrophenol-bovine serum albumin (DNP-BSA), and *p*-nitrophenyl *N*-acetyl-β-D-glucosaminide were purchased from Sigma-Aldrich (St. Louis, MO, USA), while 3-(4,5-Dimethylthiazol-2-yl)-2,5-Diphenyltetrazolium Bromide (MTT) reagent was purchased from Tokyo Chemical Industry (Tokyo, Japan). Tyrode buffer (TBF), containing 130 mM NaCl, 5 mM KCl, 1.4 mM CaCl<sub>2</sub>, 1 mM MgCl<sub>2</sub>·6H<sub>2</sub>O, 10 mM HEPES, 5.6 mM glucose, 0.1% (g/v) BSA (pH 7.2), was used for anti-allergic (β-hexosaminidase release) assay. Pinorelinol and quercetin were purchased from



Sigma-Aldrich (St. Louis, MO USA). TLC silica gel 60 F<sub>254</sub> plates were purchased from Merck (Darmstadt, Germany); methanol-*d*<sub>4</sub> (CD<sub>3</sub>OD-*d*<sub>4</sub>) and chloroform-*d* (CDCl<sub>3</sub>-*d*) were purchased from Cambridge Isotope Laboratories (Andover, MA, USA). For extraction and open column chromatography: silica gel (Wakogel C 200, pore size 7 nm, particle diameter 75–15 μm), *n*-hexane (*n*-hex), ethyl acetate (EtOAc), methanol (MeOH), ethanol (EtOH) and Chloroform (CHCl<sub>3</sub>) were purchased from Wako Pure Chemical Industries (Osaka, Japan).

### **2.2.3. Methods**

#### **2.2.3.1. HPLC Analysis of the Chemical Profile of the OMW Ethanolic Extract**

EtOH extract of OMW was redissolved in MeOH to a final concentration of 10 mg/ml for HPLC analysis. Before injection for chromatographic separation, it was filtered through Millipore 0.20 μM filters (Millex-LG, Japan). Agilent 1220–LC system (Agilent Technologies, Santa Clara, CA, USA) equipped with a vacuum degasser, autosampler, a binary pump and DAD detector (Agilent Technologies, Santa Clara, CA, USA) was used for the chromatographic separation, which was achieved by using a YMC-Triart C18 column (YMC Company, Kyoto, Japan), (150×4.6 mm, 5 μM particle size), operated at 40 °C with a flow rate of 0.8 ml/min. The mobile phases used were 0.1% formic acid in water (phase A) and acetonitrile (phase B). The analytes were eluted as follows: 0–2 min, 5% B; 2–32 min, 5–30% B; 32–37 min, 30–33% B; 37–45 min, 33–38% B; 45–50 min, 38–50% B; 50–56 min, 50–100% B; 56–60 min, 100% B. Finally, the B content was decreased to the initial conditions (5%) in 2 min and the column re-equilibrated for 3 min. A volume of 10 μL of the

extracts was injected. The detection was monitored with a DAD detector set at 240 and 280 nm. For data acquisition and monitoring the hardware, Agilent OpenLAB Chromatography Data System (CDS) EZChrom software (Agilent Technologies, Santa Clara, CA, USA) was used.

### 2.2.3.2. Fractionation and Isolation Procedure

Based on the previous report, EtOH extract of OMW exhibited stronger anti-allergic activity, by reducing degranulation by up to 56.5%<sup>22</sup>, in this section, the focus was given to it to fractionate to get active fractions for isolation of active compounds. The whole process of fractionation and identification is discussed here in detail.

The residue was subjected to silica gel open column chromatography (100 × 15 cm) previously packed with *n*-hexane and eluted with an *n*-hex-EtOAc gradient (100:0 → 0:100). Similar fractions were pooled together based on similar  $R_f$  values – monitoring was done with TLC analysis, detected by irradiating UV light at 254 nm and by spot visualization, in which the TLC plate was sprayed with 5% sulfuric acid in MeOH and burned at 100–180 °C. In the end, 10 fractions were obtained and all fractions were tested for their anti-allergic activity.

Fr. 6 (15.5 g) showed the highest anti-allergic activity, as summarized in **Figure 3**, and thus it was further purified to obtain pure bioactive compounds. The fraction was subjected to silica gel open column chromatography (65 × 6.5 cm) previously packed with *n*-hexane, eluted with the *n*-hexane-EtOAc gradient (80:20 → 10:90), and finally washed with MeOH to afford 10 sub-fractions (Fr. 6-1 to 6-10). Two sub-fractions (Fr.

6-6 and 6-7, which were eluted with *n*-hex-EtOAc (40:60), and *n*-hex-EtOAc (40:60→30:70), respectively) exhibited the highest anti-allergic activity, and low cytotoxicity simultaneously, and hence they were chosen for further purification (**Figure 4**). Two other sub-fractions (Fr. 6-5 and 6-8), were also taken for further purification since they were eluted with almost similar mobile phase composition, and lastly, the first sub-fraction (Fr. 6-1) was used as control inactive fraction, and therefore it was also purified to isolate the pure compound(s).

Beginning with the purification of the first active sub-fractions, Fr. 6-6 (367 mg), it was, firstly, subjected to silica gel open column chromatography (50 × 4.5 cm) previously packed with *n*-hexane and eluted with the *n*-hex-EtOAc gradient (80:20 → 0:100) to obtain 8 sub-sub-fractions, whereby, two of them were eluted as pure compounds **2** (46 mg) and **5** (1.0 mg). In the second step, it was subjected to MPLC system (EPCLC, Yamazen, Osaka, Japan), to afford one more compound, **4** (1.0 mg) – in both cases, elutes were monitored with TLC analysis (as previously described). Similarly, the sub-fraction, Fr. 6-7 (2.5 g) was subjected, firstly, to silica gel open column chromatography (50 × 4.5 cm) previously packed with *n*-hexane and eluted with the *n*-hex-EtOAc gradient (80:20 → 0:100) to obtain 7 sub-sub-fractions. The second sub-sub-fraction, eluted with *n*-hex-EtOAc (50:50) was further purified by chromatography repeatedly to afford compound **6** (0.7 mg), while the seventh sub-sub-fraction was eluted with *n*-hex-EtOAc (30:70) and (20:80), and it was further purified by preparative TLC to afford two compounds, **7** (1.0 mg) and **8** (8.5 mg), respectively. While, in the second step, the other sub-fractions were

purified by MPLC system connected with columns of silica gel (particle size 50  $\mu\text{m}$ , 3.0  $\times$  16.5 cm, 37 g) flashed with  $\text{CHCl}_3$ : MeOH gradient (90:10 $\rightarrow$ 0:100) to afford two more compounds, **9** (7.8 mg) and **10** (13.6 mg)

The sub-fraction Fr. 6-5 (5.913 g), was subjected to silica gel open column chromatography (50  $\times$  4.5 cm) previously packed with *n*-hexane and eluted with the *n*-hex-EtOAc gradient (90:10  $\rightarrow$  0:100) to obtain five sub-sub-fractions. The fourth and second sub-sub-fractions were further purified by chromatographic techniques to afford two compounds **2** (19.6 mg) and **3** (6.5 mg). And last but not least, is the purification of the inactive control fraction, Fr. 1 (144 g), which was eluted with the *n*-hexane-EtOAc (80:20) from the main extract. After TLC analysis, this fraction was purified further by preparative TLC to afford compound **1** (2.4 mg). Purification and isolation of all compounds originated from the active Fr. 6, are summarized in **Figure 5**. In summary, a total of ten compounds were isolated, of which, five were triterpenic compounds and the other five were polyphenolic compounds.

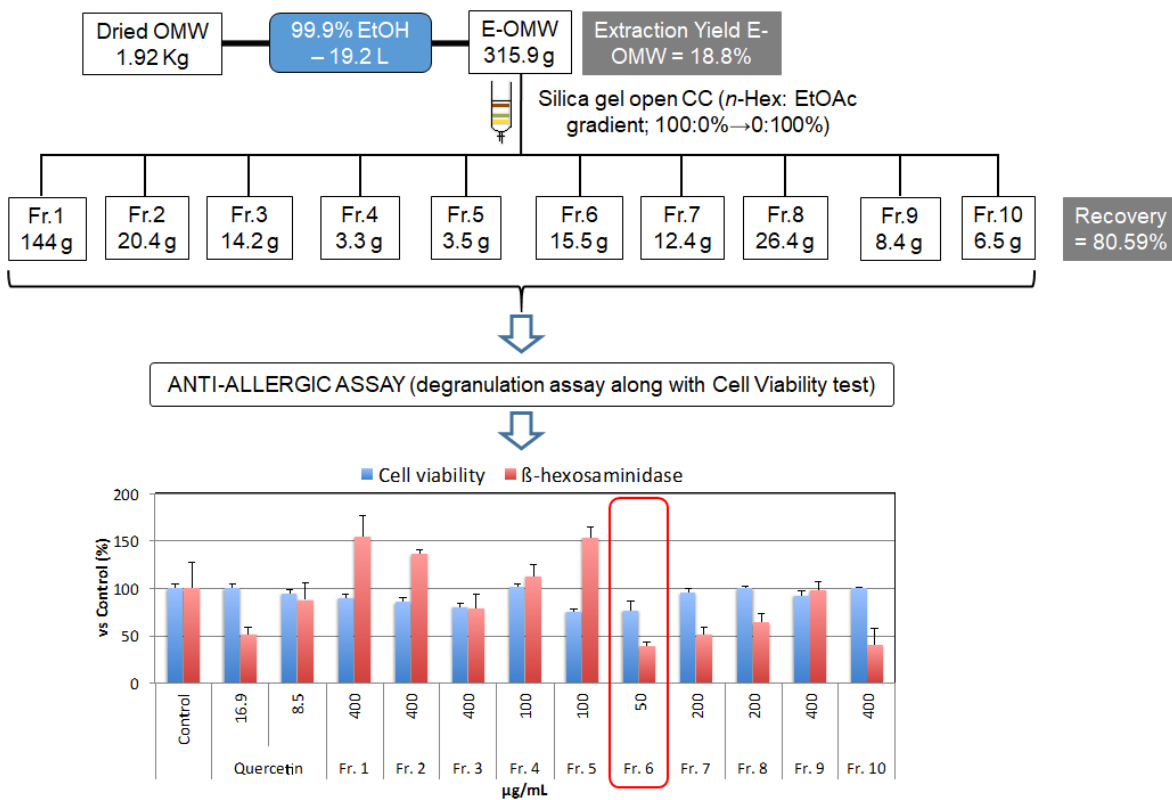


Figure 3: A summary of the bioassay-guided fractionation of OMW ethanolic extract. The red boundary shows the most active fraction, Fr. 6. Effect on RBL-2H3 cells' degranulation/ anti-allergic activity of the fractions, which was tested by measuring the amount of β-hexosaminidase released after treatment by calcium ionophore (A23187), is represented in red bars. Cytotoxicity of the compounds is presented with blue bars.

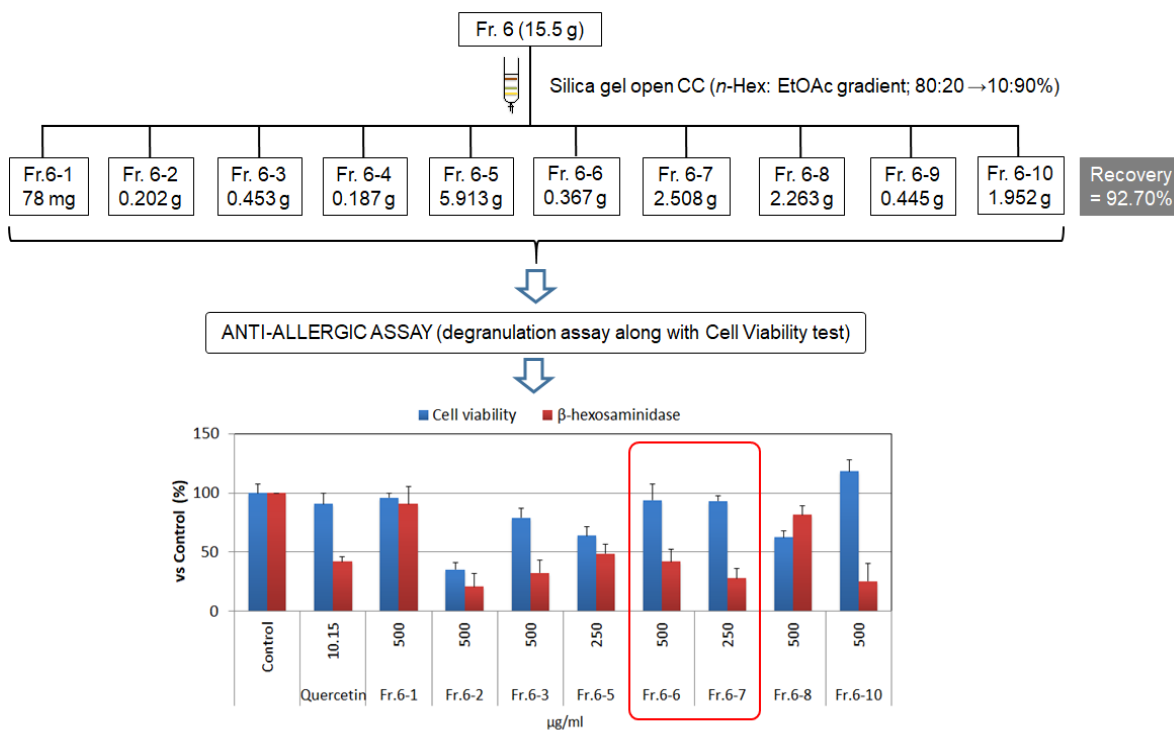


Figure 4: A summary of the bioassay-guided fractionation of the active fraction, Fr. 6. Sub-fractions Fr. 6-2 and Fr. 6-3/4 showed high activity towards inhibition of degranulation, but they were too toxic to the cells – thus we did not deal with them for further purification. Sub-fractions 6-5 and Fr. 6-8 were not active, but we proceed with their purification and isolation because they had similar TLC pattern with Fr. 6-6 and Fr. 6-7, respectively. The sub-fractions 6-10 was active, however, several trials to isolate individual compounds were done unsuccessfully.

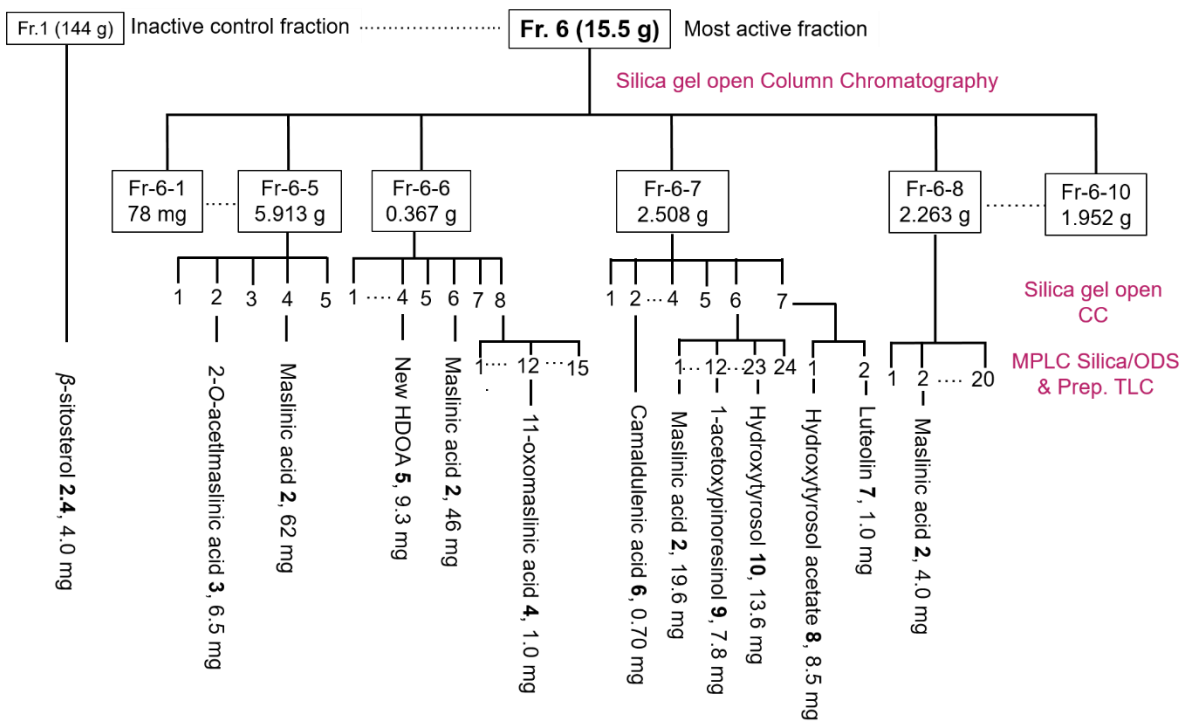


Figure 5: Purification and isolation of compounds from the active sub-fractions of the active fraction, Fr. 6 (HDOA, hemialdehydic decarboxymethylated oleuropein aglycone)

### **2.2.3.3. Procedure for the Identification of the Isolated compounds**

The isolated compounds were identified by measuring the nuclear magnetic resonance (NMR) spectroscopy; mass spectrometry (MS) and polarimetry to determine their one-dimensional (1D) and two-dimensional (2D) NMR for the elucidation of their molecular structures, molecular weights, and optical rotations respectively. In the measurement of the NMR spectroscopy, <sup>1</sup>H- and <sup>13</sup>C-, HSQC and HMBC NMR spectra were obtained from an NMR spectrometer (Bruker DRX-600; Bruker Daltonics, Billerica MA, USA) at room temperature with trimethylsilane (TMS) as an internal standard of the chemical shifts, and CD<sub>3</sub>OD or CDCl<sub>3</sub> as dissolving solvents, while EI/FAB-MS was performed on JMS 700 MStation mass spectrometer (JEOL, Tokyo, Japan). Optical rotations were measured with a JASCO DIP-370 polarimeter (JASCO, Tokyo, Japan).

### **2.1.5. Screening for the anti-allergic activity**

Both the total extract and fractions were subjected to anti-allergic activity to determine their inhibitory effect on the release of  $\beta$ -hexosaminidase from RBL-2H3 cells. Purification was done from the active fractions to isolate pure compounds, which were then subjected to a similar anti-allergic assay to determine their anti-allergic activities (IC<sub>50</sub>, half-minimum inhibitory concentration) and their cytotoxicities (CC<sub>50</sub>, half-minimum cytotoxic concentration). Cell viability (cytotoxicity) was tested in the presence of the extract/ isolated compounds. In the present study, the contents of the tested compounds resulting into  $\geq 80\%$  viable cells were defined as limited toxicity ("non-cytotoxic"), while anti-allergic activity was defined as a non-cytotoxic



concentration of the tested compound resulting into 50% inhibition  $\beta$ -hexosaminidase release. Finally, all isolated compounds were quantified and their total anti-allergic activities were compared with each other. This helped us to understand the contribution of each metabolite to the total anti-allergic properties of the OMW.

#### **2.2.3.4. Cytotoxicity Assay**

Cytotoxicity was conducted just before doing the inhibitory test on  $\beta$ -hexosaminidase release from RBL-2H3 cells. It was evaluated by an MTT proliferation assay as described by Kishikawa *et al.* (2017) with minor modifications <sup>96</sup>.

In the method, the RBL-2H3 cells were cultured on a 96-well plate at a density of  $2.5 \times 10^4$  cells/well for 24 – 30 h, and then treated with DMSO solution of the extract, or either one of the test compounds at various concentrations or with only DMSO as a control (0.5  $\mu$ L/well,  $n=3$ ) for 1 h with a dimethyl sulfoxide (DMSO) solution of the extract, or either one of the test compounds at various concentrations or with only DMSO as a control. Quercetin was used as standard since it was reported to inhibit the degranulation of RBL-2H3 cells <sup>114</sup>, and it is a polyphenolic compound – the same group as the isolated ones. Then, 10  $\mu$ L MTT reagent (at a final concentration of 0.5 mg/mL) was added in each well and incubated for 4 h followed by the replacement with 100  $\mu$ L of acidified propanol (containing 0.04 N HCl), which was then incubated overnight in the dark at room temperature. For the determination of cytotoxicity for the compounds, the cell viability of RBL-2H3 cells was calculated by the

determination of accumulated formazan derivatives in the treated cells at 570 nm in comparison with the untreated ones by using a microplate reader (iMark, Bio-Rad, Hercules, CA, USA).

Cell viability was calculated using the following formula:

$$\text{Cell viability (\%)} = (1 - \text{Abs}_{570\text{Test}} / \text{Abs}_{570\text{Control}}) \times 100$$

where;

$\text{Abs}_{570\text{Test}}$  is the absorbance at 570 nm of the test well (DMSO solution: +, test compound/ extract: +) and

$\text{Abs}_{570\text{Control}}$  is the absorbance at 570 nm of the control well (DMSO solution: +, test compound/ extract: -).

#### **2.2.3.5. $\beta$ -hexosaminidase release (degranulation) Assay**

Inhibitory effects on the release of  $\beta$ -hexosaminidase from RBL-2H3 cells was evaluated by a method as described by Yun *et al.* (2010) with some modifications<sup>131</sup>. In brief, the RBL-2H3 cells were cultured on a 96-well plate at a density of  $2.5 \times 10^4$  cells/well between 24 – 30 h and were treated for 1 h ( $0.5 \mu\text{L}$ / well,  $n = 3$ ) with a dimethyl sulfoxide (DMSO) solution of either the extract or one of the test compounds at various concentrations or with only DMSO as a control (negative). Quercetin was used as a standard drug<sup>114</sup>, as for cytotoxicity assay. To elicit the maximum release of  $\beta$ -hexosaminidase, the cells were treated with a working solution containing  $5 \mu\text{M}$  A23187, a calcium ionophore, in tyrode's buffer (pH 7.2) for 1 h. Then, the

supernatant, which contained the released  $\beta$ -hexosaminidase, was recovered. The recovered supernatant, 50  $\mu$ L, was added with the same volume of the substrate solution of 1 mM *p*-nitrophenyl-*N*-acetyl- $\beta$ -D-glucosaminide (pH 5.2) to a new 96-well plate and the mixture was then incubated in the dark at room temperature for 1 h with continuous shaking at 40 rpm to allow enzymatic reaction. The reaction was terminated by addition of 100  $\mu$ L of 100 mM sodium bicarbonate (pH 10). Finally, the absorbance was read at 405 nm using a microplate reader (iMark, Bio-Rad, Hercules, CA, USA). For the determination of the anti-allergic activity of the compounds, the percentage inhibition of degranulation ( $\beta$ -hexosaminidase release) from the RBL-2H3 cells was calculated as follows:

$$\text{Inhibition of degranulation (\%)} = \left( 1 - \frac{(\text{Abs}405_{\text{Test}} - \text{Abs}405_{\text{Blank}})}{(\text{Abs}405_{\text{Control}} - \text{Abs}405_{\text{Blank}})} \right) \times 100$$

Where;

Abs405<sub>Test</sub> is the absorbance at 405 nm of the test well (DMSO solution: +, A23187: +, test compound/extract: +),

Abs405<sub>Control</sub> is the absorbance at 405 nm of the control well (DMSO solution: +, A23187: +, test compound/extract: -), and

Abs405<sub>Blank</sub> is the absorbance at 405 nm of the blank well (DMSO solution: +, A23187: -, test compound/extract: -).

### 2.2.3.6. $\beta$ -hexosaminidase Enzymatic Inhibition Assay

Individual compounds may directly inhibit  $\beta$ -hexosaminidase enzymatic activity beyond avoiding just the release of  $\beta$ -hexosaminidase. Bearing this in mind, the inhibition of  $\beta$ -hexosaminidase enzymatic activity by the isolated compounds and quercetin was evaluated in assay similar to the one described above. A method as described by Pinho *et al.* (2014) with some modifications was adopted<sup>132</sup>. Briefly, the compounds were incubated with the supernatant of degranulated cells where  $\beta$ -hexosaminidase is present. Whereby, 50  $\mu$ l of the supernatant of cells treated with 10  $\mu$ M A23187, in presence of 50  $\mu$ l of the substrate solution, was incubated with compounds for 1 h, at 37°C. Finally, the absorbance was read at 405 nm using a microplate reader (iMark, Bio-Rad, Hercules, CA, USA), and the determination of their inhibition was calculated at concentrations slightly higher or equal to their IC<sub>50</sub> as follows:

$$\beta - \text{hexosaminidase inhibition (\%)} = (1 - \text{Abs}_{405\text{Test}} / \text{Abs}_{405\text{Control}}) \times 100$$

Where;

Abs<sub>405Test</sub> is the absorbance at 405 nm of the test well (DMSO solution: +, A23187: +, test compound/extract: +),

Abs<sub>405Control</sub> is the absorbance at 405 nm of the control well (DMSO solution: +, A23187: +, test compound/extract: -).

A schematic presentation of the protocols for RBL-2H3 cells' degranulation assay and  $\beta$ -hexosaminidase inhibitory activity is shown in **Figure 6**.

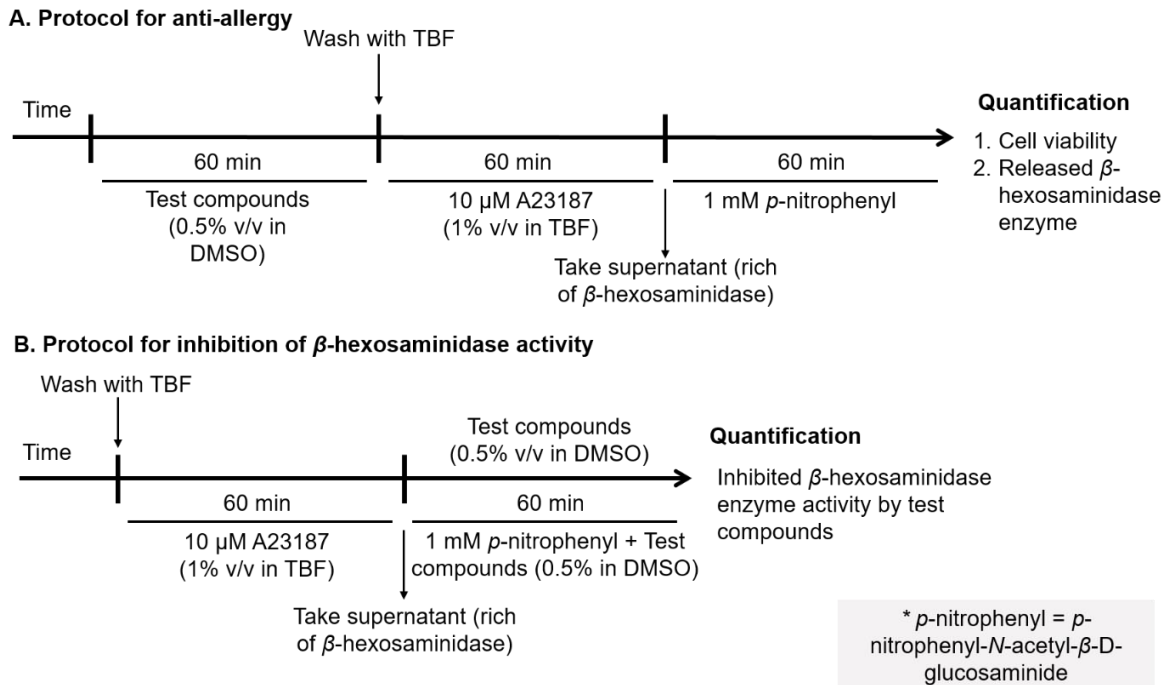


Figure 6: A schematic presentation of protocols for RBL-2H3 cells' degranulation assay using A23187 (A), and  $\beta$ -hexosaminidase inhibitory activity (B)

## **Effect of the Active Anti-allergic compounds on RBL-2H3 cells' intracellular Ca<sup>2+</sup> concentrations**

As described in detail in the introduction part of this Chapter, an overall elevation of intracellular free Ca<sup>2+</sup> levels plays an essential role in the degranulation process<sup>122,125</sup>. This means that type 1 allergy is a Ca<sup>2+</sup>-dependent action. Therefore, active anti-allergic compounds were investigated of their effect on intracellular free Ca<sup>2+</sup> concentration, and on calcium channel proteins, to characterize the possible mechanisms involved behind degranulation.

### **2.2.3.7. Intracellular Ca<sup>2+</sup> Levels Analysis by Fluorescence Technique**

Intracellular Ca<sup>2+</sup> levels were determined with Calcium Kit II-Fluo 4<sup>TM</sup> (Dojindo Laboratories, Kumamoto, Japan). A method previously described by Han *et al.* (2017) with some minor modifications was adopted<sup>133</sup>.

In the assay, RBL-2H3 cells were seeded into a 96-well black opaque cell culture plate at a density of  $2.5 \times 10^4$  cells/mL for 24 h at 37°C/ 5% CO<sub>2</sub>. After incubation, the cells were washed with Tyrode's buffer (pH 7.4) and then treated with or without the test compounds for 1 h. After the treatment of the RBL-2H3 cells, they were incubated with 10 μM of Fluo-4 AM for 45 min at room temperature in the dark. Finally, free Fluo-4 AM was removed by washing. Following a 20 s baseline recording, cells were exposed to 10 μg/ml A23187 or 100 ng/ml DNP-BSA for another 180 s. Fluorescence intensity (FI) was recorded using the FlexStation3

multi-mode microplate reader (Molecular Devices, CA, USA) with excitation wavelength at 488 nm and emission wavelength at 525 nm.

#### **2.2.3.8. qRT-PCR Analysis of the Calcium Channel Proteins**

Total RNA was prepared using RNeasy Mini Kit (QIAGEN, USA) and cDNA was transcribed using ReverTra Ace qPCR RT Master Mix with gDNA remover (Toyobo Co., Ltd, Osaka, Japan). The semi-quantitative real-time PCR (RT-PCR) was performed using THUNDERBIRD® SYBR qPCR mix (Toyobo Co., Ltd, Osaka, Japan) for STIM1, Orai1, TRPC1, IP3R and  $\beta$ -actin (which was used as the internal control). After 16-hour treatment of the anti-DNP IgE sensitized RBL-2H3 cells with the compounds followed by stimulation with DNP-BSA, PCR for RBL-2H3 was performed with primers as follows: 5'-ATGCCACGTCTTCCAATGGT-3' and 5'-TCAGCCATAGCCTTCTTGCC-3' for STIM1, 5'-GCCATAAGACGGACCGACAG-3' and 5'-ACTTAGGCATAGTGGGTGCC-3' for Orai1, 5'-AGCTGCTTATCTTCATGTGCG-3' and 5'-AGCACGAGGCCAGTTTTGTA-3' for TRPC1, 5'-AGCATCTCCTTCAACCTGGC-3' and 5'-CACAGTTGCCACAAAGCTC-3' for IP3R and 5'-GCAGGAGTACGATGAGTCCG-3' and 5'-ACGCAGCTCAGTAACAGTCC-3' for  $\beta$ -actin. The  $2^{-\Delta\Delta Ct}$  method was used to calculate the relative mRNA levels. The PCR was performed using the Agilent AriaMX Real-Time PCR system (Agilent Technologies, Santa Clara, CA, USA).

#### **2.3.4. Statistical analysis**

The values in this study are expressed as mean values  $\pm$  standard deviation (SD) of at least three independent experiments ( $n=3$ ). The significant differences between each tested group and the control group were determined using Dunnett's multiple post hoc test.  $p$ -value cut-points were set at 95% and 99% (where; \*  $p<0.05$ , \*\*  $p<0.01$ ), when the one-way analysis of variance (ANOVA) was statistically significant.



### **Part III: RESULTS AND DISCUSSION**

The RBL-2H3 cells are tumor analog of mast cells, which after being sensitized with mouse monoclonal IgE or ionophore A23187 respond by releasing inflammatory mediators from their secretory granules – degranulation. As mentioned in the methods section, the effect of the samples (extracts and pure compounds) on the degranulation of basophil was estimated based on the colorimetric assay which quantifies the amount of  $\beta$ -hexosaminidase released from the rat basophilic cells, RBL-2H3. As a result, the extract/ fraction or a pure compound is considered to have anti-allergic activity if it can inhibit mast cell degranulation and produce a significant reduction of the release of  $\beta$ -hexosaminidase. However, at first, the chemical properties of the OMW ethanolic extract was investigated by HPLC analysis.

#### **2.3.1. Chemical Properties of EtOH Extract of OMW**

The authentication of any olive product is made by the identification of the two common polyphenolic compounds found in olives, which are oleuropein and hydroxytyrosol. These compounds were detected in the OMW sample (and one of them was isolated; discussed in the next sections) following the analysis by HPLC. For the purpose of identification, standards of oleuropein and hydroxytyrosol were detected in OMW extract by HPLC at 280nm with retention times of 30.6 min and 9.19 min, respectively. Further confirmation was made by photodiode array (PDA) detector analysis in which the spectral similarities of the pure compounds were made with reference to the extracts'. A similar analysis was done for the case of the isolated compounds from OMW, and all compounds had an acceptable similarity

factor, ranging between 0.84 – 0.97. The HPLC chromatogram of the extract of OMW and the structures of oleuropein and hydroxytyrosol is shown in **Figure 7**.

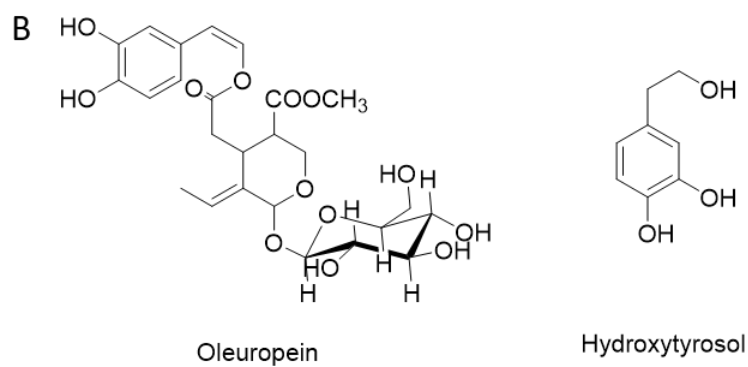
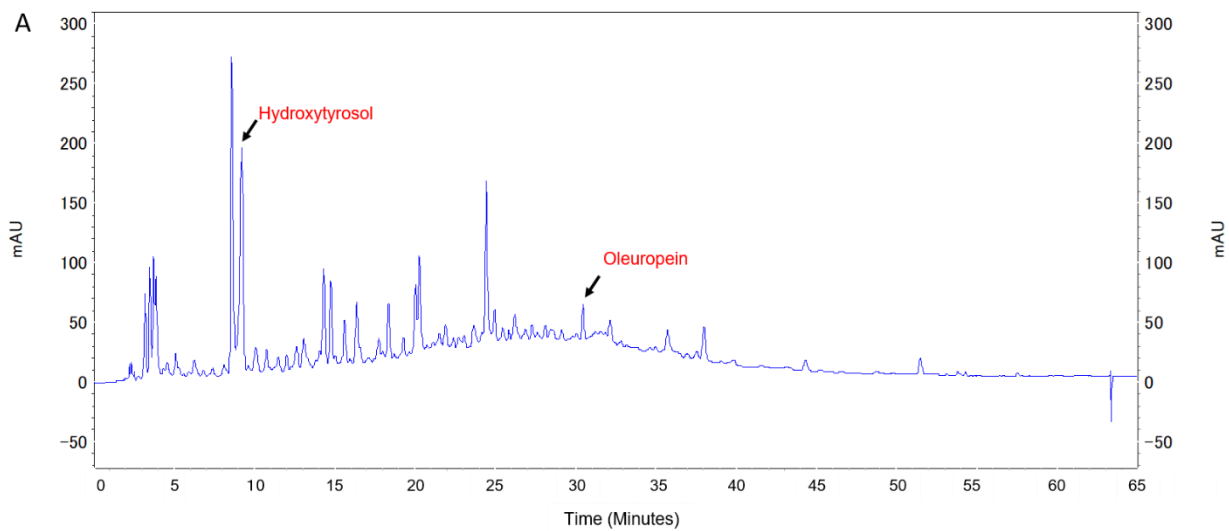


Figure 7: A) HPLC chromatogram of the EtOH extract of OMW (DAD set at  $\lambda=280$  nm). Oleuropein and hydroxytyrosol were identified by comparing their retention times and UV absorption spectra, from PDA detector, of each peak to those of authentic compounds. B) The chemical structures of oleuropein and hydroxytyrosol.

### 2.3.2. Identification of the Isolated Compounds

Ten compounds were isolated from OMW following anti-allergic assay guided fractionation. Based on their classes, five were pentacyclic triterpenes while the other five polyphenolic compounds, including one novel, a derivative of hemialdehydic decarboxymethylated oleuropein aglycone **5**, and the other four were known. The details of the new compound have been discussed below and structures of all compounds are shown in **Figure 8 (B)**.

Compound **5** was obtained as a yellowish amorphous powder with an  $[\alpha]_D^{25} = -3.91$  (c 1.0, MeOH) and UV (EtOH)  $\lambda_{max}$  228, 282 nm. Its structure was elucidated by 1D- and 2D-NMR spectroscopy and HR-FAB-MS spectrometry. A detailed analysis of NMR data in comparison with those in the literature <sup>134</sup>, suggested that compound **5** has a partial structure of the main skeleton, hemialdehydic decarboxymethylated oleuropein aglycone (HDOA). The <sup>1</sup>H NMR spectrum showed characteristic peaks suggestive of the protons of typical secoiridoid skeleton <sup>135</sup>, and these include an aldehydic proton resonating at  $\delta_H$  9.29 (d,  $J=1.8$  Hz, H-1); an olefinic proton at  $\delta_H$  6.64 (q,  $J=7.2$  Hz, H-8); a multiplet at  $\delta_H$  4.25 (H-3); an ABX system, whereby two protons were resonating at  $\delta_H$  2.65 (dd,  $J_{6a,6b}=15.0$  Hz, H-6a) and  $\delta_H$  2.54 (dd,  $J_{6b,6a}=15.0$  Hz, H-6b) and a multiplet resonating at  $\delta_H$  3.21 (H-5); lastly, a multiplet at  $\delta_H$  2.01 (H-4a/4b) and a doublet at  $\delta_H$  1.94 (3H,  $J=7.2$  Hz, H-10). The presence of the hydroxytyrosol moiety was also evident through <sup>1</sup>H NMR spectral peaks, whereby one doublet at  $\delta_H$  6.50 (2H,  $J=1.8, 8.1$  Hz, H-8') was observed which corresponds to the meta- and para-aromatic ring substitutions (as opposed to

tyrosol), and other two resonances at  $\delta_{\text{H}}$  4.10 (2H, m) and 2.72 (2H, t,  $J=7.2$  Hz) corresponding to the protons H-1' and H-2' of the ethyl chain, respectively.

The main difference between the compound **5** and the reported HDOA was at the attachment at C-3. In the  $^{13}\text{C}$ -NMR spectrum of **5**, C-3 was resonating at  $\delta_{\text{C}}$  103.0 – a slight downfield as compared to the reported one ( $\delta_{\text{C}}$  98.2). It was speculated that it could be due to the attachment of more than one oxygen atom-bonded chain. Through the HSQC spectrum, this carbon correlated to a multiplet at  $\delta_{\text{H}}$  4.26 (H-3). The long-range HMBC correlations observed from  $\delta_{\text{H}}$  4.26 (m, H-3) included the carbon signals at,  $\delta_{\text{C}}$  37.0 (C-4), 31.1 (C-5) and with other two methylene carbons resonating at  $\delta_{\text{C}}$  62.3 (C-1'') and 62.7 (C-1''') - which confirms the hypothesis that there are two oxygenated carbons attached to C-3. HSQC spectrum was more evident, as it revealed that protons at  $\delta_{\text{H}}$  3.54 (m, H-1'') and 3.63 (m, H-1''') correlated to these carbons, respectively. Through the help of HMBC, the following important correlations were seen: proton at  $\delta_{\text{H}}$  3.54 (H-1'') correlated with a methyl carbon resonating at  $\delta_{\text{C}}$  15.6, which was carefully assigned as C-2'' and with  $\delta_{\text{C}}$  103.0 (C-3). For proton at  $\delta_{\text{H}}$  3.63 (H-1'''), the same kind of correlation as for H-1'' was observed, that is, it correlated with one methyl carbon resonating at  $\delta_{\text{C}}$  15.6, which was later assigned as C-2''' and another correlation with the carbon resonating at  $\delta_{\text{C}}$  103.0 (C-3). The assignment of all  $^1\text{H}$ - and  $^{13}\text{C}$ -NMR signals were confirmed by HSQC and HMBC data and are summarized in **Table 4** and **Figure 8 (A)**.

The HR-FAB-MS spectrum of compound **5** exhibited a molecular ion peak  $[M+Na]^+$  at  $m/z$  417.1889, which was in line with the suggested elemental composition of  $C_{21}H_{30}O_7Na$  (calculated  $m/z$  417.1890). Another peak at  $m/z$  349 was observed which corresponds to the fragment  $[M-CH_3CH_2OH]^+$ . In addition, another characteristic fragment was observed at  $m/z$  241  $[M-HTYR]^+$ .

Other compounds were identified as  $\beta$ -sitosterol **1** <sup>136,137</sup>, maslinic acid **2** <sup>138</sup>, 2-*O*-acetylmaslinic acid **3** <sup>139</sup>, 11-oxomaslinic acid **4** <sup>96</sup>, camaldulenic acid **6** <sup>140</sup>, luteolin **7** <sup>141</sup>, hydroxytyrosol acetate **8** <sup>142</sup>, 1-acetoxypinoresinol **9** <sup>143</sup> and hydroxytyrosol **10** <sup>52</sup>, by comparing their NMR with those reported previously in the respectively cited references.

$\beta$ -sitosterol **1**, one of the two most abundant phytosterol in nature, is considered as a main phytosterol in the olives. Even though its bioactivities have been rarely reported from olives, it is widely known for its antioxidant and anticancer activities, for instance, through modulation of the antioxidant enzyme response in RAW 264.7 macrophages <sup>144</sup>. Maslinic acid **2** (and oleanolic acid – not isolated in this study) are known to be the main triterpenes in OMW, olive fruits, olive oil, and olive leaves <sup>145</sup>.

Maslinic acid **2** is a widely known triterpene with many biological activities ranging from antioxidant, anticancer, anti-inflammatory, antidiabetes, and liver-protective activities among many other biological activities <sup>146,147</sup>. Other triterpenes isolated in the present study, 2-*O*-acetylmaslinic acid **3**, 11-oxomaslinic acid **4**, camaldulenic

acid **6**, are derivatives of maslinic acid and one of them, camaldulenic acid **6** was isolated for the first time in olives (OMW) in the present study.

Hydroxytyrosol **10** has been reported as a major polyphenolic compound of class phenylethanoid in OMW, olive oil and olive fruits, and it has been reported to have a wide variety of biological activities including antioxidant, cardioprotective, chemopreventive, anti-inflammatory, hypoglycemic, antihypertensive, antimicrobial and antiviral <sup>17</sup>. Hydroxytyrosol acetate **8**, is an ester form of parent hydroxytyrosol and it has been previously isolated from olive oil <sup>142</sup>. However, only a limited number of literatures have cited its biological activities – neuroprotective and antioxidant activities <sup>148, 149</sup>.

For luteolin **7**, a famous flavonoid, a lot of its biological activities have been reported <sup>150–153</sup>. It is worth a mention that, the existence of esterified compounds in OMW has been reported previously. For instance, it was reported that pectin extracted from OMW was highly acetylated and it was proposed that acetylation increases its oil holding capacity <sup>154</sup>; and other researchers isolated esterified maslinic acid (2-O-acetylmasilnic acid) <sup>96</sup>.

**Table 4: <sup>1</sup>H and <sup>13</sup>C NMR data for compound 5 and hemialdehydic decarboxymethylated oleuropein aglycone (HDOA)**

No.	Compound 5 <sup>a</sup>		HDOA <sup>b</sup>	
	<sup>1</sup> H (J in Hz)	<sup>13</sup> C	<sup>1</sup> H (J in Hz)	<sup>13</sup> C
1	9.29 d (1.8)	197.2	9.14 d (1.9)	197.2
3	4.21 m	103.0	4.22 m	98.2
4	2.00 m	37.0	2.00 m	40.1
5	3.21 m	31.1	3.24 m	31.2
6a	2.65 dd (15.0)	38.7	2.62 dd (15.0)	38.5
6b	2.54 dd		2.46 dd	
7	–	174.1	–	174.1
8	6.61 q (7.2)	155.4	6.61 q (7.1)	155.5
9	–	145.3	–	145.0
10	1.94 d (7.2)	15.3	1.89 d	15.2
1'	4.10 m	66.4	4.09 m	66.5
2'	2.72 t (7.2)	35.3	2.65 t (7.0)	35.5
3'	–	130.8	–	130.7
4'	6.68 d (1.8)	116.4	6.65 d (2.1)	116.4
5'	–	144.9	–	144.8
6'	–	146.3	–	146.1
7'	6.64 d (8.4)	117.0	6.63 d (8.0)	117.0
8'	6.50 dd (8.4/1.8)	121.2	6.45 dd	121.2
OMe	–	–	3.29 s	49.9
1''	3.54 m	62.7	–	
2''	1.16 t (7.2)	15.6	–	
1'''	3.63 m	62.3	–	
2'''	1.13 t (7.2)	15.6	–	

The values of chemical shifts are in ppm; for **1** the <sup>1</sup>H and <sup>13</sup>C NMR at 600 and 150 MHz respectively while for HDOA the <sup>1</sup>H and <sup>13</sup>C NMR at 200 and 50 MHz respectively; **a** – in Methanol-*d*<sub>4</sub>(CD<sub>3</sub>OD), **b** – in Chloroform-*d* (CDCl<sub>3</sub>)



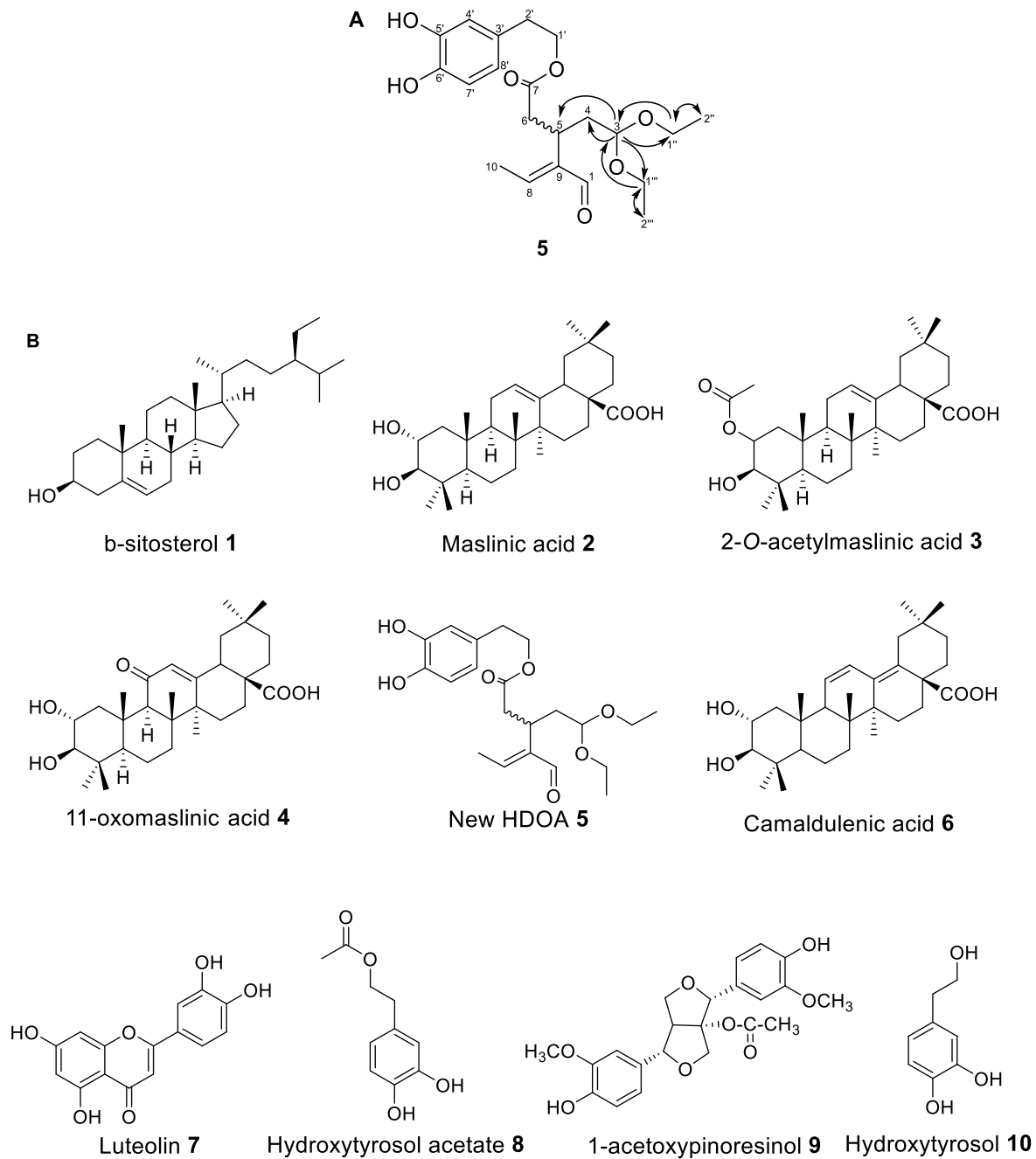


Figure 8: The chemical structures of the isolated compounds from OMW. (A) Significant HMBC correlations (solid arrows) of Compound **5**; (B) The structures of the isolated compounds from OMW (**1 – 10**)

The data used for the identification of the rest of the compounds (**1**, **2**, **3**, **4**, **6**, **7**, **8**, **9**, and **10**) is as follows;

Maslinic acid (*2 $\alpha$* , *3 $\beta$* -dihydroxyolean-12-en-28-oic acid), **2**; White amorphous solid:  $[\alpha]^{26}_D +52.2$  (*c* 1.0, MeOH):  $^1\text{H}$  NMR (600 MHz,  $\text{CD}_3\text{OD}$ )  $\delta_{\text{H}}$  5.21 (1H, dd, *J*=Hz, H-12), 3.60 (1H, ddd, *J*=4.5, 9.6, 11.4 Hz, H-2 $\beta$ ), 2.88 (1H, d, *J*=9.5 Hz, H-3 $\alpha$ ), 2.76 (1H, dd, *J*=4.1, 13.8 Hz, H-18), 1.91 (1H, m, H-16), 1.07 (3H, s, H-27), 0.95 (3H, s, H-23), 0.91 (3H, s, H-25), 0.86 (3H, s, H-30), 0.84 (3H, s, H-29), 0.74 (3H, s, H-26), 0.71 (3H, s, H-24): for  $^{13}\text{C}$  NMR (150 MHz,  $\text{CD}_3\text{OD}$ ), see **Table 5**: HR-ESI-MS *m/z* 471.3487 [M-H] $^-$ .

2-O-acetylmasilnic acid **3**; White amorphous solid:  $[\alpha]^{26}_D +25.0$  (*c* 1.0, MeOH):  $^1\text{H}$  NMR (600 MHz,  $\text{CD}_3\text{OD}$ )  $\delta_{\text{H}}$  5.25 (1H, dd, *J* = 3.5, 3.5 Hz, H-12), 4.90 (1H, m, H-2), 3.15 (1H, d, *J* = 10.2 Hz, H-3), 2.85 (1H, dd, *J* = 4.0, 14.4, H-18), 2.04 (3H, s,  $\text{COCH}_3$ ), 1.18 (3H, s, H-27), 1.05 (3H, s, H-25), 1.04 (3H, s, H-23), 0.95 (3H, s, H-29), 0.91 (3H, s, H-30), 0.85 (3H, s, H-24), 0.81 (3H, s, H-26): for  $^{13}\text{C}$  NMR (150 MHz,  $\text{CD}_3\text{OD}$ ), see **Table 5**: HR-EI-MS *m/z* 513.3581 [M - H] $^-$ .

11-oxo-maslinic acid (*2 $\alpha$* , *3 $\beta$* -dihydroxy-11-oxo-18 $\beta$ -olean-12-en-28-oic acid, **4**); Yellowish amorphous powder:  $[\alpha]^{26}_D +49.2$  (*c* 1.0, MeOH):  $^1\text{H}$ -NMR (600 MHz,  $\text{CD}_3\text{OD}$ )  $\delta_{\text{H}}$  5.55 (1H, s, H-12), 3.66 (1H, ddd, *J* = 4.2, 10.2, 10.2 Hz, H-2 $\beta$ ), 3.08 (1H, dd, *J* = 4.2, 12.6 Hz, H-1), 3.00 (1H, dd, *J* = 4.2, 13.8 Hz, H-18), 2.92 (1H, d, *J* = 9.6 Hz, H-3 $\alpha$ ), 2.48 (1H, s, H-9), 2.14 (1H, ddd, *J* = 4.2, 13.4, 13.4 Hz, H-25), 1.41 (3H,

s, H-27), 1.17 (3H, s, H-25), 1.02 (3H, s, H-23), 0.98 (3H, s, H-26), 0.96 (3H, s, H-30), 0.95 (3H, s, H-29) 0.84 (1H, dd, J = Hz, H-5), 0.82 (3H, s, H-24):  $^{13}\text{C}$ -NMR (150 MHz,  $\text{CD}_3\text{OD}$ ), see **Table 5**: HR-ESI-MS  $m/z$  485.3356  $[\text{M} - \text{H}]^-$ .

Camaldulenic acid ( $2\alpha$ ,  $3\beta$ -dihydroxy- $18\beta$ -olean-11,  $13$ -dien-28-oic acid, **6**); Colorless needles:  $[\alpha]^{26}_{\text{D}} -68.0$  ( $c$  1.0,  $\text{CHCl}_3$ ):  $^1\text{H}$ -NMR (600 MHz,  $\text{CD}_3\text{OD}$ )  $\delta_{\text{H}}$  5.61 (1H, s, H-12), 3.68 (1H, ddd, J = 11.4, 10.2, 4.6 Hz, H- $2\beta$ ), 2.19 (1H, d, J = 4.2, 12.0 Hz, H-1), 2.92 (1H, d, J = 9.6 Hz, H- $3\alpha$ ), 2.50 (1H, s, H-9), 0.99 (1H, s H-25), 0.92 (3H, s, H-27), 1.02 (3H, s, H-23), 1.01 (3H, s, H-26), 0.93 (3H, s, H-30), 0.90 (3H, s, H-29), 0.84 (1H, dd, J = Hz, H-5), 0.83 (3H, s, H-24):  $^{13}\text{C}$ -NMR (150 MHz,  $\text{CD}_3\text{OD}$ ), see **Table 5**: HR-EI-MS  $m/z$  470.3395  $[\text{M}]^+$ .

Luteolin ( $3',4',5,7$ -tetrahydroxyflavone) **7**; Yellow amorphous powder:  $[\alpha]^{26} +0$  ( $c$  1.0, MeOH):  $^1\text{H}$  NMR (600 MHz,  $\text{CD}_3\text{OD}$ )  $\delta_{\text{H}}$  7.38 (1H, dd, J=2.4, 8.4 Hz, H- $6'$ ), 7.37 (1H, d, J=2.4 Hz, H- $2'$ ), 6.90 (1H, d, J=8.4 Hz, H- $5'$ ), 6.54 (1H, s, H-3), 6.44 (1H, d, J=2.4 Hz, H-8), 6.21 (1H, d, J=2.4 Hz, H-6):  $^{13}\text{C}$  NMR (150 MHz,  $\text{CD}_3\text{OD}$ )  $\delta_{\text{C}}$  183.9 (C, C-4), 166.4 (C, C-7), 166.1 (C, C-5), 163.3 (C, C-2), 159.5 (C, C-9), 151.0 (C, C- $4'$ ), 147.1 (C, C- $3'$ ), 123.8 (C, C- $1'$ ), 120.3 (CH, C- $6'$ ), 116.8 (CH, C- $5'$ ), 114.2 (CH, C- $2'$ ), 105.4 (C, C-10), 103.9 (CH, C-3), 100.2 (CH, C-6), 95.0 (CH, C-8): HR-ESI-MS  $m/z$  285.0418  $m/z$   $[\text{M}-\text{H}]^-$ .

Hydroxytyrosol acetate ( $2$ -( $3,4$ -dihydroxyphenyl) ethyl acetate) **8**; Slight yellow amorphous solid:  $[\alpha]^{25} +0$  ( $c$  1.0,  $\text{CHCl}_3$ ):  $^1\text{H}$  NMR (600 MHz,  $\text{CDCl}_3$ )  $\delta_{\text{H}}$  6.7 (3H, m, Phenyl), 4.20 (2H, t, H- $2'$ ), 2.81 (2H, t, H- $1'$ ), 2.03 (3H, s,  $\text{OCH}_3$ ): for  $^{13}\text{C}$  NMR (150

MHz, CDCl<sub>3</sub>) δ<sub>c</sub> 171.7 (C, C=OCH<sub>3</sub>), 143.7 (C, C-3), 142.4 (C, C-4), 130.5 (CH, C-5), 121.2 (CH, C-6), 115.9 (C, C-1), 115.4 (CH, C-2), 65.3 (CH, C-2'), 34.3 (CH, C-1'), 21.0 (CH, COCH<sub>3</sub>): HR-ESI-MS *m/z* 195.0674 [M-H]<sup>-</sup>.

*1-acetoxypinoresinol* ([1*S*,4*S*,5*R*,8*R*)-4,8-bis(4-hydroxy-3-methoxy-phenyl)-3,7-dioxabicyclo [3.3.0] oct-1-yl] acetate **9**; amorphous powder: [α]<sup>25</sup> +29 (c 3.0, MeOH): <sup>1</sup>H NMR (600 MHz, CD<sub>3</sub>OD) δ<sub>H</sub> 1.68 (3H, s, OCOCH<sub>3</sub>), 3.87 (6H, s, Phenyl-OCH<sub>3</sub>), 6.74 – 7.02 (6H, m, Aromatic-H): <sup>13</sup>C NMR (150 MHz, CD<sub>3</sub>OD), see **Table 6**. HR-ESI-MS at 417.1472 *m/z* [M+H]<sup>+</sup>.

*Hydroxytyrosol* (3,4-dihydroxyphenylethanol) **10**; Yellowish liquid: <sup>1</sup>H NMR (600 MHz, CD<sub>3</sub>OD) δ<sub>H</sub> 6.66 (d, H-4), 6.52 (dd, *J*=1.8, 8.1 Hz, H-8), 3.67 (m, H-1), 2.66 (t, H-2): for <sup>13</sup>C NMR (150 MHz, CD<sub>3</sub>OD); the spectrum showed signals at δ 63.9 and 39.6 in the region of aliphatic carbons corresponding to the C-2' and C-1' carbons, respectively, it also showed signals at δ<sub>c</sub> 145.2, 143.9, 131.3, 120.6, 116.4, and 115.7 in the region of aromatic carbons, corresponding to the carbons C-2, C-1, C-4, C-5, C-6, and C-3 of the benzene ring (δ<sub>c</sub> 145.2 (CH, C-2), 143.9 (C, C-1), 131.3 (C, C-4), 120.6 (CH, C-5), 116.4 (CH, C-6) and 115.7 (C, C-3)): HR-ESI-MS *m/z* 153.0577 [M-H]<sup>-</sup>.

*β-sitosterol*, **1**; White waxy powder: <sup>1</sup>H-NMR (600 MHz, CDCl<sub>3</sub>) δ<sub>H</sub>: 5.36 (1H, m, H-6), 5.33 (1H, m, H-23), 2.27 (1H, m, H-20), 1.82 (5H, m), 3.66 (1H, m, H-3), 1.12, 1.00, 0.99, 0.92, 0.90, 0.83 (each 3H, s, CH<sub>3</sub>), 0.93 (6H, s, 2 × CH<sub>3</sub>). <sup>13</sup>C-NMR (150

MHz, CDCl<sub>3</sub>) δ<sub>c</sub>: 140.8 (C-5), 121.8 (C-6), 71.9 (C-3), 36.6 (C-10), 32.0 (C-8), 42.3 (C-4), 12.1 (C-18), 42.4 (C-13), 34.0 (C-22), 56.8 (C-14), 50.2 (C-9), 29.2 (C-16), 20.0 (C-11), 19.1 (C-19), 11.9 (C-29), 31.7 (C-2), 18.9 (C-21), 24.4 (C-15), 23.1 (C-28), 39.9 (C-12), 56.1 (C-17), 36.2 (C-20), 19.1 (C-26), 19.1 (C-27), 29.2 (C-25), 37.3 (C-1), 45.9 (C-24), 32.1 (C-7), 26.2 (C-23). HR-EI-MS *m/z* 413 [M-H]<sup>-</sup>.

**Table 5:  $^{13}\text{C}$  NMR data for the isolated triterpene compounds 2, 3, 4, and 6**

<b>Carbon</b>	<b>2<sup>a</sup></b>	<b>3<sup>a</sup></b>	<b>4<sup>a</sup></b>	<b>6<sup>a</sup></b>
1	48.9	45.1	47.2	47.8
2	68.3	74.0	69.2	69.6
3	83.2	81.0	84.2	84.6
4	39.2	40.9	40.6	39.0
5	55.2	56.5	56.2	56.4
6	18.3	20.8	18.7	19.6
7	33.0	33.6	32.9	34.3
8	39.0	39.3	45.1	40.6
9	47.4	39.5	63.0	55.8
10	38.1	55.1	39.4	37.3
11	23.7	24.6	202.7	127.2
12	122.3	123.4	128.3	126.5
13	143.9	145.3	172.9	136.5
14	41.7	45.0	46.5	41.9
15	27.4	28.0	28.9	26.4
16	23.5	23.8	23.9	41.6
17	47.5	47.2	47.2	++
18	41.0	42.7	43.4	131.0
19	46.3	47.7	45.6	38.4
20	30.7	30.8	31.7	43.3
21	33.1	34.9	34.8	33.6
22	33.0	33.6	34.0	30.7
23	28.5	28.8	29.3	29.0
24	16.5	17.4	17.5	17.0
25	16.7	17.1	18.0	19.7
26	18.2	16.9	19.9	17.0
27	25.9	26.4	24.0	24.8
28	181.0	181.8	181.0	181.5
29	33.0	33.6	33.2	23.8
30	23.5	23.8	23.8	33.0
<u>COCH<sub>3</sub></u>	–	173.3		47.8
<u>COCH<sub>3</sub></u>		20.8		

The values of chemical shifts are in ppm, **a** –  $^{13}\text{C}$ -NMR measured in Chloroform-*d*

( $\text{CDCl}_3$ ), ++ Superimposed with solvent signals

**Table 6:  $^{13}\text{C}$  NMR data for 1-acetoxypinoresinol **9****

Position	<b>9</b> <sup>a</sup>	Reference <sup>b</sup>
C-1	98.8	96.9
C-5	60.2	58.2
C-4	71.1	69.3
C-8	75.9	73.9
C-2	88.8	86.3
C-6	86.9	84.6
C-1'	129.5	127.6
C-1''	133.0	131.2
C-2'	113.9	113.0
C-2''	111.3	110.7
C-3'	147.6	146.9
C-3''	148.6	147.6
C-4'	147.6	146.4
C-4''	147.9	146.4
C-5'	115.8	114.8
C-5''	116.2	115.3
C-6'	122.8	121.3
C-6''	120.4	118.9
OCH <sub>3</sub>	56.5	55.7
<u>CH</u> <sub>3</sub> CO	20.9	20.5
CH <sub>3</sub> <u>C</u> O	171.3	168.7

The values of chemical shifts are in ppm, **a** –  $^{13}\text{C}$ -NMR measured in Methanol- $d_4$  (CD<sub>3</sub>OD), **b** –  $^{13}\text{C}$ -NMR measured in Dimethylsulfoxide- $d_6$  (DMSO)

## **Anti-allergic activity**

The investigation on the anti-allergic activities of the isolated metabolites (polyphenolic and triterpenoid compounds) from OMW was done through evaluation of their ability to inhibit RBL-2H3 cells' degranulation, and to reduce the elevation of  $[Ca^{2+}]_i$  evoked by two complementary stimuli: the calcium ionophore (A23187; simulation of events preceding degranulation) and DNP-BSA (whereby anti-DNP IgE is used; simulation of IgE dependent allergic response), and their effect on the expression of calcium channel proteins, both  $Ca^{2+}$ -influx related proteins; STIM1, Orai1, and TRPC1, and ER membrane protein; IP3R. A set of these experiments was made to assist the characterization of their mechanisms. The cell line used in this study is RBL-2H3 cells, which are rat basophilic cell line known for expressing high-affinity IgE receptors (FcεRI) – making it a perfect model to study allergy<sup>155</sup>.

### **2.3.3. Effect of the Isolated Compounds on RBL-2H3 cells' degranulation**

The ability to reduce RBL-2H3 cells' degranulation evoked by the calcium ionophore A23187 (10  $\mu$ M, 60 min exposure) by the isolated OMW compounds was evaluated by an assay as summarized in **Figure 6(A)**. Before the examination of compounds' ability to inhibit degranulation, their cytotoxic effect on RBL-2H3 cells was examined. Since two classes of compounds were isolated in this study, pentacyclic triterpenes and polyphenolic compounds, their examination were compared among themselves. With particular interest, it was found that, generally, the pentacyclic triterpenes were more toxic to the cell (cytotoxic) and less active in degranulation inhibition as



compared to their counterpart class – polyphenolic compounds. In this sub-section, a detailed one-by-one analysis of the isolated compounds has been discussed.

Beginning with the pentacyclic triterpenes (and a phytosterol), it was found that with exception to 11-oxomaslinic acid **4**, the rest of the compounds,  $\beta$ -sitosterol **1**, maslinic acid **2**, 2-O-acetylmasic acid **3** and camaldulenic acid **6** significantly affected the cell viability at as low concentration as 10  $\mu\text{g/ml}$  ( $p < 0.05$ ,  $n=3$ ), for instance,  $\beta$ -sitosterol **1** following the MTT assay (**Figure 9**, white bars). Taking account of all triterpenic compounds at 50  $\mu\text{g/ml}$ , the percentage of viable cells in each was as follows; maslinic acid **2** ( $76.9 \pm 5.4\%$ ,  $p < 0.05$ ), 2-O-acetylmasic acid **3** ( $65.3 \pm 12.5\%$ ,  $p < 0.05$ ), 11-oxomaslinic acid **4** ( $96.5 \pm 4.6\%$ ,  $p > 0.05$ ), and camaldulenic acid **6** ( $62.4 \pm 8.4\%$ ,  $p < 0.05$ ). Based on these results, 2-O-acetylmasic acid and camaldulenic acid were the most toxic to the cells. These results were consistent even after calculating their  $\text{CC}_{50}$  values. For instance, camaldulenic acid was found to have the lowest  $\text{CC}_{50}$  value of all compounds – which means it was the most toxic ( $\text{CC}_{50} = 59.1 \pm 6.5 \mu\text{g/ml}$ ) (**Table 7**).

Their antiallergic activities, based on degranulation ( $\beta$ -hexosaminidase release) assay, were either very low or could not be calculated at all due to toxicity issues. Again, 11-oxomaslinic acid came out as an exception – it was the only active one ( $\text{IC}_{50} = 14.8 \pm 1.4 \mu\text{g/ml}$  eq. to  $31.0 \mu\text{M}$ ) (**Table 7**). Some other triterpenes and a phytosterol inhibited degranulation significantly at various concentrations ( $p < 0.05$ ,  $n=3$ ) as shown in **Figure 9**. However, the exact values for their  $\text{IC}_{50}$  could not be

determined for two major reasons; one, due to their higher toxicities (as for the triterpenes maslinic acid **2**, 2-O-acetylmalinic acid **3** and camaldulenic acid **6**), or the 50%-inhibition could not be obtained as it was too inactive (as for a phytosterol,  $\beta$ -sitosterol). The results for their antiallergic activities are displayed in **Table 7**.

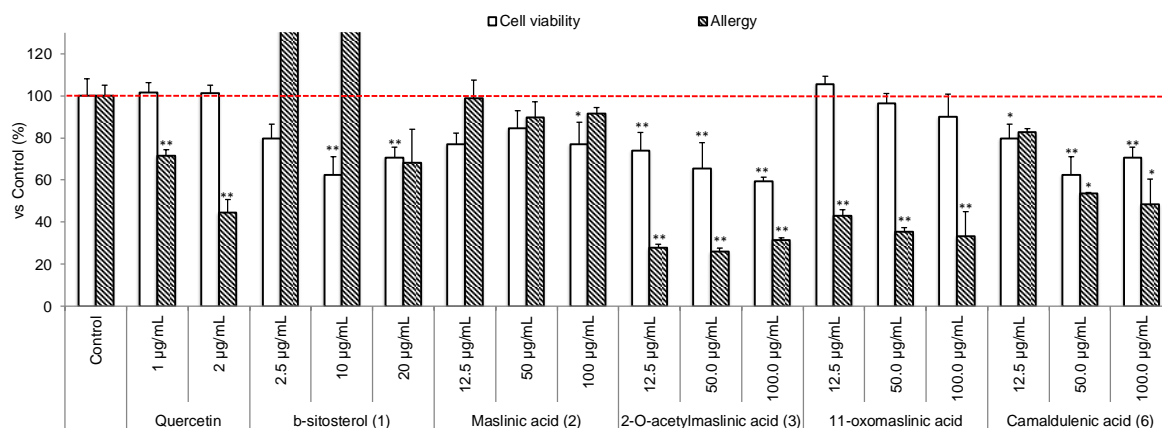


Figure 9: Inhibitory effects of tested phytosterol (1) and triterpenic compounds on RBL-2H3 cells' degranulation. Effect on RBL-2H3 cells' degranulation/ anti-allergic activity of the compounds (bars with black diagonal lines), which was tested by measuring the amount of  $\beta$ -hexosaminidase released after treatment by calcium ionophore (A23187). Cytotoxicity of the compounds is presented with white bars. The experiments were done in triplicates  $n=3$ , where: \*  $p<0.05$ , \*\*  $p<0.01$  paired t-test with respect to control (10  $\mu$ M A23187).

For the polyphenolic compounds (new HDOA **5**, Camaldulenic acid **6**, Luteolin **7**, Hydroxytyrosol acetate **8**, 1-acetoxypinoresinol **9**, Hydroxytyrosol **10**), it was found that three of them didn't significantly affect the cell viability at a wide range of concentration, up to 250 µg/ml ( $p>0.05$ ,  $n=3$ ); while, one compound (1-acetoxypinoresinol **9**) exhibited a significant reduction in cell viability ( $p<0.05$ ,  $n=3$ ) at its maximum tested concentration (50 µg/ml), as assessed by MTT reduction assay (**Figure 10(A)**, white bars). Nevertheless, its toxicity was still regarded as 'limited' because it killed less than 20% of the cells; a percentage of viable cells was  $87.4\pm 0.4\%$ .

To investigate their effect on degranulation,  $\beta$ -hexosaminidase release in their presence or absence was measured, but to be sure that the compounds affect only on degranulation, their inhibitory effect on  $\beta$ -hexosaminidase enzymatic activity was investigated, as summarized in **Figure 6(B)**, and it was observed that all compounds, tested individually, had no significant effect on enzyme inhibition ( $p>0.05$ ,  $n=3$ ) (**Figure 10(B)**). Therefore, each compound reduced degranulation (release of  $\beta$ -hexosaminidase) from RBL-2H3 cells but did not inhibit the activity of the  $\beta$ -hexosaminidase enzyme.

The comprehensive anti-allergic activity of all isolated compounds from OMW is shown in **Table 7**. The anti-allergic activities are expressed as  $IC_{50}$ , while cytotoxicity activities expressed as  $CC_{50}$ .

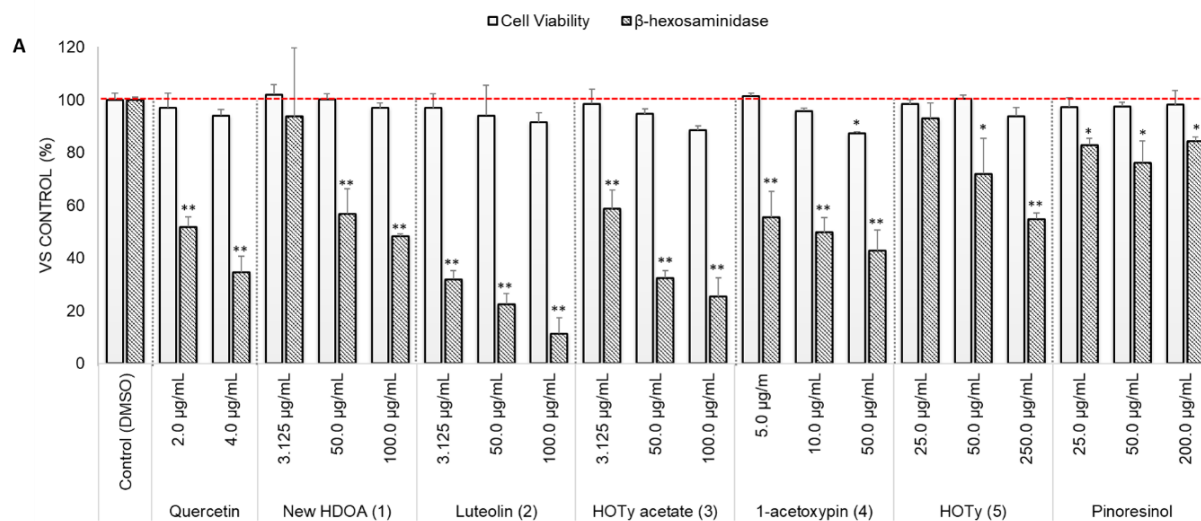
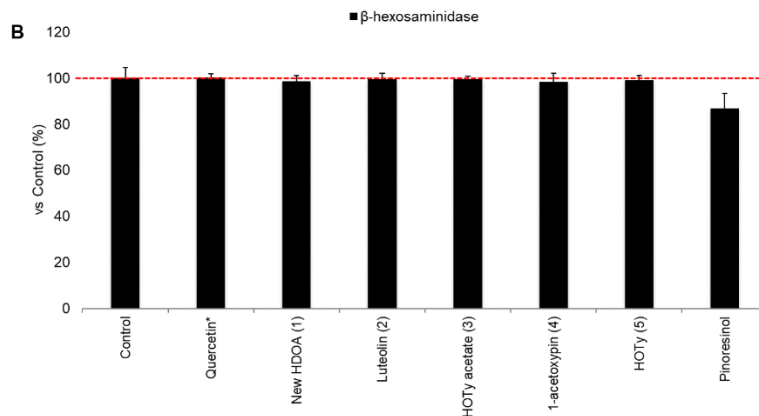


Figure 10: Inhibitory effects of tested polyphenolic compounds on RBL-2H3 cells' degranulation, and on  $\beta$ -hexosaminidase enzymatic activity. (A) Effect on RBL-2H3 cells' degranulation/ anti-allergic activity (bars with black diagonal lines), which was tested by measuring the amount of  $\beta$ -hexosaminidase release. Cytotoxicity of the compounds is presented with white bars. The experiments were done in triplicates  $n=3$ , where: \*  $p<0.05$ , \*\*  $p<0.01$  paired t-test with respect to control (10  $\mu$ M A23187). HOTy is hydroxytyrosol 10 and 1-acetoxypin is 1-acetoxypinoresinol 9.



**Figure 10 (B)** Inhibitory effect of the compounds on  $\beta$ -hexosaminidase enzymatic activity; in which the release of  $\beta$ -hexosaminidase enzyme from RBL-2H3 cells was stimulated by A23187, and then, enzyme-rich supernatant was treated with the compounds to see if they have any direct inhibitory effect on the enzyme. The experiments were done in triplicates  $n=3$ , where: Significance was measured by paired t-test with respect to control (10  $\mu$ M A23187). HOTy is hydroxytyrosol **10** and 1-acetoxypin is 1-acetoxypinoresinol **9**.

**Table 7: The anti-allergic activity (IC<sub>50</sub>) and cytotoxicity (CC<sub>50</sub>) of isolated compounds from OMW**

<b>Compound</b>	<b>IC<sub>50</sub> (µg/ml) [µM]</b>	<b>CC<sub>50</sub> (µg/ml) [µM]</b>
<i>β</i> -sitosterol <b>1</b>	>100 [>200]	>100 [>200]
Maslinic acid <b>2</b>	ND <sup>Tox</sup>	>100 [>200]
2- <i>O</i> -acetylmasic acid <b>3</b>	ND <sup>Tox</sup>	>100 [>200]
11-oxomaslinic acid <b>4</b>	14.8±1.4 [31.0]	>100 [>200]
New HDOA <b>5</b>	42.7±1.5 [108.3]	>100 [>250]
Camaldulenic acid <b>6</b>	ND <sup>Tox</sup>	59.1±6.5 [125]
Luteolin <b>7</b>	1.16±0.2 [3.9]	>100 [>350]
Hydroxytyrosol acetate <b>8</b>	7.9±1.4 [40.2]	>100 [>500]
1-acetoxypinoresinol <b>9</b>	18.2±5.8 [43.8]	>100 [>240]
Hydroxytyrosol <b>10</b>	>250 [>1620]	>250 [>1620]
Pinoresinol	>200 [>550]	>200 [>550]
Quercetin <sup>s</sup>	2.1±0.1 [6.6]	>50 [>150]

The results are expressed as Mean ± SD (*n*=3). <sup>s</sup> standard drug and ND<sup>Tox</sup> could not be determined because the exact value of IC<sub>50</sub> could not be calculated due to the higher toxicity of the respective compound to RBL-2H3 cells. Anti-allergic assay was based on A23187-induced degranulation of the basophil (RBL-2H3) cells.

**Table 8: The enzyme inhibitory effect, anti-allergic activity (IC<sub>50</sub>) and the total activities of the active isolated compounds from OMW**

Compound	Enzyme inhibition (%) <sup>a</sup>	IC <sub>50</sub> (µg/ml) [µM]	Amount (mg/kg) <sup>b</sup>	Total activity <sup>c</sup>
11-oxomaslinic acid <b>4</b>	1.49±2.1	42.7±1.5 [108.3]	0.30	7.0
New HDOA <b>5</b>	1.49±2.1	42.7±1.5 [108.3]	0.30	7.0
Luteolin <b>7</b>	0.46±2.0	1.16±0.2 [3.9]	2.67	2264.5
Hydroxytyrosol acetate <b>8</b>	0.23±1.5	7.9±1.4 [40.2]	13.34	1688.6
1-acetoxypinoresinol <b>9</b>	1.66±3.07	18.2±5.8 [43.8]	1.72	94.6
Hydroxytyrosol <b>10</b>	0.93±3.1	>250 [>1620]	89.56	ND
Quercetin <sup>s</sup>	0.26±1.3	2.1±0.1 [6.6]	–	–

The results are expressed as Mean ± SD (*n*=3). <sup>a</sup> Values indicate enzyme inhibition (%) against β-hexosaminidase at the following sample concentrations (close to their IC<sub>50</sub>): new HDOA, 50 µg/ml; luteolin, 1.5 µg/ml; hydroxytyrosol acetate, 10 µg/ml; 1-acetoxypinoresinol, 20 µg/ml; hydroxytyrosol, 250 µg/ml and pinoresinol, 200 µg/ml.

<sup>b</sup> The amount of each compound as quantified by HPLC; <sup>c</sup> Total activity was estimated using the following formula: total activity = amount (mg/kg)/IC<sub>50</sub> (mg/ml);

<sup>s</sup> standard drug, and ND could not be determined because the exact value of IC<sub>50</sub> could not be calculated.



In the degranulation assay, luteolin **7** (3.125 µg/ml), hydroxytyrosol acetate **3** (3.125 µg/ml) and 1-acetoxypinoresinol **4** (5.0 µg/ml) were able to significantly reduce degranulation by 68.1±3.2%, 41.4±7.3% and 44.6±9.9% respectively ( $p < 0.01$ ,  $n=3$ ; **Figure 10(A)**, bars with black diagonal lines). On the other hand, at their low concentrations, new HDOA **5** (3.125 µg/ml) and hydroxytyrosol **10** at 25 µg/ml did not reduce degranulation significantly ( $p > 0.05$ ,  $n=3$ ), while pinoresinol showed a reduction of degranulation at significance level  $p < 0.05$  (not  $p < 0.01$ ). Overall dose-inhibition response results (and after calculation of their  $IC_{50}$  values), showed that pinoresinol and hydroxytyrosol **10** had a weaker effect on reduction of degranulation (both of them with  $IC_{50}$  values  $> 500$  µM) compared to new HDOA **5** which had relatively good activity ( $IC_{50} = 108.3$  µM).

Finally, the total anti-allergic activities of the isolated compounds were compared (**Table 7**). Among all compounds, regardless of its relatively low abundance in OMW, luteolin still showed the highest total activity (**Table 8**), because of its low  $IC_{50}$ . As opposed to hydroxytyrosol, even though it was the most abundant metabolite, its total activity is estimated to be very low, although the exact figure could not be calculated, because of its high  $IC_{50}$  ( $> 250$  µg/ml).

New HDOA **5** is a 3,4-DHPEA (3,4-dihydroxyphenylethyl acetate) joined to a decarboxymethylated elenolic acid (EA) derivative. Taking into consideration of weak anti-allergic activity of hydroxytyrosol (3,4-DHPE),  $IC_{50} > 1000$  µM, and based on results from the previous report that even EA itself had weaker anti-allergic

activity ( $IC_{50} > 1000 \mu M$ )<sup>156</sup>, these findings strongly supports the hypothesis that the ester linkage of the two molecules (3,4-DHPEA and EA derivative) enhances its anti-allergic activity. Luteolin **7** showed the highest anti-allergic activity ( $IC_{50}=3.9 \mu M$ ) followed by hydroxytyrosol acetate **8** ( $IC_{50}=40.2 \mu M$ ) and 1-acetoxypinoresinol **9** ( $IC_{50}=43.8 \mu M$ ). On the other hand, the activity of hydroxytyrosol **5** and pinoresinol were weak ( $IC_{50}>550$  and  $>1620 \mu M$ , respectively), while that of new HDOA **5** was relatively good ( $IC_{50} =108 \mu M$ ). While the anti-allergic activities of luteolin **7** and hydroxytyrosol **10** were consistent with those of the reported elsewhere<sup>124,156</sup>, this is the first report on anti-allergic activity for new HDOA **5**, hydroxytyrosol acetate **8**, 1-acetoxypinoresinol **9** and pinoresinol.

Taking into account the difference in anti-allergic activities between hydroxytyrosol acetate **8** and hydroxytyrosol **10** ( $IC_{50}=40.2$  vs  $>1620 \mu M$ , respectively), these results strongly suggest that esterification by acetyl group in hydroxytyrosol acetate **8**, markedly increases potency towards anti-allergic effect by several folds. A similar observation was made for the case of 1-acetoxypinoresinol **9** vs pinoresinol ( $IC_{50}=43.2$  vs  $>550 \mu M$ , respectively). Again, it appears that esterification of the furofuran ring at position one (C-1) of 1-acetoxypinoresinol **9** enhances its anti-allergic activity. Based on these observations, they strongly support the hypothesis that ester linkage in the two compounds (**8** and **9**) enhances their anti-allergic activities, as previously proposed to other metabolites such as oleuropein aglycone

124.

Regarding SAR for flavonoids, the following key features are important: 1) the C-2/C-3 double bond of flavones and flavonols, 2) as the number of the hydroxyls at the C-5, C-6, C-7 of ring A and C-3', and C-4' of ring B positions increased in number, so does the activity, 3) the glycoside linkage markedly reduced the activity <sup>124,157</sup>. Both luteolin **7** and quercetin have similar structures, with all mentioned favorable structural features, making them one of the most potent anti-allergic flavonoids (IC<sub>50</sub> values 3.9 μM and 6.6 μM, respectively).

#### **2.3.4. Effect of the Isolated Compounds on Free Intracellular Ca<sup>2+</sup> Concentration, and the Expression of Ca<sup>2+</sup> Channel Proteins**

The examination of free intracellular Ca<sup>2+</sup> concentration and expression of Ca<sup>2+</sup> channel proteins in RBL-2H3 cells was done to clarify the possible mechanisms underlying the inhibitory effects of the compounds on degranulation. Briefly, cross-linking of Ag-specific IgE with newly absorbed allergens leads to a cascade of events including mobilization of Ca<sup>2+</sup> and activation of signal transduction pathways resulting into Ca<sup>2+</sup> release from the endoplasmic reticulum (ER) and influxes from extracellular space *via* store-operated Ca<sup>2+</sup> channels (SOC) or famously known as 'calcium release-activated calcium (CRAC)' channels <sup>125</sup>. This leads to an overall elevation of intracellular free Ca<sup>2+</sup> levels [Ca<sup>2+</sup>]<sub>i</sub>, which in turn plays an essential role in the degranulation process <sup>122,125,158,159</sup>.

This means that Ca<sup>2+</sup> is an essential cofactor for degranulation as it is required to regulate the granule-plasma membrane fusion and the release of mediators <sup>119</sup>. Thus,

metabolites that are capable of reducing the elevation of  $[Ca^{2+}]_i$  are potential anti-allergic. Since, generally, the polyphenolic compounds were more active than the triterpenic (and phytosterol) compounds, the study to investigate the underlying mechanisms of anti-allergic was conducted on the polyphenols only.

Fluo-4 AM (Dojindo Laboratories, Kumamoto, Japan) - a fluorescent  $Ca^{2+}$  indicator, was used to determine the free intracellular  $Ca^{2+}$  concentrations ( $[Ca^{2+}]_i$ ). The expression of  $Ca^{2+}$ -influx related proteins including stromal interaction molecule 1 (STIM1),  $Ca^{2+}$  release-activated calcium channel protein 1 (Orai1), transient receptor potential channel 1 (TRPC1), and inositol-1, 4, 5-triphosphate receptor (IP3R) were further investigated by qRT-PCR analysis. Regarding  $[Ca^{2+}]_i$ , results showed that the increased levels of intracellular  $Ca^{2+}$  after A23187 or DNP-BSA challenge at 20 seconds in the untreated cells (control), was significantly reduced after treatment with anti-allergic active compounds **5**, **7**, **8** and **9** ( $p < 0.05$ ) (**Figure 11**).

Luteolin **7** decreased  $[Ca^{2+}]_i$  significantly after challenging by A23187 suggesting that, it acts mainly by blocking the extracellular  $Ca^{2+}$  influx. Several mechanisms can be proposed, including could be the distribution of some steps in the cascade of CRAC channels activation by binding to proteins and interfering with protein-protein interactions and/or oligomerization or possible reduction of the expression of  $Ca^{2+}$  influx related protein. Even though previous research showed that luteolin inhibited the IgE-evoked degranulation<sup>124</sup>, this suggests that its main mechanism involves attenuation of  $Ca^{2+}$  levels elevation by blocking the extracellular  $Ca^{2+}$  influx.

Hydroxytyrosol acetate **8** and 1-acetoxypinoresinol **9** were found to significantly reduce the increased levels of  $[Ca^{2+}]_i$  after challenging by both A23187 and DNP-BSA (**Figure 11 (A and B)**), suggesting that their mechanisms for anti-allergic activity are beyond just blocking extracellular  $Ca^{2+}$  influx. The other mechanism could be due to inhibition of the cross-linking of high-affinity receptors for IgE, FcεRI receptors, which later interfere with the signaling pathways leading to upstream of  $[Ca^{2+}]_i$  increase <sup>133</sup>. While this is the first report for both hydroxytyrosol acetate **8** and 1-acetoxypinoresinol **9**, a similar mechanism has been previously described for oleuropein <sup>160</sup>. In fact, both hydroxytyrosol acetate **8** and oleuropein share a 3,4-dihydroxyphenylethyl acetate (3,4-DHPEA) core, and thus, these findings suggest that both **8** and oleuropein act through similar mechanisms of action, and that both C-3 and C-4 hydroxyls might be involved to modulate direct enzyme interaction via hydrogen bonds <sup>161</sup>. On the other hand, 1-acetoxypinoresinol **9** also has two hydroxyls, but not adjacent to each other (and two methoxyls), suggesting a similar mechanism as for hydroxytyrosol acetate **8**.

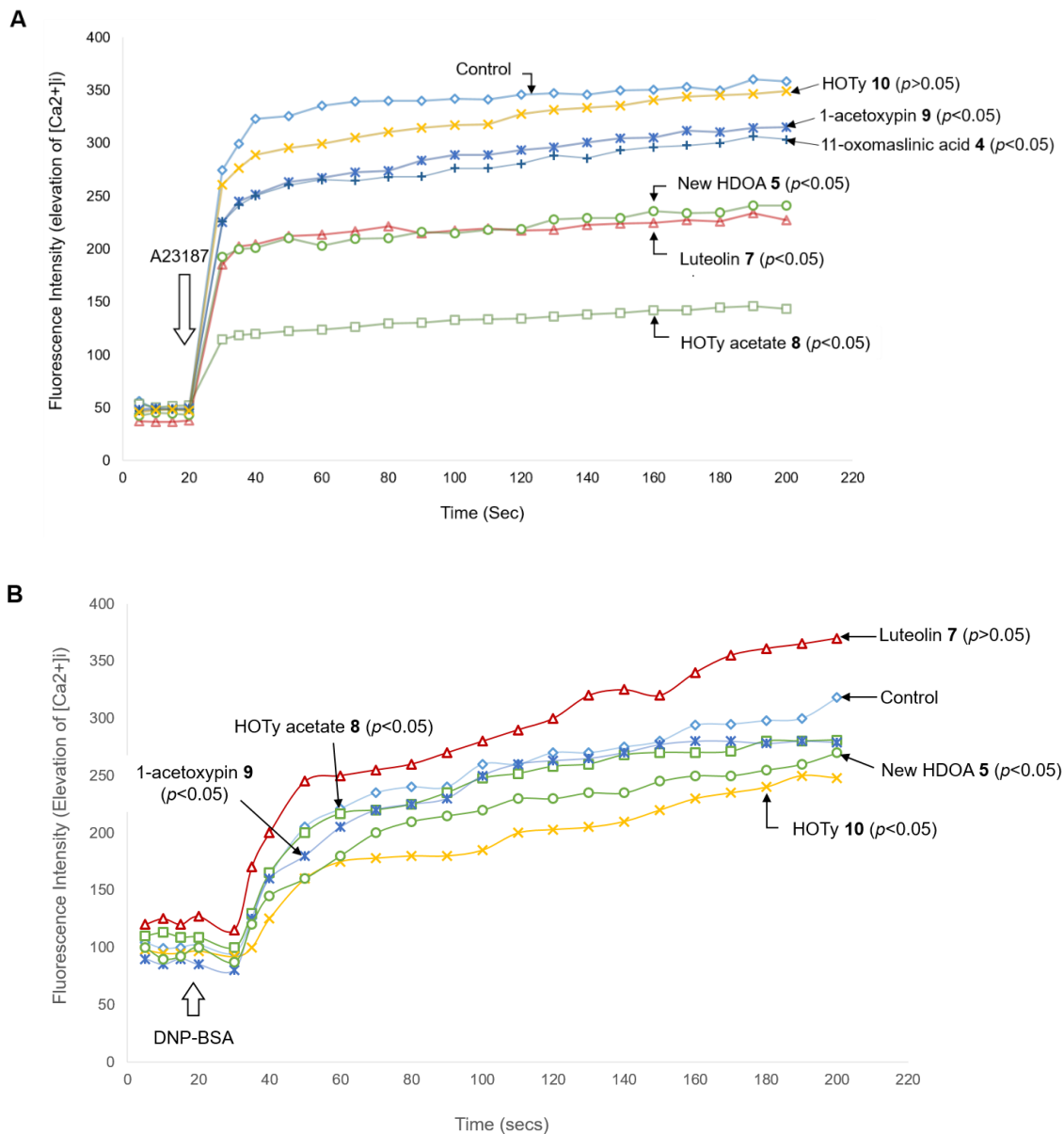


Figure 11: Effects of isolated Polyphenols on Ag-stimulated intracellular  $Ca^{2+}$  elevation in RBL-2H3 cells. (A) RBL-2H3 cells were treated without or with new HDOA, luteolin, HOTy acetate, 1-acetoxypin or HOTy for 60 min. Then, cells were stimulated without (for first 20 secs), then with A23187 (for 180 secs), during all this time intracellular  $Ca^{2+}$  levels were

measured. The arrow shows time at which A23187 was challenged. (B) IgE-sensitized RBL-2H3 cells were treated without or with new HDOA, luteolin, HOTy acetate, 1-acetoxypin or HOTy for 60 min. Then, cells were stimulated without (for first 20 secs), then with DNP-BSA (for 180 secs), during all this time intracellular  $Ca^{2+}$  levels were measured. Statistical significance differences (*p*-value) were determined relative to the control (only A23187 or DNP-BSA, without treatment with the compounds). Arrow: the time at which A23187 or DNP-BSA was challenged, light blue squares: control, green circles: new HDOA **5**, wine-red triangle: luteolin **7**, green squares: hydroxytyrosol acetate **8**, blue cross-marks: 1-acetoxypinoresinol **9** and yellow cross-marks: hydroxytyrosol **10**.

Surprisingly, regardless of its weak anti-allergic activity ( $IC_{50} > 1620 \mu M$ ), hydroxytyrosol **10** decreased  $[Ca^{2+}]_i$  levels after challenging by DNP-BSA. This suggests that hydroxytyrosol **10** might, at least partially, interact with IgE high affinity Fc $\epsilon$ RI as hydroxytyrosol acetate **8** does. This partial similarity in their mechanism of action could be due to the presence of a 3,4-dihydroxyphenylethyl (3,4-DHPE) core in both **8** and **10**. The 3,4-DHPE core, like the esterified form 3,4-DHPEA, has C-3 and C-4 hydroxyls which might be involved in the interaction with tyrosine kinase enzyme. However, its weak activity, **10**, has been correlated with a lack of ester linkage, which is present in the active counterpart, hydroxytyrosol acetate **8**. It is worth noting that, similar mechanism of inhibition of the cross-linking of Fc $\epsilon$ RI by hydroxytyrosol has been reported elsewhere <sup>160</sup>.

Based on qRT-PCR results, the expression levels of Orai1, STIM1, and TRPC1 were significantly decreased by new HDOA **5**, luteolin **7**, and quercetin (standard drug) ( $p < 0.05$ , **Figure 12 (B)**, **(C)**, and **(D)**). Moreover, there was no significant difference in the expression levels of IP3R mRNA, a receptor expressed on the ER membrane ( $p > 0.05$ , **Figure 12 (A)**), in the presence or absence of these compounds, indicating that they did not have had an effect on the depletion of ER  $Ca^{2+}$  store. These results suggest that they stabilize membrane by inhibiting the  $Ca^{2+}$  influx due to the lower expression of calcium channel proteins ( $Ca^{2+}$ -influx related proteins – Orai1, STIM1, and TRPC1). Generally, standard (quercetin) and luteolin **7** were found to act in a similar way, i.e, by reducing the expression levels of Orai1, STIM1 and TRPC1 but



not IP3R (**Figure 12(A)-(D)**). This may be related to the similarities in their chemical structures.

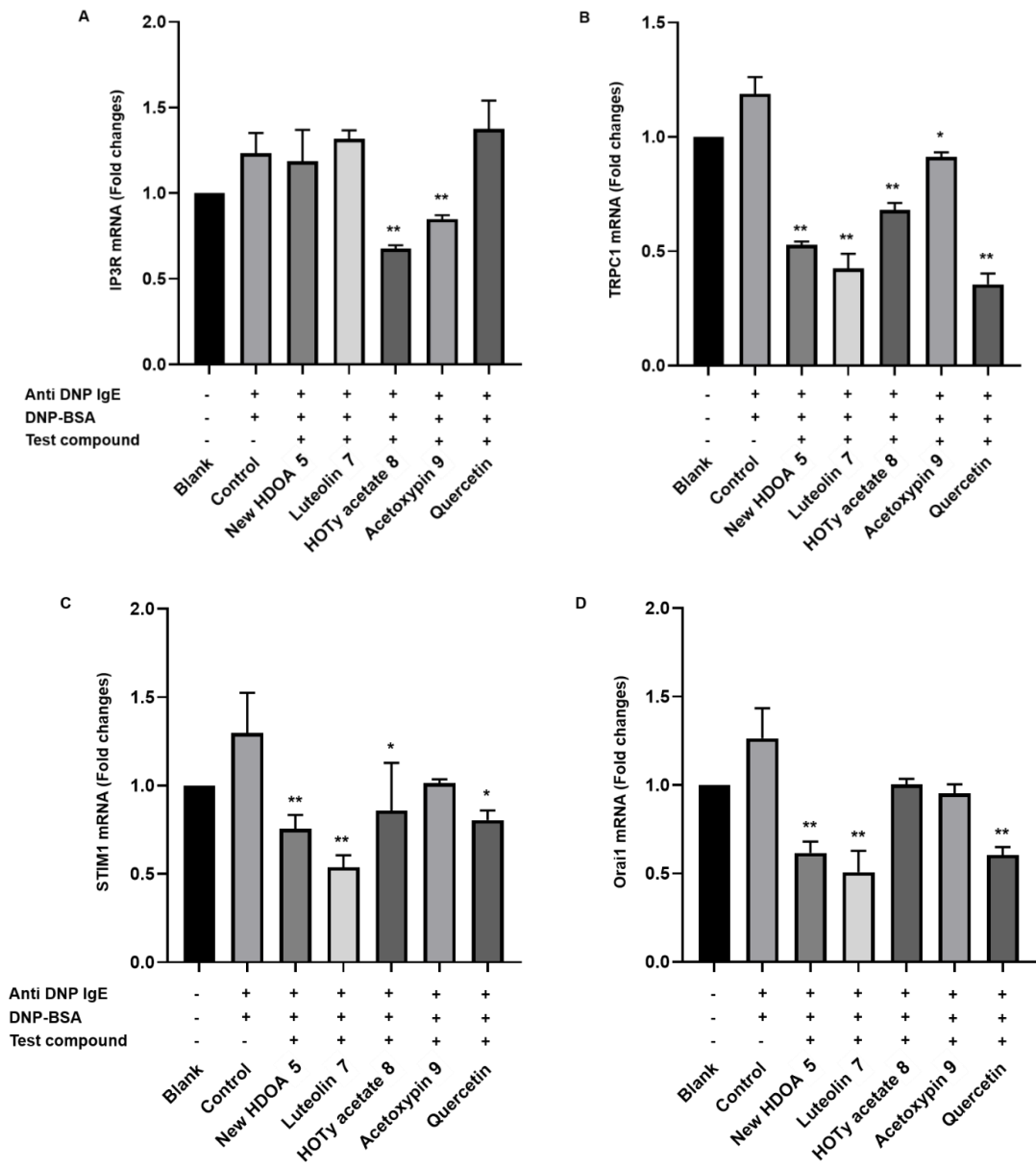


Figure 12: Effect of polyphenolic compounds on the expression of RBL-2H3 cells' calcium channel proteins. (A) The mRNA relative expression of IP3R, (B) The mRNA relative expression of TRPC1, (C) The mRNA relative expression of STIM1, and (D) The mRNA relative expression of Orai1. Where  $*p < 0.05$ ,  $**p < 0.001$  significantly different from control.

Hydroxytyrosol acetate **8**, significantly decreased the expression of STIM1 and TRPC1, but not Orai1, while 1-acetoxypinoresinol **9** decreased the expression of only TRPC1 ( $p < 0.05$ , **Figure 12(C)** and **(D)**). Intriguingly, both hydroxytyrosol acetate **8** and 1-acetoxypinoresinol **9** significantly reduced the expression of IP3R ( $p < 0.05$ , **Figure 12(A)**), indicating their effect on depletion of ER  $\text{Ca}^{2+}$  store. This is in line with  $[\text{Ca}]_i$  measurements, whereby results suggested that these compounds' mechanism is beyond just blocking extracellular  $\text{Ca}^{2+}$  influx. Thus, RT-PCT confirms the hypothesis that their mechanism of action goes beyond just blocking extracellular  $\text{Ca}^{2+}$  influx. Therefore, it is evident that cell uptake of these compounds may be higher, considering their lipophilicity, compared to compounds **5**, **7**, and quercetin - likely due to the presence of an ester linkage. A similar mechanism has been proposed for lipophilic compounds <sup>132</sup>.

It is known that crosslinking of antigen receptors activates the breakdown of phosphatidylinositol-4,5-bisphosphate to generate inositol-1,4,5-trisphosphate (IP3) and diacylglycerol, whereby IP3 binds its receptors, IP3R, located on the ER surface, and activates the release of  $\text{Ca}^{2+}$  in the cytoplasm. This event, known as 'store depletion', in turn, activates  $\text{Ca}^{2+}$ -influx related proteins – STIM1, Orai1, and TRPC1 – famously known as SOC or CRAC channels <sup>126</sup>. Thus, these results confirm that for compounds with presumably higher cell uptake like hydroxytyrosol acetate **8** and 1-acetoxypinoresinol **9** might be acting, firstly, by causing store depletion in ER (decreased expression of the IP3R); and secondly, to the  $\text{Ca}^{2+}$ -influx related proteins.

Generally, it was confirmed that all active polyphenolic compounds, new HDOA **5**, luteolin **7**, hydroxytyrosol acetate **8** and 1-acetoxypinoresinol **9**, act mainly as “mast cell stabilizers” by reducing mediator release <sup>162</sup>, through their inhibitory effect of extracellular Ca<sup>2+</sup> influx due to the lower expression of, two or more, calcium channel proteins. To my knowledge, this is the first study to address the anti-allergic activity of Olive lignans (pinoresinol and 1-acetoxypinoresinol), hydroxytyrosol acetate, and the new oleuropein aglycone (new HDOA), and their possible underlying mechanisms by which they reduce degranulation. While the other two (hydroxytyrosol and luteolin) have been previously reported, but their mechanism by which they reduce degranulation was not fully studied.

#### **Part IV: CONCLUSION**

In conclusion, as “stabilizers”, the isolated polyphenolic compounds reduce the release of allergic mediators by blocking extracellular  $\text{Ca}^{2+}$  influxes. Although the results are based on *in-vitro* assays, they give important preliminary data on the anti-allergic potential of OMW, especially through its polyphenolic constituents. This means that OMW can be regarded as an important source of lead compounds which might be used as ingredients in different anti-allergic formulations such as food supplements or functional foods, or for structural modification to improve and develop new anti-allergic drugs.

## Part V: CHAPTER SUMMARY

In this chapter, the isolation and anti-allergic activity (degranulation reduction) of six polyphenolic compounds, one of them being novel, from olive mill wastes (OMW) were reported. Additionally, their ability to reduce intracellular  $\text{Ca}^{2+}$  levels and expression of calcium channel proteins in RBL-2H3 cells were evaluated, to assist the possible characterization of the mechanisms involved. We found that only one pentacyclic triterpene and four polyphenolic compounds were active. The triterpene, 11-oxomaslinic acid **4** (31.0  $\mu\text{M}$ ), and the polyphenols, a novel compound, new hemialdehydic decarboxymethylated oleuropein aglycone, HDOA **5** ( $\text{IC}_{50}$ =108.3  $\mu\text{M}$ ), hydroxytyrosol acetate **8** ( $\text{IC}_{50}$ =40.2  $\mu\text{M}$ ) and 1-acetoxypinoresinol **9** ( $\text{IC}_{50}$ =43.8  $\mu\text{M}$ ) reduced intracellular  $\text{Ca}^{2+}$  levels after challenging by both A23187 and DNP-BSA, suggesting a mechanism beyond just blockage of extracellular  $\text{Ca}^{2+}$  influx. While luteolin **7**, despite its strongest activity ( $\text{IC}_{50}$ =3.9  $\mu\text{M}$ ), reduced  $\text{Ca}^{2+}$  levels only after challenging by A23187, suggesting its main mechanism is by blocking extracellular  $\text{Ca}^{2+}$  influx. The qRT-PCR analysis confirmed further that each compound decreased the expression of, two or more, calcium channel proteins suggesting that they act as 'mast cell stabilizers' by reducing the expression of calcium channel proteins. This work attracts more attention to OMW as a potential source of lead compounds for structural modification to improve and develop new anti-allergic drugs.

### **CHAPTER 3**

**Postprandial hyperglycemia lowering effect of the isolated compounds from olive mill wastes – an inhibitory activity and kinetics studies on  $\alpha$ -glucosidase and  $\alpha$ -amylase enzymes**

## **Part I: INTRODUCTION – DIABETES**

### **3.1.1. Diabetes Mellitus**

Diabetes mellitus (DM) is a chronic metabolic disease characterized by elevated blood glucose (persistent hyperglycemia) resulting from either, when the pancreas does not produce enough insulin, a hormone that regulates blood glucose (type 1), or when the body cannot effectively respond to the insulin it produces <sup>100</sup>. Type 2 (previously called non-insulin-dependent or adult-onset diabetes) results from the body's ineffective to respond to/ use insulin it produces. Type 2 is the commonest form that accounts for 90-95% of all diabetic cases <sup>102</sup>. Major diabetic symptoms include excessive urination and thirst, constant hunger, weight loss, vision changes, and fatigue. These symptoms are more prevalent in type 1, but often less marked or absent at all in type 2. That is why type 2 may go undiagnosed for many years until complications have already arisen <sup>102,163</sup>.

WHO lists DM among four priority noncommunicable diseases (NCDs) targeted for action as it causes global public health problem. Both the number of cases and the prevalence of diabetes have been steadily increasing over the past few decades; it was reported that 422 million people were affected by 2014 <sup>100</sup>, and it is projected to affect 552 million people by 2030 <sup>163</sup>. Postprandial hyperglycemia (PPHG) is an independent risk factor for the development of macrovascular complications <sup>164</sup>, which may lead into life-threatening complications such as cerebrovascular and



cardiovascular diseases <sup>165</sup>, thus, controlling PPHG is of vital importance to prevent diabetes and its complications <sup>166,167</sup>.

The rise of glucose levels in the blood, postprandially, is a result of carbohydrates hydrolysis, a process primarily catalyzed by the enzymes  $\alpha$ -glucosidase and  $\alpha$ -amylase <sup>168</sup>. In the process, salivary  $\alpha$ -amylase enzyme hydrolyzes carbohydrates to disaccharides and oligosaccharides which are then hydrolyzed further by the  $\alpha$ -glycosidase enzyme to monosaccharides such as glucose which is then absorbed through the small intestines into the blood, and the remaining oligosaccharides are hydrolyzed by the pancreatic  $\alpha$ -amylase to glucose and maltose <sup>169</sup>. Therefore, inhibition of these enzymes results in a massive reduction of PPHG blood levels.

### 3.1.2. Research Gap and Way-forward

Until to date, drugs used to inhibit the activity of carbohydrate hydrolyzing enzymes are synthetic. Despite their efficacy in controlling blood glucose levels, continuous and long term use of most of them is associated with undesirable adverse side effects especially, gastrointestinal disturbances such as flatulence, abdominal pain, and diarrhea <sup>170</sup>. Other classes of antidiabetic drugs are associated with metabolic syndromes such as weight gain, drug resistance, and sometimes liver inflammation such as hepatitis and lactic acidosis <sup>171</sup>. Besides, all of these synthetic drugs need high technology for their production and thus they are expensive, which limits their accessibility to many patients, especially those in rural areas and in developing countries <sup>172</sup>. Hence, there is urgency for the need to search for new antidiabetics which are effective, cheap, and low toxicity.

As a result, investigation for antidiabetics from natural sources has gained a lot of attention as they can offer all stated advantages <sup>173</sup>. This is because they constitute secondary metabolites with a wide structural diversity that possesses a broad spectrum of bioactivities including anti-diabetic. Researchers have proved that some medicinal plants/ consumption of functional foods effectively inhibit  $\alpha$ -glycosidase and  $\alpha$ -amylase and thus may prevent the development of diabetes <sup>174</sup>. In the present study, the  $\alpha$ -glucosidase and  $\alpha$ -amylase enzymes inhibitors from olive mill wastes (OMW) were investigated.

## **Screening for the anti-diabetic activity of olive mill wastes and its isolated compounds: an inhibitory activity on $\alpha$ -glucosidase and $\alpha$ -amylase enzymes**

Even though some studies reported about antidiabetic properties of virgin olive oil (VOO), all studies were based on epidemiological facts, whereby they correlated olive oil major fatty acids, especially oleic acid, and antidiabetic effect of VOO <sup>175-177</sup>. However, there is a lack of enough evidence about the effectiveness of minor secondary metabolites found in other olive parts apart from VOO. These include OMW and/ or olive leaves. In this chapter, the antidiabetic activity of the OMW and its recovered compounds was investigated by the bioassay-guided fractionation approach, as a way of creating agricultural demand and thus solving/ reducing the existing environmental damages caused by OMW <sup>18,23,178,179</sup>.

The antidiabetic activity assay was investigated on its ability to reduce the postprandial hyperglycemia (PPHG) by inhibiting carbohydrate digesting enzymes -  $\alpha$ -glucosidase and  $\alpha$ -amylase enzymes. Also, enzyme inhibitory kinetics analysis of the most active compounds was investigated to assist the possible characterization of the mechanisms of inhibition involved.

## Part II: EXPERIMENTAL

### 3.2.1. Material and Sample

Dried OMW was collected from an olive farm in Ukiha (Kyushu, Japan) in December 2018. The freeze-dried sample of OMW (350.48 g) was, at first defatted with 3.6 L *n*-hexane (to afford extracted 38.55 g of *n*-hex extract), and then extracted by maceration at 200 rpm with 3.6 L of MeOH at r.t. for 72 h – this process was repeated two times for exhaustive extraction. After evaporation under reduced pressure at 45°C, 27.15 g extract was obtained.

### 3.2.2. Chemicals and Reagents

The enzyme  $\alpha$ -glucosidase (isolated from *Saccharomyces cerevisiae*) was purchased from Oriental Yeast Co. (Tokyo, Japan), while  $\alpha$ -amylase (from the porcine pancreas) was from Sigma-Aldrich (St. Louis, MO, USA) and acarbose was obtained from Wako Pure Chemical Industries (Osaka, Japan). The deionized water (18 M $\Omega$  cm) was obtained by using a Milli-Q purification system from Millipore (Bedford, MA, USA), LC-MS grade acetonitrile, and formic acid were used to prepare chromatographic mobile phases. Commercial pure standard of (+)-pinoresinol was purchased from Sigma-Aldrich (St. Louis, MO, USA). Silica gel and solvents used for extraction and open column chromatography were purchased from Wako Pure Chemical Industries (Osaka, Japan), while TLC silica gel 60 F<sub>254</sub> plates were from Merck (Darmstadt, Germany), and chloroform-*d* (CDCl<sub>3</sub>) and methanol-*d*<sub>4</sub> (CD<sub>3</sub>OD), were purchased from Cambridge Isotope Laboratories (Andover, MA, USA).

### 3.2.3. Methods

#### 3.2.3.1. Analysis of the Chemical Profile of OMW Extract by UPLC/qTOF-MS

The powdered OMW (100 mg) was extracted by sonication with 10 mL of MeOH for 45 min at 30 °C. The extracted solution was then filtered, and this process was repeated twice for exhaustive extraction. Then, the combined filtrate was evaporated to dryness at reduced pressure by a rotary evaporator at 45 °C. The residue was finally reconstituted in MeOH to a final concentration of 200 µg/ml. Before injection for chromatographic separation, it was filtered twice through Millipore 0.20 µm PTFE filters (Millex-LG, Japan).

Agilent 1290 Series UPLC system equipped with 1290 photodiode array detector (DAD) (Agilent Technologies, Santa Clara, CA, USA) coupled to an Agilent 6545 q-TOF hybrid mass spectrometer (MS) with dual electrospray ionization (ESI) source for simultaneous spraying of a mass reference solution that enabled continuous calibration of detected  $m/z$  ratios was used for the analysis of the samples. An injection volume of 2 µL and a flow rate of 0.2 mL/min was used. The mobile phases were 0.1% (v/v) formic acid aqueous solution (phase A) and 0.1% (v/v) formic acid acetonitrile (phase B). Separation of the analytes was achieved through Agilent Poroshell 120 EC C-18 column (100 × 2.1 mm inner diameter, 2.7 µm particle size, Agilent Technologies, Santa Clara, CA, USA) at 40 °C. The gradient method was as follows: 4% B to 100% B in 15 min, and 100% A for 2.5 min. At last, re-equilibration was done for 3.5 min. The dual ESI source operated in negative ionization using the

following conditions: nebulizer gas at 35 psi and drying gas flow rate and temperature at 10 L/min and 325 °C, respectively. The capillary voltage was set at 3500 V, while the fragmentor, skimmer, and octapole voltages were fixed at 130, 65, and 750 V, respectively.

The data were acquired in centroid mode in the extended dynamic range (2 GHz). The full scan was carried out at 1.5 spectra per second within the  $m/z$  range of 100–1700. A continuous internal calibration was performed during analyses, to ensure the desired mass accuracy of recorded ions, with the use of signals at  $m/z$  112.9855 (ammonium-abstracted TFA/ TFA anion) and  $m/z$  1033.9881 (trifluoroformate adduct of hexakis[1H,1H,3H, tetrafluoropropox]phosphazine). For data acquisition and monitoring the hardware, Agilent MassHunter Workstation software (Agilent Technologies, Santa Clara, CA, USA) was used.

The obtained UPLC/QTOF-MS raw data were further processed by Agilent MassHunter Qualitative Analysis software (version B.10.00, Agilent, USA). The extracted ion chromatograms (EICs) algorithm was applied to extract and identify all metabolites from the total ion chromatograms (TICs) of the extract according to their metabolic features including  $m/z$ , retention time and ion intensities, whereby, reference was made from a standard mix. After identification of all metabolites by Agilent MassHunter Qualitative Analysis software, the raw data were then transferred to Agilent MassHunter Quantitative Analysis software version B.10.00

(Agilent Technologies, Santa Clara, CA, USA) for making calibration curve and quantification.

### **3.2.3.2. Procedure for Extraction and Isolation**

Before starting fractionation and isolation, both the *n*-hexane extract obtained after defatting and MeOH extract obtained after maceration of OMW (section 3.2.1) were subjected to  $\alpha$ -glucosidase inhibitory activity. Following  $\alpha$ -glucosidase inhibitory assay, MeOH extract exhibited stronger inhibitory activity (**Figure 16**), and hence it was subjected to LLE to obtain *n*-hexane (7645.9 mg), dichloromethane, DCM (899.11 mg), ethyl acetate, EtOAc (1680.20 mg) and aqueous (12927.29 mg) fractions. The  $\alpha$ -glucosidase inhibitory activity showed that only DCM and EtOAc fractions were most active while the *n*-hexane was the least active, Their IC<sub>50</sub> values are shown in the results and discussion section (**Table 13**). Therefore, fractionation and isolation proceeded with the most active fractions (DCM and EtOAc Fr). The scheme to summarize the extraction protocol used in the present study is shown in **Figure 13**.

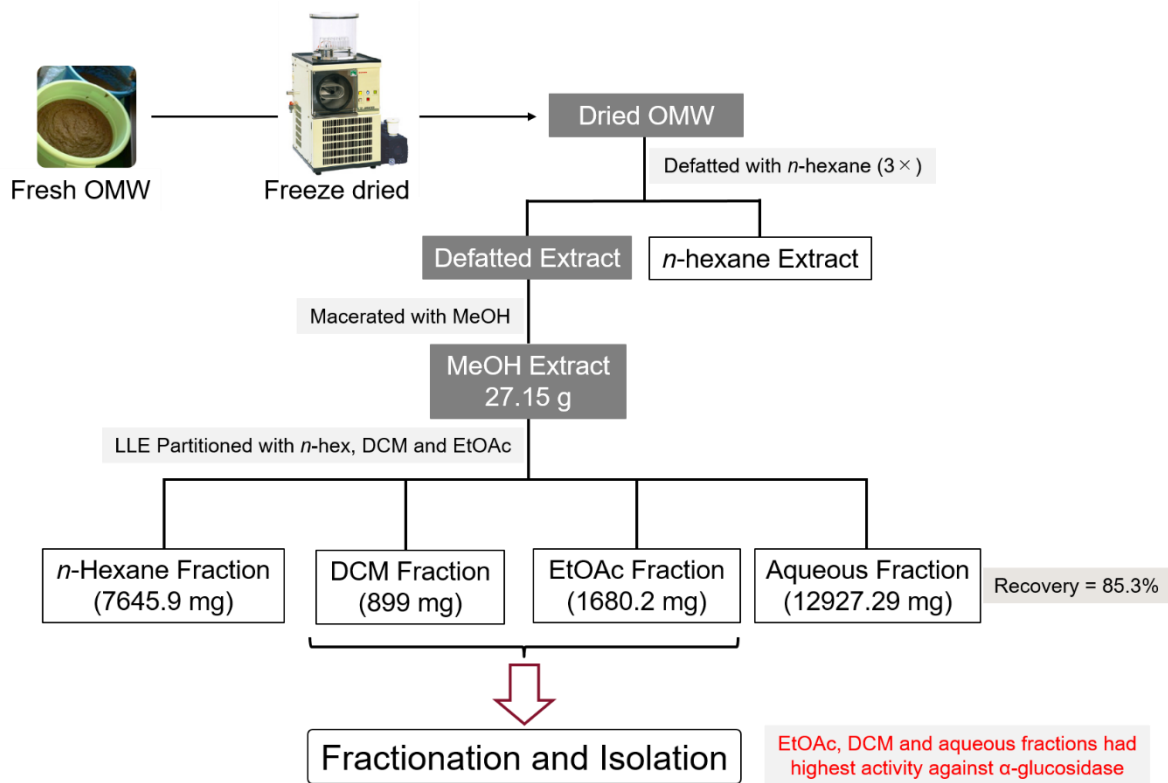


Figure 13: General extraction and LLE protocol of OMW as guided by  $\alpha$ -glucosidase inhibitory activity. In the first step, the defatted extract was more active than *n*-hexane extract and that is why it was further fractionated to several fractions by LLE technique



Each of these fractions was separately subjected to the medium pressure liquid chromatography (MPLC) system (BUCHI, Reverelis Prep Purification System, Switzerland) and further purification, when necessary, was achieved by preparative TLC or MPLC system again. In both cases, elutes were monitored with TLC analysis. To begin with the DCM fraction; it was purified by the BUCHI MPLC system connected with the C-18 column (particle size 35-45  $\mu\text{m}$ , 40 g) flushed with the Water-MeOH system (95:5 $\rightarrow$ 0:100) resulting into 95 collected tubes, each containing 25 mL elute. After TLC analysis of the elutes from flasks number 83-95, eluted with Water-MeOH (5:95 $\rightarrow$ 0:100), were confirmed to contain a pure compound **1** (37 mg). Also, while elutes in the flask number 77, eluted with Water-MeOH (15:85) came out as pure compound **2** (39.7 mg), other elutes from flask number 81 which was eluted with Water-MeOH (10:90) by MPLC in the first purification step, it was further purified in the second step by preparative TLC using *n*-hex-EtOAc (30:70) to afford pure compound **2** (4.0 mg) – making a total of 43.7 mg for compound **2**. Then, for the EtOAc fraction; its first purification step was done with the BUCHI MPLC system connected with the C-18 column (particle size 35-45  $\mu\text{m}$ , 3.0 $\times$ 16.5 cm, 40 g), flushed by Water-MeOH system (95:5 $\rightarrow$ 0:100) to afford 120 collected tubes (each with 25 mL elutes).

Sub-fractions from flasks number 77 to 120 (187.4 mg), eluted with Water-MeOH (20:80 $\rightarrow$ 0:100), were further purified by Yamazen MPLC system (EPCLC, Yamazen, Osaka, Japan) connected with silica gel column (particle size 50  $\mu\text{m}$ , 3.0 $\times$ 16.5 cm, 40 g) flashed with  $\text{CHCl}_3$ -MeOH gradient (90:10 $\rightarrow$ 0:100), then by preparative TLC

eluted with *n*-hex-EtOAc (30:70) and (20:80), to afford compounds **3** (1.6 mg) and **4** (8.0 mg), respectively. The sub-fractions from flask number 1 to 7 (23.3 mg) eluted with Water-MeOH (95:5), was further purified by the BUCHI MPLC system connected with the C-18 column flashed with Water-MeOH gradient (95:5→85:15) to afford compound **7** (4.0 mg). Elutes from flask 13 to 60 (680.3 mg) eluted with Water-MeOH (90:10→30:70), were further purified by Yamazen MPLC system connected with the silica gel column flashed with *n*-hex-EtOAc gradient (30:70→0:100), and lastly washed with MeOH to afford four sub-fractions. The first, most polar, sub-fraction was purified by preparative TLC ran by EtOAc: MeOH: Hex = 9:1:1 to afford compound **5** (3.0 mg) and **6** (4.5 mg).

### **3.2.3.3. Identification of the Isolated compounds**

The NMR spectra of the compounds were recorded on Bruker DRX-600 spectrometer (Bruker Daltonics, Billerica MA, USA) at room temperature with trimethylsilane (TMS) as the internal standard of the chemical shifts, CD<sub>3</sub>OD or CDCl<sub>3</sub> as dissolving solvent and the chemical shifts were expressed as  $\delta$  values. HR-ESI-MS and HR-FAB-MS were performed on quadrupole time-of-flight (qTOF) mass spectrometer (Agilent Technologies, Santa Clara, CA, USA) and JMS 700 MStation mass spectrometer (JEOL, Tokyo, Japan).

#### 3.2.3.4. Assay for $\alpha$ -glucosidase inhibitory activity

The method used to assay the  $\alpha$ -glucosidase inhibitory activity of the compound was adopted as described by Fatmawati *et al.* (2011)<sup>180</sup>. Briefly, 100  $\mu$ l of an appropriate solvent such as DMSO, water or a mixture of them with or without (control) samples and 100  $\mu$ l of the enzyme ( $\alpha$ -glucosidase, 5 U/ml in 0.15 M HEPES buffer) were added to 100  $\mu$ l of the substrate (0.1 M sucrose solution, made by dissolving into 0.15 M HEPES buffer), and the mixture was homogenized by vortexing for 5 s and then incubated at 37 °C for 30 min to allow enzymatic reaction. After incubation, the reaction was stopped by heating at 100 °C for 10 min in block incubator. The formation of glucose was determined by means of glucose oxidase method using a BF-5S Biosensor (Oji Scientific Instruments, Hyogo, Japan). The  $\alpha$ -glucosidase inhibitory activity of each sample was calculated by the following equation:

$$\text{Inhibition (\%)} = [A_c - A_s] / A_c \times 100$$

Where;  $A_c$  is the average value of control and  $A_s$  is the average value of the sample ( $n=3$ ).

#### 3.2.3.5. Assay for $\alpha$ -amylase inhibitory activity

The  $\alpha$ -amylase inhibitory effect was assayed according to the procedure as described by Xiao *et al.* (2006)<sup>181</sup>, with some minor modifications. Briefly, 0.2% (w/v) potato starch solution, phosphate buffer with or without (control) samples, were mixed with PPA in phosphate buffer to start the enzyme reaction. After incubation at 37 °C for 30 min, the reaction was stopped by the addition of 0.4 M HCl. Then, 100

μL of 5 mM KI was added and absorbance was read at 660 nm (Corona Electric Co, Japan). All samples were assayed in triplicates ( $n=3$ ). The percent inhibitory activity (%) was calculated as follows:

$$\text{Inhibition (\%)} = \{1 - (A_2 - A_1) / (A_4 - A_3)\} \times 100$$

Where,  $A_1$  is the average absorbance of the incubated solution containing the sample, starch, and  $\alpha$ -amylase;  $A_2$  is the average absorbance of an incubated solution containing sample and starch;  $A_3$  is the average absorbance of an incubated solution containing starch and  $\alpha$ -amylase;  $A_4$  is the average absorbance of an incubated solution containing starch only ( $n=3$ ).

#### **3.2.3.6. Analysis of $\alpha$ -Glucosidase Enzyme Inhibitory Kinetics**

Inhibitory kinetics analysis was performed on the most active compounds. In order to evaluate the inhibition type of the active compounds against  $\alpha$ -glucosidase, the enzyme activity was quantified at increasing concentrations of the substrate (sucrose) at constant enzyme concentration, in the absence or presence of the inhibitors (active compounds) at different concentrations – whereby, three different concentrations were used (ranging from 0  $\mu$ M to the one near their respective  $IC_{50}$ -values). Briefly, enzyme (5 U/mL), dissolved in 100 mM HEPES buffer, was pre-incubated at 37°C with the inhibitor (most active compound, individually) for 5 min. The substrate (sucrose) at different concentrations was added to the pre-incubated mixture of enzyme-inhibitor and incubated at 37°C in the reaction mixture for 30 min. The inhibition type (competitive, uncompetitive, non-competitive or mixed), were

determined by Lineweaver-Burk plot analysis of the data which was calculated from the result according to Michaelis-Menten kinetics, whereby the plots of  $1/V$  versus  $1/S$  were constructed, where  $S$  is the substrate concentration and  $V$  is the reaction velocity<sup>182</sup>. The types of inhibition parameters (to determine the values of  $K_m$ ,  $K_i$ , and  $V_{max}$ ) were calculated by SigmaPlot 12.3 software (Systat Software Inc., CA, USA).

#### **3.2.4. Data Analysis**

The data values in the present study were expressed as Mean  $\pm$  standard deviation (S.D.) of at least three independent experiments ( $n=3$ ). The significant differences between each tested group and the control group were determined using Dunnett's multiple post hoc test.  $p$ -value cutpoint was set at 95% (where;  $p < 0.05$ ), when the one-way analysis of variance (ANOVA) was statistically significant. The inhibitory bar graphs of the isolated compounds (and fractions) were drawn by using Microsoft Excel 2016.

## Part III: RESULTS AND DISCUSSION

### 3.3.1. The Structure of the Identified Isolated compounds

A total of seven compounds were isolated from OMW, including one novel, 3,4-dihydroxyphenyl-2-methoxyethanol **5** – a methoxy derivative of hydroxytyrosol. The chemical structures of all compounds are shown in **Figure 14 (B)**.

Compound **5** was obtained as a yellowish amorphous liquid with a UV (EtOH)  $\lambda_{\max}$  228, 280 nm. Its structure was elucidated by 1D- and 2D-NMR spectroscopy and HR-ESI-MS. The analysis of NMR data in comparison with that in the literature <sup>52</sup>, suggested that compound **5** has the main skeleton of the hydroxytyrosol which was evident through both <sup>1</sup>H NMR spectral peaks, whereby a doublet at  $\delta_{\text{H}}$  6.72 (d, 1H,  $J=2.1$  Hz, H-2) and a doublet-doublet at  $\delta_{\text{H}}$  6.53 (dd, 1H,  $J=2.0$  Hz,  $J=8.0$  Hz H-6) were observed, which entails the ABX system – meta- and para-aromatic ring substitution. The other two resonances corresponding to the protons H-1' and H-2' of the ethyl chain were observed resonating at  $\delta_{\text{H}}$  4.09 (dd, 2H,  $J=3.8$  Hz,  $J=8.2$  Hz, H-1') and  $\delta_{\text{H}}$  3.48 (dd, 2H,  $J=3.8$  Hz,  $J=11.7$  Hz H-2'), respectively. The first difference between **5** and hydroxytyrosol **7** was observed at H-1', which was resonating at a more downfield region as compared to that of hydroxytyrosol ( $\delta_{\text{H}}$  2.67, t, 2H). Another main difference was observed through the <sup>13</sup>C NMR spectrum at the region of aliphatic carbons. These signals were observed resonating at  $\delta_{\text{C}}$  84.7 and 66.4, which were later assigned for C-1' and C-2', respectively through HSQC – both

of them being more downfield as compared to the reported ones ( $\delta\text{C}$  63.9 and 39.0). These data were suggestive of the possible attachment at C-1'.

The long-range HMBC correlations observed from  $\delta\text{H}$  4.09 (H-1') included the carbons resonating at  $\delta\text{C}$  130.3 (C-1), 118.3 (C-6), 66.4 (C-2') and 55.2 (-OCH<sub>3</sub>). Bearing in mind of the ABX substitution in the aromatic ring, confirming the presence of an oxygenated carbon attached to C-1'. Furthermore, the correlations between C-1' and C-2'; and C-1' and -OCH<sub>3</sub> were seen through <sup>1</sup>H-<sup>1</sup>H COSY spectrum. The assignment of all <sup>1</sup>H- and <sup>13</sup>C NMR signals were confirmed by HSQC and HMBC data and are summarized in **Table 9** and **Figure 14 (A)**. The HR-ESI-MS spectrum of compound **5** showed a molecular ion peak [M-H]<sup>-</sup> at  $m/z$  183.0639, which was agreeable with the suggested molecular formula of C<sub>9</sub>H<sub>11</sub>O<sub>4</sub><sup>-</sup> (calculated  $m/z$  183.0663). Some molecular peaks were observed at  $m/z$  151.0391 and 167.078, corresponding to the fragments [M-CH<sub>3</sub>OH]<sup>-</sup> and [M-OH]<sup>-</sup>, respectively.

**Table 9: <sup>1</sup>H and <sup>13</sup>C NMR data for compound 5 and hydroxytyrosol**

No.	Compound 5		Reference (Hydroxytyrosol)	
	<sup>1</sup> H (J in Hz)	<sup>13</sup> C	<sup>1</sup> H (J in Hz)	<sup>13</sup> C
1		131.3		130.3
2	6.72 d (2.0)	115.7	6.72 d (2.1)	113.5
3		145.2		145.0
4		143.9		144.7
5	6.68 d (8.0)	116.4	6.67 d (8.0)	113.4
6	6.53 dd (2.0, 8.0)	120.6	6.61 dd (2.0, 8.0)	118.3
1'	4.09 dd (3.8, 8.2)	84.7	2.67 t (7.2)	39.0
2'	3.48 dd (3.8, 8.2)	66.4	3.68 t (7.2)	63.9
<u>OCH</u> <sub>3</sub>	3.21 s	55.2	–	–

The values of chemical shifts are expressed in ppm; for **5** the <sup>1</sup>H and <sup>13</sup>C NMR at 600 and 150 MHz respectively. In both cases, the compounds were dissolved in Methanol-*d*<sub>4</sub> (CD<sub>3</sub>OD)



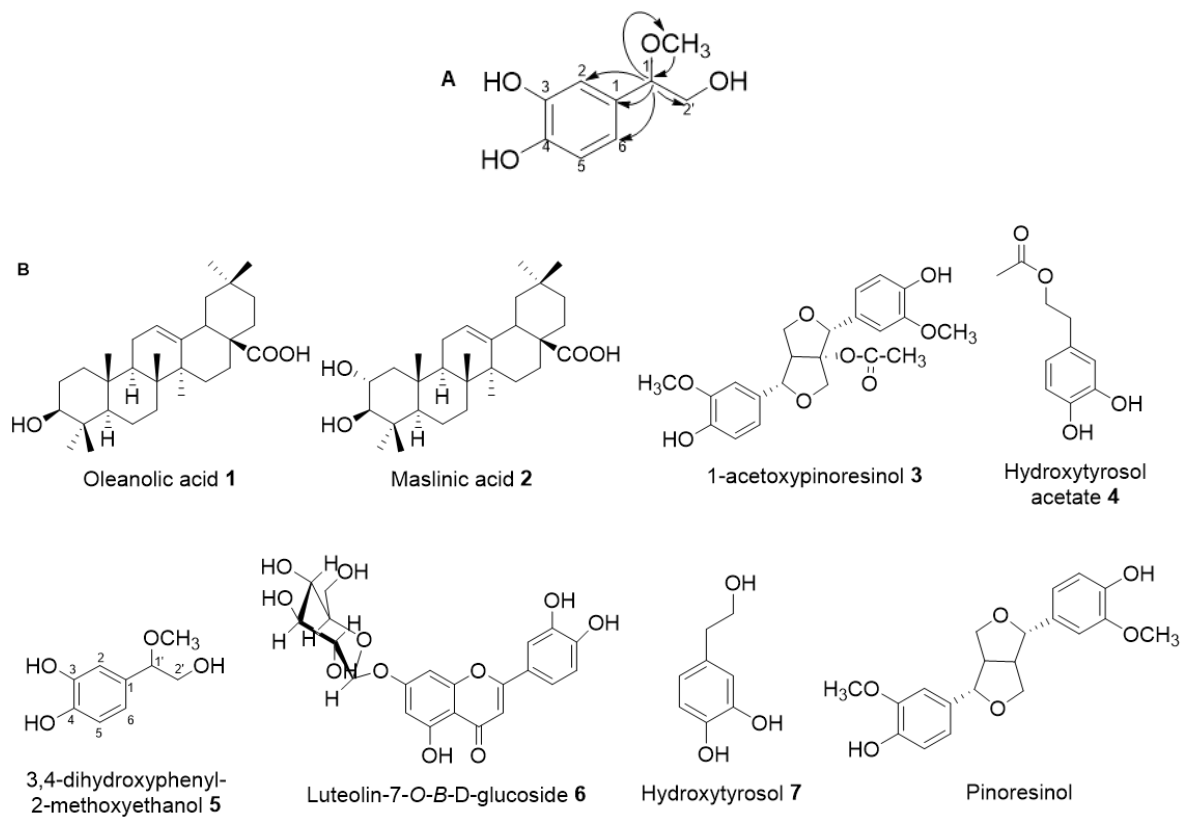


Figure 14: The chemical structures of the isolated compounds from OMW.

Other compounds were identified as oleanolic acid **1**<sup>138</sup>, maslinic acid **2**<sup>138</sup>, 1-acetoxypinoresinol **3**<sup>143</sup>, hydroxytyrosol acetate **4**<sup>142</sup>, luteolin-7-O- $\beta$ -D-glucoside **6**<sup>183</sup> and hydroxytyrosol **7**<sup>52</sup>. The data used for the identification of these compounds is as follows:

Oleanolic acid (*3 $\beta$ -hydroxyolean-12-en-28-oic acid*), **1**; White amorphous solid:  $[\alpha]^{26}_D +65.6$  (c 1.0, MeOH): <sup>1</sup>H NMR (600 MHz, CD<sub>3</sub>OD)  $\delta_H$  5.28 (1H, dd, J=Hz, H-12), 3.20 (1H, dd, J=4.3, 9.6, 11.4 Hz, H-2 $\beta$ ), 2.88 (1H, d, J=9.5 Hz, H-3 $\alpha$ ), 2.82 (1H, dd, J=4.3, 13.7 Hz, H-18), 1.98 (1H, ddd, J=4.2, 13.7, 13.7 Hz, H-16), 1.13 (3H, s, H-27), 0.98 (3H, s, H-23), 0.93 (3H, s, H-25), 0.91 (3H, s, H-30), 0.90 (3H, s, H-29), 0.77 (3H, s, H-26), 0.76 (3H, s, H-24): for <sup>13</sup>C NMR (150 MHz, CD<sub>3</sub>OD), see **Table 10**: HR-ESI-MS *m/z* 455.3534 [M-H]<sup>-</sup>.

Maslinic acid (*2 $\alpha$ , 3 $\beta$ -dihydroxyolean-12-en-28-oic acid*), **2**; Same data were obtained as the ones in chapter 2.

1-acetoxypinoresinol (*(1S,4S,5R,8R)-4,8-bis(4-hydroxy-3-methoxy-phenyl)-3,7-dioxabicyclo [3.3.0] oct-1-yl acetate*) **3**; Same data were obtained as the ones in chapter 2.

Hydroxytyrosol acetate (*2-(3,4-dihydroxyphenyl) ethyl acetate*) **4**; Same data were obtained as the ones in chapter 2.

Luteolin-7-O- $\beta$ -D-glucoside (3',4',5-trihydroxyflavon-7-O- $\beta$ -D-glucoside) **6**;

Yellowish powder:  $^1\text{H}$  NMR (600 MHz,  $\text{CD}_3\text{OD}$ )  $\delta^{\text{H}}$  7.32 (1H, dd,  $J=2.2, 8.1$  Hz, H-6'), 7.15 (1H, d,  $J=1.8$  Hz, H-2'), 6.87 (1H, d,  $J=8.4$  Hz, H-5'), 6.45 (1H, s, H-3), 6.35 (1H, d,  $J=1.3$  Hz, H-8), 6.21 (1H, d,  $J=1.6$  Hz, H-6):  $^{13}\text{C}$  NMR (150 MHz,  $\text{CD}_3\text{OD}$ )  $\delta^{\text{C}}$  181.0 (C-4), 162.2 (C-7), 161.4 (C-5), 168.9 (C-2), 158.4 (C-9), 152.8 (C-4'), 152.0 (C-3'), 124.1 (C-1'), 121.3 (C-6'), 118.2 (C-5'), 114.2 (C-2'), 107.9 (C-10), 104.9 (C-3), 104.3 (C-6), 95.1 (C-8). The anomeric carbon of sugar moiety, C-1, was seen at  $\delta^{\text{C}}$  101.1. Other carbons of sugar were seen at  $\delta^{\text{C}}$  68.2 (C-2), 72.5 (C-3), 69.7 (C-4), 78.5 (C-5), 61.6 (C-6): HR-EI-MS at 447.0933  $m/z$   $[\text{M-H}]^-$ .

Hydroxytyrosol (3,4-dihydroxyphenylethanol) **7**; Same data were obtained as the ones in chapter 2.

**Table 10:  $^{13}\text{C}$  NMR data for the isolated triterpene compounds 1 and 2 (Oleanolic acid 1 and Maslinic acid 2)**

<b>Carbon</b>	<b>1<sup>a</sup></b>	<b>2<sup>a</sup></b>
1	38.4	48.9
2	27.1	68.3
3	79.1	83.2
4	38.8	39.2
5	55.3	55.2
6	18.3	18.3
7	33.1	33.0
8	39.3	39.0
9	47.7	47.4
10	37.1	38.1
11	23.4	23.7
12	122.6	122.3
13	143.6	143.9
14	41.6	41.7
15	27.2	27.4
16	23.4	23.5
17	47.7	47.5
18	41.0	41.0
19	46.5	46.3
20	30.7	30.7
21	33.1	33.1
22	32.7	33.0
23	28.1	28.5
24	15.6	16.5
25	16.6	16.7
26	17.2	18.2
27	26.0	25.9
28	183.1	181.0
29	33.1	33.0
30	23.6	23.5

The values of chemical shifts are in ppm, a – in Chloroform-*d* ( $\text{CDCl}_3$ )

### 3.3.2. Chemical Profile of the Extract by UPLC/QTOF-MS

The characteristic profiles of the isolated compounds were investigated with highly sensitive UPLC/QTOF-MS. All the isolated compounds (and (+)-pinoresinol) were identified based on their retention times, mass spectral and DAD (280 nm) data with the isolated ones or available standards, for the case of (+)-pinoresinol (**Table 11**). For compounds like oleanolic acid **1** and maslinic acid **2**, which do not have a chromophore, their detection was based only on their retention times and MS data. MS detection was made at negative ionization mode as the compounds gave a strong response in negative-ion mode. Moreover, it has been proven to be effective for olive metabolites <sup>184</sup>. In all cases, the identification of the compounds in the extract was highly accurate with an error of  $\pm 5$  ppm only. The presentation of different chromatograms (extracted ion chromatogram, EIC, and DAD chromatogram) of the OMW extract are shown in **Figure 15**.

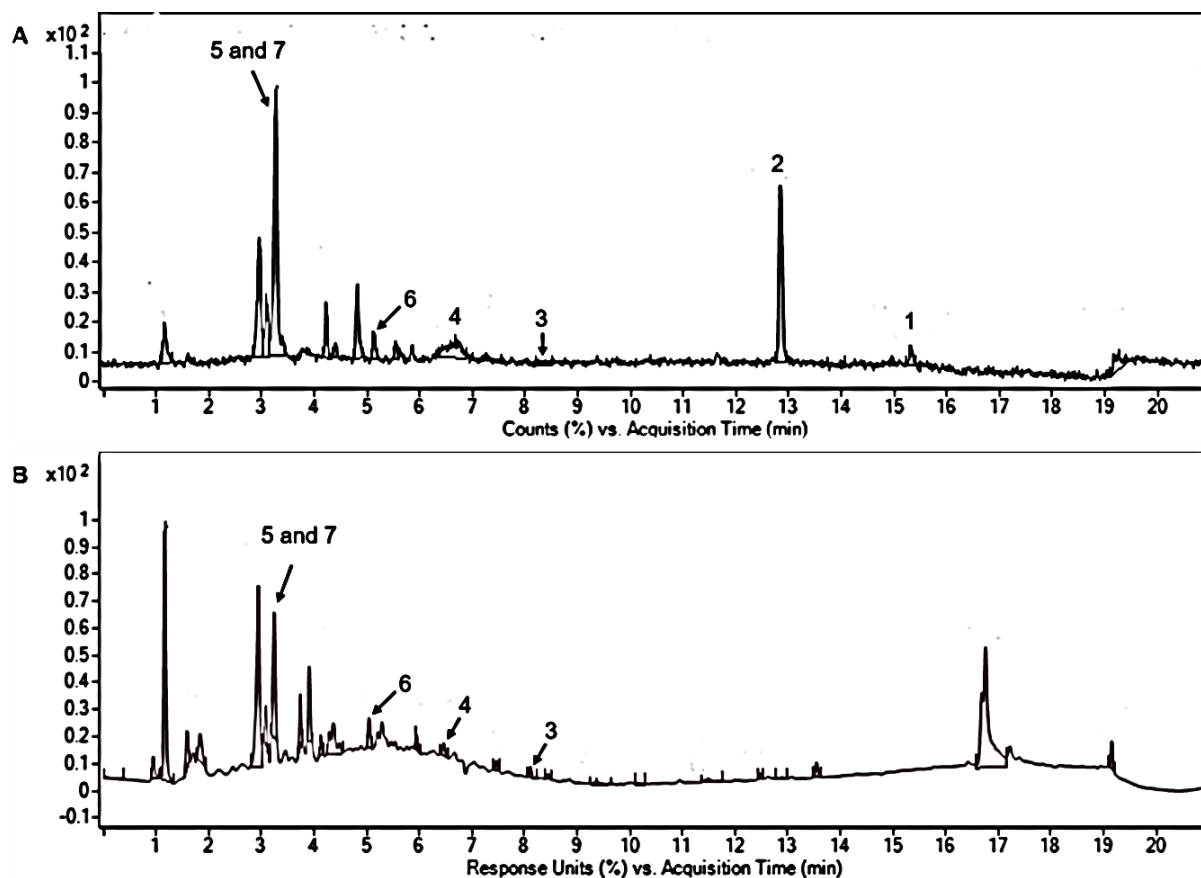


Figure 15: The chromatograms of OMW total extract, 200 ppm (A) Extracted ion chromatogram (EIC) scan, and; (B) DAD chromatogram ( $\lambda=280$  nm) scan. The compounds were identified as oleanolic acid **1**, maslinic acid **2**, 1-acetoxypinoresinol **3**, hydroxytyrosol acetate **4**, 3,4-dihydroxyphenyl-2-methoxyethanol **5**, luteolin-7-*O*- $\beta$ -D-glucoside **6** and hydroxytyrosol **7**, respectively, by comparing their retention times, mass spectral and DAD data of each peak to those of the isolated pure ones or authentic one (for the case of (+)-pinoresinol). Compounds **1** and **2** could not be seen at the DAD scan as they can't absorb UV at wavelength 280 nm.

**Table 11: Characterization of the isolated compounds (and (+)-pinoresinol) from the OMW extract by UPLC/QTOF-MS.**

Peak No.	Retention time, $t_R$ (min)	Formula	$[M-H]^-$ ( $m/z$ <i>exp</i> )	$[M-H]^-$ ( $m/z$ <i>theo</i> )	Error (ppm)	Identification
1	15.295	C <sub>30</sub> H <sub>48</sub> O <sub>3</sub>	455.3534	455.3530	0.8784	Oleanolic acid
2	12.829	C <sub>30</sub> H <sub>48</sub> O <sub>4</sub>	471.3487	471.3480	1.4851	Maslinic acid
3	8.313	C <sub>22</sub> H <sub>24</sub> O <sub>8</sub>	415.1390	415.1398	-1.9271	1-acetoxypinoresinol
4	6.674	C <sub>10</sub> H <sub>12</sub> O <sub>4</sub>	195.0674	195.0663	5.6391	Hydroxytyrosol acetate
5	3.381	C <sub>9</sub> H <sub>12</sub> O <sub>4</sub>	183.0663	183.0663	0.0000	3,4-dihydroxyphenyl-2-methoxyethanol
6	5.123	C <sub>21</sub> H <sub>20</sub> O <sub>11</sub>	447.0933	447.0933	0.0000	Luteolin-7-O- $\beta$ -D-glucoside
7	3.268	C <sub>8</sub> H <sub>10</sub> O <sub>3</sub>	153.0577	153.0577	0.0000	Hydroxytyrosol
(+)- pinoresinol	7.43	C <sub>20</sub> H <sub>22</sub> O <sub>6</sub>	357.1331	357.1344	-3.6401	(+)-pinoresinol

### 3.3.3. Inhibitory Effect of the Isolated Compounds on $\alpha$ -Glucosidase and $\alpha$ -Amylase Enzymes

As stated in the Method section, both the defatted (*n*-hexane) extract and MeOH extracts were subjected to  $\alpha$ -glucosidase inhibitory assay and found that MeOH had stronger inhibitory activity (**Figure 16**). The results were consistent even after calculation of their IC<sub>50</sub> values, whereby MeOH extract was more potent than *n*-hexane extract – IC<sub>50</sub> values 85.6±4.8 and >500  $\mu$ g/ml, respectively (**Table 12**). Then, because of its higher inhibition, MeOH extract was further fractionated by LLE to afford *n*-hexane fraction, dichloromethane (DCM), and ethyl acetate (EtOAc) fractions. After the assay, it was found that DCM and EtOAc exhibited significantly higher  $\alpha$ -glucosidase inhibitory activity than *n*-hexane ( $p < 0.05$ ). Similarly, this was consistent even after the calculations of the IC<sub>50</sub> values (**Table 13**).

Therefore, DCM and EtOAc fractions proceeded for the isolation of compounds. In addition to  $\alpha$ -glucosidase inhibitory activity, the isolated compounds were also tested for their  $\alpha$ -amylase inhibitory activity. Their  $\alpha$ -glucosidase and  $\alpha$ -amylase inhibitory activities are presented in **Figure 17**. The isolated compounds showed different inhibitory activities against both enzymes ( $\alpha$ -glucosidase and  $\alpha$ -amylase). Interestingly, compounds that exhibited stronger inhibitory activity against  $\alpha$ -glucosidase enzymatic activity (**1, 2, 3, and 6**) are the same ones which showed stronger inhibitory activity against the  $\alpha$ -amylases (**Figure 17**).



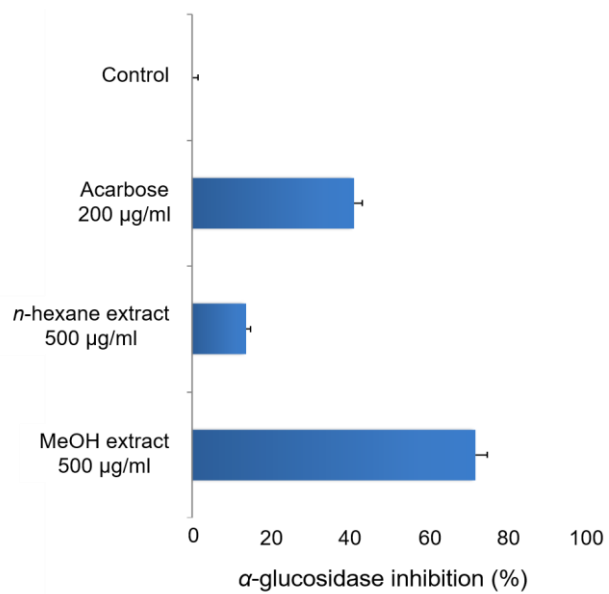


Figure 16:  $\alpha$ -glucosidase inhibitory activity of *n*-hexane, methanol extracts, and acarbose. The experiments were done in triplicates ( $n=3$ ).

**Table 12: IC<sub>50</sub> values for  $\alpha$ -glucosidase inhibitory activity of *n*-hexane, methanol extracts, and acarbose**

Sample	IC <sub>50</sub> ( $\mu$ g/ml) <sup>a</sup>
<i>n</i> -hexane extract	>500
Methanol extract	85.6 $\pm$ 4.8
Acarbose <sup>b</sup>	234.6 $\pm$ 3.7

<sup>a</sup> The inhibitory effect is expressed as the Mean $\pm$ SD values of the IC<sub>50</sub> in triplicates ( $n=3$ ). <sup>b</sup> Positive control (standard drug).

**Table 13: IC<sub>50</sub> values for  $\alpha$ -glucosidase inhibitory activity of the MeOH fractions following LLE**

Sample	IC <sub>50</sub> ( $\mu$ g/ml) <sup>a</sup>
<i>n</i> -hexane fraction	>500
DCM fraction	64.7 $\pm$ 5.5
EtOAc fraction	159.2 $\pm$ 18.3
Acarbose <sup>b</sup>	234.6 $\pm$ 2.7

<sup>a</sup> The inhibitory effect is expressed as the Mean $\pm$ SD values of the IC<sub>50</sub> in triplicates (*n*=3). <sup>b</sup> Positive control (standard drug).

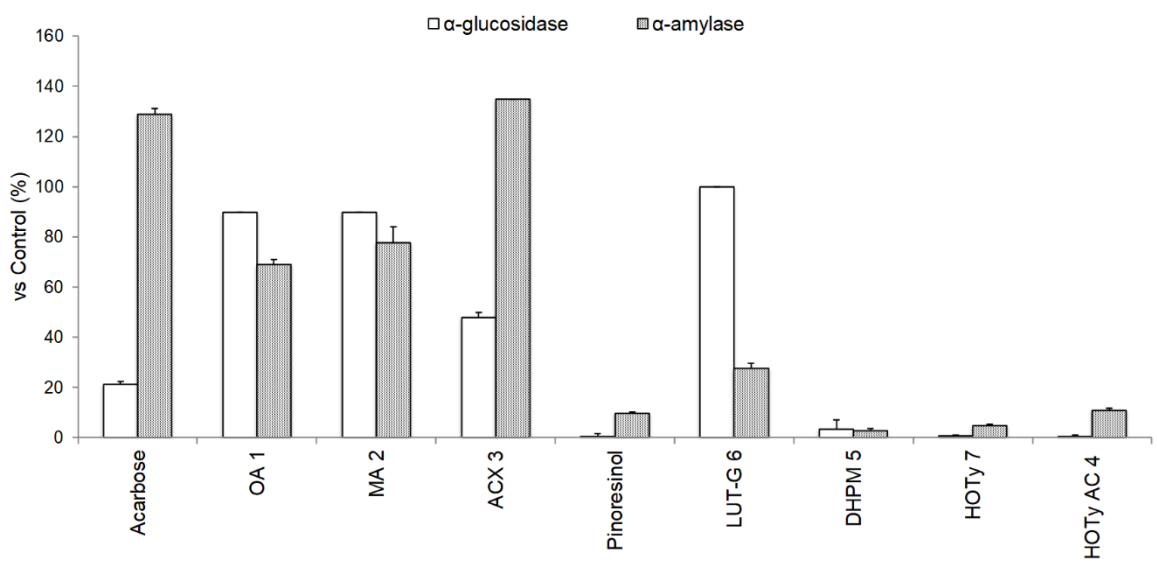


Figure 17: Inhibitory effects of the isolated compounds on the enzymatic activity of  $\alpha$ -glucosidase and  $\alpha$ -amylase enzymes – all compounds presented at a concentration of 150  $\mu$ M. Effect on  $\alpha$ -glucosidase inhibitory activity is presented with white bars, while the effect on  $\alpha$ -amylase inhibitory activity is presented with bars with black dots. The  $\alpha$ -glucosidase inhibitory activity was quantified by measuring the amount of glucose oxide formed at the end of the reaction, while inhibitory activity on  $\alpha$ -amylase was measured by a quantitative starch-iodine method. In both cases, the experiments were done in triplicates  $n=3$  (results are expressed as Mean $\pm$ S.D.), where: OA, oleanolic acid; MA, maslinic acid; ACX, 1-acetoxypinoresinol; LUT-G, luteolin-7-*O*- $\beta$ -D-glucoside; DHPM, 3,4-dihydroxyphenyl-2-methoxyethanol; HOTy, hydroxytyrosol, and HOTy Ac, hydroxytyrosol acetate.

When compared to the standard drug, acarbose, their inhibitory activity on  $\alpha$ -glucosidase was higher than that of acarbose ( $p < 0.05$ ); while for the case of  $\alpha$ -amylase, acarbose had stronger inhibitory activity than them ( $p < 0.05$ ).

In general, the results show that even though both fractions exhibited a stronger inhibitory activity, the activities of individual compounds from the respective fractions varies widely (from highly active to poorly/ not active). For instance, hydroxytyrosol acetate **4**, 3,4-dihydroxyphenyl-2-methoxyethanol **5**, and hydroxytyrosol **7**, which were isolated from the active EtOAc fraction, showed inhibitory activity of less than 10% at highest tested concentrations (1000  $\mu$ M and 500  $\mu$ M for  $\alpha$ -glucosidase and  $\alpha$ -amylase, respectively). This may suggest that there is a possibility of either an additive or synergism effect for the overall activity of the fraction(s), or some minor compounds, which were not isolated, may have contributed to the overall stronger inhibitory activity of the fractions. The synergism effect of plant extracts/ fractions has been widely known in phytochemistry<sup>185,186</sup>.

Finally, their total activities were compared (**Table 14**). Generally, the total activity for both  $\alpha$ -glucosidase and  $\alpha$ -amylase enzymes was highest for oleanolic acid **1** and maslinic acid **2** when compared to other active compounds (**3** and **6**). This is because, apart from having strong inhibitory activity, low  $IC_{50}$  values, but also they are more abundant than compounds **3**, and **6** in OMW. Another instance is observed to 1-acetoxypinoresinol **3**; regardless of its strongest  $\alpha$ -amylase inhibitory activity, but its total activity for  $\alpha$ -amylase was lower than that of **1** and **2**.

**Table 14: The enzymatic inhibitory activity (IC<sub>50</sub>), the total amount in dry weight and the total activity of the isolated compounds from OMW**

Compound	IC <sub>50</sub> (μM) [μg/mL]		Amount (mg/kg dried OMW)	Total activity <sup>b</sup>	
	α-glucosidase	α-amylase		α-glucosidase	α-amylase
Oleanolic acid <b>1</b>	33.5±0.6 [15.3]	81.3±2.7 [37.1]	82.1	5,359.5	2,212.9
Maslinic acid <b>2</b>	34.5±1.4 [16.3]	67.0±5.4 [31.7]	180.0	11,042.9	5,678.2
1-acetoxypinoresinol <b>3</b>	313.1±12.5 [130.4]	13.9±3.9 [5.5]	1.13	8.7	205.5
Hydroxytyrosol acetate <b>4</b>	>1000 [>200]	>500 [>100]	21.46	ND	ND
3,4-dihydroxyphenyl-2-methoxyethanol <b>5</b>	>1000 [>200]	>500 [>100]	128.79	ND	ND
Luteolin-7-O-β-D-glucoside <b>6</b>	26.6±0.8 [11.9]	404.7±0.0 [181.5]	46.71	3,925.2	256.6
Hydroxytyrosol <b>7</b>	>1000 [>200]	>500 [>100]	303.03	ND	ND
(+)-pinoresinol	>1000 [>400]	>500 [>200]		ND	ND
Acarbose <sup>a</sup>	323.4±4.2 [208.8]	15.0±1.3 [9.7]			

The results are expressed as Mean ± SD (*n*=3). Where; <sup>a</sup> standard drug and ND could not be determined since the exact value of IC<sub>50</sub> could not be calculated (beyond maximum tested concentration); <sup>b</sup> Total activity of each compound was

estimated mathematically by using the following formula: total activity = amount  
(mg/kg)/IC<sub>50</sub> (mg/ml).

#### 3.3.4. Effect of the Active Isolated Compounds Enzyme Kinetics

Due to their stronger inhibitory activity against the  $\alpha$ -glucosidase enzyme, oleanolic acid **1**, 1-acetoxypinoresinol **3**, and luteolin-7-*O*- $\beta$ -D-glucoside **6** were investigated further for their possible underlying mechanisms of inhibition of the enzyme. In the experiment,  $\alpha$ -glucosidase was treated with these compounds, individually, using sucrose as the substrate (1 – 33 mM) to determine the inhibition type. To obtain the  $K_i$  constant of the inhibitors in the media, sucrose was used as a substrate, and three different inhibitor concentrations were used in the reaction medium. As a result, three diverse fixed concentrations of inhibitor Lineweaver-Burk graphs which were utilized to calculate  $V_{max}$  and other inhibition parameters<sup>187</sup>. After analysis of the Lineweaver–Burk plots and based on the best ‘fit results’ and ‘goodness to fit’ analysis, it was concluded that oleanolic acid **1** is a partial mixed inhibitor<sup>188</sup>, luteolin-7-*O*- $\beta$ -D-glucoside **6** is a non-competitive inhibitor, while 1-acetoxypinoresinol **3** is a partial uncompetitive inhibitor to the  $\alpha$ -glucosidase enzyme<sup>189</sup>. The Lineweaver-Burk plots of the reaction of  $\alpha$ -glucosidase and the active compounds are shown in **Figure 18**.

The mixed type of inhibition by oleanolic acid **1** is similar to non-competitive inhibition, as of luteolin-7-*O*- $\beta$ -D-glucoside **6**, except that binding of the substrate or the inhibitor affects the enzyme’s binding affinity for the other<sup>190</sup>. The findings of oleanolic acid **1** and luteolin-7-*O*- $\beta$ -D-glucoside **6** inhibition types are in line with the previous report on oleanane-type pentacyclic triterpene acids and flavonoid luteolin, respectively<sup>191,192</sup>.



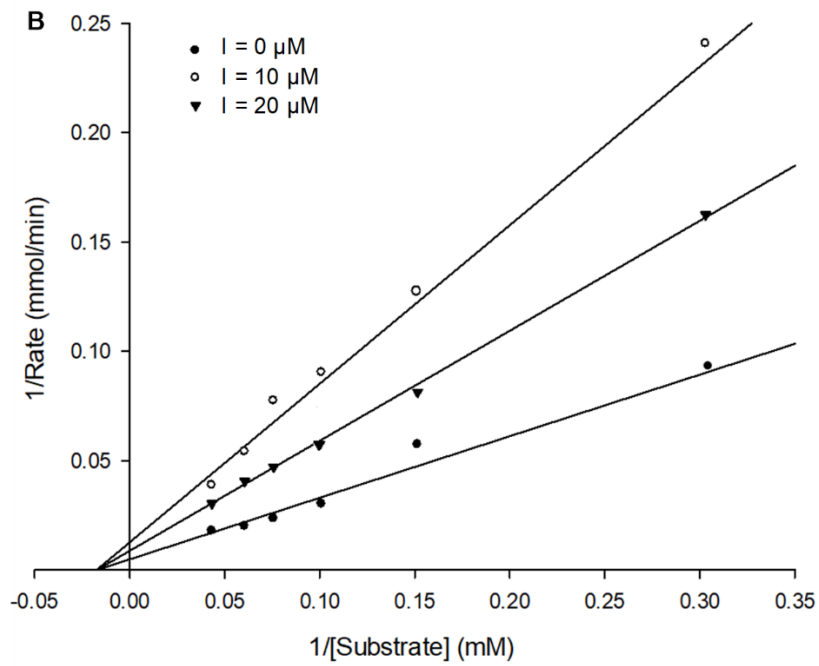
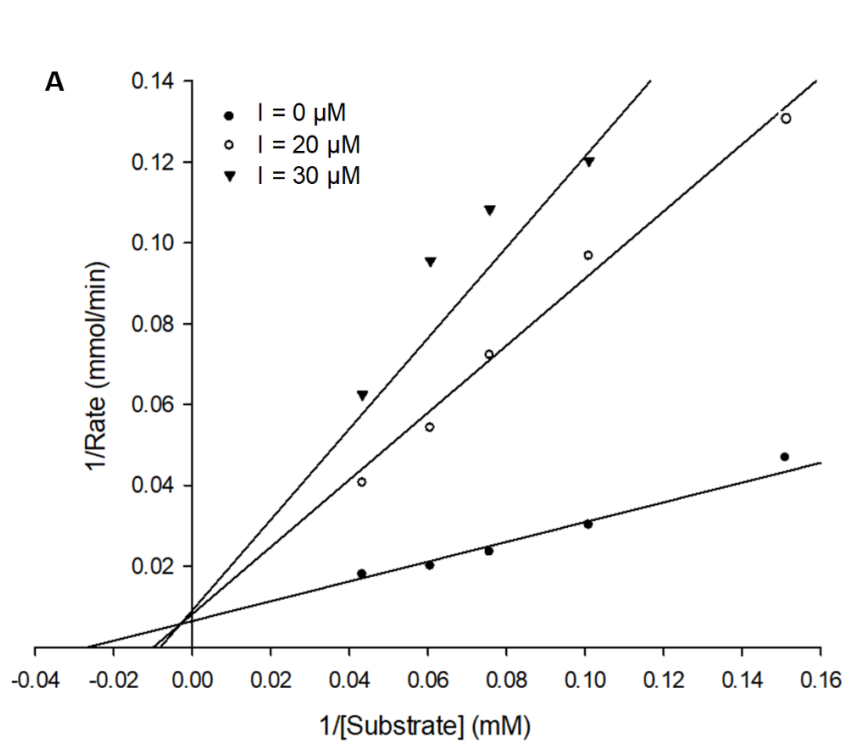


Figure 18 (A) & (B)

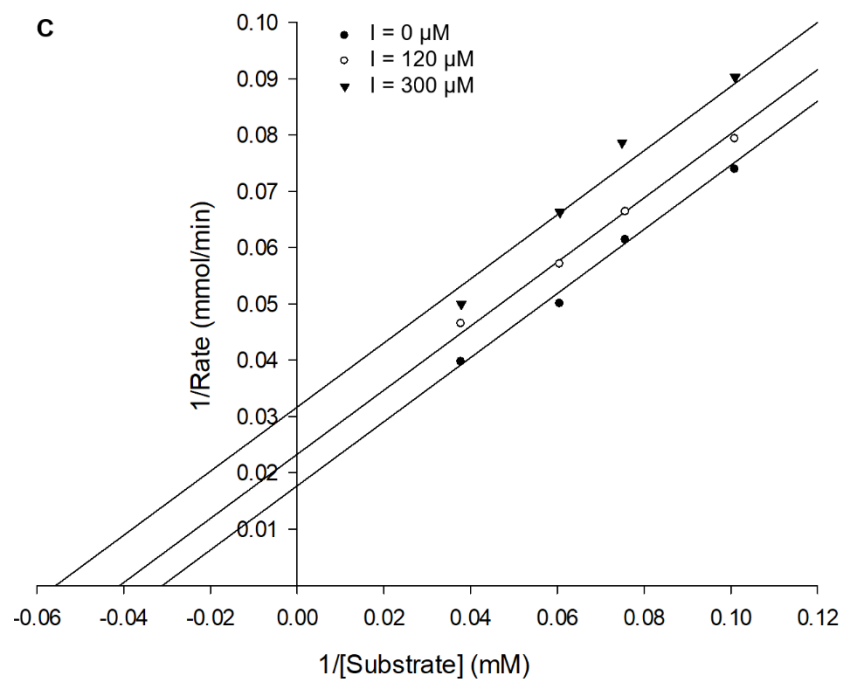


Figure 18: Kinetic analysis of  $\alpha$ -glucosidase inhibition. Lineweaver-Burk plots of the reaction of  $\alpha$ -glucosidase in the presence of the active compounds. (A) Oleanolic acid **1**, (B) Luteolin-7-*O*- $\beta$ -D-glucoside **6**, and (C) 1-acetoxypinoresinol **3**. The concentration of sucrose was measured in the absence or presence of inhibitors at different concentrations (I, Inhibitor; dark circles, no inhibitor; dark triangles, low concentration; black-lined transparent circles, high concentration).

On the other hand, this is the first report on lignan 1-acetoxypinoresinol **3**. As an uncompetitive inhibitor, 1-acetoxypinoresinol **3** binds to the enzyme at the same time as the enzyme's substrate, that is, it binds to the enzyme-substrate complex (it neither binds to the enzyme itself nor to the substrate) and this type of inhibition cannot be overcome but can only be reduced by increasing the substrate concentration <sup>193</sup>. Thus for all inhibition types, mixed type, non-competitive, and uncompetitive,  $K_i$  value, which measures the affinity of the inhibitor for an enzyme, is usually greater than 1 ( $K_i > 1$ ) <sup>190</sup> – for oleanolic acid **1**,  $K_i = 8.4$ ; luteolin-7-O- $\beta$ -D-glucoside **6**,  $K_i = 12.7$ ; and 1-acetoxypinoresinol  $K_i = 61.1$ . Moreover, this shows the fact that all these compounds have a quite different structure from that of substrate for the enzyme, and that is why they can't inhibit the enzyme competitively.

## Discussion

The raise of postprandial glucose levels in plasma is a result of the hydrolysis of carbohydrates, such as starch and sucrose – a process that is primarily catalyzed by two hydrolase enzymes;  $\alpha$ -glucosidase and  $\alpha$ -amylase. While  $\alpha$ -amylases specifically hydrolyze internal  $\alpha$ -1,4-glycosidic bond of starch to yield maltose and glucose,  $\alpha$ -glucosidases which are a series of enzymes found in the brush border of enterocytes hydrolyze both starch and sucrose down to glucose <sup>168,169</sup>. These processes are known to happen in the upper portion of the small intestine and are known to potentially raise plasma glucose, especially in diabetic patients <sup>194</sup>. Thus, the inhibitors of  $\alpha$ -glucosidase and  $\alpha$ -amylase enzymes are currently used, clinically as first-line drugs, for example, acarbose and voglibose, to reduce glucose postprandial (PPHG) plasma levels in patients with Type 2 diabetes. These drugs are capable of lengthening the duration time of carbohydrate absorption and hence reducing plasma glucose levels over time <sup>195</sup>.

The present study was designed to evaluate whether metabolites from OMW may be used to reduce carbohydrate hydrolysis by inhibiting these enzymes involved in diabetes and its complications, in comparison with acarbose. Generally, olives have been reported to have several biological activities including antioxidant <sup>17</sup> and anti-inflammatory <sup>196</sup>, among many others. These activities may, indirectly, help to reduce oxidative stresses and inflammatory bodies which may contribute to diabetes <sup>197,198</sup>. The antidiabetic activity has also been reported by several studies <sup>175–177,199,200</sup>. So far, for antidiabetic activity, reports are only on phenolic acids and olive fatty acids –

but no reports on other olive phenolic compounds, nor, on olive triterpenes. Moreover, the mechanism of inhibition of olives against  $\alpha$ -glucosidase and  $\alpha$ -amylase was not demonstrated in the previous studies.

In this study, it was observed that the triterpenes oleanolic acid **1** and maslinic acid **2** had good inhibitory activity against both enzymes, which is in line with the previous studies <sup>201</sup>. They (oleanolic acid **1** and maslinic acid **2**) have also been reported, previously, to have significant blood glucose-lowering effect *in vivo* studies. For example, oleanolic acid reported to lower blood glucose levels in STZ-induced diabetic rats <sup>202</sup>; and reduced glycogen levels and glycogenic enzymes in rats <sup>203</sup>. For maslinic acid; it was reported to reduce blood glucose levels by inhibiting glycogen phosphorylase <sup>204</sup>. The results of the present study suggest that the oleanane skeleton may be responsible for their anti-diabetic activity. This is not uncommon as previous research showed that other oleanane-type triterpenes, apart from oleanolic and maslinic acids, were also active. For instance, corosoric acid showed strong inhibitory activity not only *in vitro* against both  $\alpha$ -glucosidase and  $\alpha$ -amylase enzymes <sup>194</sup> but also reported having a significant effect on lowering post-challenge plasma glucose levels *in vivo* <sup>205</sup>. Considering the higher abundances of oleanolic **1** and maslinic acids **2** in OMW and their total activities for both  $\alpha$ -glucosidase and  $\alpha$ -amylase, these data attract more attention to OMW as a potential source of PPHG-lowering agents.

Furthermore, two phenolic compounds (1-acetoxypinoresinol **3** and luteolin-7-O- $\beta$ -D-glucoside **6**) showed stronger inhibitory activity, while the rest, three of them (**4**, **7**

and (+)-pinoresinol) had very weak activities against both  $\alpha$ -glucosidase and  $\alpha$ -amylase enzymes. 1-acetoxypinoresinol **3** showed a very strong inhibitory activity against both enzymes – with the strongest inhibitory activity for  $\alpha$ -amylase,  $IC_{50}=13.9 \mu\text{M}$  vs  $15.0 \mu\text{M}$  of acarbose; while for  $\alpha$ -glucosidase,  $IC_{50}=313.1 \mu\text{M}$  vs  $323.4 \mu\text{M}$ . Regardless of its strongest activity against  $\alpha$ -amylase, its total activity was lower than that of oleanolic acid **1** and maslinic acid **2**. This is accounted for by its low abundance in OMW, as opposed to **1** and **2** which were more abundant by several folds compared to **3** (**Table 12**). On the other hand, the inhibitory activity of (+)-pinoresinol, a compound with a closely related chemical structure to **3**, was very weak ( $IC_{50} > 500 \mu\text{g/mL}$  against both enzymes). Taking into account the differences in their inhibitory activities, between 1-acetoxypinoresinol **3** vs (+)-pinoresinol, it is arguably that esterification of the furofuran ring at position one (C-1) of 1-acetoxypinoresinol **3** enhances its  $\alpha$ -glucosidase and  $\alpha$ -amylase enzymatic inhibitory activity. While the inhibitory activities of **1** and **2** were consistent with those reported elsewhere <sup>201</sup>, this is the first report on antidiabetic activity for 1-acetoxypinoresinol **3** and (+)-pinoresinol. Luteolin-7-*O*- $\beta$ -D-glucoside **6** was more active against  $\alpha$ -glucosidase and relatively poor activity against  $\alpha$ -amylase. These findings are in line with the ones previously reported about flavonoid glycosides <sup>206–208</sup>.

The least active phenolic compounds, hydroxytyrosol **7**, hydroxytyrosol acetate **4** and 3,4-dihydroxyphenyl-2-methoxyethanol **5**, share a common structural feature – the presence of a 3,4-dihydroxyphenylethyl (3,4-DHPE) moiety. All of them had weak

inhibitory activity against both  $\alpha$ -glucosidase and  $\alpha$ -amylase. These findings show that even with several modifications, for instance, esterification of hydroxytyrosol at the ethyl –OH (to form hydroxytyrosol acetate) or alkylation at the ethyl C-2 (to form the new compound, 3,4-dihydroxyphenyl-2-methoxyethanol). Again, this is the first report on their inhibitory effect on hydrolase enzymes  $\alpha$ -glucosidase and  $\alpha$ -amylase. Previously, only the inhibitory activity of a phenolic extract from virgin olive oil (VOO) was reported to have an inhibitory effect on these enzymes; it was more active against  $\alpha$ -glucosidase than it was for  $\alpha$ -amylase. However, the researchers did not go further to test the inhibitory activity of individual phenolic compounds <sup>209</sup>.

Most studies that have reported about antidiabetic properties of olives and virgin olive oil, are based on epidemiological facts, whereby they correlated olive fatty acids, especially oleic acid, and antidiabetic effect of virgin olive oil <sup>175–177,199</sup>. Contrary, the current findings clearly showed that *n*-hexane fraction, which contains all fatty acids including up to 75% oleic acid <sup>200</sup>, had a poor inhibitory activity. Therefore, the present study gives evidence that not only fatty acids constituents that offer antidiabetic properties, but also other metabolites, such as triterpenes and phenolic compounds contribute to the antidiabetic properties. And it was consistent with one study whereby some researchers reported about the effectiveness of olive phenolic acids on  $\alpha$ -glucosidase and  $\alpha$ -amylase inhibitory activity <sup>209</sup>.

In general, this study confirmed that some metabolites in OMW are potential inhibitors of the hydrolase enzymes involved in the Type 2 DM – olive lignan (1-

acetoxypinoresinol **3**), pentacyclic triterpenes (oleanolic acid **1** and maslinic acid **2**), and luteolin-7-*O*- $\beta$ -D-glucoside **6**. This is the first study to address the  $\alpha$ -glucosidase and  $\alpha$ -amylase inhibitory activity of olive lignans ((+)-pinoresinol and 1-acetoxypinoresinol), as well as, hydroxytyrosol derivatives including the new compound, 3,4-dihydroxyphenyl-2-methoxyethanol, and hydroxytyrosol acetate. While the other compounds (**1**, **2**, and **6**) have been reported in the previous studies, but this is the first study that quantifies their contribution (of individual metabolite) in the OMW dry mass to the total inhibitory activity against  $\alpha$ -glucosidase and  $\alpha$ -amylase enzymes (antidiabetic).



#### **Part IV: CONCLUSION**

In summary, the results from this study clearly show that some compounds from OMW are potential inhibitors of  $\alpha$ -glucosidase and  $\alpha$ -amylase enzymes, which are involved in the hydrolysis of carbohydrates to generate glucose (PPHG) – one of the very first steps in the pathogenesis of diabetes. The mechanism of  $\alpha$ -glucosidase inhibition by active compounds was demonstrated, one of them being an olive lignan, 1-acetoxypinoresinol which has been reported for the first time. These results potentiate OMW as an important source of lead compounds for antidiabetic formulations, food supplements, or for modification to develop new antidiabetic drugs. It is, therefore, worth mentioning that, OMW (and its metabolites) will be valuable for further study, prevention, and/or treatment of Type 2 diabetes.

## Part V: CHAPTER SUMMARY

In this chapter, the isolated seven compounds from olive mill wastes (OMW), one of them being novel, and their antidiabetic potential through inhibition of  $\alpha$ -glucosidase and  $\alpha$ -amylase enzymes were investigated. To assist the possible characterization of the mechanisms involved, we analyzed the inhibitory kinetics of the active compounds. Oleanolic acid **1**, maslinic acid **2**, 1-acetoxypinoresinol **3**, and luteolin-7-*O*- $\beta$ -D-glucoside **6** exhibited stronger inhibitory activity against both enzymes, with  $IC_{50}$ -values less than or close to that of acarbose. Other compounds; pinoresinol and hydroxytyrosol-containing compounds (hydroxytyrosol acetate **4**, hydroxytyrosol **7**, and the novel one, 3,4-dihydroxyphenyl-2-methoxyethanol **5**) showed weak inhibitory activity against both enzymes ( $IC_{50} > 500 \mu M$ ). These findings suggest that; first, the esterification of C-1 of furofuran ring, is the key feature for the stronger inhibitory activity of 1-acetoxypinoresinol **3** against both enzymes ( $IC_{50} = 13.9 \mu M$ , and  $313 \mu M$  for  $\alpha$ -amylase and  $\alpha$ -glucosidase, respectively), as compared to pinoresinol; second, oleanane skeleton of the triterpenes (**1** and **2**), is optimum for the  $\alpha$ -glucosidase and  $\alpha$ -amylase inhibitory activity; while, hydroxytyrosol-moiety may be responsible for the weak activity of **4**, **5**, and **7**. Additionally, kinetics analysis of **1**, **6**, and **3**, revealed that they inhibit  $\alpha$ -glucosidase in a mixed-type, non-competitive and uncompetitive mechanisms, respectively. Their mechanisms were confirmed by measuring their affinity for the enzyme ( $K_i$ ), and they all (**1**, **6**, and **3**) had a higher affinity for the enzyme,  $K_i > 1$ . This work adds more value to OMW for

further studies as a potential source of lead antidiabetic compounds for the prevention and/ or treatment of Type 2 diabetes.

## **CHAPTER 4**

**Anti-Alzheimer's activity of olive leaves cultivars: Cultivar-specific metabolic profiling of olive leaves by LCMS based non-targeted metabolomics for determining AChE inhibitor metabolites**

## **Part I: INTRODUCTION – ALZHEIMER’S DISEASE**

### **4.1.1. Dementia and Alzheimer’s Disease (AD)**

Dementia is a major global burden with 44.4 million patients worldwide in 2013, with that number estimated to increase to 135 million by 2050 <sup>103</sup>. The most common cause of dementia is Alzheimer’s disease (AD), which accounts for 50% - 75% of all cases <sup>210</sup>. AD is more prevalent with aging – it is characterized by a severe, progressive memory loss accompanied by several neuropathological lesions such as the formation of senile plaques <sup>211–213</sup>. AD is now considered a global burden because, beyond its debilitating effects on patients, it presents with other two major socio-economic problems; high medical costs and a high requirement for care <sup>103</sup>. It is estimated that the global medical care for dementia (of which, the majority of cases are AD) is about US \$ 604 billion, which is 1% of the global GDP <sup>214</sup>. This means that dealing with an individual patient is very expensive, for instance, in the United States, the total annual societal cost per patient with AD ranges between US \$42,000 - \$56,000 <sup>104</sup>.

AD’s other core symptoms, apart from impairments of memory, include impairment of judgment, and other cognitive functions, as well as a reduction in the levels of acetylcholine (ACh) neurotransmitter – together, they are caused by synaptic loss and neuronal death <sup>101</sup>. As a result, many AD patients start presenting with a wide range of behavioral symptoms from psychosis to aggression to depression <sup>215</sup>.

Today, they are collectively known as behavioral disturbances, collectively known as behavioral and psychological symptoms of dementia (BPSD).

The cholinergic hypothesis of AD has provided the rationale for the pharmacotherapy of the disease since the last two decades <sup>211</sup>. This theory is based on the finding that a loss of cholinergic activity, commonly observed in the brains of AD patients, have suggested a role of ACh in learning and memory <sup>213,216</sup>, and that is why AD has a variety of symptoms including psycho-behavior disturbances, cognitive impairment, memory deficits, and learning disturbance <sup>217</sup>. Moreover, the cholinergic hypothesis is supported further by randomized clinical trials (CTs), in which it was found to contribute up to 19% of all AD etiologies – based on 2173 RCTs <sup>218</sup>. Thus, acetylcholinesterase (AChE) inhibitors are currently approved therapy for the treatment of AD, and generally, only a limited number of drugs are commercially available, hence raising the urgent need to research for new drugs. **Figure 19** summarizes cholinergic hypothesis of AD.

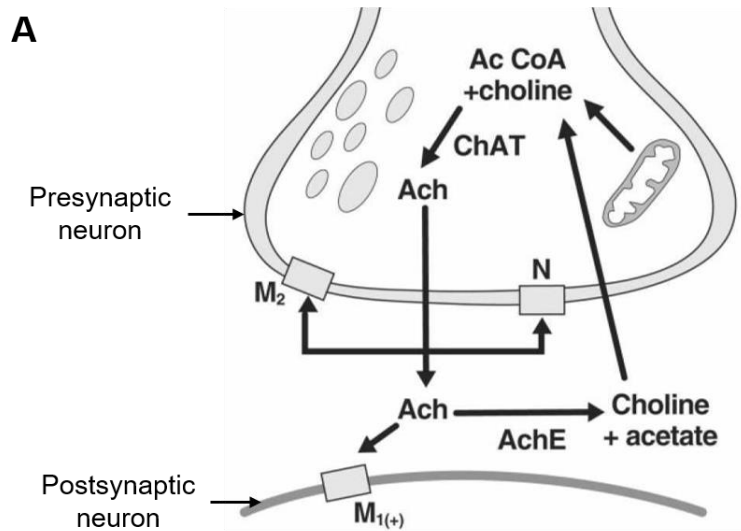


Figure 19: (A) Physiology of the cholinergic synapse. Choline is the critical substrate for the synthesis of acetylcholine (ACh). Acetyl coenzyme A (Ac CoA), along with the enzyme choline acetyltransferase (ChAT) are critical for the synthesis of acetylcholine (ACh). Once the neurotransmitter acetylcholine is released into the synapse, it binds (activates) postsynaptic receptor (M<sub>1</sub>), thus transmitting a signal from one neuron to the other. The excess neurotransmitter in the synaptic cleft is broken down by the enzyme acetylcholinesterase (AChE) into choline and acetate, which are returned by an uptake mechanism for recycling into acetyl coenzyme A. In AD, there is an increased AChE enzymatic activity that leads to cholinergic deficits leads to cognitive decline and memory loss. (B) Pathophysiological condition, in AD patients. Source for (A): 219.

#### **4.1.2. Olives and Treatment of AD: Research Gap and Way Forward**

Olives, through its major biophenol (hydroxytyrosol), are known to inhibit the activity of the AChE enzyme <sup>220</sup>. There is, however, still scarce of information describing the potential of other compounds in the olive which otherwise might be contributing to the activity. To make matters even difficult, there are so many cultivars or varieties of olive leaves that differ in their effectiveness. This means that a powerful tool to identify a wide range of low-molecular-weight compounds such as secondary metabolites is needed to solve this major challenge, and when coupled to high-tech analytical software such as Chemometrics, it becomes easier to associate between the metabolites and phenotype – in this case, cultivar type <sup>221,222</sup>.

Therefore, in this study, the metabolomics approach was employed for the unbiased evaluation of the anti-AChE properties of extracts of olive leaves cultivars and to identify bioactive compounds among cultivars. This is, to my knowledge, the first report about the MP-driven bioactivity evaluation of olive leaves cultivar extracts related to the anti-AChE activity.

#### **4.1.3. Metabolomics approach**

Metabolomics is the part of the 'omics' fields that focus on the wide variety of low molecular weight metabolites present in biological system/ sample (urine, blood, tissues, plant sample like leaves or roots). It can be defined as a comprehensive analysis of the whole metabolome under a given set of conditions – it may involve identification/ quantification of metabolites of a biological system <sup>223</sup>. The metabolites



in plant or any animal sample closely related, such as plant cultivars might differ depending on several factors such as chemical reactions taking place in the organism, or from exogenous sources such as climate or geographical location, nutrients used, drugs, and so on <sup>224,225</sup>. This technique is very efficient and effective in the identification of the bioactive metabolites in the complex biological system including those of closely related samples such as cultivars <sup>226</sup>.

The most common techniques used to perform metabolomics are NMR and MS <sup>223</sup>. Literature cites MS-based metabolomics as especially important for the largest metabolite coverage with the highest sensitivity <sup>227</sup>. It is usually coupled to different separation techniques such as liquid chromatography (LC), gas chromatography (GC) or capillary electrophoresis (CE). Due to high sensitivity of MS-based metabolomics, it can identify, quantify, and serve both for targeted and non-targeted metabolomics studies <sup>225</sup>. In the present study, we employed an LC coupled to high-resolution mass spectrometry (LC-MS)-based non-targeted metabolomics.

LC-MS offers an advantage in covering a wider range of low-molecular-weight secondary metabolites <sup>221</sup>. And by metabolic profiling, MP technique, the association between the metabolites and phenotype can be detected as well as for the evaluation of bioactivity and identification of metabolites conferring beneficial properties <sup>222,228</sup>. Coupled with chemometric methods, such as multivariate analysis (PCA, PLS-DA), the approach may be useful for the evaluation of specific biological property of crude extract and identifying specific bioactive metabolites in extracts.

This approach finds to be useful for the unbiased evaluation of the pharmaceutical properties of crude plant extracts and to identify specific bioactive metabolites in extracts.

## Part II: EXPERIMENTAL

### 4.2.1. Materials and Sample

The samples of fresh olive leaves cultivars were received monthly from January to December 2019 from an olive company's farm in Ukiha (Kyushu Island, Japan). During collection, the samples were harvested randomly. They were immediately ground with liquid nitrogen ( $-196\text{ }^{\circ}\text{C}$ ) in the laboratory, then freeze-dried for 5 days before ground further to fine homogeneous powder and were stored at  $-20\text{ }^{\circ}\text{C}$  prior to further analysis. In total, 18 cultivars of olive leaves as shown in **Table 15** have been received monthly and tested for the anti-AChE activity – for cultivars from January to June 2019. From July to December, the samples could not be tested due to time limitations.

In the end, six cultivars – three of them being active and the other three were not active, were chosen for further metabolomics studies to determine the AChE inhibitor metabolites. Six cultivars that were used for non-targeted metabolomics study to identify the anti-AChE metabolites. These were;

- a. Most active ones; Berhudar ( $n=3$ ), Frantoio ( $n=3$ ), and Lucca ( $n=3$ )
- b. Least active ones; Cippressino ( $n=3$ ), Hinakase ( $n=3$ ), and Nevadillo ( $n=3$ ).

### 4.2.2. Chemicals and reagents

The deionized water (18 M $\Omega$  cm) was purified by using a Milli-Q Ultrapure Water System RFU424CA (Advantec, Tokyo, Japan), LC-MS grade acetonitrile and LC-MS grade formic acid and, purchased from Wako Pure Chemical Industries (Osaka,

Japan) were used to prepare chromatographic mobile phases. Acetylthiocholine iodide (ATCI) was purchased from Tokyo Chemical Industry (Tokyo, Japan). Galantamine hydrobromide and acetylcholinesterase (AChE) 500 U/mg, were purchased from Sigma (St. Louis, MO, USA). 5,5-dithiobis [2-nitrobenzoic acid] (DTNB), NaOH, and DMSO were purchased from Wako Pure Chemical Industries, Ltd. (Osaka, Japan).

### **4.2.3. Methods**

#### **4.2.3.1. Procedure for Extraction of Olive Leaves Cultivars**

Extraction of Olive leaves was done by ordinary maceration, whereby, 100 mg of leaves sample (for each cultivar, 18 samples) were dissolved in 10 ml of extracting solvent, EtOH: Water (8:2) and macerated at r.t, 200 rpm for 2 h, then sonicated for 45 minutes. After sonication, all samples were centrifuged at 1680 g for 10 min and the supernatant was collected and were evaporated to dryness under reduced pressure in a rotary evaporator at 35 °C to obtain the dried extracts. The average extraction yield for all Olive cultivars ranged between 25.0 – 35.0% (w/w). The dried residues (extracts) were then dissolved in DMSO to prepare different concentrations to test for their inhibitory activity against AChE.

**Table 15: Leaf Size of the Sampled Leaves Cultivars**

	Cultivar Name	Physical dimension (l×w = cm × cm)*
1	Ascolana	6.07×1.45
2	Arbequina	4.38×1.07
3	Santa Caterina	2.28×0.94
4	Gemlik	2.9×1.14
5	Correggiolo	5.26×1.7
6	Cipressino	6.44×1.66
7	Taggiasca	6.88×1.74
8	Nevadillo blanco/ Hojiblanca	5.2×1.7
9	Frantoio	5.42×1.24
10	Berhudar	5.16×1.28
11	Pendolino	5.88×1.32
12	Maurino	4.88×0.96
13	Mission	6.16×1.35
14	Moraiolo	5.24×1.54
15	Lucca	5.1×1.8
16	Lechin de Sevilla	4.4×1.66
17	Leccino	5.2×1.82
18	Hinakase	-

\* The dimensions presented as Mean of 5 different leaves ( $n=5$ ) <sup>b</sup> Water content expressed in %

#### **4.2.3.2. Assay for AChE inhibitory activity**

AChE inhibition activity was measured using Ellman's method <sup>229,230</sup>. AChE hydrolyzes the substrate ACTI into acetate and thiocholine. In a neutral or alkaline medium; thiocholine reacts with DTNB to give yellow-colored 2-nitro-5-thiobenzoate, which can be detected spectrophotometrically at 405 nm. Briefly, in a 96-well plate, 25 mL of 15 mM ACTI, 125 mL of 3 mM DTNB in buffer B (50 mM Tris-HCl, pH 8, 0.1 M NaCl, 0.02 M MgCl<sub>2</sub>.6H<sub>2</sub>O), 50 mL of buffer A (50 mM Tris-HCl, pH 8, 0.1% BSA) and 25 mL of the test sample were mixed, and the absorbance was measured using a microplate reader (Corona, Japan) at 405 nm every 60 s for ten times.

Then, 25 mL of AChE (0.25 U mL<sup>-1</sup> in buffer A) was added and the absorbance was measured ten times every 60 s. A solution of 25% DMSO was used as a negative control. The absorbance was plotted against time and the enzyme activity was calculated from the slope of the line, and so was obtained and expressed as a percentage compared to an assay using a buffer without any inhibitor.

#### **4.2.3.3. Sample Preparation for Untargeted LCMS-Based Metabolomics**

The powder of olive leaves of each cultivar, 500 mg, was extracted by sonication with 50 mL of aqueous EtOH (70%, v/v) for 45 min at 30 °C. The extracted solution was then filtered, and this process was repeated twice for the evaluation of the recovery percentage of the extraction system. Then, the combined filtrate was evaporated to dryness at reduced pressure by a rotary evaporator at 45 °C. The

residue was finally reconstituted in MeOH to a final concentration of 200 µg/ml. Before injection for chromatographic separation, it was filtered twice through Millipore 0.20 µM PTFE filters (Millex-LG, Japan).

#### **4.2.3.4. UPLC/QTOF-MS Analysis of the Olive Leaves Cultivar Extracts**

Agilent 1290 Series UPLC system, consisting of vacuum degasser, cooled autosampler, rapid resolution binary pump, and thermostatted column compartment (Agilent Technologies, Santa Clara, CA, USA) hyphenated to an Agilent 6545 Q-TOF hybrid mass spectrometer (MS) equipped with a dual Agilent Jet Stream (AJS) electrospray ionization (ESI) source (Agilent Technologies, Santa Clara, CA, USA), for simultaneous spraying of a mass reference solution that enabled continuous calibration of detected  $m/z$  ratios was used for analysis.

The chromatographic separation was performed on a reversed-phase Zorbax Eclipse Plus C18 analytical column (100 × 3.0 mm i.d, 1.8 µm particle size, Agilent Technologies, Santa Clara, CA, USA) coupled to a guard column Agilent Eclipse Plus C18 (3.0 × 5 mm, 3.8 µm particle size) and an inline-filter. An injection volume of 2 µL and a flow rate of 0.4 mL/min was used for elution. The mobile phases were 0.1% (v/v) formic acid in aqueous solution (eluent A) and 0.1% (v/v) formic acid in acetonitrile (eluent B). The gradient elution method was as follows: isocratic step at 4% B for 2 min, 4 to 100% B in 15 min, then 100% B was maintained for 2 min, and then re-equilibrated for 3 min. The column oven was maintained at 40 °C.

The dual ESI source operated in negative ionization set at the following conditions: nebulizer gas pressure: 35 psi; drying gas flow rate: 10 L/min; gas temperature; 325 °C. The capillary voltage was set at 3.5 kV, while skimmer voltage: 65 V; octapole voltage: 750 V; dielectric capillary exit (fragmentor voltage): 130 V. The data were acquired in both centroid and profile modes in the extended dynamic range (2 GHz). The instrument was calibrated and tuned according to procedures recommended by the manufacturer. Accurate mass spectra were acquired in the  $m/z$  range 50–1100 in all-ion fragmentation (AIF) mode, where a single high-resolution full scan is acquired, including three sequential experiments at three alternating collision energies (one full scan at 0 eV, followed by one MS/MS scan at 10 eV, followed by MS/MS scan at 20 eV, and then followed by another one MS/MS scan at 40 eV). The data acquisition rate was 4 scans per second. To ensure the desired mass accuracy of recorded ions, a continuous internal calibration was performed during analyses with the use of reference solution signals at  $m/z$  112.9855 (TFA anion) and  $m/z$  1033.9881 (trifluoroformate adduct of hexakis[1H,1H,3H, tetrafluoropropox]phosphazine).

The internal reference solution was introduced into the ESI source via a T-junction using an Agilent Series 1290 isocratic pump (Agilent Technologies, Santa Clara, CA, USA). For data acquisition and monitoring the hardware, Agilent MassHunter Workstation software (Agilent Technologies, Santa Clara, CA, USA) was used. Mass accuracy of <5 ppm was expected for the potential metabolite co-elution and isobaric compounds.



#### 4.2.4. Data Processing and Statistical Analysis

The Agilent MassHunter Profinder (version B.08.00, Agilent Technologies, USA) was used for processing the obtained raw UPLC/QTOF-MS full single MS data. Batch Recursive Feature Extraction algorithm was employed for a full single MS data, in which all ions with identical elution profiles and related  $m/z$  values were extracted as molecular features (MFs) characterized mainly by retention time (RT), intensity in the apex of the chromatographic peak, and accurate mass. Other main parameters during the extraction of MFs were optimized as follows; two intensity threshold settings 5000 and 10,000 counts per second (cps) were tested for the MFs extraction while peak filter thresholds were tested at 600 and 1000 counts, both in the full scan RT range of 20 min. The test below 5000 cps was not done as low-abundance ions can be hard to identify if the precursor ion intensity is low, generally below 5000 counts for an Agilent Q-TOF <sup>231</sup>.

Finally, the thresholds of peak filters and metabolite filters were set at 1000 counts and 5000 counts, respectively, to produce an optimized matrix containing fewer biased and redundant data. To perform subtraction of MFs from the background, such as polymers or plasticizers and other contaminating compounds, analysis of the blank sample (aqueous methanol 95:5 v/v) was carried out under identical instrument settings and the background MFs were removed. Using background-subtracted data, files in compound exchange format (.cef files) were created for each sample and imported into the Agilent Mass Profiler Professional (MPP) software

package (version 14.5) (Agilent Technologies, Santa Clara, CA, USA) for further processing of the differential analysis, whereby alignment, normalization, defining the sample sets, and filtering of the MFs were applied. In the alignment step, all metabolites whose absolute abundance were greater than 5000 counts across the sample set were aligned by RT and accurate mass ( $m/z$ ) using the tolerance 0.1 min and 15 ppm, respectively.

Then, a stepwise reduction of the MFs number was performed based on frequency, abundance of the respective MFs in the cultivars, results of one-way analysis of variance (ANOVA), and fold change. In order to lower the relatively large differences among the MFs abundances, mean-centered and logarithmic transformation on the data was performed. To take a deep look at whether the difference between six cultivars exists, the MPP software enabled the conduction of multivariate analysis; unsupervised principal component analysis (PCA) and supervised partial least square discrimination analysis (PLS-DA) of the data. The validation of the obtained PLS-DA predictive model was done by using a cross-validation procedure in which its prediction accuracy was tested. Finally, the selected marker compounds (MFs) were analyzed by Agilent MassHunter Qualitative Analysis software (version B.10.00, Agilent Technologies, USA) for MS/MS data acquisition for molecular formula estimation to establish their IDs based on fragmentation pattern.

The  $IC_{50}$  values were calculated from plots of log concentration of inhibitor concentration against the percentage inhibition curves using Microsoft Excel 2016.

The data were expressed as Mean  $\pm$  standard deviation (S.D.) of at least three independent experiments ( $n=3$ ).

## Part III: RESULTS AND DISCUSSION

### 4.3.1. Anti-AChE Activity of Olive Leaves Cultivars

A total of 90 samples (18 olive leaves cultivars harvested in five months, Jan to May) were analyzed for their AChE inhibitory activity in the present report. The analysis shows that, firstly, all cultivars of March harvest exhibited the strongest inhibitory activity against the enzyme – whereby, at 500 µg/ml, their inhibitory rate was by more than 85% (whereby the inhibitory effect of the standard, galanthamine IC<sub>50</sub> was 1.7 µg/ml, while that of hydroxytyrosol, a known anti-AChE in olives, was 9.5 µg/ml). Secondly, all cultivars of April and May harvest exhibited relatively weak inhibitory activity, a similar observation was made for January harvest – both January, April, and May cultivars, all of them, had IC<sub>50</sub> > 500 µg/ml (Data not shown).

Even though there were some inconsistencies in the cultivars' activity, it was found that cultivars like Frantoio, Berhudar, Lucca, and Arbequina showed consistently higher activity from January through March – with peak activity on March (**Figure 20**). Therefore, from this data, three most active olive leaves cultivars; Frantoio, Berhudar, and Lucca, and three least active cultivars; Cippressino, Nevadillo Blanco, and Hinakase cultivars were chosen for further analysis by non-targeted metabolomics approach to find out the major cause of these differences among them, and also to test the power of the approach in predicting the effectiveness of the cultivars.

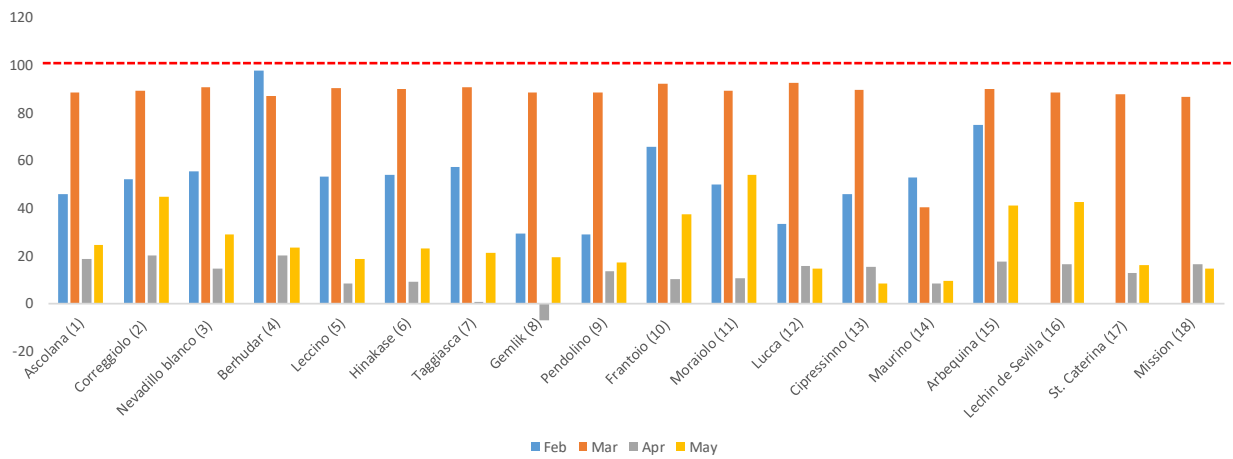
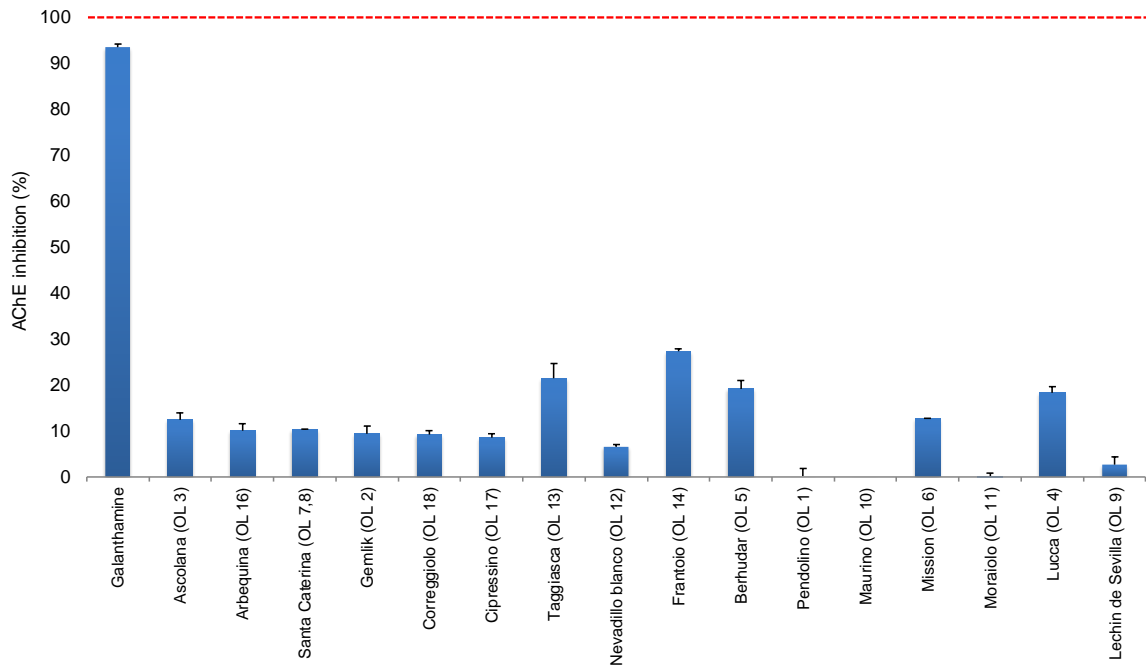


Figure 20: AChE inhibitory activity of Olive leaves cultivars at 500 µg/ml (upper figure, January harvest; Lower figure, February to May harvest)

#### 4.3.2. Validation of the UPLC/QTOF-MS Analytical Method

The metabolites were extracted with aqueous EtOH (70%, v/v), separated on a reversed-phase (C18) column, and analyzed by MS in the negative mode<sup>184</sup>. Since it was a non-target approach, we set both UPLC separation and MS detection with generic settings during the method development, to obtain metabolic profiles containing as many compounds as possible covering both highly polar and less-polar ones. For validation of the method, the quality control (QC) specimen, prepared by taking 10  $\mu$ L samples from each of the six cultivar groups and pooled together, and the acquisition of the QC specimen was the same as that of all other samples. Before experimental data acquisition, we did five consecutive injections of the QC specimen to obtain a stable QTOF-MS system. Immediately after five injections of the QC, the acquisition of data for samples was then launched. In the sequence, a QC sample was analyzed every 10 samples throughout the whole analysis.

Since good reproducibility and stability of metabolite retention times (RTs) represent an important parameter for method validation, as it is closely associated with the outcome of the aligning procedure performed across the sample set, 10 sets of data obtained via the acquisition of QC specimen was used to assess the repeatability of the method. Five characteristic ions ( $m/z$  315.1085 with retention time 4.66 min;  $m/z$  623.1981 with retention time 6.53 min;  $m/z$  539.1824 with retention time 7.39 min;  $m/z$  319.1186 with retention time 8.22 min;  $m/z$  471.3487 with retention time 13.62 min) were chosen to examine the shifts in RTs,  $m/z$ , peak area, and peak intensity

to assess the stability of the system. Based on repeated measurements, the typical RT variability was found to be 0.3 s or a relative standard deviation (RSD) of less than 0.1%, while for peak area for each peak was less than 15%. The result is summarized in **Table 16**. The experiment gave excellent stability and repeatability of the system, which means that it yielded reasonable data that can be further processed to obtain credible results.

**Table 16: The variability of retention times (RT), impulse *m/z* and peak areas in 10 sets of data obtained via acquisition of QC specimen**

<b>RT (Min)</b>	<b><i>m/z</i></b>	<b>Diff (ppm)</b>	<b>RSD (RT)</b>	<b>RSD (Area)</b>
<b>4.659</b>	315.1085	0.32 - 2.54	0.07%	7.7%
<b>6.528</b>	623.1981	0.16 - 3.85	0.07%	9.4%
<b>7.393</b>	539.1782	0.74 - 3.71	0.06%	5.8%
<b>8.219</b>	319.1199	0.62 - 3.76	0.05%	8.8%
<b>13.629</b>	471.3479	0.21 – 3.82	0.08%	13.4%



### 4.3.3. Metabolite Profiling (MP)

For metabolic profiling/ data mining, a high-resolution Q-TOF LC/MS metabolomics workflow for unbiased metabolomics study of cultivar-specific metabolites was developed. The metabolites were separated on RP column and analyzed by MS in the negative mode <sup>184</sup>. Both UPLC separation and MS detection were set to obtain MPs containing as many compounds as possible covering both highly polar and less-polar ones. The combined TCC obtained for the six cultivars seemed closely similar with (Figure 21). Most major peaks found in the total ion chromatograms (TICs) of the individual cultivars.

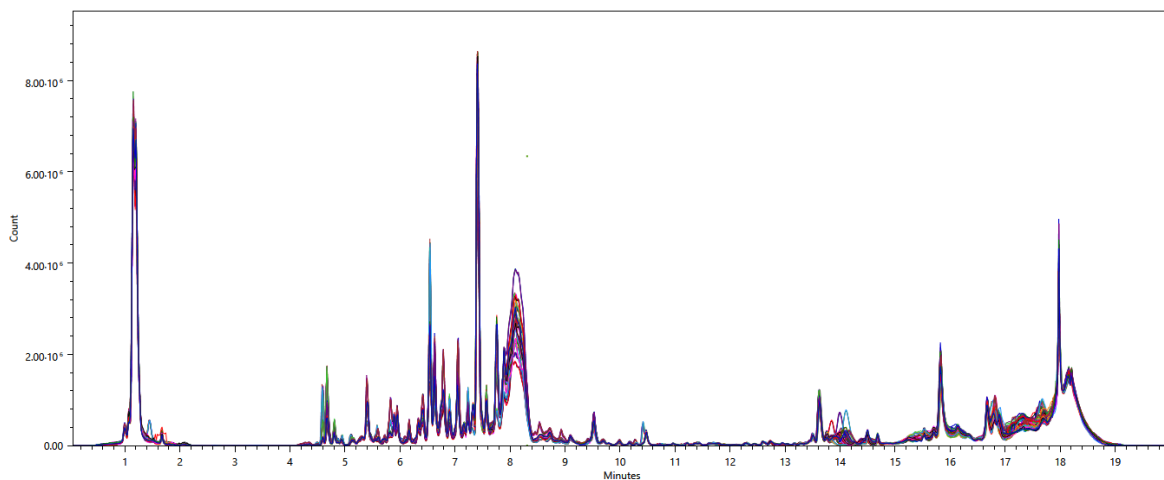


Figure 21: Combined TCC obtained from the six olive leaves cultivars

### 4.3.4. Data Mining and Pre-treatment

Taking into consideration the complexity of the raw data obtained by LC/MS analysis (Figure 21), the manual data inspection to distinguish the chemical profile among the cultivars is not possible, or else, it would be time demanding and not efficient at

all. For this reason, in data mining, several analytical software to extract metabolites from the cultivars were employed and coupled to chemometric software for further treatment. Bearing in mind that multiple signals can originate during ESI ionization of a single compound, it means that, for a complex set of data such as extracts (as we are dealing with), ESI can result into an extremely high amounts of signals. Therefore, to reduce this possible drawback causing signal redundancy, ions with accurate  $m/z$  values differences corresponding to adducts, isotopes or multiply charged species, supposing they had an identical elution profile, were merged and further handled as a single variable.

In the process, firstly, the secondary metabolites in the cultivar samples mined from LC/MS analysis to get the raw data were further processed with MassHunter Profinder software to recognize the ion peaks and the chemical metabolites. An algorithm enabling automated extraction of ions corresponding to compounds present in the samples was employed, “find compounds by molecular feature” (MFs) algorithm. The obtained extracted metabolites (MFs) were exported as compound exchange format (.cef) files, and these files were then imported into Mass Profiler Professional (MPP) software (Agilent Technologies, USA) for further differential analysis including alignment, normalization, defining the sample sets, filtering by frequency (FbF).

Usually, the number of obtained MFs aligned across the sample set was significantly influenced by the intensity threshold setting used during the data mining procedure

(not shown here). Due to that fact, before multivariate analysis (PCA and PLS-DA), the data dimensionality was reduced so that to use the most important marker compounds for the olive leaves cultivar discrimination. Several filtering procedures were applied to initial MFs (which were 1194 MFs, after removal of MFs extracted from the blank samples).

In the first step, all the MFs that were not present in at least 50% of samples in at least one group were removed, in this case, a cultivar type – the number was reduced to 1109 MFs. The next phase involved filtering based on *p*-values calculated for each MF by one-way ANOVA. The *p*-value cut-off of 0.05 was applied as the filtering criterion to ensure that only MFs which differ in the respective cultivars with 95% statistical significance are passed on and further processed – here the number was reduced to 644 MFs. Then, the last filtering step was performed using a fold change (FC) analysis, which finds MFs with high abundance ratios between two cultivar samples, picking out only MFs with  $FC \geq 2.0$  – the number was reduced further to 418 MFs. Lastly, a careful inspection of resultant EICs of each MF from the FC analysis was performed to avoid any false positive MFs. As a result, many MFs were regarded as false positive and hence were removed from each of the filtered MF groups. The final number of MFs obtained after manual recursion was reduced to 66 MFs only (**Table 17**). **Figure 22** shows all 1194 metabolites aligned among 18 samples (A), most of the metabolites presented low frequency, which was confirmed by the mass-retention curve of metabolites after alignment (**Figure 22(B)**).

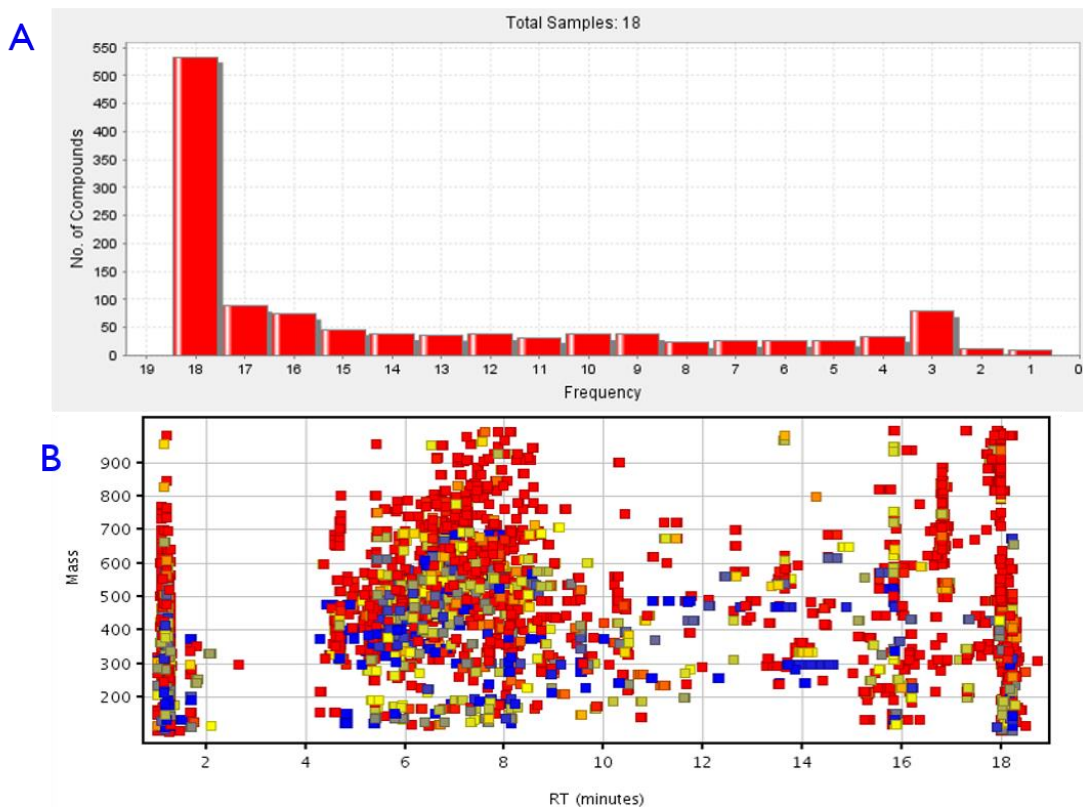


Figure 22: **(A)** The overall situation of aligned metabolites in 18 cultivar samples, and **(B)** the mass-retention curve of aligned metabolites. Where; red color represents the lower frequency metabolites, while the higher frequency metabolites are marked by blue color.

**Table 17: The overview of final MFs obtained in negative ion mode**

<b>No.</b>	<b><i>m/z</i></b>	<b>RT (Min)</b>	<b>No.</b>	<b><i>m/z</i></b>	<b>RT (Min)</b>
<b>1</b>	624.2061	<b>6.54</b>	<b>23</b>	540.1852	<b>7.98</b>
<b>2</b>	584.212	<b>7.76</b>	<b>24</b>	336.1199	<b>6.58</b>
<b>3</b>	448.1014	<b>6.63</b>	<b>25</b>	818.225	<b>7.44</b>
<b>4</b>	524.1883	<b>7.89</b>	<b>26</b>	834.2187	<b>7.05</b>
<b>5</b>	316.1155	<b>4.67</b>	<b>27</b>	472.3539	<b>13.76</b>
<b>6</b>	578.1618	<b>6.79</b>	<b>28</b>	378.1309	<b>8.07</b>
<b>7</b>	432.1066	<b>7.06</b>	<b>29</b>	464.0956	<b>6.61</b>
<b>8</b>	378.1308	<b>8.07</b>	<b>30</b>	618.3923	<b>14.68</b>
<b>9</b>	390.1163	<b>5.39</b>	<b>31</b>	270.052	<b>8.93</b>
<b>10</b>	702.238	<b>7.23</b>	<b>32</b>	652.1978	<b>7.76</b>
<b>11</b>	570.1953	<b>7.33</b>	<b>33</b>	494.1414	<b>7.86</b>
<b>12</b>	422.2336	<b>17.64</b>	<b>34</b>	724.2188	<b>6.56</b>
<b>13</b>	138.0308	<b>8.06</b>	<b>35</b>	356.1112	<b>5.82</b>
<b>14</b>	556.1798	<b>6.53</b>	<b>36</b>	514.204	<b>7.41</b>
<b>15</b>	402.1516	<b>5.83</b>	<b>37</b>	478.1478	<b>6.66</b>
<b>16</b>	608.2108	<b>6.89</b>	<b>38</b>	306.0769	<b>5.80</b>
<b>17</b>	286.0471	<b>8.24</b>	<b>39</b>	516.0878	<b>6.63</b>
<b>18</b>	302.0426	<b>8.31</b>	<b>40</b>	342.0946	<b>5.10</b>
<b>19</b>	342.1173	<b>1.12</b>	<b>41</b>	776.2351	<b>7.00</b>
<b>20</b>	404.1311	<b>5.89</b>	<b>42</b>	300.1203	<b>5.12</b>
<b>21</b>	390.1173	<b>4.69</b>	<b>43</b>	558.2297	<b>7.96</b>
<b>22</b>	318.0623	<b>1.21</b>	<b>44</b>	462.1745	<b>4.95</b>

\* Intensity threshold 5,000 cps

**Table 17, continue...**

<b>No.</b>	<b><i>m/z</i></b>	<b>RT (Min)</b>
<b>45</b>	622.1900	<b>6.54</b>
<b>46</b>	402.1882	<b>6.34</b>
<b>47</b>	354.0953	<b>5.47</b>
<b>48</b>	594.1577	<b>5.71</b>
<b>49</b>	980.2781	<b>7.22</b>
<b>50</b>	472.3537	<b>12.73</b>
<b>51</b>	196.0737	<b>7.38</b>
<b>52</b>	432.1174	<b>7.06</b>
<b>53</b>	506.1819	<b>1.20</b>
<b>54</b>	390.1156	<b>4.35</b>
<b>55</b>	484.2302	<b>7.78</b>
<b>56</b>	286.0478	<b>7.04</b>
<b>57</b>	320.1267	<b>6.63</b>
<b>58</b>	358.1414	<b>6.91</b>
<b>59</b>	326.1001	<b>5.59</b>
<b>60</b>	964.2818	<b>7.53</b>
<b>61</b>	384.1025	<b>4.67</b>
<b>62</b>	594.1571	<b>6.42</b>
<b>63</b>	624.2062	<b>6.78</b>
<b>64</b>	646.1861	<b>6.54</b>
<b>65</b>	448.1010	<b>7.23</b>
<b>66</b>	624.2061	<b>6.54</b>

\* Intensity threshold 5,000 cps

#### 4.3.5. Identification of the Cultivar Biomarkers

In the present study, we tried to identify the compounds which can be used as cultivar markers. The identification is necessary to know and identify these compounds and to accomplish this purpose the availability of standards for the marker compounds could facilitate simpler tests for identification of specific cultivar. By using the single MS accurate mass data for the pseudo molecular ion and its isotopes, a molecular formula for each marker compound can be generated. Those formulae that provide the best fit of this data can be used to search private and public databases of possible compounds. Using these data to search the databases (such as PubChem, ChemSpider and MetLin) results in a suspect identification of the compounds. Moreover, applying the Q-TOF, accurate MS/MS of the suspect  $m/z$  gives further identification of the compounds. However, without any idea of what a compound might be, even both accurate MS and MS/MS data would be difficult to interpret to obtain a compound structure. Thus, it remains a significant bottleneck in non-targeted metabolomics to correctly annotate the biological identity of a detected molecular feature (MF)/ compound <sup>232–234</sup>. Therefore, for the final confirmation, standard compounds of the indicated compounds were required.

Since it requires several steps to pass before confirmation of the proposed compound (MF), several guidelines have been proposed for metabolite identification. In the present study, one of the most frequently used guidelines known as Metabolite Standard Initiative (MSI) was adopted <sup>235</sup>. The MSI defined four levels of metabolite identification. The highest level (level 1) is based on matching two or more

orthogonal properties [e.g., accurate mass (AM), retention time (RT)/index, isotopic pattern, MS/MS spectrum] of an authentic reference standard analyzed under the same condition as the metabolite of interest. This level of structural information provides a high level of confidence in metabolite identity but is resource-intensive. Level 2 is based on matching the accurate mass (AM), retention time (RT), and isotopic pattern (AMRT + IP), while the lowest level (level 4) is based on matching only one orthogonal property, especially the accurate mass MS only (AM).

Based on our results, of the 66 MFs, only 29 gave a result from a database – their molecular formula estimation and subsequent tentative identification of these MFs as marker compounds was performed based on accurate mass only, AM (level 4 of MSI), and the error was found to be within acceptable limits ranging between -3 to 2 ppm (see the result in **Appendix i**). However, 5 markers (out of 29 MFs identified), were detected in multiple retention times. For example; MF #3 with  $m/z$  448.101 was detected at RTs 7.23 min and 6.63 min; MF #48 with  $m/z$  594.1577 at RTs 5.71 min and 6.42 min; and MF #9  $m/z$  390.1163 at RTs 4.35 and 5.39 min. Based on the current AM-only identification, it is still hard to conclude the true identity of these markers – in the next steps, comparison with the standards' RTs, MS/MS, and isotopic patterns will be done.

Based on the EICs of the olive leaves cultivars, we could propose some of the MFs as specific marker compounds for a certain cultivar. For instance; the marker specific for Cippressino cultivar is  $m/z$  137.0246 [M-H]<sup>-</sup>, RT 8.02 min; for Hinakase cultivars



are  $m/z$  577.1583 [M-H]<sup>-</sup>, RT 6.79 min, and  $m/z$  401.1461 [M-H]<sup>-</sup>, RT 5.84 min (both shown on the top-most row in **Figure 23**). The marker  $m/z$  515.0804 [M-H]<sup>-</sup>, RT 6.63 min, could be used to differentiate Lucca cultivar from other five cultivars (middle row in **Figure 23**). On the other hand, we observed that, some markers were found in almost equal amount, thus they are not specific and cannot be used to discriminate the cultivars. For instance, the markers  $m/z$  539.1791 [M-H]<sup>-</sup>, RT 7.41 min; and  $m/z$  471.3493 [M-H]<sup>-</sup>, RT 13.74 min (bottom-most row in **Figure 23**). Based on AM-only identification, these 'non-specific' markers were oleuropein and maslinic acid, respectively – major compounds reported in olives.

Lastly but not least, is the marker  $m/z$  569.1880 [M-H]<sup>-</sup>, RT 7.33 min; this marker can be used to differentiate Cippressino cultivar from Nevadillo cultivar (middle row in **Figure 23**).

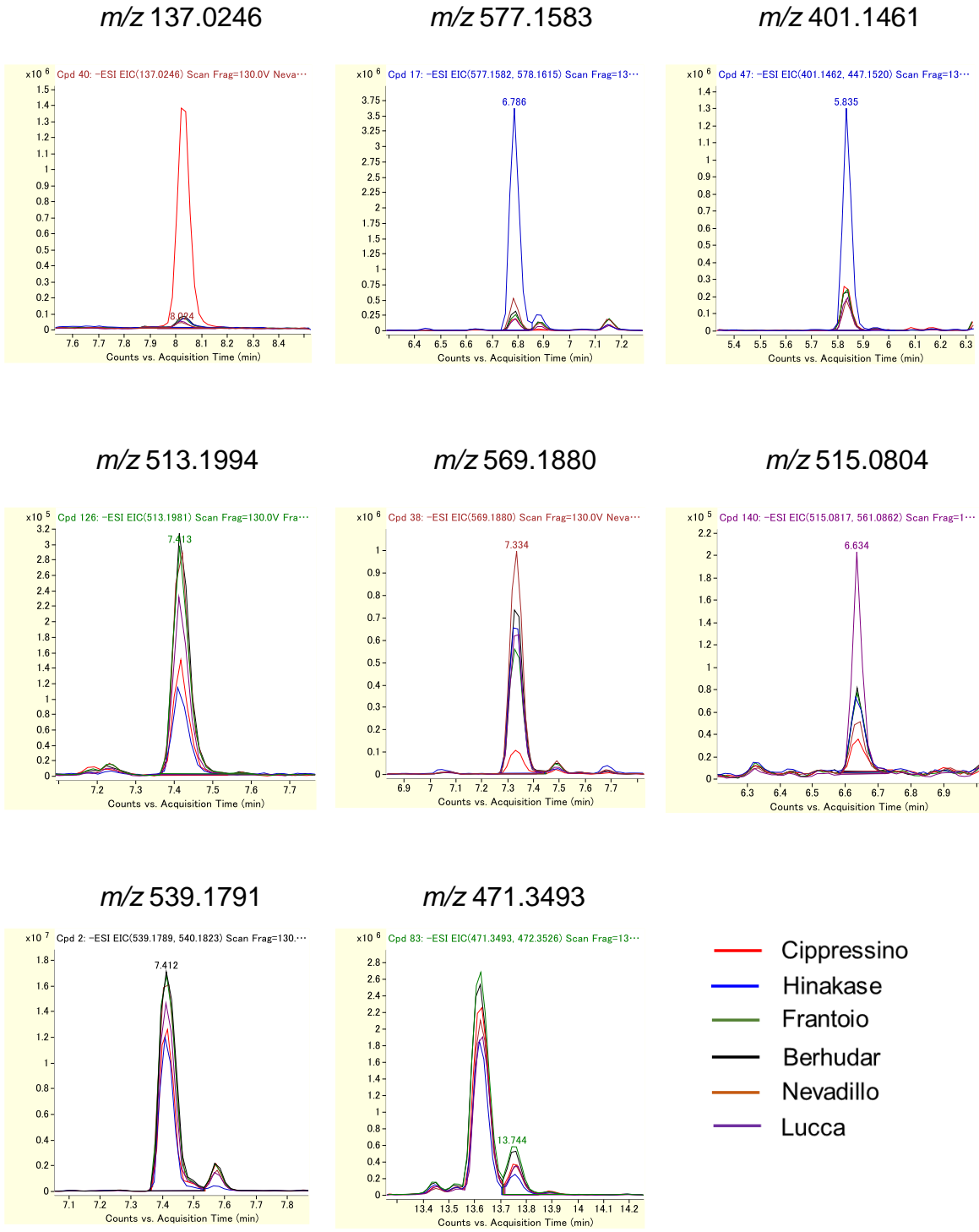


Figure 23: EIC of possible markers to discriminate olive leaves cultivars in the negative ionization mode ([M-H]).

#### **4.3.6. Multivariate Analysis**

In multivariate analysis of the samples, unsupervised PCA and supervised PLS-DA models were applied for QC and discrimination analysis, respectively. Following the above data pre-treatment, PCA score plot was employed in the first phase of multivariate analysis for the data to evaluate sample clustering according to the olive cultivar. Before going to the results of the multivariate analysis obtained in the present study, below is a description of the PCA and PLS-DA.

Principal component analysis (PCA) is employed unsupervised pattern recognition technique enabling data dimensionality reduction, and at the same time retaining maximum variability of the data. PCA is often applied as the first step of the data analysis for the detection of the patterns in the measured data. PCA allows data visualization by retaining as much as possible the information present in the original data even after the reduction of data dimensionality. It means that PCA transforms the original measured variables into new uncorrelated variables called “principal components, PCs”. Each PC represents a linear combination of the original measured variables. Thus, PCA affords a group of orthogonal axes that represent the directions of greatest variance in data. The first component (PC1) accounts for the maximum of the total variance in the Y-axis direction, the second, PC2 is uncorrelated with the first and accounts for the residual maximum variance in the X-axis direction, while PC3 is correlated roughly with the two. In many instances for practicality, only those components that account for a large percentage of the total

variance are retained. The betterness of the clustering ability of the PCA is defined by the component scores <sup>236,237</sup>.

Partial least square (PLS) is a commonly used supervised pattern recognition method that is capable of class prediction. PLS modeling is a multivariate projection method for modeling a relationship between dependent (Y) and independent variables (X) <sup>238</sup>. The major principle of PLS is to find the components in the input matrix (X) that describe as much as possible the relevant variations in the input variables and at the same time have a maximal correlation with that in Y. In other words, PLS models both X and Y simultaneously to find the latent variables in X that will predict the latent variables in Y <sup>237</sup>. The partial least squares discriminant analysis, also known as discriminant PLS (PLS-DA), aims to find the variables and directions in the multivariate space which discriminate the established classes in the calibration set. An optimal number of latent variables can be estimated by using cross-validation or external test sets. In PLS-DA, the Y matrix is constructed with zeros and ones. It is consisted of as many columns as there are classes and an observation had the value 1 for the class it belongs to and 0 for the rest. The X matrix consists of the original (pre-processed) data. The only difference between PLS-DA and PCA is that, the later uses the information of matrix X only, while PLS-DA takes into account both the information in matrix X and Y <sup>236</sup>.

Based on my findings, **Figure 24** illustrates a clear clustering among the cultivars. Cippessino cultivar was clearly separated from the other cultivars in PC1 by 25.0%

of the variance. On the other hand, Hinakase cultivar was also clearly separated from the rest in PC3 by 10.2% of the variance. The rest of the cultivars (Frantoio, Berhudar, Lucca, and Nevadillo blanco cultivars) were alienated in PC2 by 22.4% of the variance (**Figure 24**).

For the demonstration of the discrimination potential offered by the PCA score plot data, PLS-DA was employed – it is a commonly used supervised pattern recognition method that is capable of class prediction. It was, thus, employed to build and validate a model for olive leaves cultivar classification. It was, thus, used to construct and validate a statistical model for cultivar classification. The result of the cultivar classification is summarized in **Table 18**. The prediction ability was 98.15%, representing the percentage of the samples correctly classified. However, that is slightly lower than 100% – due to incorrect assignment of one Berhudar cultivar sample as Frantoio. However, an excellent separation among the cultivars was observed by PLS-DA scores plot as shown in **Figure 25**.

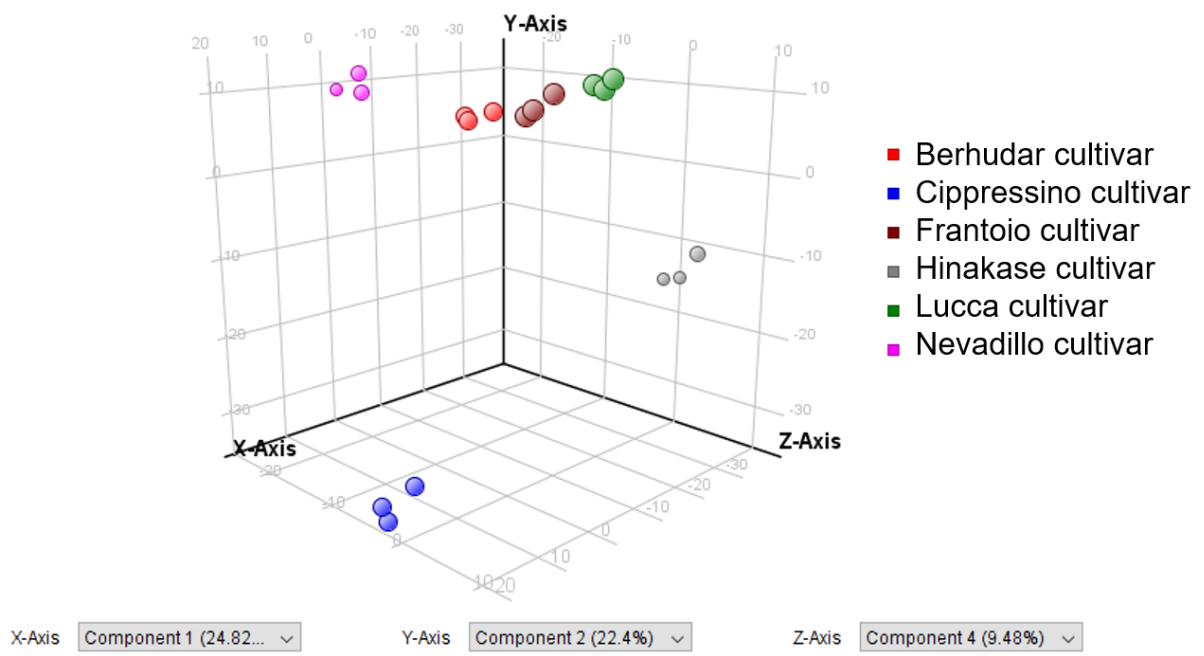


Figure 24: 3D PCA scores plot of olive leaves cultivars

**Table 18: The overview classification results obtained by the PLS-DA model**

	[Ber] (Predict)	[Cip] (Predict)	[Fra] (Predict)	[Hin] (Predict)	[Luc] (Predict)	[Nev] (Predict)	Accuracy (%)
True [Ber]	8	0	1*	0	0	0	88.889
True [Cip]	0	9	0	0	0	0	100
True [Fra]	0	0	9	0	0	0	100
True [Hin]	0	0	0	9	0	0	100
True [Luc]	0	0	0	0	9	0	100
True [Nev]	0	0	0	0	0	9	100
Prediction Ability (%)							98.148

Where Ber, Berhudar cultivar; Cip, Cipressino cultivar; Fra, Frantoio cultivar; Hin, Hinakase cultivar; Luc, Lucca cultivar; Nev, Nevadillo blanco cultivar. \* wrong prediction.

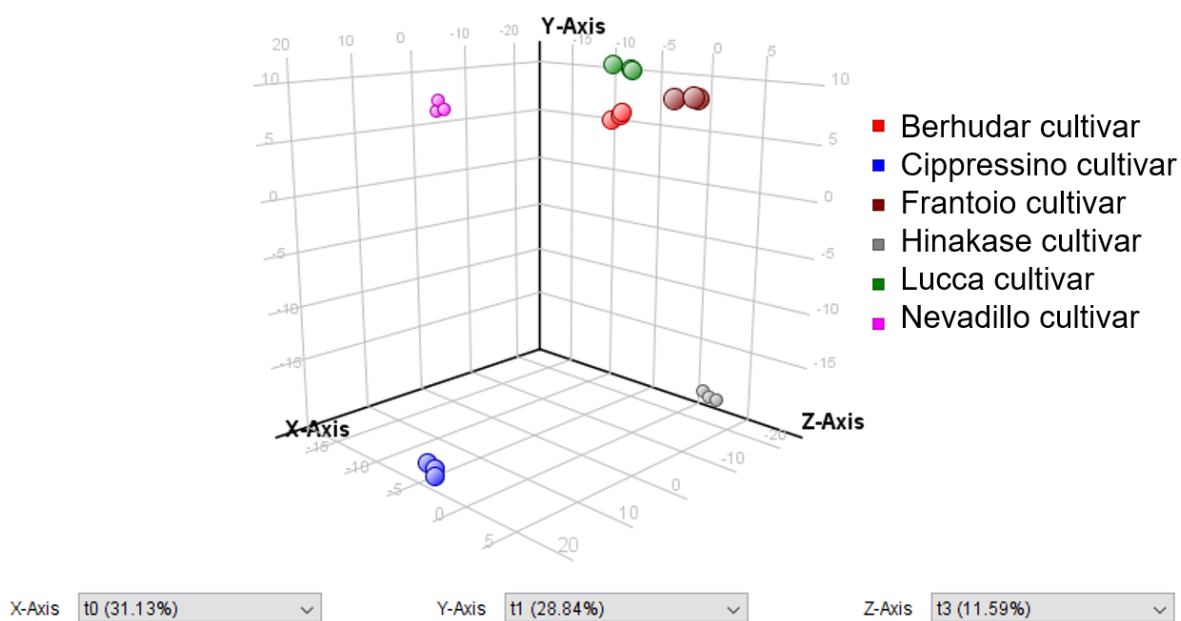


Figure 25: 3D PLS-DA scores plot of olive leaves cultivars



## Part IV: CONCLUSION

This study demonstrates that accurate-mass Q-TOF LC/MS is a powerful technique for the metabolic profiling of olive leaves from various cultivars. Data mining techniques such as molecular feature extraction (MFE) in combination with chemometric software such as MPP help to rapidly and efficiently align and filter data. Significant markers were obtained among the six cultivars of olive leaves – with demonstrated cultivar-specific markers that can be used to differentiate one cultivar from others. It was found that, so far, the markers can be used to discriminate these six groups of cultivars. Moreover, there was a clear difference in metabolite constitute among the active cultivars (Lucca, Frantoio, and Berhudar) and inactive cultivars (Cippressino, Navadillo Blanco, and Hinakase) following multivariate analysis (PCA score plots). A PLS-DA model was created, providing reasonable confidence and an excellent accuracy (98.15%). Even though the conclusion could not be reached at this point, of what metabolites contributes most to the anti-AChE activity, our findings seem to be promising to give possible reasons for the difference among cultivars. To confirm the identity/ structures of the metabolites, MS/MS analysis and comparison with the standard compounds, isobaric coelution, and ion ratios will be done.

## Part V: CHAPTER SUMMARY

Following HPLC analysis of the eighteen (18) olive leaves cultivars and their bioactivities against AChE enzymes, six of them were chosen to further study their metabolites which contributes to the anti-AChE activity (anti-AD) by employing the non-targeted metabolomics approach. The aim of this study was to establish a comprehensive analytical workflow for the application of liquid LC/MS to non-targeted metabolomics with a high level of accuracy in metabolite identification, employing the all ion fragmentation (AIF) approach as opposed to conventional and commonly used auto-MS/MS fragmentation <sup>238</sup>. Aiming at accomplishing the purpose of the present study, high-resolution mass spectrometry-based metabolomics was developed by coupling reversed-phase (RP) for metabolite screening while applying the AIF mode that includes 4 sequential full scans at 0, 10, 20, and 40 eV collision energies.

In summary, this study has explored the usefulness of olive leaves against Alzheimer's disease. It provides evidence that some cultivars are more active than others. This creates further agricultural demands for the olive leaves as a potential anti-AD preventive drug. Nonetheless, tentative identification of markers with accurate MS/MS, retention times (RTs), isotopic pattern, and ion ratio (when necessary), followed by molecular structure correlation generated some potential candidates, is still under investigation.

**CHAPTER 5**  
**CONCLUSION AND RECOMMENDATION**

It is widely known from ancient times that olive oil has been used as not only food but also as a folk medicine for the treatment of several ailments, such as cardiovascular diseases and topical disorders. With time, researchers established the scientific evidence as a base to some traditional uses of the VOO – notably for treating dermatitis, eczema, xerosis, and other types of inflammation, among many other uses linking the importance of the metabolites present in VOO, especially the major biophenols – oleuropein and hydroxytyrosol. A well-established scientific base for the health benefits of VOO has led to an increase in its demand that, in turn, has led to an increased OOBPs production, and thus new ways to utilize these wastes (by-products) are needed. This study was done in an effort to address the possible ways of utilization of OOBPs in human health – a focus was given to the use of the recovered bioactive metabolites in human diseases – allergy, diabetes mellitus, and Alzheimer's disease (AD).

The isolated metabolites exhibited promising anti-allergic and anti-diabetic activities whereby the anti-allergic active metabolites acted mainly as 'mast cell stabilizers' to reduce degranulation in RBL-2H3 cells through reducing the intracellular  $Ca^{2+}$  levels by decreasing the expression of calcium channel proteins. The most potent metabolite being luteolin ( $IC_{50}=3.9 \mu M$ ). For the anti-diabetic activity, the metabolites inhibited the carbohydrate digesting enzymes,  $\alpha$ -glucosidase and  $\alpha$ -amylase, either in uncompetitive, non-competitive or in partial mixed fashion to reduce postprandial hyperglycemia (PPHG), a major cause of diabetes – with oleanolic acid being the most potent ( $IC_{50}=33.4 \mu M$ ). Generally, the phenolic compounds were more active

than triterpenoids against allergic sensitization, and the vice versa was true when it came to anti-diabetic activity. This was confirmed further after calculation of the individual metabolite's "total activity" to understand the contribution of each metabolite to the respective biological activity.

To understudy the chemical profile of the OOBPs, the samples of different olive leaves cultivars were used. Following the difference in their anti-AChE activity, only six were chosen for further studies (three most active and three least active ones). A novel HRMS-based metabolomics approach by LC/Q-TOF-MS employing the all-ion fragmentation (AIF) acquisition mode in data mining, coupled to chemometrics analysis (MPP software) was developed. A total of 66 metabolites (as molecular features, MFs) were detected – 6 MFs as triterpenoids and 23 MFs as phenolic compounds. The novel developed AIF-based workflow was also used for screening specific biomarkers of different cultivars, and thus it can be a useful platform not only for investigating the metabolome in the selection of the specific biomarkers in closely related samples, e.g, cultivars, but also in the identification of active anti-AChE metabolites in the cultivars.

These findings highlight the chemical and biological importance of the OOBPs and their metabolites. Even though the findings of this study are based on *in-vitro* assays, they highlight the potential of OOBPs and their constituents against allergy, diabetes, and AD. This, in turn, adds more value and attracts more attention to OOBPs as an important source of lead compounds that may be used as ingredients in food

additives, food supplements, or for structural modification to develop novel drugs for the management/ treatment of allergies, AD and diabetes mellitus. Thus, they can no longer be regarded as 'wastes' to dispose of but as 'cheap source of highly valuable metabolites'.

In summary, the findings presented in this thesis provide a further scientific base about the functional aspects of OOBPs that will lead to their utilization as they constitute useful bioactive metabolites with interesting biological potentials; anti-allergic, anti-diabetic, and anti-AChE activities. The utilization of OOBPs for human health could play an important role in the recycling of these by-products which could contribute to the integrated use of available resources in the olive industry or others such as cosmetic, pharmaceutical, and food industries. This could result in an overall environmental gain.

## APPENDICES

### Appendix i: Tentative identification of the olive leaves cultivar markers

S/No	MF	RT (min)	ID (based on MS)	Error (ppm)
1	624.2061	<b>6.54</b>	Verbascoside	0.92838
2	584.212	<b>7.76</b>		
3	448.1014	<b>6.63</b>	Luteolin-7-O- $\beta$ -glucoside	1.871232
4	524.1883	<b>7.89</b>	Ligstroside	-2.053647
5	316.1155	<b>4.67</b>	Hydroxytyrosol-4- $\beta$ -glucoside	-1.004695
6	578.1618	<b>6.79</b>		
7	432.1066	<b>7.06</b>		
8	378.1308	<b>8.07</b>	3,4-DHPEA-EA	-3.088079
9	390.1163	<b>5.39</b>	Oleoside	0.226855
10	702.238	<b>7.23</b>	Oleuropeinyl monoglucoside	1.26097
11	570.1953	<b>7.33</b>		
12	422.2336	<b>17.64</b>		
13	138.0308	<b>8.06</b>		
14	556.1798	<b>6.53</b>	Secologanoside	1.06854
15	402.1516	<b>5.83</b>	Secologanic acid	-2.479407
16	608.2108	<b>6.89</b>		
17	286.0471	<b>8.24</b>	Luteolin	-2.237389
18	302.0426	<b>8.31</b>		
19	342.1173	<b>1.12</b>		
20	404.1311	<b>5.89</b>	Methyloleoside	-1.979552
21	390.1173	<b>4.69</b>		
22	318.0623	<b>1.21</b>		

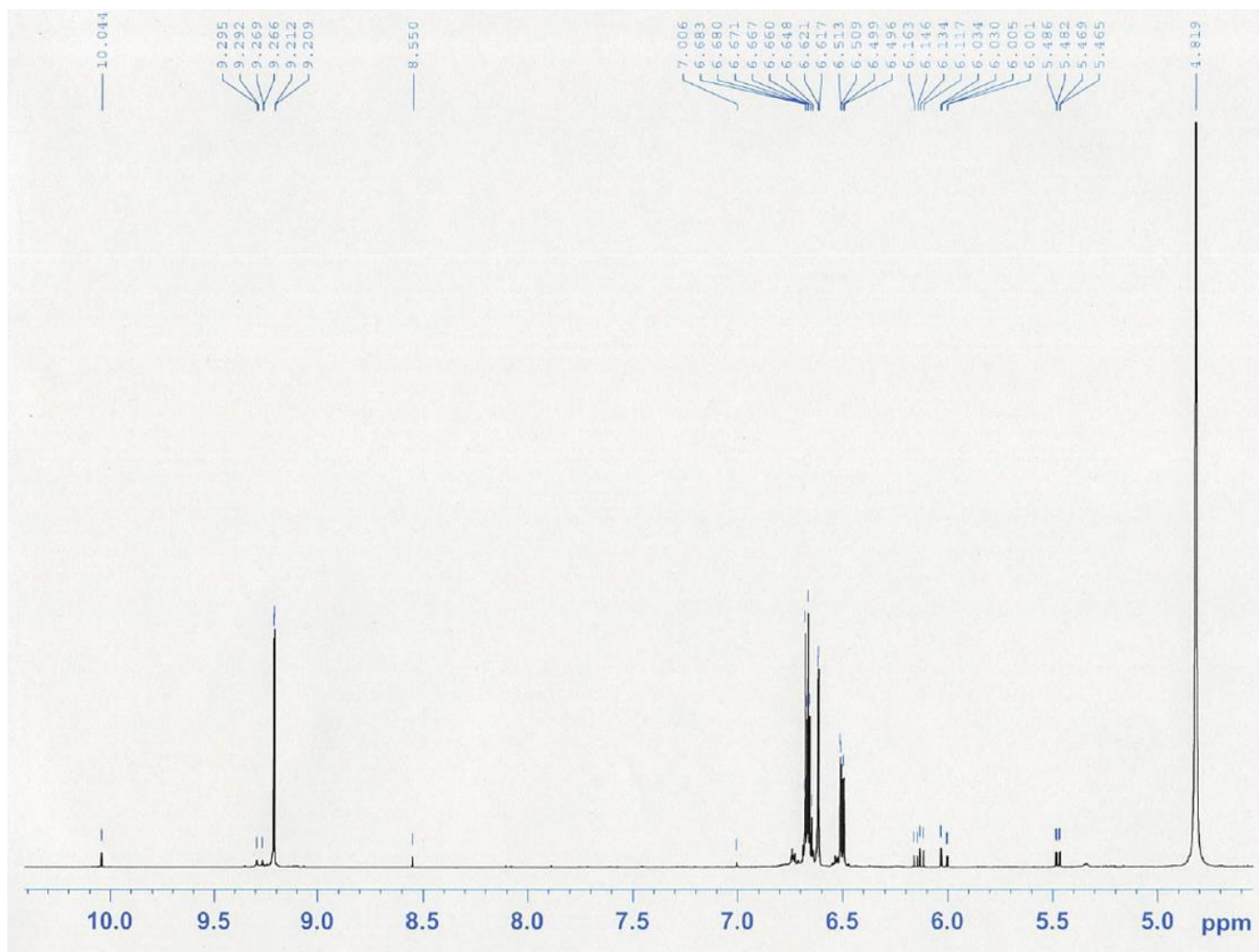
23	540.1852	<b>7.98</b>	Oleuropein	1.497452
24	336.1199	<b>6.58</b>		
25	818.225	<b>7.44</b>		
26	834.2187	<b>7.05</b>		
27	472.3539	<b>13.76</b>	Maslinic acid/ Isomaslinic acid	-2.879189
28	378.1309	<b>8.07</b>	3,4-DHPEA-EA/ Oleuropein aglycone	1.143253
29	464.0956	<b>6.61</b>		
30	618.3923	<b>14.68</b>		
31	270.052	<b>8.93</b>	Apigenin	0.653946
32	652.1978	<b>7.76</b>		
33	494.1414	<b>7.86</b>		
34	724.2188	<b>6.56</b>		
35	356.1112	<b>5.82</b>		
36	514.204	<b>7.41</b>		
37	478.1478	<b>6.66</b>		
38	306.0769	<b>5.8</b>		
39	516.0878	<b>6.63</b>		
40	342.0946	<b>5.1</b>		
41	776.2351	<b>7</b>		
42	300.1203	<b>5.12</b>	Hydroxytyrosol rhamnoside	2.00919
43	558.2297	<b>7.96</b>		
44	462.1745	<b>4.95</b>		
45	622.19	<b>6.54</b>		
46	402.1882	<b>6.34</b>		
47	354.0953	<b>5.47</b>	Scopolin	0.615089
48	594.1577	<b>5.71</b>	Vicenin-2	-1.296455



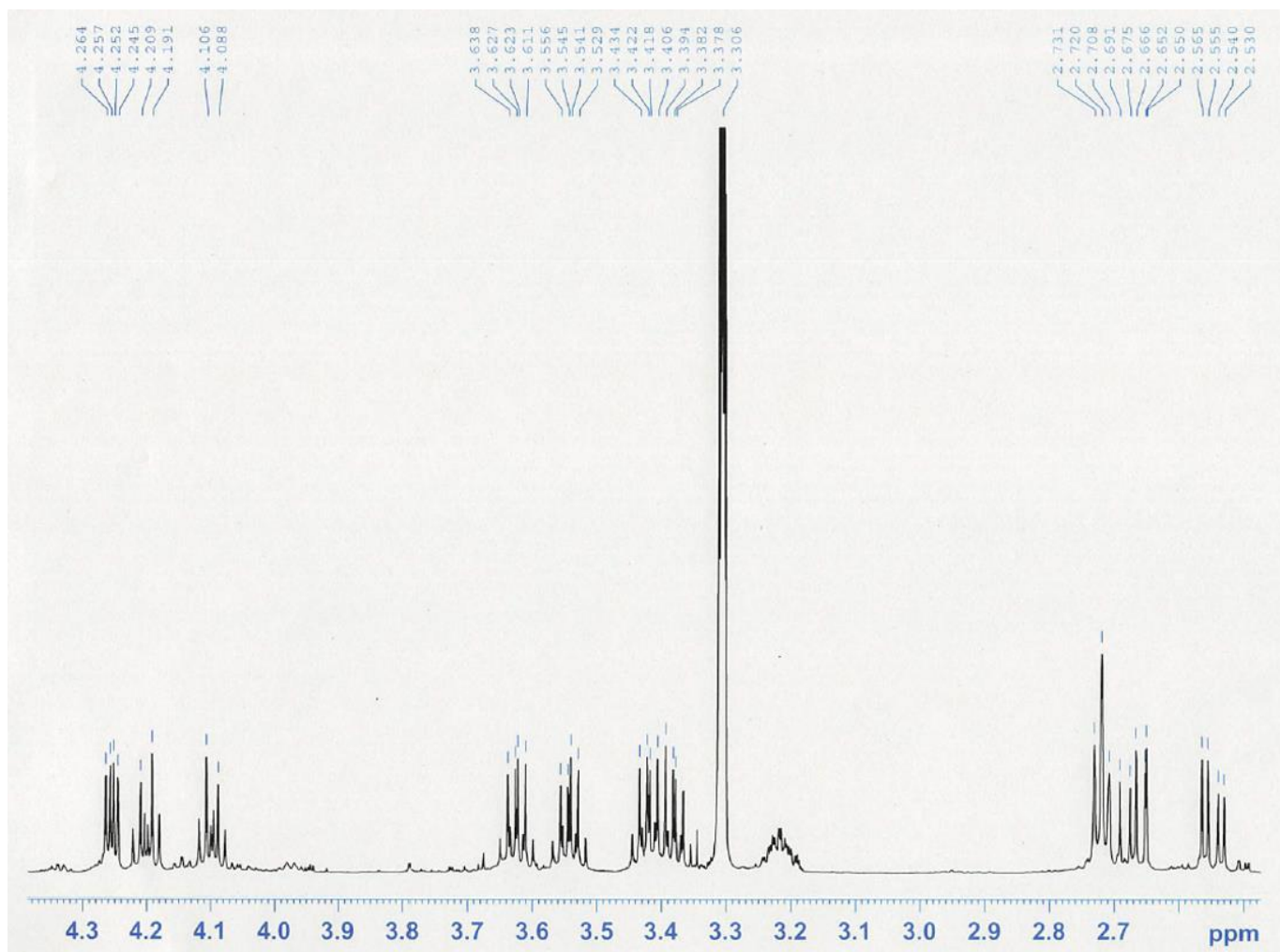
49	980.2781	<b>7.22</b>		
50	472.3537	<b>12.73</b>	Maslinic acid/ Isomaslinic acid	-2.879189
51	196.0737	<b>7.38</b>	Hydroxytyrosol acetate	0.719118
52	432.1174	<b>7.06</b>		
53	506.1819	<b>1.2</b>		
54	390.1156	<b>4.35</b>	Oleoside **	-1.567482
55	484.2302	<b>7.78</b>		
56	286.0478	<b>7.04</b>	Luteolin	0.209755
57	320.1267	<b>6.63</b>	3,4-DHPEA-EDA	2.222875
58	358.1414	<b>6.91</b>	Pinoresinol	0.665658
59	326.1001	<b>5.59</b>		
60	964.2818	<b>7.53</b>		
61	384.1025	<b>4.67</b>		
62	594.1571	<b>6.42</b>	Vicenin-2 **	-2.306287
63	624.2062	<b>6.78</b>	Verbascoside **	1.248788
64	646.1861	<b>6.54</b>		
65	448.101	<b>7.23</b>	Luteolin-7-O- $\beta$ - glucoside **	0.978575
66	624.2061	<b>6.54</b>	Verbascoside **	1.088584

\*\* multiple identified markers. Identification is based on accurate mass (AM) only  
(level 4 of MSI)

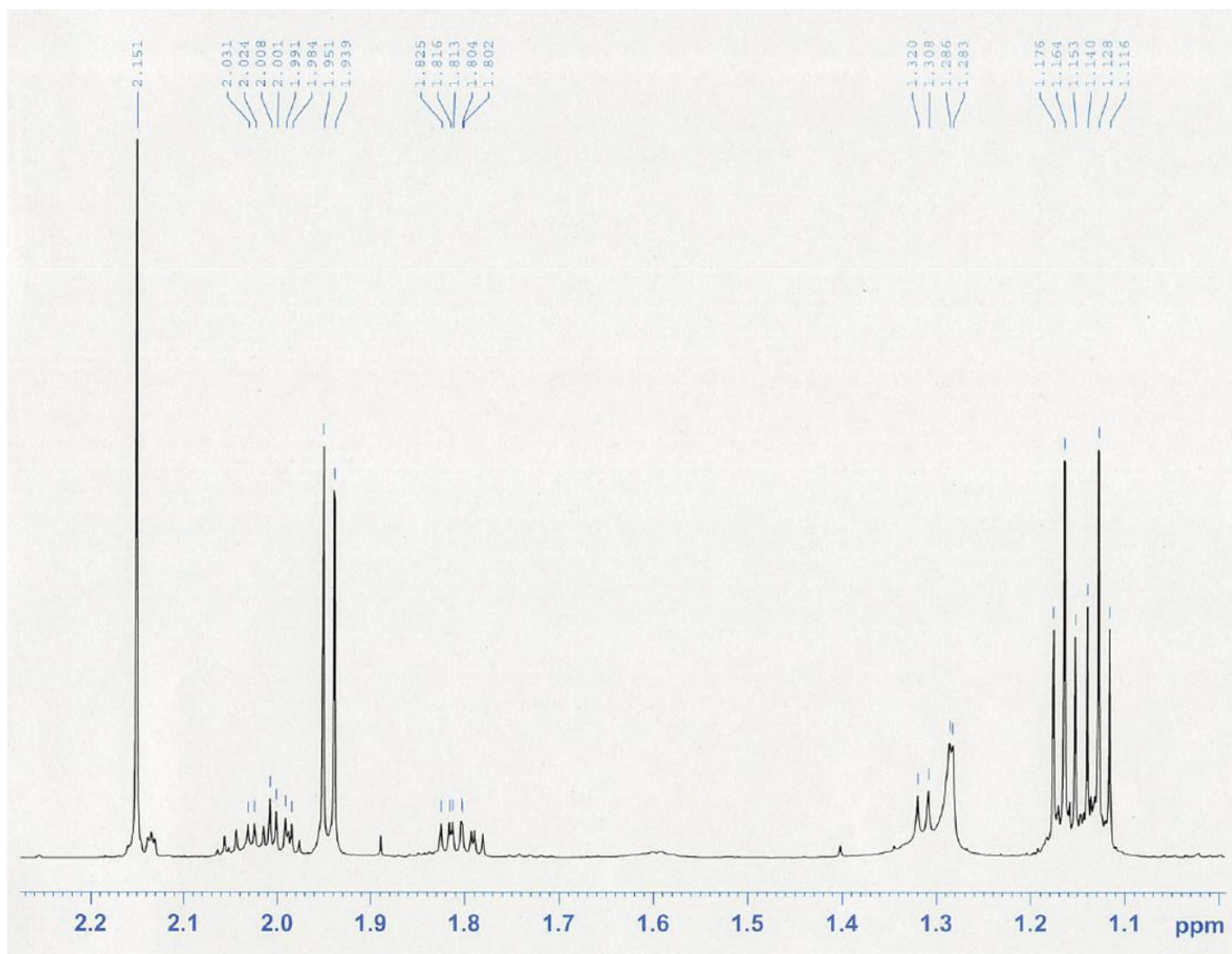
Appendix ii: <sup>1</sup>H-NMR (whole region) for the novel compound, new HDOA



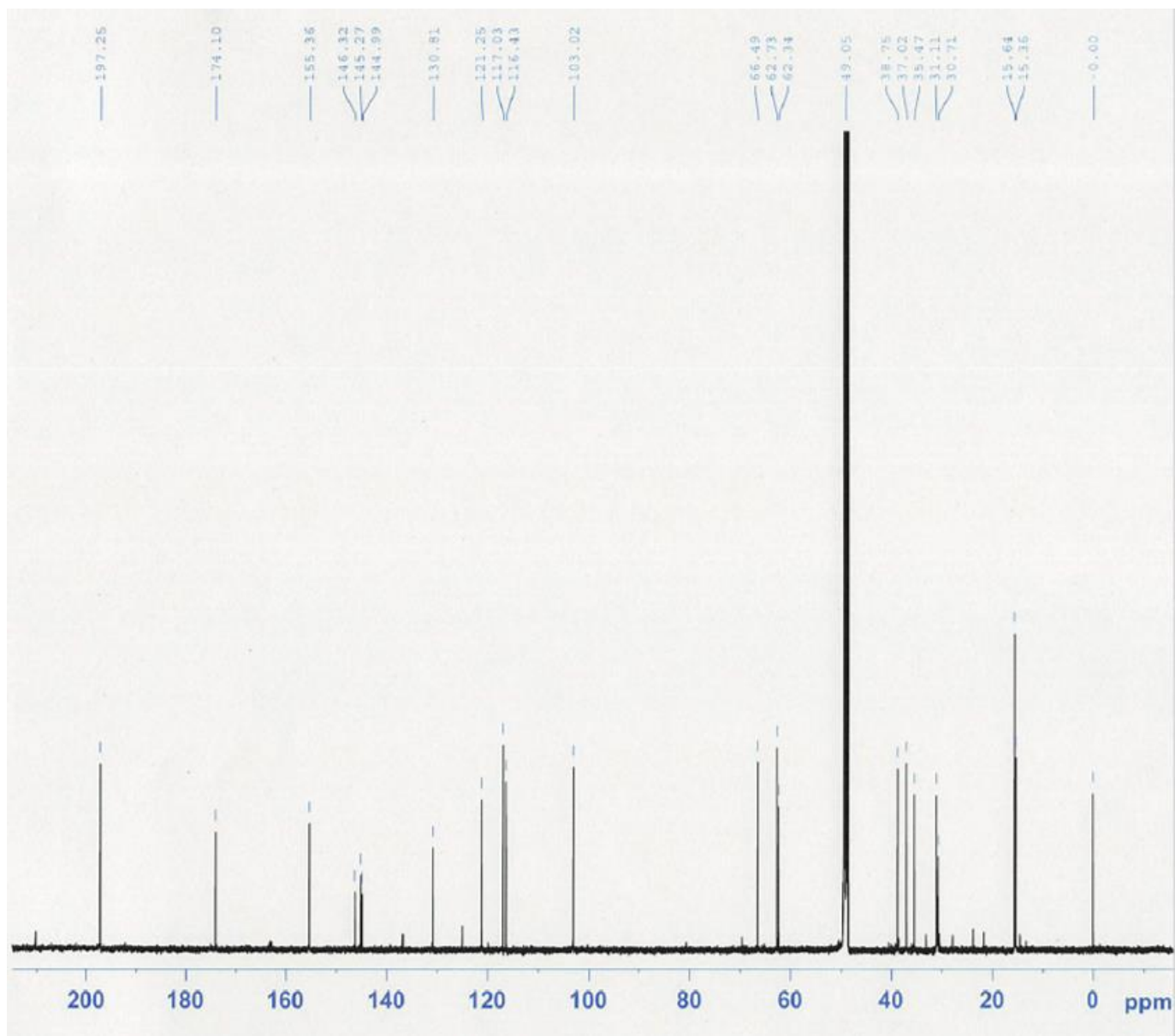
Appendix iii:  $^1\text{H-NMR}$  ( $\delta\text{H}$  4.5 to 2.5 ppm) for the novel compound, new HDOA



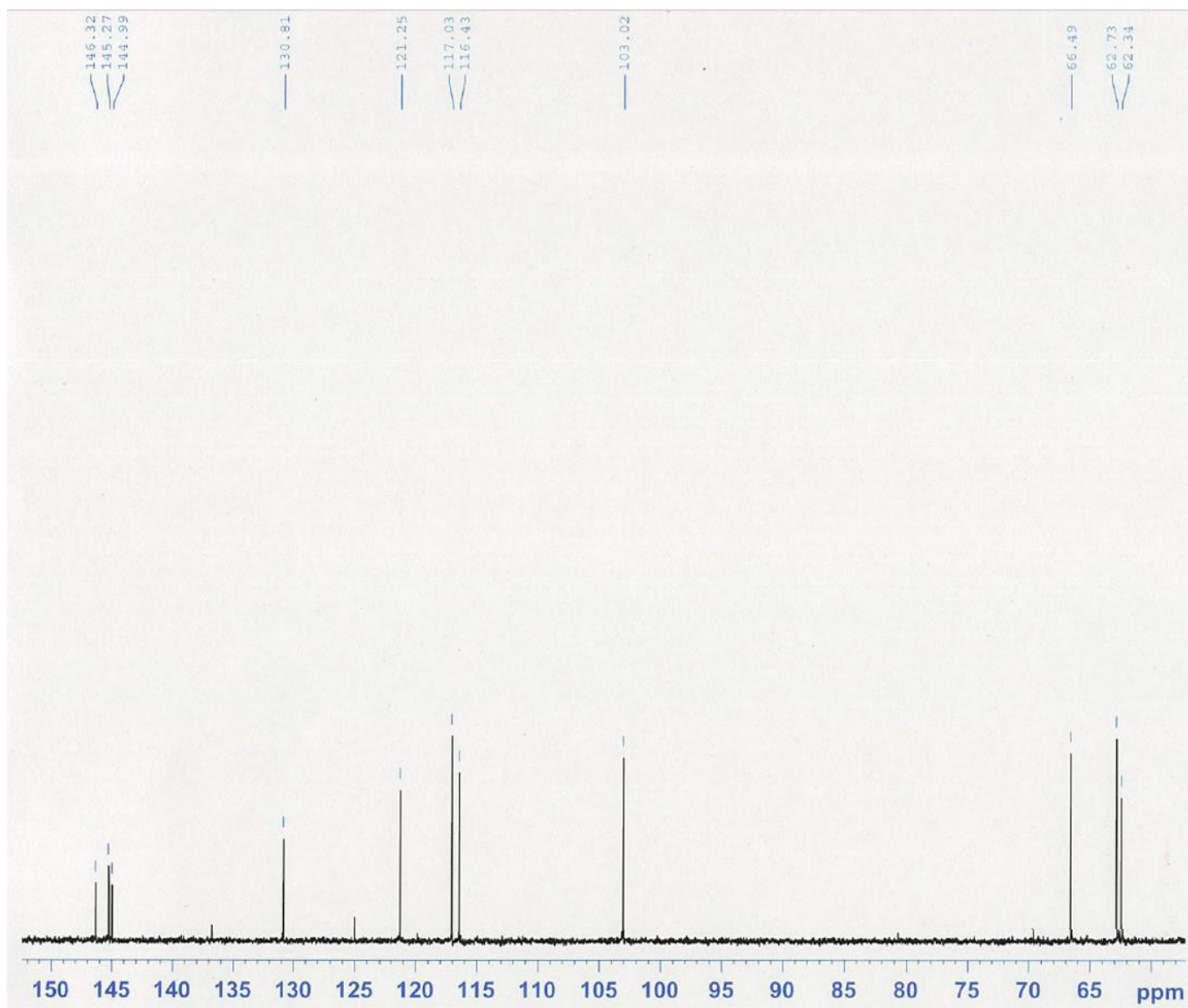
Appendix iv:  $^1\text{H-NMR}$  ( $\delta\text{H}$  2.3 to 1.0 ppm) for the novel compound, new HDOA



Appendix v:  $^{13}\text{C}$ -NMR (whole spectra) for the novel compound, new HDOA

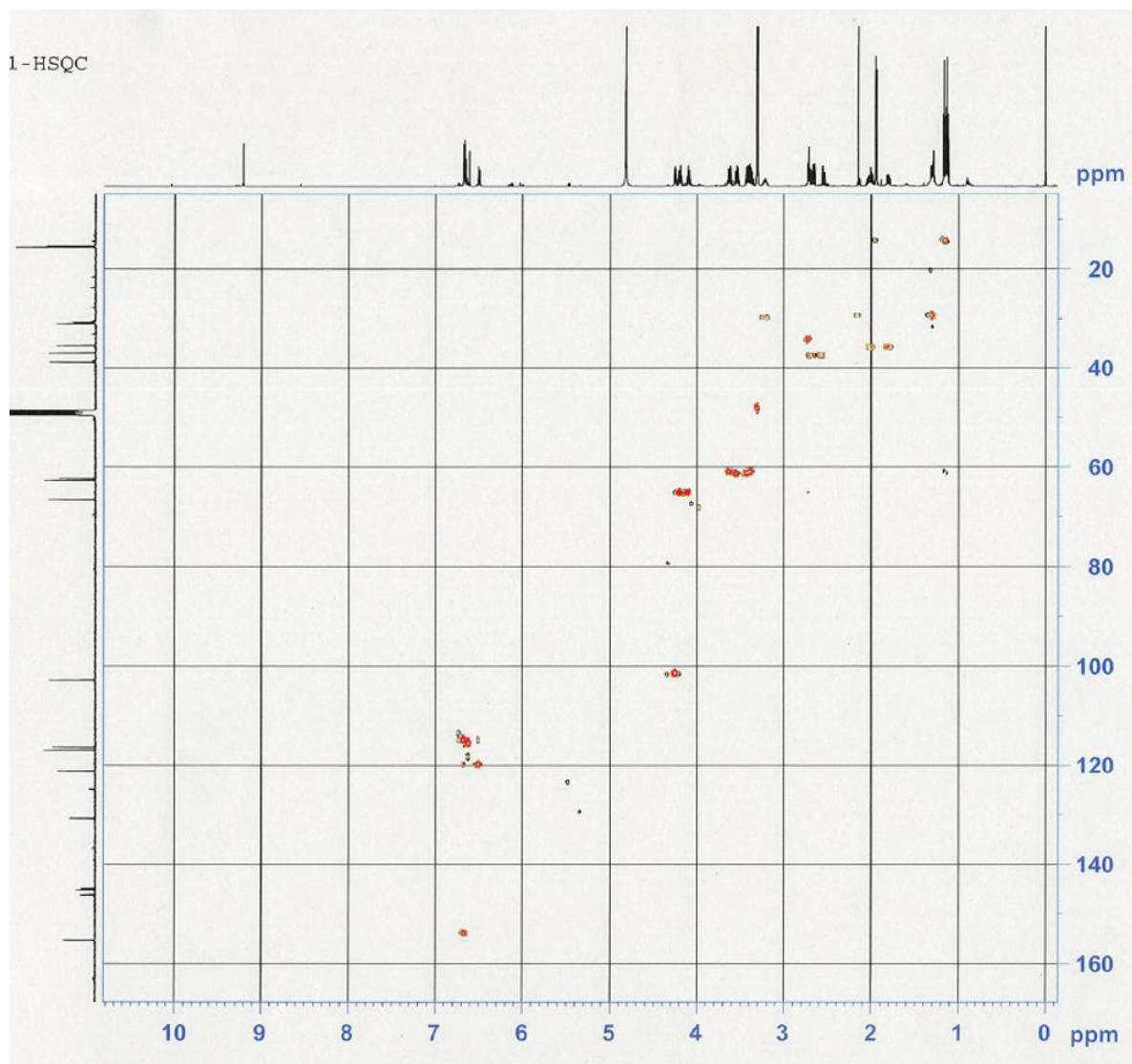


Appendix vi:  $^{13}\text{C}$ -NMR ( $\delta\text{H}$  65.0 to 150.0 ppm) for the novel compound, new HDOA

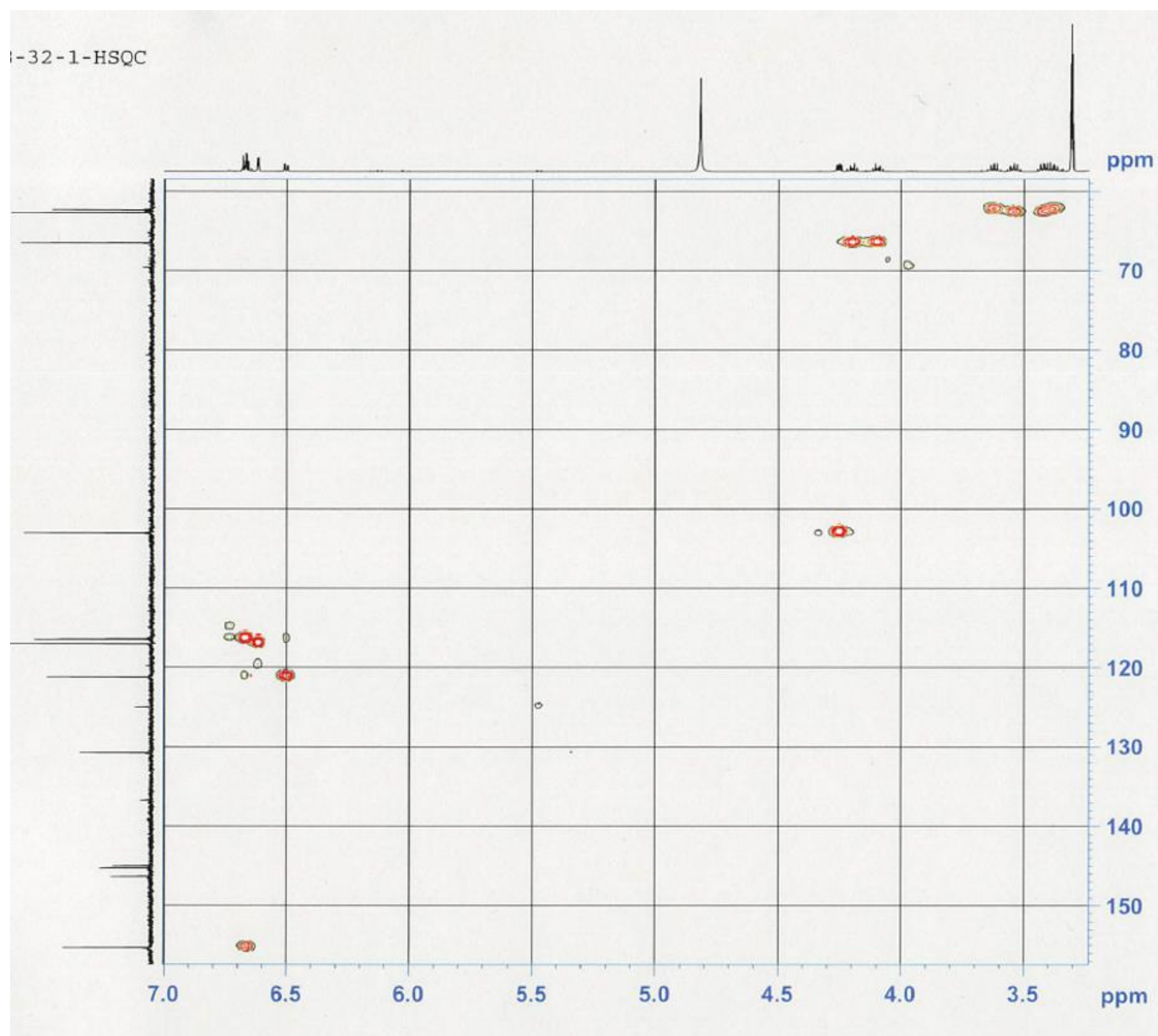




Appendix vii: HSQC-NMR (whole spectra) for the novel compound, new HDOA

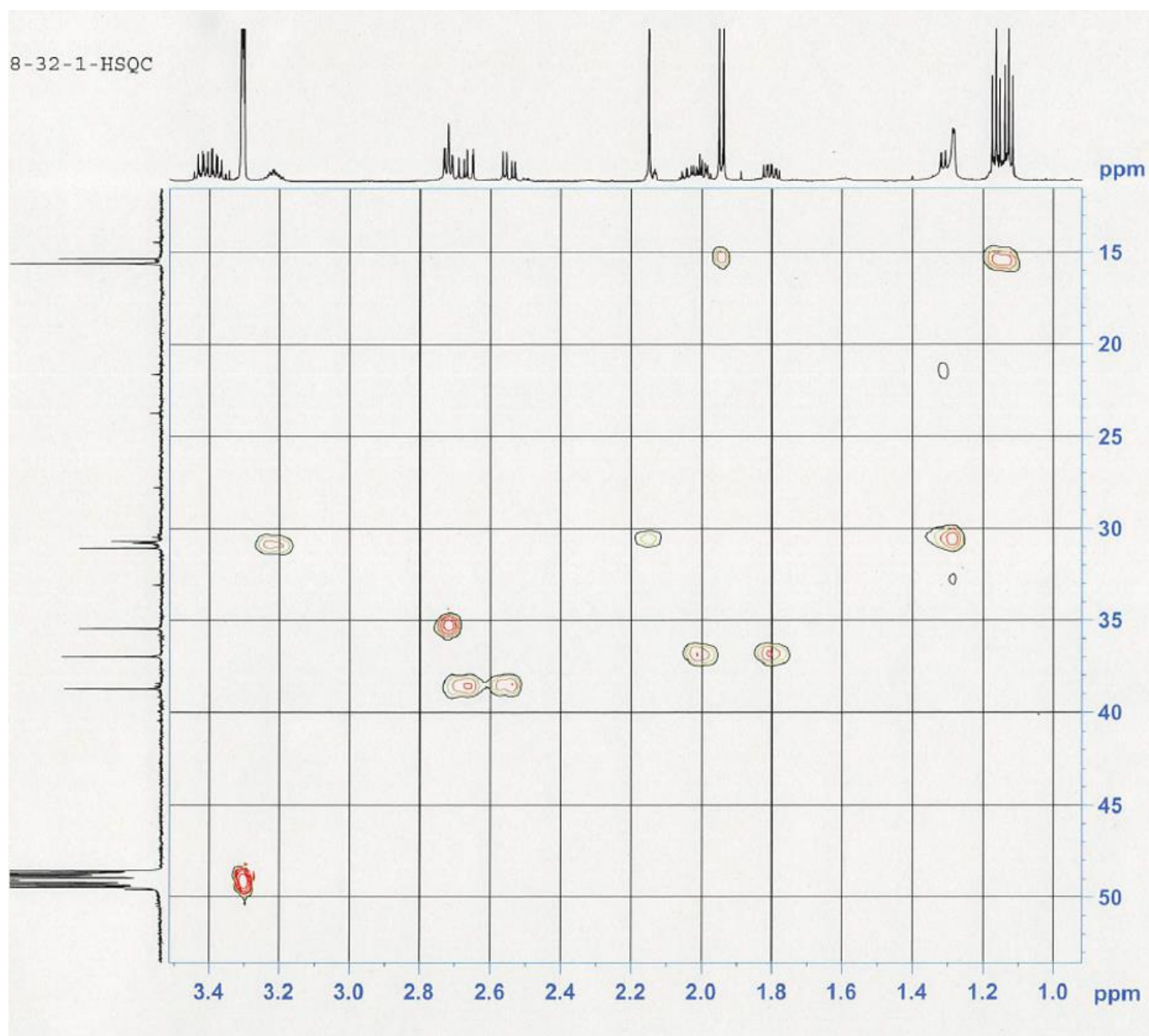


Appendix viii: HSQC-NMR ( $\delta$ H 7.0 to 3.5 ppm) for the novel compound, new HDOA

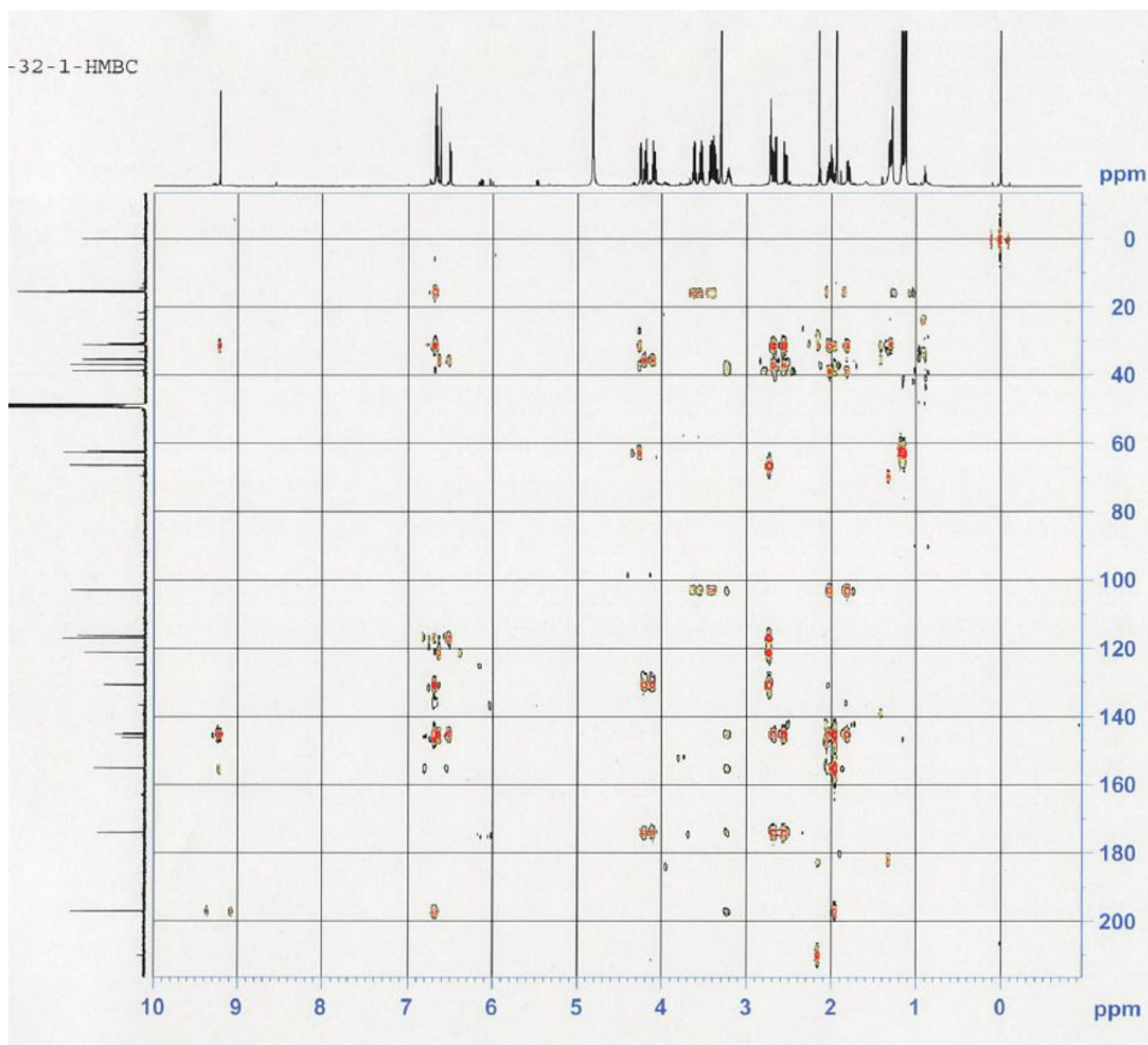




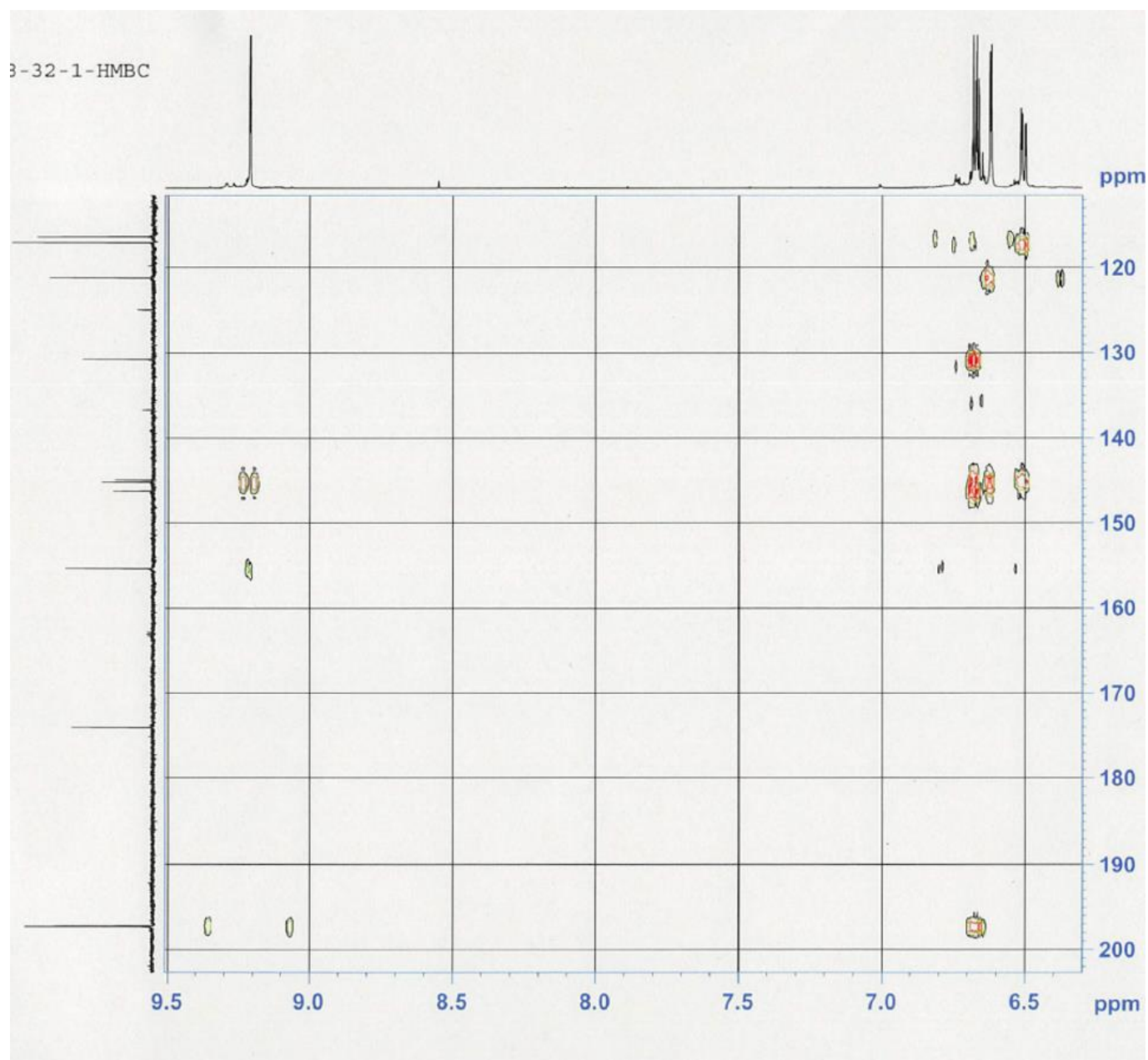
Appendix ix: HSQC-NMR ( $\delta$ H 3.5 to 1.0 ppm) for the novel compound, new HDOA



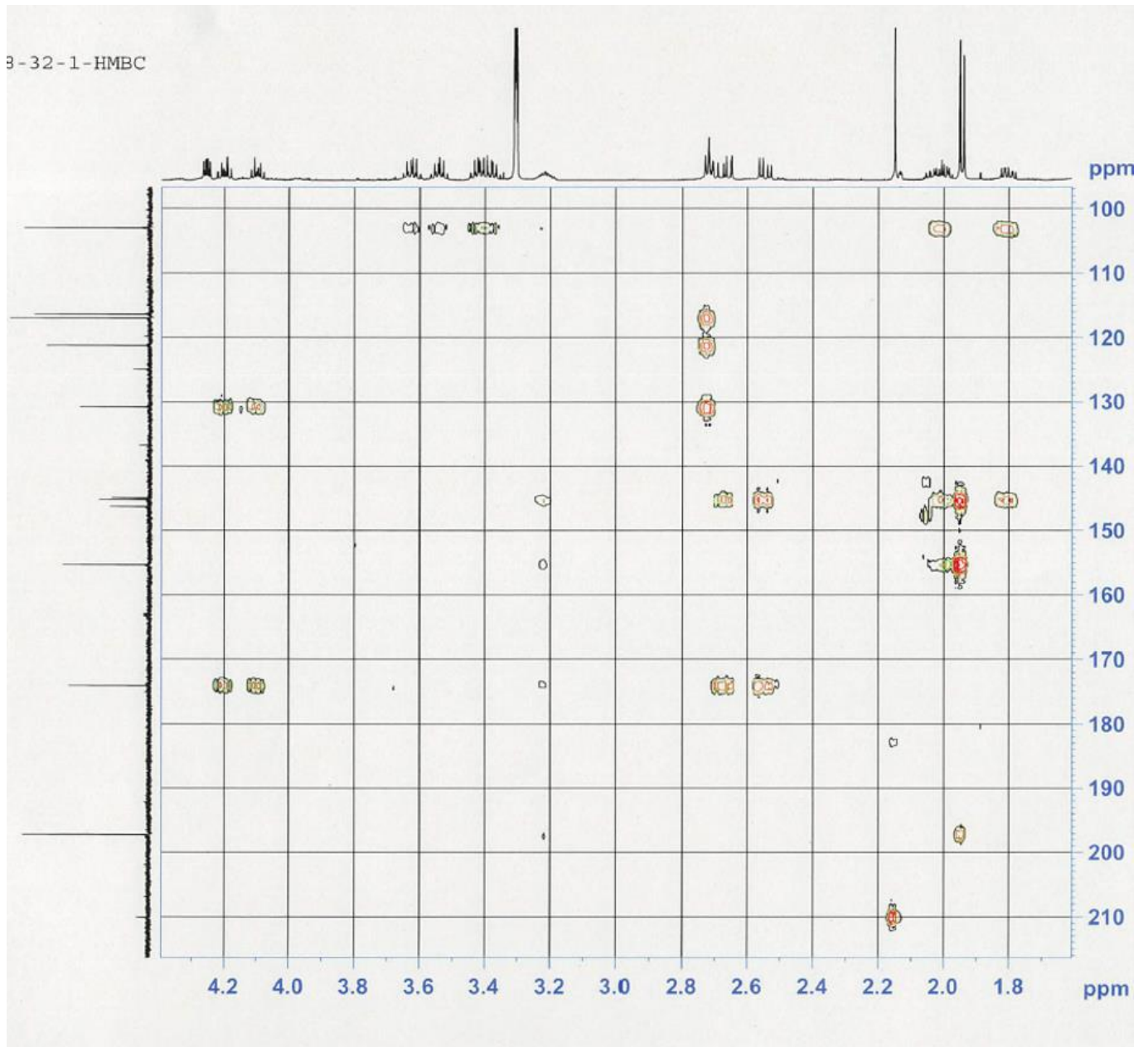
Appendix x: HMBC-NMR (whole spectra) for the novel compound, new HDOA



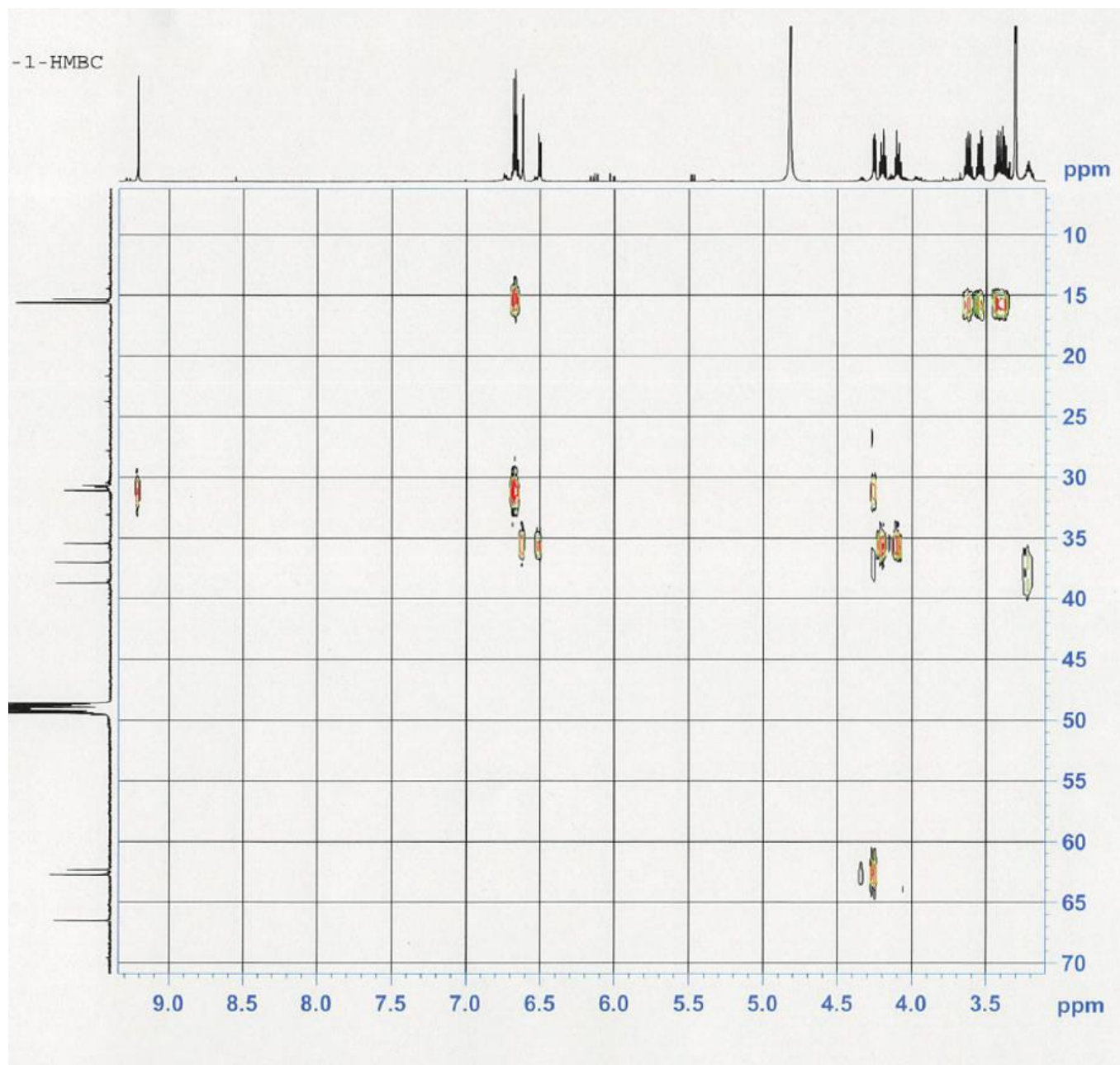
Appendix xi: HMBC-NMR ( $\delta$ H 9.5 to 6.5 ppm) for the novel compound, new HDOA



Appendix xii: HMBC-NMR ( $\delta$ H 4.4 to 1.7 ppm) for the novel compound, new HDOA



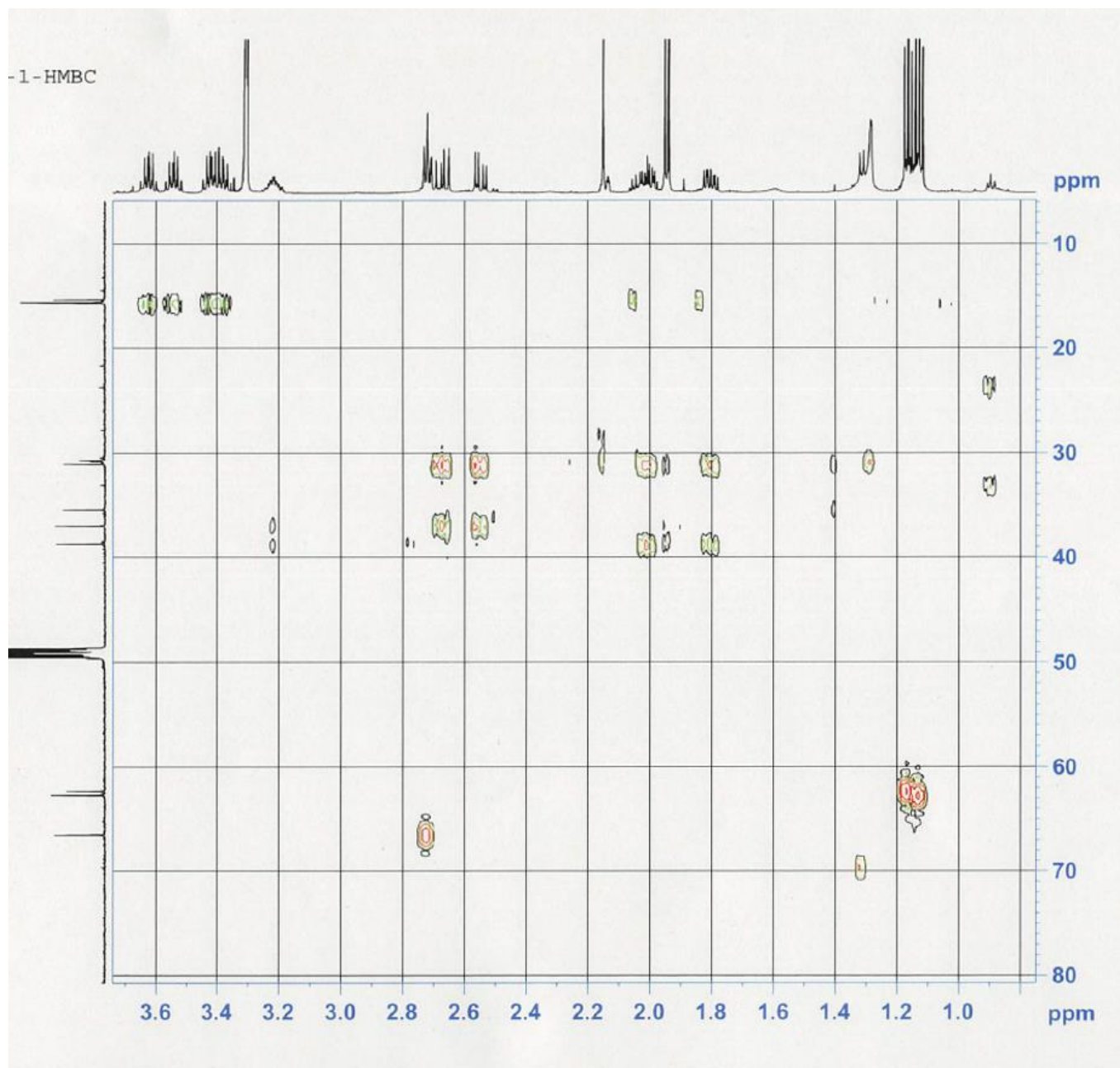
Appendix xiii: HMBC-NMR ( $\delta$ H 9.0 to 3.5 ppm) for the novel compound, new HDOA





Appendix xiv: HMBC-NMR ( $\delta$ H 3.7HDO to 1.0 ppm) for the novel compound, new

HDOA



## Appendix xv: LR-FAB-MS of the novel compound, new HDOA

[ Mass Spectrum ]

Data : 28-32-1-FABposi-LR Date : 25-Jan-2018 15:25

Instrument : MStation JMS-700

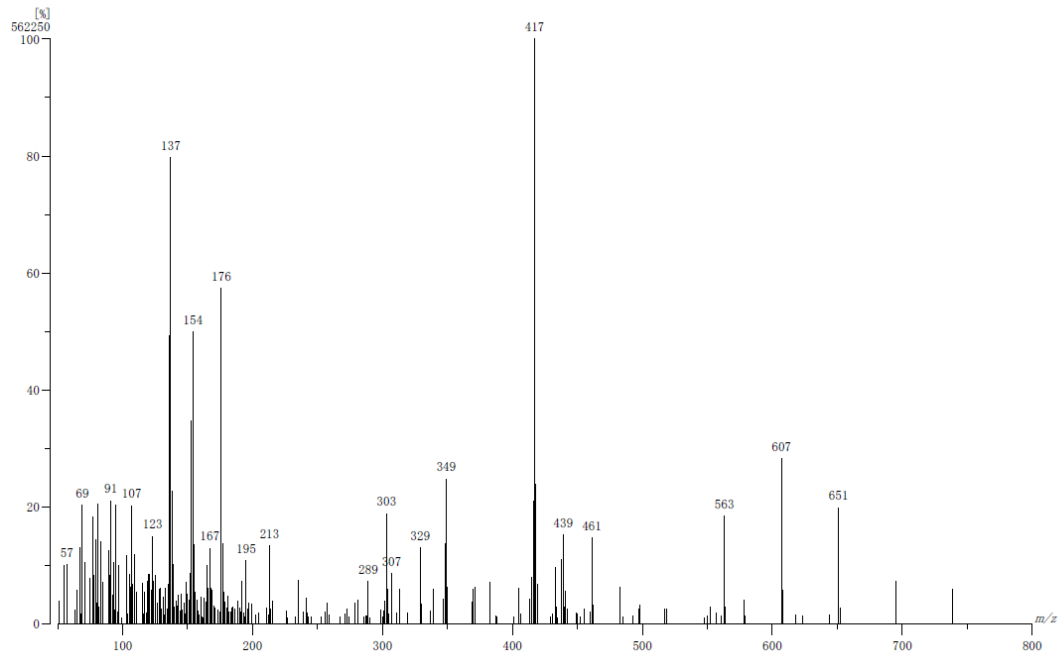
Note : IMCE Kyushu Univ.

Ion Mode : FAB+

Scan# : (10,15)

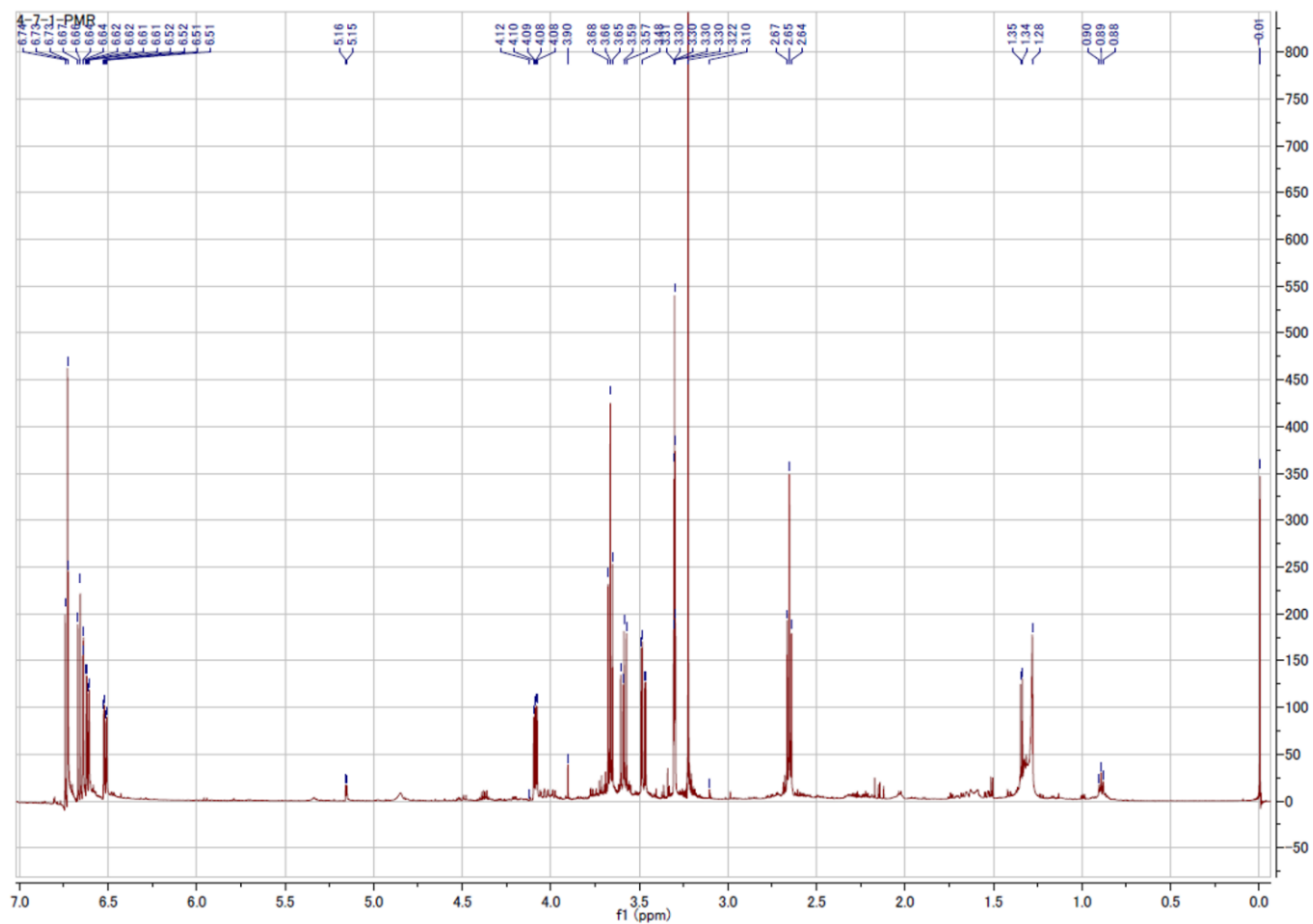
Cut Level : 1.00 %

Matrix:3NBA



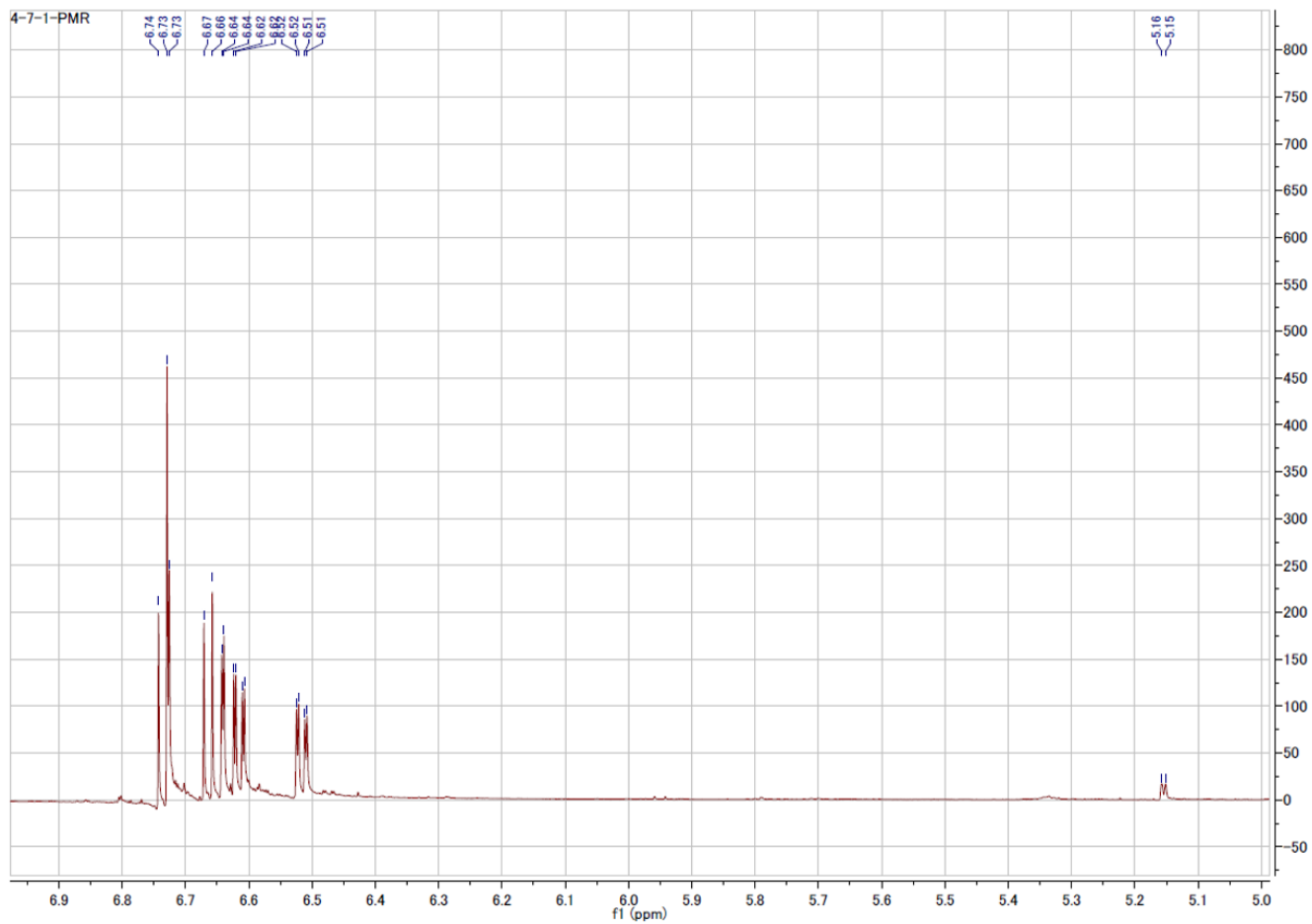
Appendix xvi: <sup>1</sup>H-NMR (whole region) for the novel compound, 3,4-dihydroxyphenyl-

2-methoxyethanol

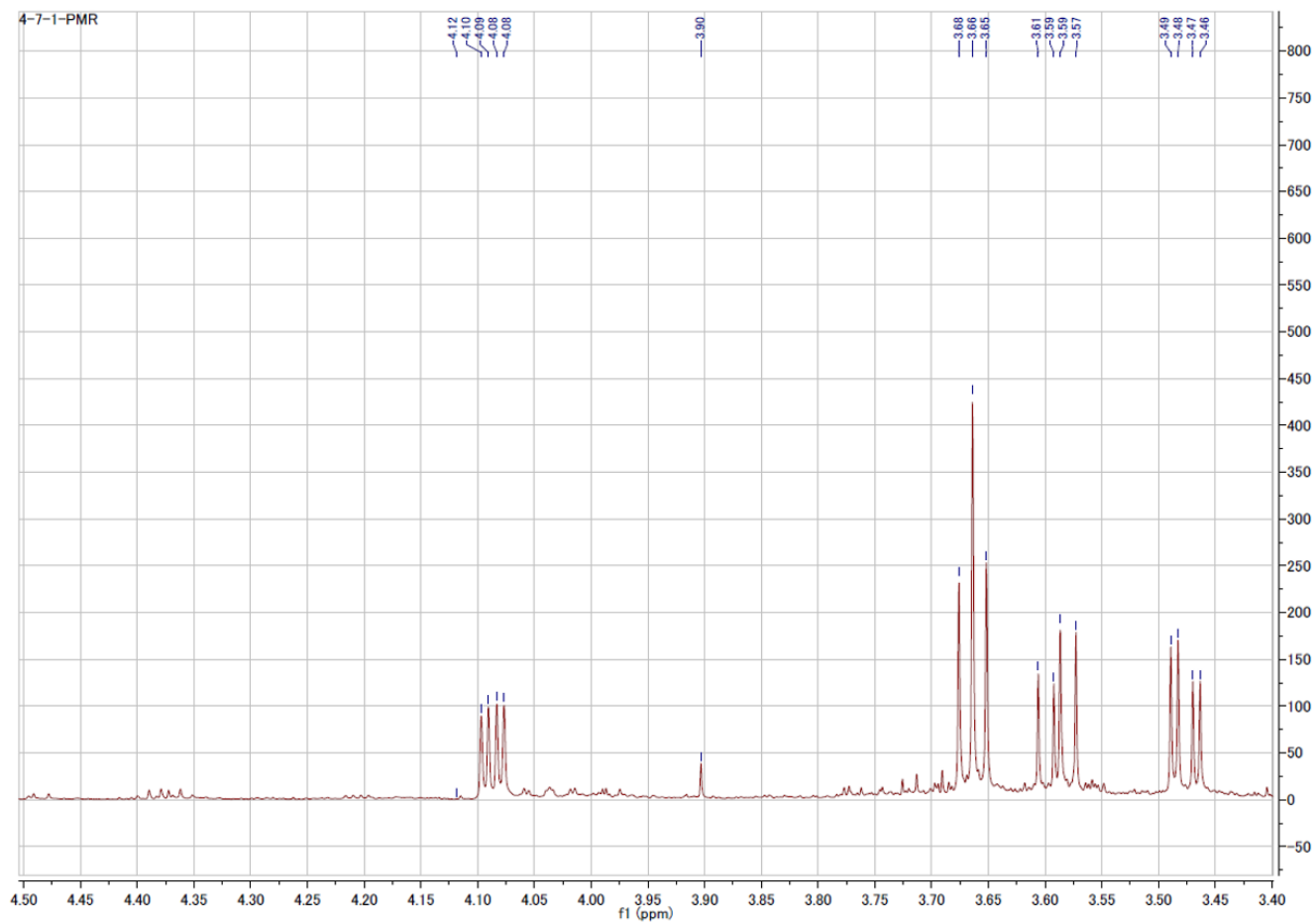




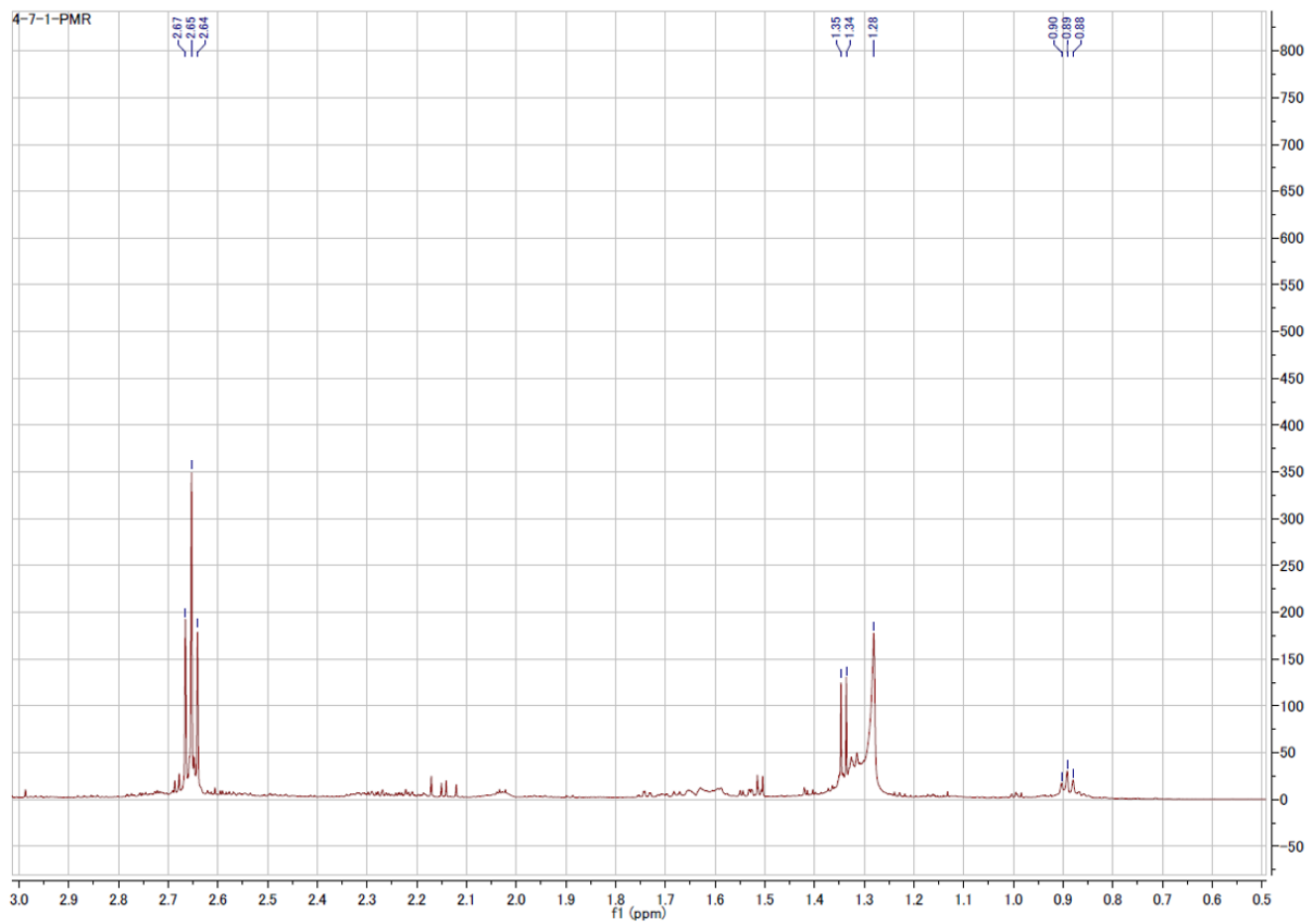
Appendix xvii:  $^1\text{H-NMR}$  (region  $\delta\text{H}$  7.0 to 5.0 ppm) for the novel compound, 3,4-dihydroxyphenyl-2-methoxyethanol



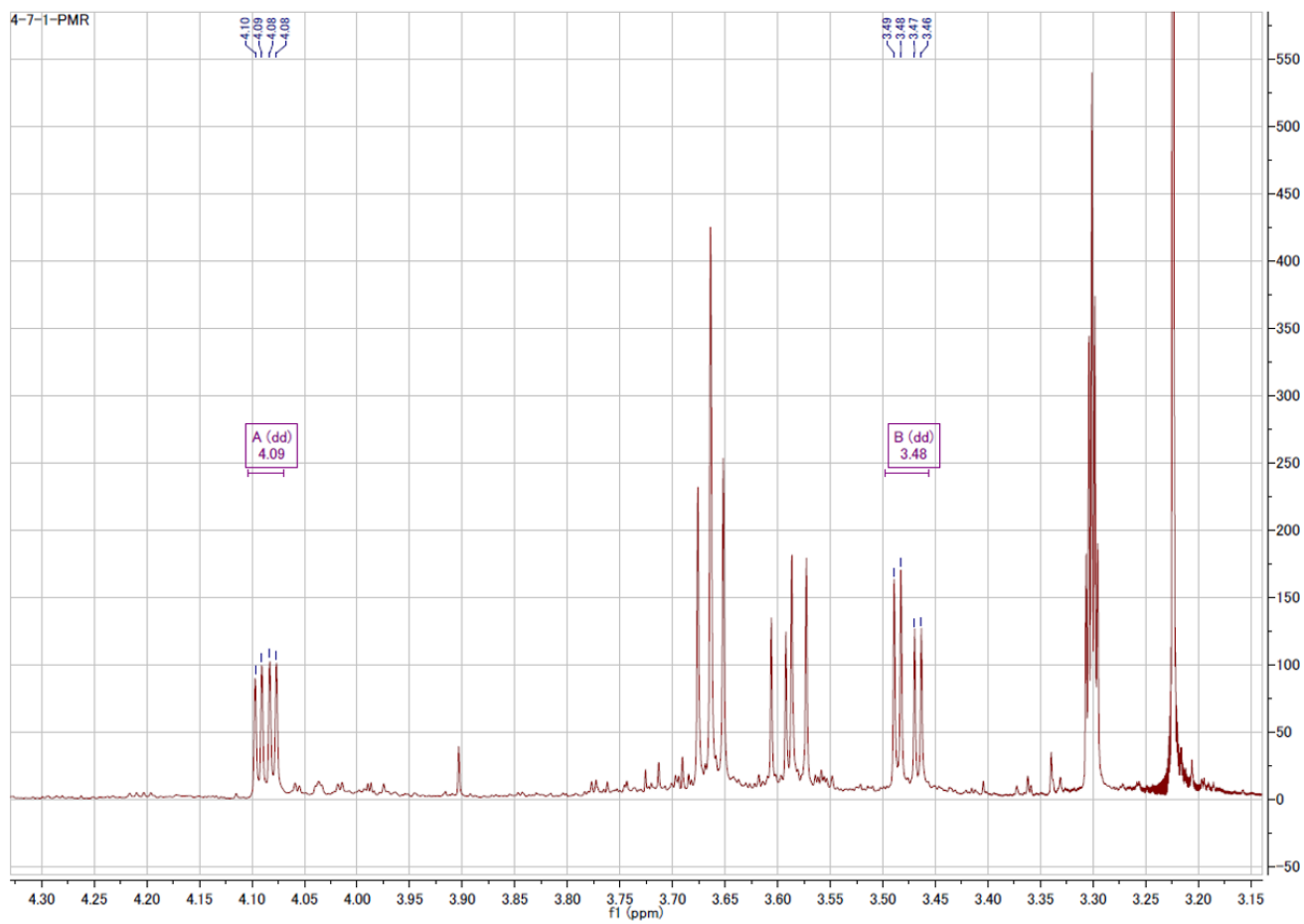
Appendix xviii:  $^1\text{H-NMR}$  (region  $\delta\text{H}$  4.5 to 3.5 ppm) for the novel compound, 3,4-dihydroxyphenyl-2-methoxyethanol



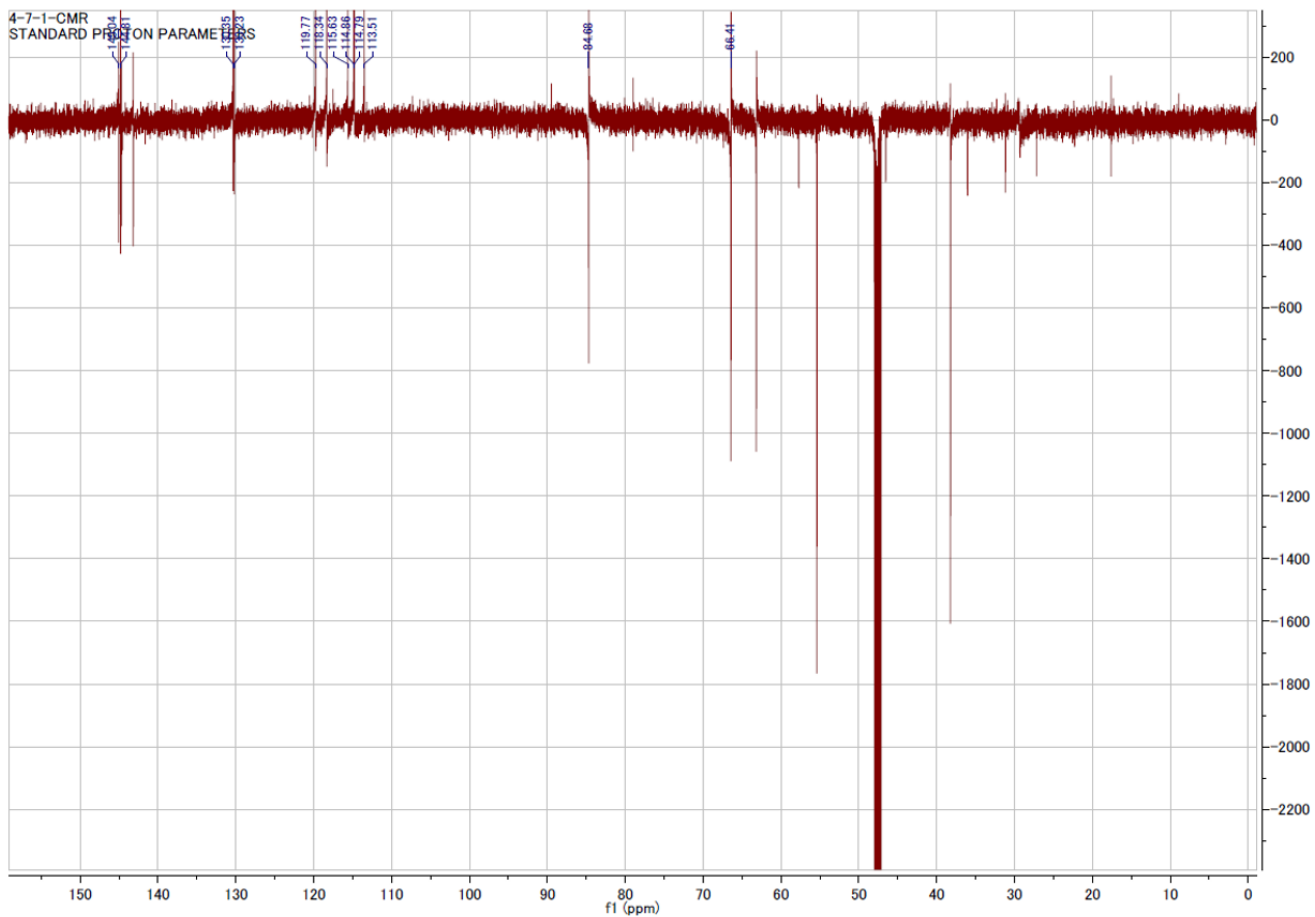
Appendix xix:  $^1\text{H-NMR}$  (region  $\delta\text{H}$  3.0 to 0.5 ppm) for the novel compound, 3,4-dihydroxyphenyl-2-methoxyethanol



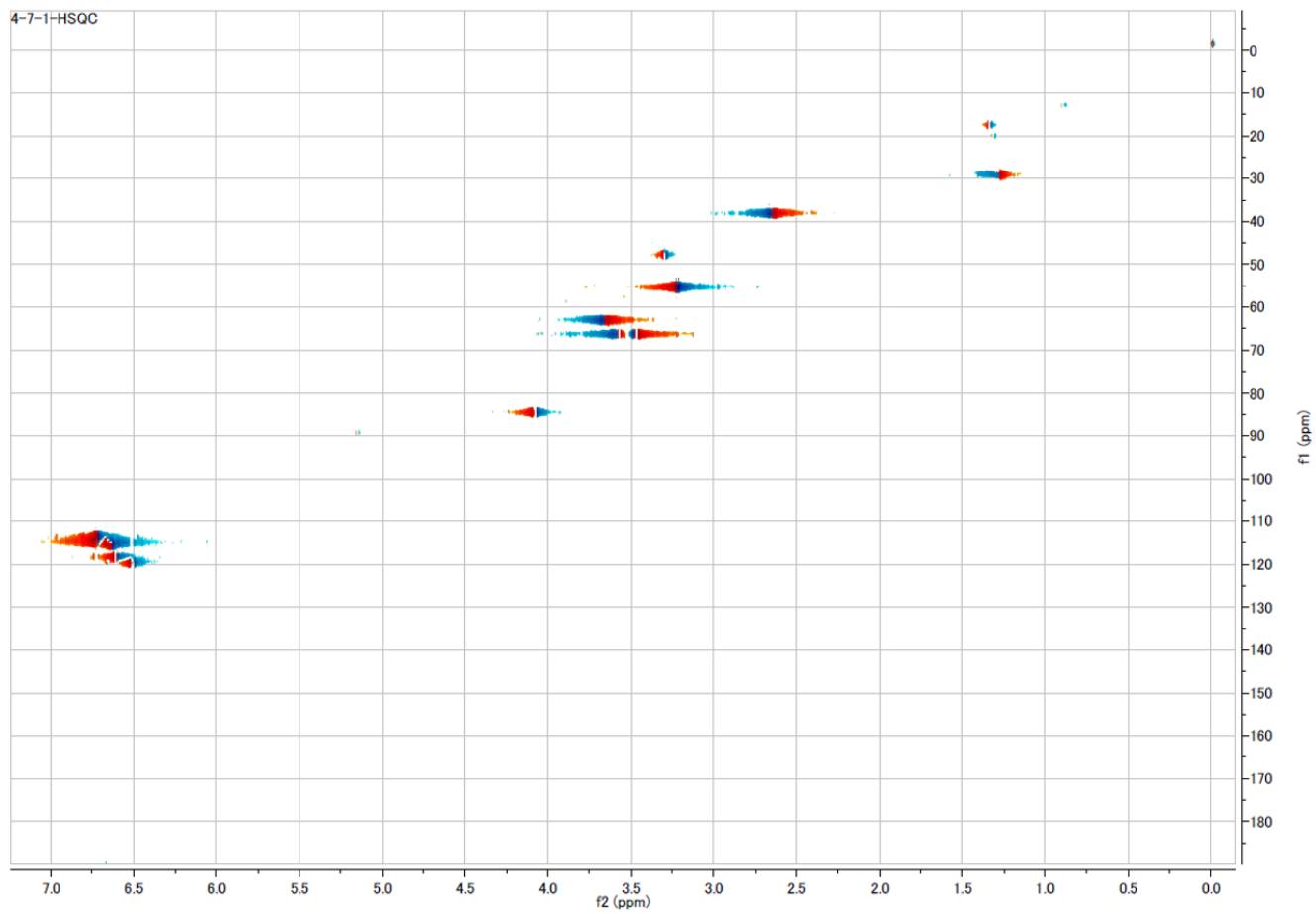
Appendix xx:  $^1\text{H-NMR}$  (H-1' and H-2') for the novel compound, 3,4-dihydroxyphenyl-2-methoxyethanol



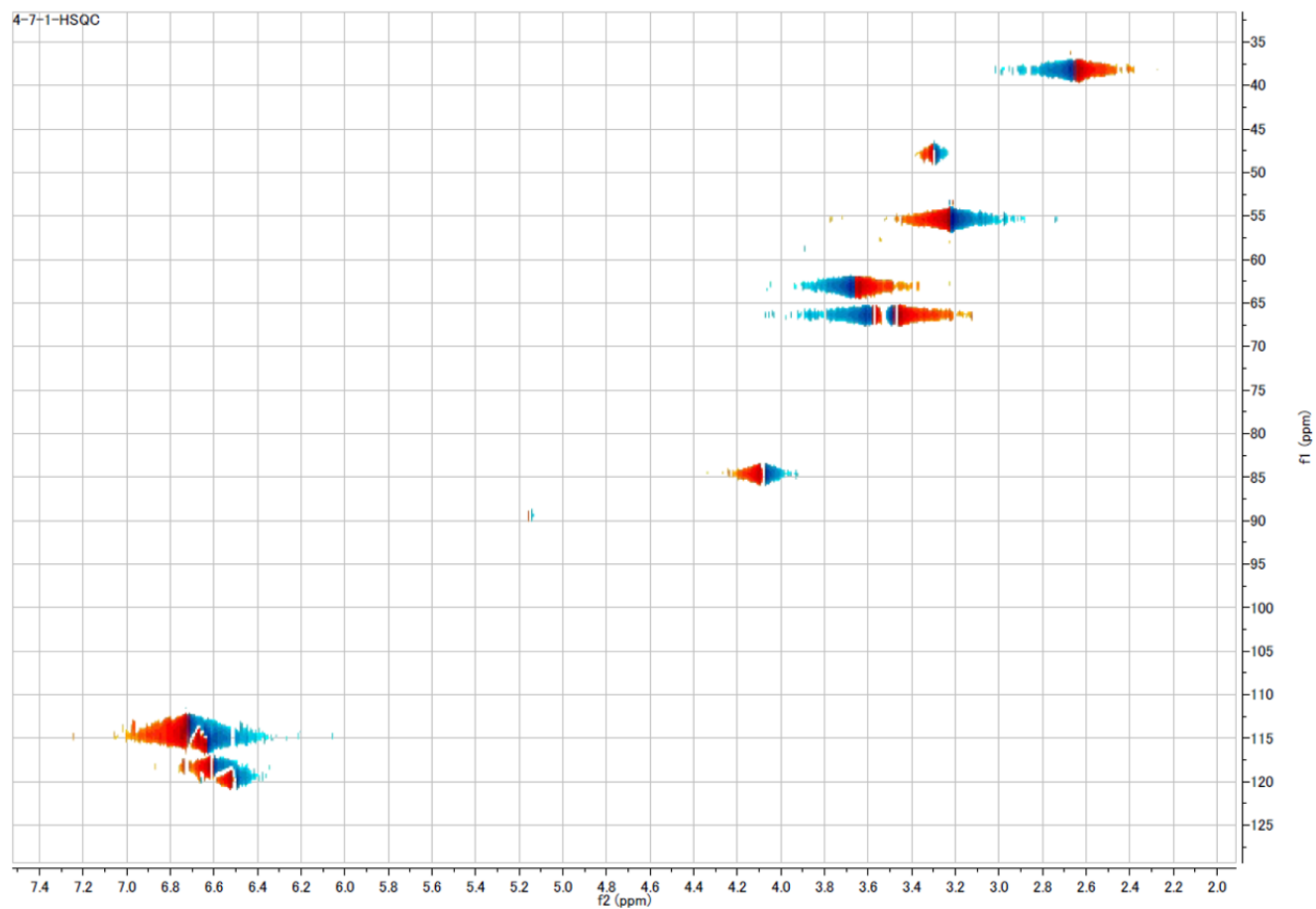
Appendix xxi:  $^{13}\text{C}$ -NMR (whole region) for the novel compound, 3,4-dihydroxyphenyl-2-methoxyethanol



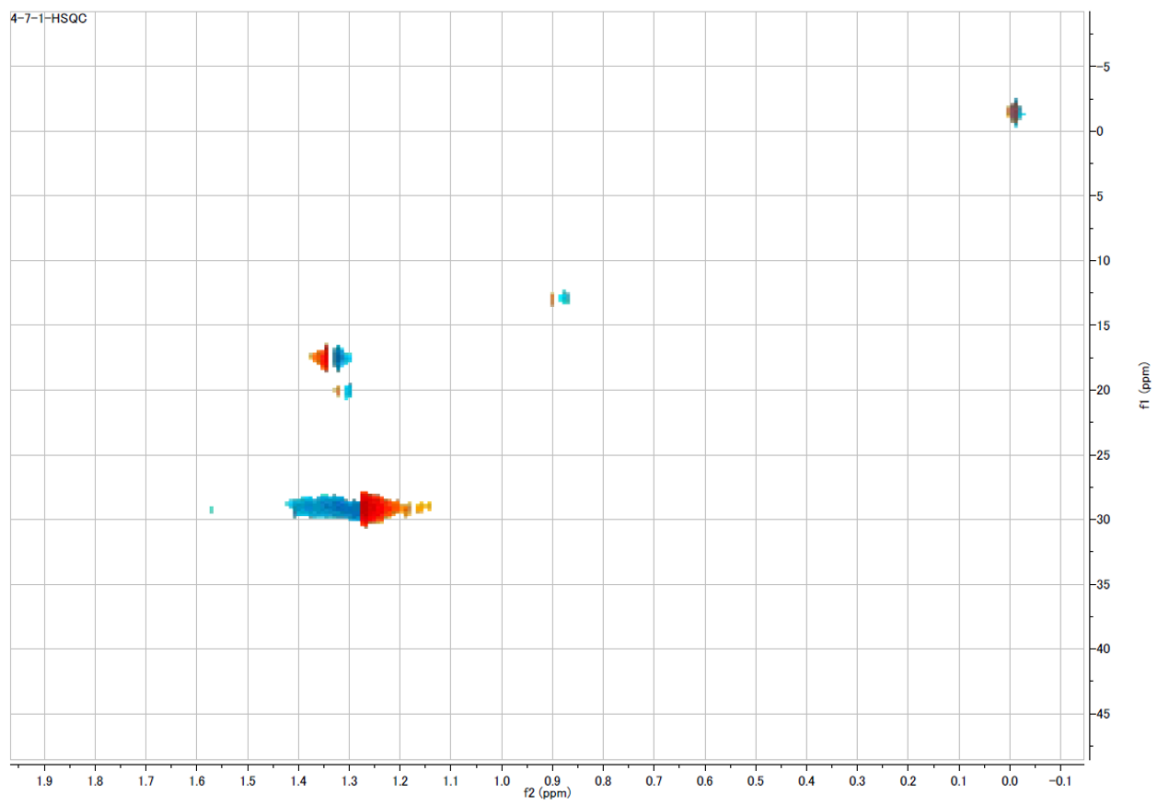
Appendix xxii: HSQC-NMR (whole region) for the novel compound, 3,4-dihydroxyphenyl-2-methoxyethanol



Appendix xxiii: HSQC-NMR (region  $\delta$ H 7.0 to 2.0 ppm) for the novel compound, 3,4-dihydroxyphenyl-2-methoxyethanol

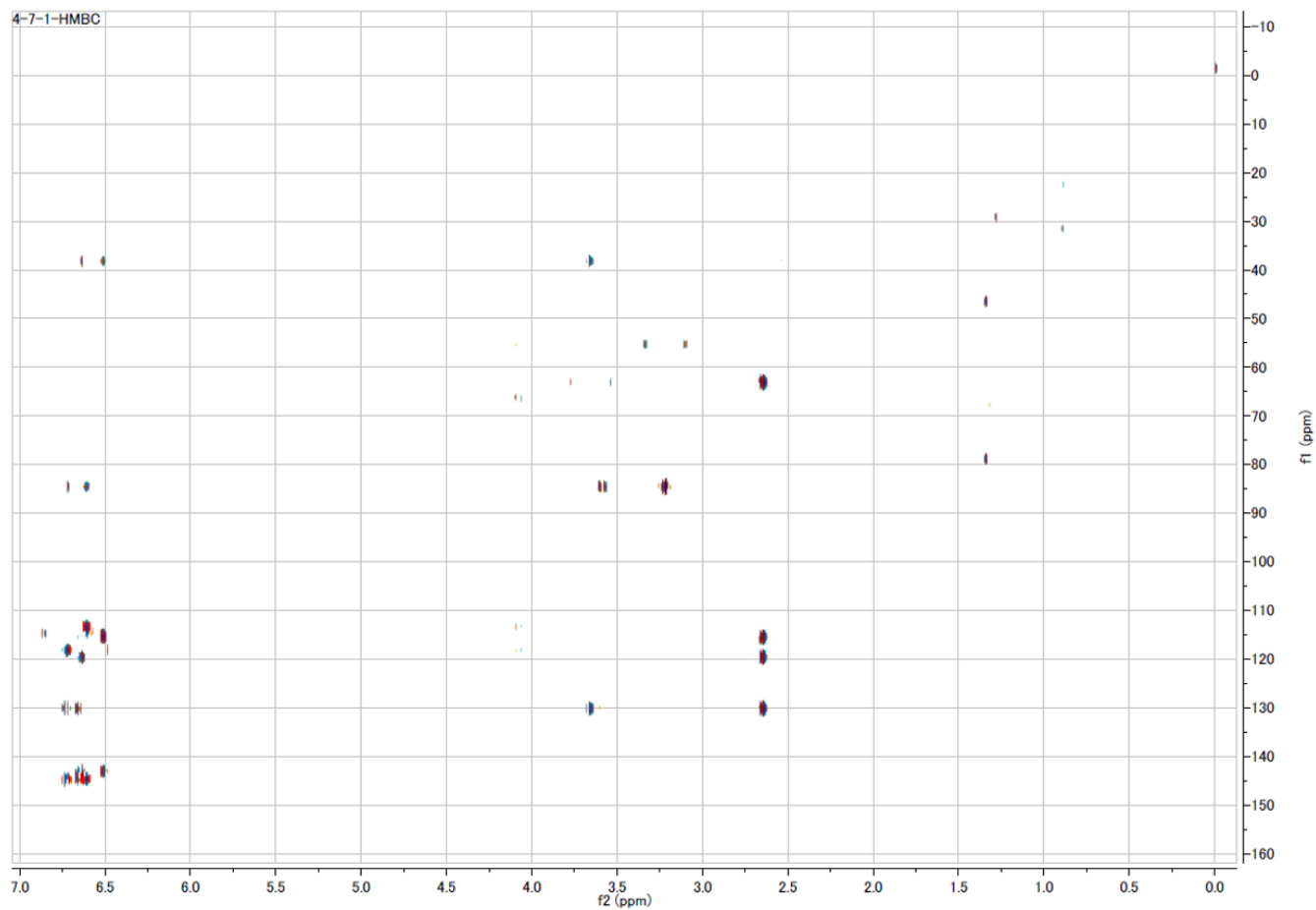


Appendix xxiv: HSQC-NMR (region  $\delta$ H 2.0 to 0.0 ppm) for the novel compound, 3,4-dihydroxyphenyl-2-methoxyethanol



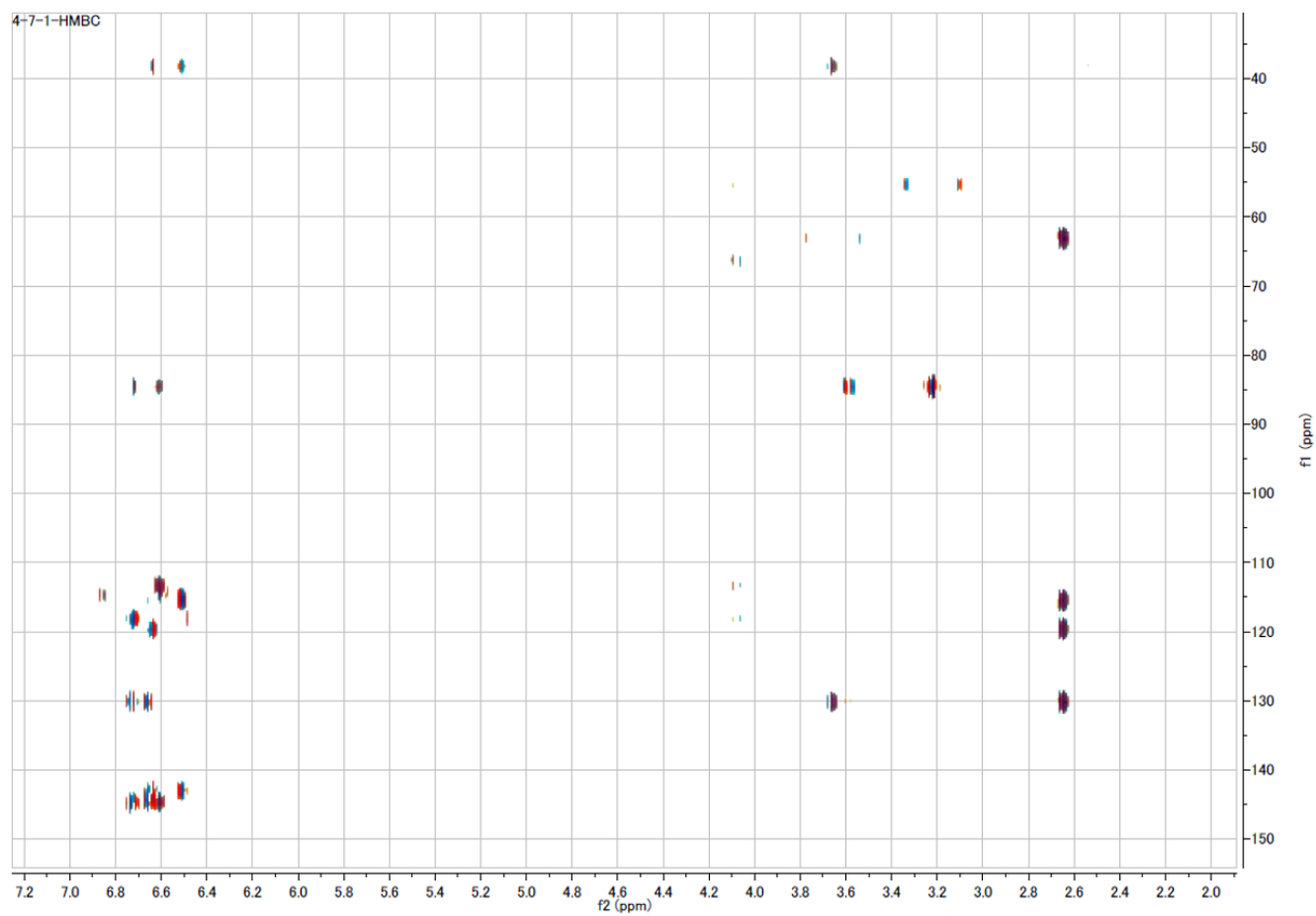


Appendix xxv: HMBC-NMR (whole region) for the novel compound, 3,4-dihydroxyphenyl-2-methoxyethanol

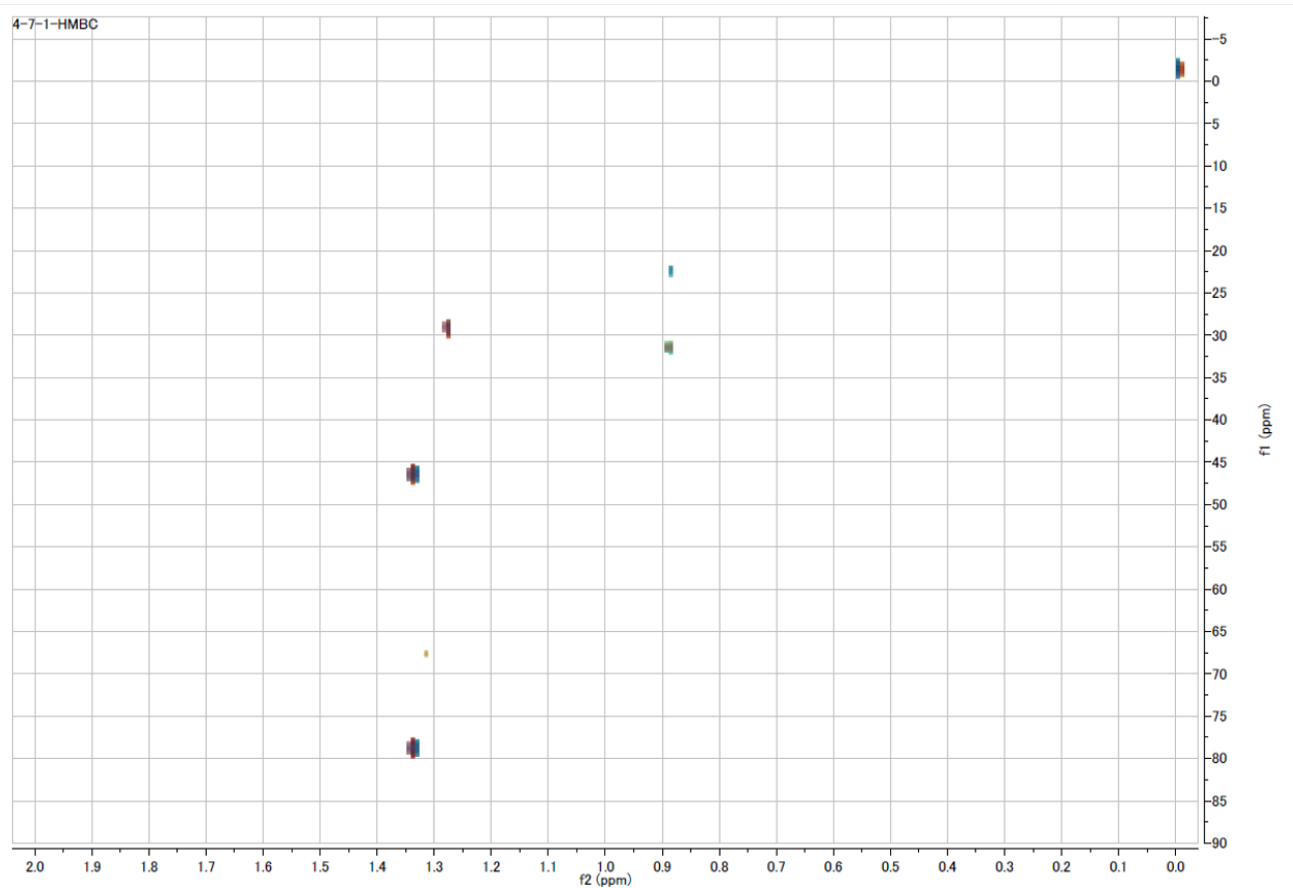


Appendix xxvi: HMBC-NMR (region  $\delta$ H 7.0 to 2.0 ppm) for the novel compound 5 -

3,4-dihydroxyphenyl-2-methoxyethanol



Appendix xxvii: HMBC-NMR (region  $\delta$ H 2.0 to 0.0 ppm) for the novel compound, 3,4-dihydroxyphenyl-2-methoxyethanol

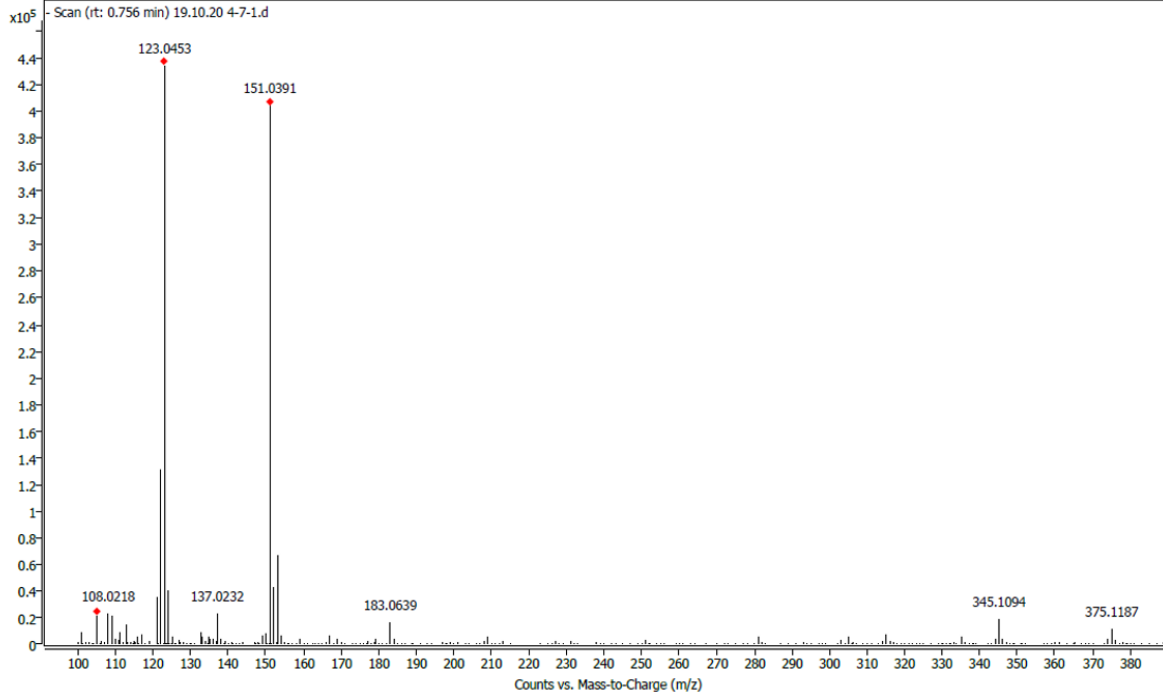


# Appendix xxviii: HR-ESI-MS of the novel compound, 3,4-dihydroxyphenyl-2-methoxyethanol

## Spectrum Plot Report



Name	19.10.20 4-7-1	Rack Pos.	Instrument	Instrument 1	Operator
Inj. Vol. (ul)	5	Plate Pos.	IRM Status	All ions missed	
Data File	19.10.20 4-7-1.d	Method (Acq)	Short Column Modified.m	Comment	Acq. Time (Local)
					10/20/2019 3:32:48 PM (UTC+09:00)



## References

- (1) Molina Alcaide, E.; Nefzaoui, A. Recycling of Olive Oil By-Products: Possibilities of Utilization in Animal Nutrition. *Int. Biodeterior. Biodegrad.* **1996**, *38* (3–4), 227–235. [https://doi.org/10.1016/s0964-8305\(96\)00055-8](https://doi.org/10.1016/s0964-8305(96)00055-8).
- (2) Fernández-Bolaños, J.; Rodríguez, G.; Rodríguez, R.; Guillén, R.; Jiménez, A. Extraction of Interesting Organic Compounds from Olive Oil Waste. *Grasas y Aceites* **2006**, *57* (1), 95–106. <https://doi.org/10.3989/gya.2006.v57.i1.25>.
- (3) Vossen, P. Olive Oil: History, Production, and Characteristics of the World's Classic Oils. *HortScience* **2007**, *42* (5), 1093–1100.
- (4) Ghanbari, R.; Anwar, F.; Alkharfy, K. M.; Gilani, A. H.; Saari, N. Valuable Nutrients and Functional Bioactives in Different Parts of Olive (*Olea Europaea* L.)-a Review. *International journal of molecular sciences*. Molecular Diversity Preservation International March 12, 2012, pp 3291–3340. <https://doi.org/10.3390/ijms13033291>.
- (5) De Leonardis, A.; Aretini, A.; Alfano, G.; MacCiola, V.; Ranalli, G. Isolation of a Hydroxytyrosol-Rich Extract from Olive Leaves (*Olea Europaea* L.) and Evaluation of Its Antioxidant Properties and Bioactivity. *Eur. Food Res. Technol.* **2008**, *226* (4), 653–659. <https://doi.org/10.1007/s00217-007-0574-3>.

- (6) S. Z., T. R. A.; J., G.; Sreekrishnan. Technologies for Olive Mill Wastewater (OMW) Treatment - a Review. *J. Chem. Technol. Biotechnol.* **2006**, *81*, 1475–1485. <https://doi.org/10.1002/jctb>.
- (7) Vinha, A. F.; Ferreres, F.; Silva, B. M.; Valentão, P.; Gonçalves, A.; Pereira, J. A.; Oliveira, M. B.; Seabra, R. M.; Andrade, P. B. Phenolic Profiles of Portuguese Olive Fruits (*Olea Europaea* L.): Influences of Cultivar and Geographical Origin. *Food Chem.* **2005**, *89* (4), 561–568. <https://doi.org/10.1016/j.foodchem.2004.03.012>.
- (8) Kapellakis, I. E.; Tsagarakis, K. P.; Crowther, J. C. Olive Oil History, Production and by-Product Management. *Rev. Environ. Sci. Biotechnol.* **2008**, *7* (1), 1–26. <https://doi.org/10.1007/s11157-007-9120-9>.
- (9) Roselló-Soto, E.; Barba, F. J.; Parniakov, O.; Galanakis, C. M.; Lebovka, N.; Grimi, N.; Vorobiev, E. High Voltage Electrical Discharges, Pulsed Electric Field, and Ultrasound Assisted Extraction of Protein and Phenolic Compounds from Olive Kernel. *Food Bioprocess Technol.* **2015**, *8* (4), 885–894. <https://doi.org/10.1007/s11947-014-1456-x>.
- (10) Sayadi, S.; Allouche, N.; Jaoua, M.; Aloui, F. Detrimental Effects of High Molecular-Mass Polyphenols on Olive Mill Wastewater Biotreatment. *Process Biochem.* **2000**, *35*, 725–735.
- (11) Azbar, N.; Bayram, A.; Filibeli, A.; Muezzinoglu, A.; Sengul, F.; Ozer, A. A

Review of Waste Management Options in Olive Oil Production. *Crit. Rev. Environ. Sci. Technol.* **2004**, 34 (3), 209–247.  
<https://doi.org/10.1080/10643380490279932>.

- (12) Ouallagui, Z. B.; Ouaziz, M. B.; An, J. H.; Oukhris, M. B.; Igane, G. R.; Riha, I. F.; Emai, H. J.; Ki, I. F.; Horbel, H. G.; Soda, H. I.; et al. Valorization of Olive Processing By-Products : Characterization , Investigation of Chemico-Biological Activities and Identification of Active Compounds. *J. Arid L. Stud.* **2012**, 64 (22 (1)), 61–64.
- (13) Galanakis, C. M. Olive Oil Production Sector: Environmental Effects and Sustainability Challenges. In *Olive Mill Waste: Recent advances for Sustainable management*, Souilem, S., El-Abbassi, A., Kiai, H., Hafidi, A., Sayadi, S., Galanakis, C. M., Eds.; Elsevier: Oxford, 2017; pp 1–28.  
<https://doi.org/10.1080/01436590050004300>.
- (14) Bouknana, D.; Hammouti, B.; Salghi, R.; Jodeh, S.; Zarrouk, A.; Warad, I.; Aouniti, A.; Sbaa, M. Physicochemical Characterization of Olive Oil Mill Wastewaters in the Eastern Region of Morocco. *J. Mater. Environ. Sci.* **2014**, 5 (4), 1039–1058.
- (15) Galanakis, C. M. Recovery of High Added-Value Components from Food Wastes: Conventional, Emerging Technologies and Commercialized Applications. *Trends Food Sci. Technol.* **2012**, 26 (2), 68–87.

<https://doi.org/10.1016/j.tifs.2012.03.003>.

- (16) de Jong, E.; Jungmeier, G. Biorefinery Concepts in Comparison to Petrochemical Refineries. In *Industrial Biorefineries and White Biotechnology*; Ashok, P., Rainer, H., Christian, L., Mohammad, T., Madhavan, N. (Eds), Eds.; Elsevier B.V.: Waltham, USA, 2015; pp 3–33. <https://doi.org/10.1016/B978-0-444-63453-5.00001-X>.
- (17) Obied, H. K.; Allen, M. S.; Bedgood, D. R.; Prenzler, P. D.; Robards, K.; Stockmann, R. Bioactivity and Analysis of Biophenols Recovered from Olive Mill Waste. *J. Agric. Food Chem.* **2005**, *53* (4), 823–837. <https://doi.org/10.1021/jf048569x>.
- (18) Visioli, F.; Romani, A.; Mulinacci, N.; Zarini, S.; Conte, D.; Vincieri, F. F.; Galli, C. Antioxidant and Other Biological Activities of Olive Mill Waste Waters. *J. Agric. Food Chem.* **1999**, *47* (8), 3397–3401. <https://doi.org/10.1021/jf9900534>.
- (19) Visioli, F.; Bellosta, S.; Galli, C. Cardioprotective Properties of Olive Oil-Derived Polyphenols. *Atherosclerosis* **1997**, *134*, 336.
- (20) Sheabar, F. Z.; Neeman, I. Separation and Concentration of Natural Antioxidants from the Rape of Olives. *J. Am. Oil Chem. Soc.* **1988**, *65* (6), 990–993. <https://doi.org/10.1007/BF02544526>.



- (21) Servili, M.; Taticchi, A.; Esposto, S.; Urbani, S.; Selvaggini, R.; Montedoro, G. F. Effect of Olive Stoning on the Volatile and Phenolic Composition of Virgin Olive Oil. *J. Agric. Food Chem.* **2007**, *55* (17), 7028–7035.  
<https://doi.org/10.1021/jf070600i>.
- (22) Kishikawa, A.; Ashour, A.; Zhu, Q.; Yasuda, M.; Ishikawa, H.; Shimizu, K. Multiple Biological Effects of Olive Oil By-Products Such as Leaves, Stems, Flowers, Olive Milled Waste, Fruit Pulp, and Seeds of the Olive Plant on Skin. *Phyther. Res.* **2015**, *29* (6), 877–886. <https://doi.org/10.1002/ptr.5326>.
- (23) Obied, H. K.; Bedgood Jr, D. R.; Prenzler, P. D.; Robards, K. Bioscreening of Australian Olive Mill Waste Extracts : Biophenol Content , Antioxidant , Antimicrobial and Molluscicidal Activities. *Food Chem. Toxicol.* **2007**, *45*, 1238–1248. <https://doi.org/10.1016/j.fct.2007.01.004>.
- (24) Peralbo-Molina, Á.; Luque deCastro, M. D. Potential of Residues from the Mediterranean Agriculture and Agrifood Industry. *Trends Food Sci. Technol.* **2013**, *32* (1), 16–24. <https://doi.org/10.1016/j.tifs.2013.03.007>.
- (25) Herrero, M.; Temirzoda, T. N.; Segura-Carretero, A.; Quirantes, R.; Plaza, M.; Ibañez, E. New Possibilities for the Valorization of Olive Oil By-Products. *J. Chromatogr. A* **2011**, *1218* (42), 7511–7520.  
<https://doi.org/10.1016/j.chroma.2011.04.053>.
- (26) Mulinacci, N.; Romani, A.; Galardi, C.; Pinelli, P.; Giaccherini, C.; Vincieri, F.

F. Polyphenolic Content in Olive Oil Waste Waters and Related Olive Samples. *J. Agric. Food Chem.* **2001**, *49* (8), 3509–3514.

<https://doi.org/10.1021/jf000972q>.

- (27) Amro, B.; Aburjai, T.; Al-Khalil, S. Antioxidative and Radical Scavenging Effects of Olive Cake Extract. *Fitoterapia* **2002**, *73* (6), 456–461.  
[https://doi.org/10.1016/S0367-326X\(02\)00173-9](https://doi.org/10.1016/S0367-326X(02)00173-9).
- (28) Hassen, I.; Casabianca, H.; Hosni, K. Biological Activities of the Natural Antioxidant Oleuropein: Exceeding the Expectation - A Mini-Review. *J. Funct. Foods* **2015**, *18* (2015), 926–940.  
<https://doi.org/10.1016/j.jff.2014.09.001>.
- (29) Speroni, E.; Guerra, M. C.; Minghetti, A.; Crespi-Perellino, N.; Pasini, P.; Piazza, F.; Roda, A. Oleuropein Evaluated in Vitro and in Vivo as an Antioxidant. *Phyther. Res.* **1998**, *12* (SUPPL. 1), 1997–1999.  
[https://doi.org/10.1002/\(SICI\)1099-1573\(1998\)12:1+<S98::AID-PTR263>3.0.CO;2-M](https://doi.org/10.1002/(SICI)1099-1573(1998)12:1+<S98::AID-PTR263>3.0.CO;2-M).
- (30) Czerwińska, M.; Kiss, A. K.; Naruszewicz, M. A Comparison of Antioxidant Activities of Oleuropein and Its Dialdehydic Derivative from Olive Oil, Oleacein. *Food Chem.* **2012**, *131* (3), 940–947.  
<https://doi.org/10.1016/j.foodchem.2011.09.082>.
- (31) Saija, A.; Trombetta, D.; Tomaino, A.; Lo Cascio, R.; Princi, P.; Uccella, N.;

Bonina, F.; Castelli, F. "In Vitro" Evaluation of the Antioxidant Activity and Biomembrane Interaction of the Plant Phenols Oleuropein and Hydroxytyrosol. *Int. J. Pharm.* **1998**, *166* (2), 123–133.  
[https://doi.org/10.1016/S0378-5173\(98\)00018-0](https://doi.org/10.1016/S0378-5173(98)00018-0).

- (32) Omar, S. H. Cardioprotective and Neuroprotective Roles of Oleuropein in Olive. *Saudi Pharm. J.* **2010**, *18* (3), 111–121.  
<https://doi.org/10.1016/J.JSPS.2010.05.005>.
- (33) Andrikopoulos, N. K.; Antonopoulou, S.; Kaliora, A. C. Oleuropein Inhibits LDL Oxidation Induced by Cooking Oil Frying By-Products and Platelet Aggregation Induced by Platelet-Activating Factor. *LWT - Food Sci. Technol.* **2002**, *35* (6), 479–484. <https://doi.org/https://doi.org/10.1006/fstl.2002.0893>.
- (34) Ruíz-Gutiérrez, V.; Muriana, F. J. G.; Maestro, R.; Graciani, E. Oleuropein on Lipid and Fatty Acid Composition of Rat Heart. *Nutr. Res.* **1995**, *15* (1), 37–51. [https://doi.org/https://doi.org/10.1016/0271-5317\(95\)91651-R](https://doi.org/https://doi.org/10.1016/0271-5317(95)91651-R).
- (35) Gutierrez, V. R.; De La Puerta, R.; Catalá, A. The Effect of Tyrosol, Hydroxytyrosol and Oleuropein on the Non-Enzymic Lipid Peroxidation of Rat Liver Microsomes. *Mol. Cell. Biochem.* **2001**, *217* (1–2), 35–41.  
<https://doi.org/10.1023/A:1007219931090>.
- (36) Alirezaei, M.; Dezfoulian, O.; Neamati, S.; Rashidipour, M.; Tanideh, N.; Kheradmand, A. Oleuropein Prevents Ethanol-Induced Gastric Ulcers via

Elevation of Antioxidant Enzyme Activities in Rats. *J. Physiol. Biochem.*

**2012**, 68 (4), 583–592. <https://doi.org/10.1007/s13105-012-0177-8>.

- (37) Jemai, H.; Feki, A. E. L.; Sayadi, S. Antidiabetic and Antioxidant Effects of Hydroxytyrosol and Oleuropein from Olive Leaves in Alloxan-Diabetic Rats. *J. Agric. Food Chem.* **2009**, 57 (19), 8798–8804. <https://doi.org/10.1021/jf901280r>.
- (38) Ahmadvand, H.; Noori, A.; Dehnoo, M. G.; Bagheri, S.; Cheraghi, R. A. Hypoglycemic, Hypolipidemic and Antiatherogenic Effects of Oleuropein in Alloxan-Induced Type 1 Diabetic Rats. *Asian Pacific J. Trop. Dis.* **2014**, 4 (S1). [https://doi.org/10.1016/S2222-1808\(14\)60481-3](https://doi.org/10.1016/S2222-1808(14)60481-3).
- (39) Duarte, J.; Perez, O.; Zarzuelo, A.; Jimenez, J.; Perez-Vizcaino, F.; Tamargo, J. Effects of Oleuropeoside in Isolated Guinea-Pig Atria. *Planta Med.* **1993**, 59 (4), 318–322. <https://doi.org/10.1055/s-2006-959690>.
- (40) Haloui, E.; Marzouk, B.; Marzouk, Z.; Bouraoui, A.; Fenina, N. Hydroxytyrosol and Oleuropein from Olive Leaves: Potent Anti-Inflammatory and Analgesic Activities. *J. Food, Agric. Environ.* **2011**, 9 (3–4), 128–133.
- (41) De La Puerta, R.; Gutierrez, V. R.; Hoult, J. R. S. Inhibition of Leukocyte 5-Lipoxygenase by Phenolics from Virgin Olive Oil. *Biochem. Pharmacol.* **1999**, 57 (4), 445–449. [https://doi.org/10.1016/S0006-2952\(98\)00320-7](https://doi.org/10.1016/S0006-2952(98)00320-7).

- (42) Bisignano, G.; Tomaino, A.; Lo Cascio, R.; Crisafi, G.; Uccella, N.; Saija, A. On the In-Vitro Antimicrobial Activity of Oleuropein and Hydroxytyrosol. *J. Pharm. Pharmacol.* **1999**, *51*, 971–974.  
<https://doi.org/10.1211/0022357991773258>.
- (43) Furneri, P. M.; Piperno, A.; Saija, A.; Bisignano, G. Antimycoplasmal Activity of Hydroxytyrosol. *Antimicrob. Agents Chemother.* **2004**, *48* (12), 4892–4894. <https://doi.org/10.1128/AAC.48.12.4892-4894.2004>.
- (44) Zorić, N.; Kopjar, N.; Bobnjarić, I.; Horvat, I.; Tomić, S.; Kosalec, I. Antifungal Activity of Oleuropein against *Candida Albicans*-the in Vitro Study. *Molecules* **2016**, *21* (12). <https://doi.org/10.3390/molecules21121631>.
- (45) Lee-Huang, S.; Zhang, L.; Huang, P. L.; Chang, Y. T.; Huang, P. L. Anti-HIV Activity of Olive Leaf Extract (OLE) and Modulation of Host Cell Gene Expression by HIV-1 Infection and OLE Treatment. *Biochem. Biophys. Res. Commun.* **2003**, *307* (4), 1029–1037. [https://doi.org/10.1016/S0006-291X\(03\)01292-0](https://doi.org/10.1016/S0006-291X(03)01292-0).
- (46) Mahmoudi, A.; Ghorbel, H.; Feki, I.; Bouallagui, Z.; Guermazi, F.; Ayadi, L.; Sayadi, S. Oleuropein and Hydroxytyrosol Protect Rats' Pups against Bisphenol A Induced Hypothyroidism. *Biomed. Pharmacother.* **2018**, *103*, 1115–1126. <https://doi.org/https://doi.org/10.1016/j.biopha.2018.03.004>.
- (47) -ÖZKAYA, F. D.; ÖZKAYA, M. T. Oleuropein Using as an Additive for Feed

and Products Used for Humans. *J. Food Process. Technol.* **2011**, *02* (03).

<https://doi.org/10.4172/2157-7110.1000113>.

- (48) Khalatbary, A. R.; Ahmadvand, H. Neuroprotective Effect of Oleuropein Following Spinal Cord Injury in Rats. *Neurol. Res.* **2012**, *34* (1), 44–51. <https://doi.org/10.1179/1743132811Y.0000000058>.
- (49) Pourkhodadad, S.; Alirezaei, M.; Moghaddasi, M.; Ahmadvand, H.; Karami, M.; Delfan, B.; Khanipour, Z. Neuroprotective Effects of Oleuropein against Cognitive Dysfunction Induced by Colchicine in Hippocampal CA1 Area in Rats. *J. Physiol. Sci.* **2016**, *66* (5), 397–405. <https://doi.org/10.1007/s12576-016-0437-4>.
- (50) Ceccon, L.; Saccù, D.; Procida, G.; Cardinali, S. Liquid Chromatographic Determination of Simple Phenolic Compounds in Waste Waters from Olive Oil Production Plants. *J. AOAC Int.* **2001**, *84* (6), 1739–1744. <https://doi.org/10.1093/jaoac/84.6.1739>.
- (51) Funes, L.; Fernández-Arroyo, S.; Laporta, O.; Pons, A.; Roche, E.; Segura-Carretero, A.; Fernández-Gutiérrez, A.; Micol, V. Correlation between Plasma Antioxidant Capacity and Verbascoside Levels in Rats after Oral Administration of Lemon Verbena Extract. *Food Chem.* **2009**, *117* (4), 589–598. <https://doi.org/10.1016/j.foodchem.2009.04.059>.
- (52) Capasso, R.; Evidente, A.; Avolio, S.; Solla, F. A Highly Convenient

Synthesis of Hydroxytyrosol and Its Recovery from Agricultural Waste

Waters. *J. Agric. Food Chem.* **1999**, *47* (4), 1745–1748.

<https://doi.org/10.1021/jf9809030>.

- (53) Visioli, F.; Caruso, D.; Plasmati, E.; Patelli, R.; Mulinacci, N.; Romani, A.; Galli, G.; Galli, C. Hydroxytyrosol, as a Component of Olive Mill Waste Water, Is Dose- Dependently Absorbed and Increases the Antioxidant Capacity of Rat Plasma. *Free Radic. Res.* **2001**, *34* (3), 301–305.  
<https://doi.org/10.1080/10715760100300271>.
- (54) Casalino, E.; Calzaretti, G.; Sblano, C.; Landriscina, V.; Tecce, M. F.; Landriscina, C. Antioxidant Effect of Hydroxytyrosol (DPE) and Mn<sup>2+</sup> in Liver of Cadmium-Intoxicated Rats. *Comp. Biochem. Physiol. - C Toxicol. Pharmacol.* **2002**, *133* (4), 625–632. [https://doi.org/10.1016/S1532-0456\(02\)00180-1](https://doi.org/10.1016/S1532-0456(02)00180-1).
- (55) Manna, C.; Galletti, P.; Cucciolla, V.; Montedoro, G.; Zappia, V. Olive Oil Hydroxytyrosol Protects Human Erythrocytes against Oxidative Damages. *J. Nutr. Biochem.* **1999**, *10* (3), 159–165. [https://doi.org/10.1016/S0955-2863\(98\)00085-0](https://doi.org/10.1016/S0955-2863(98)00085-0).
- (56) Leger, C. L.; Kadiri-Hassani, N.; Descomps, B. Decreased Superoxide Anion Production in Cultured Human Promonocyte Cells (THP-1) Due to Polyphenol Mixtures from Olive Oil Processing Wastewaters. *J. Agric. Food*

*Chem.* **2000**, *48* (10), 5061–5067. <https://doi.org/10.1021/jf991349c>.

- (57) Hu, T.; He, X.-W.; Jiang, J.-G.; Xu, X.-L. Hydroxytyrosol and Its Potential Therapeutic Effects. *J. Agric. Food Chem.* **2014**, *62* (7), 1449–1455. <https://doi.org/10.1021/jf405820v>.
- (58) Loru, D.; Incani, A.; Deiana, M.; Corona, G.; Atzeri, A.; Melis, M.; Rosa, A.; Dessì, M. Protective Effect of Hydroxytyrosol and Tyrosol against Oxidative Stress in Kidney Cells. *Toxicol. Ind. Health* **2009**, *25* (5), 301–310. <https://doi.org/10.1177/0748233709103028>.
- (59) Fabiani, R.; De Bartolomeo, A.; Rosignoli, P.; Servili, M.; Montedoro, G. F.; Morozzi, G. Cancer Chemoprevention by Hydroxytyrosol Isolated from Virgin Olive Oil through G1 Cell Cycle Arrest and Apoptosis. *Eur. J. Cancer Prev.* **2002**, *11* (4), 351–358.
- (60) Ragione, F. Della; Cucciolla, V.; Borriello, A.; Pietra, V. Della; Pontoni, G.; Racioppi, L.; Manna, C.; Galletti, P.; Zappia, V. Hydroxytyrosol, a Natural Molecule Occurring in Olive Oil, Induces Cytochrome c-Dependent Apoptosis. *Biochem. Biophys. Res. Commun.* **2000**, *278* (3), 733–739. <https://doi.org/10.1006/BBRC.2000.3875>.
- (61) Bertelli, M.; Kiani, A. K.; Paolacci, S.; Manara, E.; Kurti, D.; Dhuli, K.; Bushati, V.; Miertus, J.; Pangallo, D.; Baglivo, M.; et al. Hydroxytyrosol: A Natural Compound with Promising Pharmacological Activities. *J. Biotechnol.*



**2020**, 309, 29–33.

<https://doi.org/https://doi.org/10.1016/j.jbiotec.2019.12.016>.

- (62) Fuccelli, R.; Fabiani, R.; Rosignoli, P. Hydroxytyrosol Exerts Anti-Inflammatory and Anti-Oxidant Activities in a Mouse Model of Systemic Inflammation. *Molecules* **2018**, 23 (12).  
<https://doi.org/10.3390/molecules23123212>.
- (63) Beerens, K.; Desmet, T.; Soetaert, W.; Elbein, A. D.; Pan, Y. T.; Pastuszak, I.; Carroll, D.; Equilibria, P.; The, I. N.; Golovina, E. A.; et al. NII-Electronic Library Service. *Chem. Pharm. Bull.* **2012**, 14 (4), 369–375.  
<https://doi.org/10.1248/cpb.37.3229>.
- (64) Crespo, M. C.; Tomé-Carneiro, J.; Pintado, C.; Dávalos, A.; Visioli, F.; Burgos-Ramos, E. Hydroxytyrosol Restores Proper Insulin Signaling in an Astrocytic Model of Alzheimer's Disease. *BioFactors* **2017**, 43 (4), 540–548.  
<https://doi.org/10.1002/biof.1356>.
- (65) Peng, Y.; Hou, C.; Yang, Z.; Li, C.; Jia, L.; Liu, J.; Tang, Y.; Shi, L.; Li, Y.; Long, J.; et al. Hydroxytyrosol Mildly Improve Cognitive Function Independent of APP Processing in APP/PS1 Mice. *Mol. Nutr. Food Res.* **2016**, 60 (11), 2331–2342. <https://doi.org/10.1002/mnfr.201600332>.
- (66) Di Benedetto, R.; Vari, R.; Scazzocchio, B.; Filesi, C.; Santangelo, C.; Giovannini, C.; Matarrese, P.; D'Archivio, M.; Masella, R. Tyrosol, the Major

Extra Virgin Olive Oil Compound, Restored Intracellular Antioxidant Defences in Spite of Its Weak Antioxidative Effectiveness. *Nutr. Metab. Cardiovasc. Dis.* **2007**, *17* (7), 535–545.  
<https://doi.org/https://doi.org/10.1016/j.numecd.2006.03.005>.

- (67) Damiani, E.; Belaid, C.; Carloni, P.; Greci, L. Comparison of Antioxidant Activity Between Aromatic Indolinonic Nitroxides and Natural and Synthetic Antioxidants. *Free Radic. Res.* **2003**, *37* (7), 731–741.  
<https://doi.org/10.1080/1071576031000102169>.
- (68) Vivancos, M.; Moreno, J. J. Effect of Resveratrol, Tyrosol and  $\beta$ -Sitosterol on Oxidised Low-Density Lipoprotein-Stimulated Oxidative Stress, Arachidonic Acid Release and Prostaglandin E2 Synthesis by RAW 264.7 Macrophages. *Br. J. Nutr.* **2008**, *99* (6), 1199–1207.  
<https://doi.org/10.1017/S0007114507876203>.
- (69) Lesage-Meessen, L.; Navarro, D.; Maunier, S.; Sigoillot, J. C.; Lorquin, J.; Delattre, M.; Simon, J. L.; Asther, M.; Labat, M. Simple Phenolic Content in Olive Oil Residues as a Function of Extraction Systems. *Food Chem.* **2001**, *75* (4), 501–507. [https://doi.org/10.1016/S0308-8146\(01\)00227-8](https://doi.org/10.1016/S0308-8146(01)00227-8).
- (70) Sun-Waterhouse, D.; Zhou, J.; Miskelly, G. M.; Wibisono, R.; Wadhwa, S. S. Stability of Encapsulated Olive Oil in the Presence of Caffeic Acid. *Food Chem.* **2011**, *126* (3), 1049–1056.

<https://doi.org/10.1016/j.foodchem.2010.11.124>.

- (71) Quiles, J. L.; Farquharson, A. J.; Simpson, D. K.; Grant, I.; Wahle, K. W. J. Olive Oil Phenolics: Effects on DNA Oxidation and Redox Enzyme mRNA in Prostate Cells. *Br. J. Nutr.* **2002**, *88* (3), 225–234.  
<https://doi.org/10.1079/bjn2002620>.
- (72) Aziz, N. H.; Farag, S. E.; Mousa, L. A.; Abo-Zaid, M. A. Comparative Antibacterial and Antifungal Effects of Some Phenolic Compounds. *Microbios* **1998**, *93* (374), 43–54.
- (73) Cardinali, A.; Pati, S.; Minervini, F.; D'Antuono, I.; Linsalata, V.; Lattanzio, V. Verbascoside, Isoverbascoside, and Their Derivatives Recovered from Olive Mill Wastewater as Possible Food Antioxidants. *J. Agric. Food Chem.* **2012**, *60* (7), 1822–1829. <https://doi.org/10.1021/jf204001p>.
- (74) Kostyuk, V. A.; Potapovich, A. I.; Lulli, D.; Stancato, A.; De Luca, C.; Pastore, S.; Korkina, L. Modulation of Human Keratinocyte Responses to Solar UV by Plant Polyphenols As a Basis for Chemoprevention of Non-Melanoma Skin Cancers. *Curr. Med. Chem.* **2013**, *20* (7), 869–879.  
<https://doi.org/10.2174/0929867311320070003>.
- (75) Campo, G.; Marchesini, J.; Bristot, L.; Monti, M.; Gambetti, S.; Pavasini, R.; Pollina, A.; Ferrari, R. The in Vitro Effects of Verbascoside on Human Platelet Aggregation. *J. Thromb. Thrombolysis* **2012**, *34* (3), 318–325.

<https://doi.org/10.1007/s11239-012-0757-z>.

- (76) Kang, D. G.; Lee, Y. S.; Kim, H. J.; Lee, Y. M.; Lee, H. S. Angiotensin Converting Enzyme Inhibitory Phenylpropanoid Glycosides from *Clerodendron Trichotomum*. *J. Ethnopharmacol.* **2003**, *89* (1), 151–154. [https://doi.org/10.1016/S0378-8741\(03\)00274-5](https://doi.org/10.1016/S0378-8741(03)00274-5).
- (77) Díaz, A. M.; Abad, M. J.; Fernández, L.; Silván, A. M.; De Santos, J.; Bermejo, P. Phenylpropanoid Glycosides from *Scrophularia Scorodonia*: In Vitro Anti-Inflammatory Activity. *Life Sci.* **2004**, *74* (20), 2515–2526. <https://doi.org/10.1016/j.lfs.2003.10.008>.
- (78) Romero, C.; Brenes, M.; García, P.; Garrido, A. Hydroxytyrosol 4- $\beta$ -D-Glucoside, an Important Phenolic Compound in Olive Fruits and Derived Products. *J. Agric. Food Chem.* **2002**, *50* (13), 3835–3839. <https://doi.org/10.1021/jf011485t>.
- (79) Yang Kuo, L. M.; Zhang, L. J.; Huang, H. T.; Lin, Z. H.; Liaw, C. C.; Cheng, H. L.; Lee, K. H.; Morris-Natschke, S. L.; Kuo, Y. H.; Ho, H. O. Antioxidant Lignans and Chromone Glycosides from *Eurya Japonica*. *J. Nat. Prod.* **2013**, *76* (4), 580–587. <https://doi.org/10.1021/np3007638>.
- (80) Mascaraque, C.; Aranda, C.; Ocón, B.; Monte, M. J.; Suárez, M. D.; Zarzuelo, A.; Marín, J. J. G.; Martínez-Augustin, O.; de Medina, F. S. Rutin Has Intestinal Antiinflammatory Effects in the CD4<sup>+</sup> CD62L<sup>+</sup> T Cell Transfer

Model of Colitis. *Pharmacol. Res.* **2014**, *90*, 48–57.

<https://doi.org/https://doi.org/10.1016/j.phrs.2014.09.005>.

- (81) Selloum, L.; Bouriche, H.; Tigrine, C.; Boudoukha, C. Anti-Inflammatory Effect of Rutin on Rat Paw Oedema, and on Neutrophils Chemotaxis and Degranulation. *Exp. Toxicol. Pathol.* **2003**, *54* (4), 313–318.  
<https://doi.org/https://doi.org/10.1078/0940-2993-00260>.
- (82) Kamalakkannan, N.; Prince, P. S. M. Antihyperglycaemic and Antioxidant Effect of Rutin, a Polyphenolic Flavonoid, in Streptozotocin-Induced Diabetic Wistar Rats. *Basic Clin. Pharmacol. Toxicol.* **2006**, *98* (1), 97–103.  
[https://doi.org/10.1111/j.1742-7843.2006.pto\\_241.x](https://doi.org/10.1111/j.1742-7843.2006.pto_241.x).
- (83) Gautam, R.; Singh, M.; Gautam, S.; Rawat, J. K.; Saraf, S. A.; Kaithwas, G. Rutin Attenuates Intestinal Toxicity Induced by Methotrexate Linked with Anti-Oxidative and Anti-Inflammatory Effects. *BMC Complement. Altern. Med.* **2016**, *16* (1), 1–6. <https://doi.org/10.1186/s12906-016-1069-1>.
- (84) Zang, L. Y.; Cosma, G.; Gardner, H.; Shi, X.; Castranova, V.; Vallyathan, V. Effect of Antioxidant Protection by P-Coumaric Acid on Low-Density Lipoprotein Cholesterol Oxidation. *Am. J. Physiol. - Cell Physiol.* **2000**, *279* (4 48-4), 954–960. <https://doi.org/10.1152/ajpcell.2000.279.4.c954>.
- (85) Abdel-Wahab, M. H.; El-Mahdy, M. A.; Abd-Ellah, M. F.; Helal, G. K.; Khalifa, F.; Hamada, F. M. A. Influence of P-Coumaric Acid on Doxorubicin-Induced

Oxidative Stress in Rat's Heart. *Pharmacol. Res.* **2003**, *48* (5), 461–465.

[https://doi.org/https://doi.org/10.1016/S1043-6618\(03\)00214-7](https://doi.org/https://doi.org/10.1016/S1043-6618(03)00214-7).

- (86) Kiliç, I.; Yeşiloğlu, Y. Spectroscopic Studies on the Antioxidant Activity of P-Coumaric Acid. *Spectrochim. Acta - Part A Mol. Biomol. Spectrosc.* **2013**, *115*, 719–724. <https://doi.org/10.1016/j.saa.2013.06.110>.
- (87) Ojha, D.; Patil, K. N. P-Coumaric Acid Inhibits the Listeria Monocytogenes RecA Protein Functions and SOS Response: An Antimicrobial Target. *Biochem. Biophys. Res. Commun.* **2019**, *517* (4), 655–661. <https://doi.org/10.1016/j.bbrc.2019.07.093>.
- (88) Boz, H. P-Coumaric Acid in Cereals: Presence, Antioxidant and Antimicrobial Effects. *Int. J. Food Sci. Technol.* **2015**, *50* (11), 2323–2328. <https://doi.org/10.1111/ijfs.12898>.
- (89) Sharma, B. R.; Gautam, L. N. S.; Adhikari, D.; Karki, R. A Comprehensive Review on Chemical Profiling of Nelumbo Nucifera: Potential for Drug Development. *Phyther. Res.* **2017**, *31* (1), 3–26. <https://doi.org/10.1002/ptr.5732>.
- (90) Stanely Mainzen Prince, P.; Rajakumar, S.; Dhanasekar, K. Protective Effects of Vanillic Acid on Electrocardiogram, Lipid Peroxidation, Antioxidants, Proinflammatory Markers and Histopathology in Isoproterenol Induced Cardiotoxic Rats. *Eur. J. Pharmacol.* **2011**, *668* (1–2), 233–240.

<https://doi.org/10.1016/j.ejphar.2011.06.053>.

- (91) Tai, A.; Sawano, T.; Ito, H. Antioxidative Properties of Vanillic Acid Esters in Multiple Antioxidant Assays. *Biosci. Biotechnol. Biochem.* **2012**, *76* (2), 314–318. <https://doi.org/10.1271/bbb.110700>.
- (92) Vinothiya, K.; Ashokkumar, N. Modulatory Effect of Vanillic Acid on Antioxidant Status in High Fat Diet-Induced Changes in Diabetic Hypertensive Rats. *Biomed. Pharmacother.* **2017**, *87*, 640–652. <https://doi.org/https://doi.org/10.1016/j.biopha.2016.12.134>.
- (93) Rodis, P. S.; Karathanos, V. T.; Mantzavinou, A. Partitioning of Olive Oil Antioxidants between Oil and Water Phases. *J. Agric. Food Chem.* **2002**, *50* (3), 596–601. <https://doi.org/10.1021/jf010864j>.
- (94) Lee, O. H.; Lee, B. Y. Antioxidant and Antimicrobial Activities of Individual and Combined Phenolics in *Olea Europaea* Leaf Extract. *Bioresour. Technol.* **2010**, *101* (10), 3751–3754. <https://doi.org/10.1016/j.biortech.2009.12.052>.
- (95) Mwakalukwa, R.; Ashour, A.; Amen, Y.; Niwa, Y.; Tamrakar, S. Anti-Allergic Activity of Polyphenolic Compounds Isolated from Olive Mill Wastes. *J. Funct. Foods* **2019**, *58* (April), 207–217. <https://doi.org/10.1016/j.jff.2019.04.058>.
- (96) Kishikawa, A.; Amen, Y.; Shimizu, K. Anti-Allergic Triterpenes Isolated from

Olive Milled Waste. *Cytotechnology* **2017**, 69 (2), 307–315.

<https://doi.org/10.1007/s10616-016-0058-z>.

- (97) D'Amato, G.; Vitale, C.; De Martino, A.; Viegi, G.; Lanza, M.; Molino, A.; Sanduzzi, A.; Vatrella, A.; Annesi-Maesano, I.; D'Amato, M. Effects on Asthma and Respiratory Allergy of Climate Change and Air Pollution. *Allergy Asthma Immunol. Rese4qrch* **2016**, 8 (5), 391–395.

<https://doi.org/10.1186/s40248-015-0036-x>.

- (98) D'amato, G.; Karl, B.; Cecchi, L.; Isabella, A.-M.; Sanduzzi, A.; Liccardi, G.; Vitale, C.; Stanziola, A.; D'amato, M. Climate Change and Air Pollution - Effects on Pollen Allergy and Other Allergic Respiratory Diseases. *Allergo J. Internatonal* **2014**, 23, 17–23. <https://doi.org/10.1007/s40629-014-0003-7>.

- (99) Gowshall, M.; Taylor-Robinson, S. D. The Increasing Prevalence of Non-Communicable Diseases in Low-Middle Income Countries: The View from Malawi. *Int. J. Gen. Med.* **2018**, 11, 255–264.

<https://doi.org/10.2147/IJGM.S157987>.

- (100) World Health Organization. Global Report on Diabetes. *Isbn* **2016**, 978, 88.

[https://doi.org/ISBN 978 92 4 156525 7](https://doi.org/ISBN%20978%204%20156525%207).

- (101) Alzheimer's Association. 2014 Alzheimer's Disease Facts and Figures. *Alzheimers. Dement.* **2014**, 10 (2), e47–e92.

<https://doi.org/10.1016/j.jalz.2014.02.001>.



- (102) American Diabetes Association. Diagnosis and Classification of Diabetes Mellitus. *Diabetes Care* **2014**, 37 (SUPPL.1), 81–90.  
<https://doi.org/10.2337/dc14-S081>.
- (103) Sugino, H.; Watanabe, A.; Amada, N.; Yamamoto, M.; Ohgi, Y.; Kostic, D.; Sanchez, R. Global Trends in Alzheimer Disease Clinical Development: Increasing the Probability of Success. *Clin. Ther.* **2015**, 37 (8), 1632–1642.  
<https://doi.org/10.1016/j.clinthera.2015.07.006>.
- (104) Hurd, M. D.; Martorell, P.; Delavande, A.; Mullen, K. J.; Langa, K. M. Monetary Costs of Dementia in the United States. *N. Engl. J. Med.* **2013**, 368 (14), 1326–1334. <https://doi.org/10.1056/NEJMsa1204629>.
- (105) Grosso, G. Dietary Antioxidants and Prevention of Non-Communicable Diseases. *Antioxidants* **2018**, 7 (7), 17–19.  
<https://doi.org/10.3390/antiox7070094>.
- (106) Nediani, C.; Ruzzolini, J.; Romani, A.; Calorini, L. Oleuropein, a Bioactive Compound from *Olea Europaea* L., as a Potential Preventive and Therapeutic Agent in Non-Communicable Diseases. *Antioxidants* **2019**, 8 (12).  
<https://doi.org/10.3390/antiox8120578>.
- (107) Gavahian, M.; Mousavi Khaneghah, A.; Lorenzo, J. M.; Munekata, P. E. S.; Garcia-Mantrana, I.; Collado, M. C.; Meléndez-Martínez, A. J.; Barba, F. J. Health Benefits of Olive Oil and Its Components: Impacts on Gut Microbiota

Antioxidant Activities, and Prevention of Noncommunicable Diseases.

*Trends Food Sci. Technol.* **2019**, *88* (February), 220–227.

<https://doi.org/10.1016/j.tifs.2019.03.008>.

- (108) Mangge, H. Antioxidants, Inflammation and Cardiovascular Disease. *World J. Cardiol.* **2014**, *6* (6), 462. <https://doi.org/10.4330/wjc.v6.i6.462>.
- (109) Peña-Oyarzun, D.; Bravo-Sagua, R.; Diaz-Vega, A.; Aleman, L.; Chiong, M.; Garcia, L.; Bambs, C.; Troncoso, R.; Cifuentes, M.; Morselli, E.; et al. Autophagy and Oxidative Stress in Non-Communicable Diseases: A Matter of the Inflammatory State? *Free Radic. Biol. Med.* **2018**, *124* (May), 61–78. <https://doi.org/10.1016/j.freeradbiomed.2018.05.084>.
- (110) Galli, S. J.; Tsai, M.; Piliponsky, A. M. The Development of Allergic Inflammation. *Nature* **2008**, *454*, 445.
- (111) Jackson, K. D.; Howie, L. D.; Akinbami, L. J. Trends in Allergic Conditions Among Children : *NCHC Data Br.* **2013**, No. 121, 1–8.
- (112) Broide, D. H. Immunomodulation of Allergic Disease. *Annu. Rev. Med.* **2009**, *60* (1), 279–291. <https://doi.org/10.1146/annurev.med.60.041807.123524>.
- (113) Joseph, N.; Palagani, R.; Nh, S.; Jain, V.; Joseph, N. Prevalence , Severity and Risk Factors of Allergic Disorders among People in South India. *Afr. Health Sci.* **2016**, *16* (1), 201–209.

- (114) Kawai, M.; Hirano, T.; Higa, S.; Arimitsu, J.; Maruta, M.; Kuwahara, Y.; Ohkawara, T.; Hagihara, K.; Yamadori, T.; Shima, Y.; et al. Flavonoids and Related Compounds as Anti-Allergic Substances. *Allergol. Int.* **2007**, *56* (2), 113–123. <https://doi.org/10.2332/allergolint.R-06-135>.
- (115) Matricardi, P. M. The Allergy Epidemic, In Cezmi A. Akdis and Ioana Agache, (Eds.). *Global Atlas of Allergy* (Pp. 113-114). In *European Academy of Allergy and Clinical Immunology*; 2014. <https://doi.org/10.1016/j.orgel.2007.03.001>.
- (116) Loh, W.; Tang, M. L. K. The Epidemiology of Food Allergy in the Global Context. *Int. J. Environ. Res. Public Health* **2018**, *15* (2043). <https://doi.org/10.3390/ijerph15092043>.
- (117) Harvima, I. T.; Levi-Schaffer, F.; Draber, P.; Friedman, S.; Polakovicova, I.; Gibbs, B. F.; Blank, U.; Nilsson, G.; Maurer, M. Molecular Targets on Mast Cells and Basophils for Novel Therapies. *J. Allergy Clin. Immunol.* **2014**, *134* (3), 530–544. <https://doi.org/10.1016/j.jaci.2014.03.007>.
- (118) Siracusa, M. C.; Kim, B. S.; Spergel, J. M.; Artis, D. Basophils and Allergic Inflammation. *J. Allergy Clin. Immunol.* **2013**, *132* (4), 789–801. <https://doi.org/10.1016/j.jaci.2013.07.046>.
- (119) Nishida, K.; Yamasaki, S.; Ito, Y.; Kabu, K.; Hattori, K.; Tezuka, T.; Nishizumi, H.; Kitamura, D.; Goitsuka, R.; Geha, R. S.; et al. Fc $\epsilon$ RI-

Mediated Mast Cell Degranulation Requires Calcium-Independent  
Microtubule-Dependent Translocation of Granules to the Plasma Membrane.  
*J. Cell Biol.* **2005**, *170* (1), 115–126. <https://doi.org/10.1083/jcb.200501111>.

- (120) Siraganian, R. P.; Zhang, J.; Suzuki, K.; Sada, K. Protein Tyrosine Kinase Syk in Mast Cell Signaling. *Mol. Immunol.* **2002**, *38* (16–18), 1229–1233. [https://doi.org/10.1016/S0161-5890\(02\)00068-8](https://doi.org/10.1016/S0161-5890(02)00068-8).
- (121) Rivera, J. Molecular Adapters in FcεRI Signaling and the Allergic Response. *Curr. Opin. Immunol.* **2002**, *14* (6), 688–693. [https://doi.org/10.1016/S0952-7915\(02\)00396-5](https://doi.org/10.1016/S0952-7915(02)00396-5).
- (122) Hansen, I.; Klimek, L.; Mösges, R.; Hörmann, K. Mediators of Inflammation in the Early and the Late Phase of Allergic Rhinitis. *Curr. Opin. Allergy Clin. Immunol.* **2004**, *4* (3), 159–163.
- (123) Matsubara, Y.; Murakami, Y.; Kobayashi, M.; Morita, Y.; Tamiya, E. Application of On-Chip Cell Cultures for the Detection of Allergic Response. *Biosens. Bioelectron.* **2004**, *19* (7), 741–747. <https://doi.org/10.1016/j.bios.2003.08.001>.
- (124) Matsuda, H.; Nakamura, S.; Yoshikawa, M. Recent Progress in Study on the Biologically-Active Natural Products Degranulation Inhibitors from Medicinal Plants in Antigen-Stimulated Rat. *Chem. Pharm. Bull.* **2016**, *64* (2), 96–103.

- (125) Vig, M.; Kinet, J. Calcium Signaling in Immune Cells. *Direct* **2009**, *10* (1), 21–28. <https://doi.org/10.1038/ni.f.220/activated>.
- (126) Parekh, A. B.; Putney, J. W. Store-Operated Calcium Channels. *Physiol. Rev.* **2005**, *85*, 757–810. <https://doi.org/10.1016/B978-0-12-378630-2.00301-7>.
- (127) Zhang, S. L.; Yu, Y.; Roos, J.; Kozak, J. A.; Deerinck, T. J.; Ellisman, M. H.; Stauderman, K. A.; Cahalan, M. D. STIM1 Is a Ca<sup>2+</sup> Sensor That Activates CRAC Channels and Migrates from the Ca<sup>2+</sup> Store to the Plasma Membrane. *Nature* **2005**, *437* (7060), 902–905. <https://doi.org/10.1038/nature04147>.
- (128) Feske, S.; Gwack, Y.; Prakriya, M.; Srikanth, S.; Puppel, S. H.; Tanasa, B.; Hogan, P. G.; Lewis, R. S.; Daly, M.; Rao, A. A Mutation in Orai1 Causes Immune Deficiency by Abrogating CRAC Channel Function. *Nature* **2006**, *441* (7090), 179–185. <https://doi.org/10.1038/nature04702>.
- (129) Baba, Y.; Nishida, K.; Fujii, Y.; Hirano, T.; Hikida, M.; Kurosaki, T. Essential Function for the Calcium Sensor STIM1 in Mast Cell Activation and Anaphylactic Responses. *Nat. Immunol.* **2008**, *9* (1), 81–88. <https://doi.org/10.1038/ni1546>.
- (130) Kishikawa, A. The Effect of the Ethanol Extract of Olive Milled Waste on Allergic Reaction of Basophil and Ca<sup>2+</sup> Signal Transduction of Keratinocyte,

Kyushu University, 2017.

- (131) Yun, S. S.; Kang, M. Y.; Park, J. C.; Nam, S. H. Comparison of Anti-Allergenic Activities of Various Polyphenols in Cell Assays. **2010**, *53* (3), 139–140. <https://doi.org/10.3839/jabc.2010.026>.
- (132) Pinho, B. R.; Sousa, C.; Valentao, P.; Oliveira, J. M. A.; Andrade, P. B. Modulation of Basophils' Degranulation and Allergy- Related Enzymes by Monomeric and Dimeric Naphthoquinones. *PLoS One* **2014**, *9* (2), 1–10. <https://doi.org/10.1371/journal.pone.0090122>.
- (133) Han, S.; Sun, L.; He, F.; Che, H. Anti-Allergic Activity of Glycyrrhizic Acid on IgE-Mediated Allergic Reaction by Regulation of Allergy- Related Immune Cells. *Sci. Rep.* **2017**, No. June, 1–9. <https://doi.org/10.1038/s41598-017-07833-1>.
- (134) Montedoro, G.; Servili, M.; Baldioli, M.; Selvaggini, R.; Miniati, E.; Macchioni, A. Simple and Hydrolyzable Compounds in Virgin Olive Oil. 3. Spectroscopic Characterizations of the Secoiridoid Derivatives. *J. Agric. Food Chem.* **1993**, *41* (11), 2228–2234. <https://doi.org/10.1021/jf00035a076>.
- (135) Gariboldi, P.; Jommi, G.; Verotta, L. Secoiridoids from *Olea Europaea*. *Phytochemistry* **1986**, *25* (4), 865–869. [https://doi.org/10.1016/0031-9422\(86\)80018-8](https://doi.org/10.1016/0031-9422(86)80018-8).

- (136) Kim, D. K.; Lim, J. P.; Kim, J. W.; Park, H. W.; Eun, J. S. Antitumor and Antiinflammatory Constituents from *Celtis Sinensis*. *Arch. Pharm. Res.* **2005**, *28* (1), 39–43. <https://doi.org/10.1007/BF02975133>.
- (137) Kovganko, N. V.; Kashkan, Z. N.; Borisov, E. V.; Batura, E. . <sup>13</sup>C-NMR of Beta-Sitosterol Derivatives with Oxidized Rings A and B. *Bioorg. Chem.* **1999**, *35* (6), 646–649.
- (138) Kundu, A. P. <sup>13</sup>C Nmr Spectra of Pentacyclic Triterpenoids-a and Some Salient Features. *Phytochemistry* **1994**, *37* (6), 1517–1575. [https://doi.org/10.1016/S0031-9422\(00\)89569-2](https://doi.org/10.1016/S0031-9422(00)89569-2).
- (139) Thoison, O.; Sévenet, T.; Niemeyer, H. M.; Russell, G. B. Insect Antifeedant Compounds from *Nothofagus Dombeyi* and *N. Pumilio*. *Phytochemistry* **2004**, *65* (14), 2173–2176. <https://doi.org/10.1016/j.phytochem.2004.04.002>.
- (140) Begum, S.; Siddiqui, B. S. Triterpenoids from the Leaves of *Eucalyptus Camaldulensis* Var. *Obtusa*. *J. Nat. Prod.* **1997**, *60*, 20–23.
- (141) Flamini, G.; Pardini, M.; Morelli, I. A Flavonoid Sulphate and Other Compounds from the Roots of *Centaurea Bracteata*. *Phytochemistry* **2001**, *58* (8), 1229–1233. [https://doi.org/10.1016/S0031-9422\(01\)00345-4](https://doi.org/10.1016/S0031-9422(01)00345-4).
- (142) Brenes, M.; García, A.; García, P.; Rios, J. J.; Garrido, A. Phenolic Compounds in Spanish Olive Oils. *J. Agric. Food Chem.* **1999**, *47* (9), 3535–

3540. <https://doi.org/10.1021/jf990009o>.

- (143) Tsukamoto, H.; Hisada, S.; Nishibe, S. Lignans from Bark of the Olea Plants. I. *Chem. Pharm. Bull. (Tokyo)*. **1984**, *32* (7), 2730–2735.  
<https://doi.org/10.1248/cpb.37.3229>.
- (144) Vivancos, M.; Moreno, J. J.  $\beta$ -Sitosterol Modulates Antioxidant Enzyme Response in RAW 264.7 Macrophages. *Free Radic. Biol. Med.* **2005**, *39* (1), 91–97. <https://doi.org/10.1016/j.freeradbiomed.2005.02.025>.
- (145) Sánchez-Quesada, C.; López-Biedma, A.; Warleta, F.; Campos, M.; Beltrán, G.; Gaforio, J. J. Bioactive Properties of the Main Triterpenes Found in Olives, Virgin Olive Oil, and Leaves of *Olea Europaea*. *J. Agric. Food Chem.* **2013**, *61* (50), 12173–12182. <https://doi.org/10.1021/jf403154e>.
- (146) Lozano-Mena, G.; Sánchez-González, M.; Juan, M. E.; Planas, J. M. Maslinic Acid, a Natural Phytoalexin-Type Triterpene from Olives - A Promising Nutraceutical? *Molecules* **2014**, *19* (8), 11538–11559.  
<https://doi.org/10.3390/molecules190811538>.
- (147) Liu, J.; Sun, H.; Duan, W.; Mu, D.; Zhang, L. Maslinic Acid Reduces Blood Glucose in KK-Ay Mice. *Biol. Pharm. Bull.* **2007**, *30* (11), 2075–2078.  
<https://doi.org/10.1248/bpb.30.2075>.
- (148) González-Correa, J. A.; Navas, M. D.; Lopez-Villodres, J. A.; Trujillo, M.;



Espartero, J. L.; De La Cruz, J. P. Neuroprotective Effect of Hydroxytyrosol and Hydroxytyrosol Acetate in Rat Brain Slices Subjected to Hypoxia–Reoxygenation. *Neurosci. Lett.* **2008**, *446* (2–3), 143–146.  
<https://doi.org/10.1016/J.NEULET.2008.09.022>.

- (149) Trujillo, M.; Mateos, R.; De Teran, L. C.; Espartero, J. L.; Cert, R.; Jover, M.; Alcudia, F.; Bautista, J.; Cert, A.; Parrado, J. Lipophilic Hydroxytyrosyl Esters. Antioxidant Activity in Lipid Matrices and Biological Systems. *J. Agric. Food Chem.* **2006**, *54* (11), 3779–3785. <https://doi.org/10.1021/jf060520z>.
- (150) Lin, Y.; Shi, R.; Wang, X.; Shen, H. Luteolin , a Flavonoid with Potential for Cancer Prevention and Therapy. *Curr. Cancer Drug Targets* **2008**, *8*, 634–646. <https://doi.org/10.2174/156800908786241050>.
- (151) López-lázaro, M. Distribution and Biological Activities of the Flavonoid Luteolin. *Mini Rev. Med. Chem.* **2009**, *9*, 31–59.  
<https://doi.org/10.2174/138955709787001712>.
- (152) Maria, E. S.; Krystyna, D. Luteolin as an Anti-Inflammatory and Neuroprotective Agent: A Brief Review. *Brain Res. Bull.* **2015**, *119*, 1–11.  
<https://doi.org/10.1016/j.brainresbull.2015.09.002>.
- (153) Nagao, A.; Seki, M.; Kobayashi, H. Inhibition of Xanthine Oxidase by Flavonoids. *Biosci. Biotechnol. Biochem.* **1999**, *63* (10), 1787–1790.  
<https://doi.org/10.1271/bbb.63.1787>.

- (154) Rubio-Senent, F.; Rodríguez-Gutiérrez, G.; Lama-Muñoz, A.; Fernández-Bolaños, J. Pectin Extracted from Thermally Treated Olive Oil By-Products: Characterization, Physico-Chemical Properties, In vitro Bile Acid and Glucose Binding. *Food Hydrocoll.* **2015**, *43*, 311–321.  
<https://doi.org/10.1016/j.foodhyd.2014.06.001>.
- (155) Choi, Y.; Kim, M. S.; Hwang, J. K. Inhibitory Effects of Panduratin A on Allergy-Related Mediator Production in Rat Basophilic Leukemia Mast Cells. *Inflammation* **2012**, *35* (6), 1904–1915. <https://doi.org/10.1007/s10753-012-9513-y>.
- (156) Sato, A.; Shinozaki, N.; Tamura, H. Secoiridoid Type of Antiallergic Substances in Olive Waste Materials of Three Japanese Varieties of *Olea Europaea*. *J. Agric. Food Chem.* **2014**, *62* (31), 7787–7795.  
<https://doi.org/10.1021/jf502151b>.
- (157) Sato, A.; Tamura, H. High Antiallergic Activity of 5,6,4'-Trihydroxy-7,8,3'-Trimethoxyflavone and 5,6-Dihydroxy-7,8,3',4'-Tetramethoxyflavone from Eau de Cologne Mint (*Mentha × Piperita Citrata*). *Fitoterapia* **2015**, *102*, 74–83. <https://doi.org/10.1016/j.fitote.2015.02.003>.
- (158) Matsubara, M.; Masaki, S.; Ohmori, K.; Karasawa, A.; Hasegawa, K. Differential Regulation of IL-4 Expression and Degranulation by Anti-Allergic Olopatadine in Rat Basophilic Leukemia (RBL-2H3) Cells. *Biochem.*

*Pharmacol.* **2004**, 67 (7), 1315–1326.

<https://doi.org/10.1016/J.BCP.2003.12.008>.

(159) Putney, J. W.; Tomita, T. Phospholipase C Signaling and Calcium Influx.

*Adv. Biol. Regul.* **2013**, 52 (1), 152–164.

<https://doi.org/10.1016/j.advenzreg.2011.09.005>.

(160) Persia, F. A.; Mariani, M. L.; Fogal, T. H.; Penissi, A. B. Hydroxytyrosol and Oleuropein of Olive Oil Inhibit Mast Cell Degranulation Induced by Immune and Non-Immune Pathways. *Phytomedicine* **2014**, 21 (11), 1400–1405.

<https://doi.org/10.1016/j.phymed.2014.05.010>.

(161) Sarkhel, S.; Desiraju, G. R. N–H...O, O–H...O, and C–H...O Hydrogen Bonds in Protein-Ligand Complexes: Strong and Weak Interactions in Molecular Recognition. *Proteins Struct. Funct. Bioinforma.* **2003**, 54 (2), 247–259. <https://doi.org/10.1002/prot.10567>.

(162) Sun, N.; Wang, J.; Zhou, C.; Wang, C.; Wang, S.; Che, H. Cell-Based Immunological Assay: Complementary Applications in Evaluating the Allergenicity of Foods with FAO/WHO Guidelines. *Food Res. Int.* **2014**, 62, 735–745. <https://doi.org/10.1016/j.foodres.2014.04.033>.

(163) International Diabetes Federation. *IDF Diabetes Atlas 5th Edition*; 2011.

<https://doi.org/10.1007/978-90-481-3271-3>.

- (164) Gin, H.; Rigalleau, V. Post-Prandial Hyperglycemia. Post-Prandial Hyperglycemia and Diabetes. *Diabetes Metab.* **2000**, *26* (4), 265—272.
- (165) Eringa, E. C.; Serne, E. H.; Meijer, R. I.; Schalkwijk, C. G.; Houben, A. J. H. M.; Stehouwer, C. D. A.; Smulders, Y. M.; Van Hinsbergh, V. W. M. Endothelial Dysfunction in (Pre)Diabetes: Characteristics, Causative Mechanisms and Pathogenic Role in Type 2 Diabetes. *Rev. Endocr. Metab. Disord.* **2004**, *14* (1), 39–48. <https://doi.org/10.1007/s11154-013-9239-7>.
- (166) Ceriello, A.; Hanefeld, M.; Leiter, L.; Monnier, L.; Moses, A.; Owens, D.; Tajima, N.; Tuomilehto, J. Postprandial Glucose Regulation and Diabetic Complications. *Arch. Intern. Med.* **2004**, *164* (19), 2090–2095.
- (167) Henry, W. L. Perspectives in Diabetes. *J. Natl. Med. Assoc.* **2005**, *54* (1), 476–478. <https://doi.org/10.2337/diabetes.52.1.1>.
- (168) Watanabe, J.; Kawabata, J.; Kurihara, H.; Niki, R. Isolation and Identification of  $\alpha$ -Glucosidase Inhibitors from Tochu-Cha ( *Eucommia Ulmoides* ). *Biosci. Biotechnol. Biochem.* **1997**, *61* (1), 177–178. <https://doi.org/10.1271/bbb.61.177>.
- (169) Taslimi, P.; Aslan, H. E.; Demir, Y.; Oztaskin, N.; Maraş, A.; Gulçin, İ.; Beydemir, S.; Goksu, S. Diarylmethanon, Bromophenol and Diarylmethane Compounds: Discovery of Potent Aldose Reductase,  $\alpha$ -Amylase and  $\alpha$ -Glycosidase Inhibitors as New Therapeutic Approach in Diabetes and

Functional Hyperglycemia. *Int. J. Biol. Macromol.* **2018**, *119*, 857–863.

<https://doi.org/10.1016/j.ijbiomac.2018.08.004>.

(170) Phung, O. J.; Scholle, J. M. Effect of Noninsulin Antidiabetic Drugs Added to Metformin Therapy on Glycemic Control , Weight Gain , and Hypoglycemia in Type 2 Diabetes. *J. Am. Med. Assoc.* **2010**, *303* (14), 1410–1418.

(171) Derosa, G.; Maffioli, P.  $\alpha$ -Glucosidase Inhibitors and Their Use in Clinical Practice. *Arch. Med. Sci.* **2012**, *8* (5), 899–906.

<https://doi.org/10.5114/aoms.2012.31621>.

(172) Mohiuddin, M.; Arbain, D.; Islam, A. K. M. S.; Ahmad, M. S.; Ahmad, M. N. Alpha-Glucosidase Enzyme Biosensor for the Electrochemical Measurement of Antidiabetic Potential of Medicinal Plants. *Nanoscale Res. Lett.* **2016**, *11* (1), 1–12. <https://doi.org/10.1186/s11671-016-1292-1>.

(173) Tringali, C. *Bioactive Compounds from Natural Sources; Isolation, Characterisation and Biological Properties*, First Edit.; Tringali, C., Ed.; Taylor & Francis: Ney York, 2001.

(174) Demir, Y.; Durmaz, L.; Taslimi, P.; Gulçin, İ. Antidiabetic Properties of Dietary Phenolic Compounds: Inhibition Effects on  $\alpha$ -Amylase, Aldose Reductase, and  $\alpha$ -Glycosidase. *Biotechnol. Appl. Biochem.* **2019**, *66* (5), 781–786. <https://doi.org/10.1002/bab.1781>.

- (175) Madigan, C.; Ryan, M.; Owens, D.; Collins, P.; Tomkin, G. H. Dietary Unsaturated Fatty Acids in Type 2 Diabetes; Higher Levels of Postprandial Lipoprotein on a Linoleic Acid–Rich Sunflower Oil Diet Compared with an Oleic Acid–Rich Olive Oil Diet. *Diabetes Care* **2000**, *23* (10), 1472–1477.
- (176) Nyomba. G., Berard.L., M. L. Facilitating Access to Glucometer Reagent Increases Blood Glucose Self Monitoring Frequency and Improves Glycaemic Control: A Prospective Study in Insulin-Treated Diabetic Patients. *Diabet. Med.* **2004**, *21* (2), 103–113. [https://doi.org/10.1046/j.1464.](https://doi.org/10.1046/j.1464.2004.02102.x)
- (177) Pérez-martínez, P.; García-ríos, A.; Delgado-lista, J.; Pérez-jiménez, F.; López-, J. Mediterranean Diet Rich in Olive Oil and Obesity , Metabolic Syndrome and Diabetes Mellitus. *Curr. Pharm. Des.* **2011**, *17* (8), 769–777.
- (178) Goula, A. M.; Lazarides, H. N. Integrated Processes Can Turn Industrial Food Waste into Valuable Food By-Products and / or Ingredients : The Cases of Olive Mill and Pomegranate Wastes. *J. Food Eng.* **2015**, *167*, 45–50. <https://doi.org/10.1016/j.jfoodeng.2015.01.003>.
- (179) Alfano, G.; Lustrato, G.; Lima, G.; Vitullo, D.; Ranalli, G. Characterization of Composted Olive Mill Wastes to Predict Potential Plant Disease Suppressiveness. *Biol. Control* **2011**, *58* (3), 199–207. <https://doi.org/10.1016/j.biocontrol.2011.05.001>.
- (180) Fatmawati, S.; Shimizu, K.; Kondo, R. Ganoderol B: A Potent  $\alpha$ -Glucosidase

Inhibitor Isolated from the Fruiting Body of *Ganoderma Lucidum*.

*Phytomedicine* **2011**, *18* (12), 1053–1055.

<https://doi.org/10.1016/j.phymed.2011.03.011>.

- (181) Xiao, Z.; Storms, R.; Tsang, A. A Quantitative Starch-Iodine Method for Measuring Alpha-Amylase and Glucoamylase Activities. *Anal. Biochem.* **2006**, *351* (1), 146–148. <https://doi.org/10.1016/j.ab.2006.01.036>.
- (182) Nelson, D. L.; Cox, M. M. Enzyme Kinetics as an Approach to Understanding Mechanism. *Lehninger Principles of Biochemistry*.; WH Freeman & Co.: New York, 2014; pp 200–212.
- (183) Agrawal, P. K.; Bansal, M. C.; Porter, L. J.; Foo, L. Y. *Carbon-13 NMR of Flavonoids*; Agrawal, P. K., Ed.; Elsevier Science Publishers B.V: Amsterdam, 1989; Vol. 39. <https://doi.org/10.1016/B978-0-444-87449-8.50014-6>.
- (184) Peralbo-Molina, Á.; Priego-Capote, F.; Luque De Castro, M. D. Tentative Identification of Phenolic Compounds in Olive Pomace Extracts Using Liquid Chromatography-Tandem Mass Spectrometry with a Quadrupole-Quadrupole-Time-of-Flight Mass Detector. *J. Agric. Food Chem.* **2012**, *60* (46), 11542–11550. <https://doi.org/10.1021/jf302896m>.
- (185) Caesar, L. K.; Cech, N. B. Synergy and Antagonism in Natural Product Extracts: When 1 + 1 Does Not Equal 2. *Nat. Prod. Rep.* **2019**, *36* (6), 869–

888. <https://doi.org/10.1039/c9np00011a>.

- (186) Britton, E. R.; Kellogg, J. J.; Kvalheim, O. M.; Cech, N. B. Biochemometrics to Identify Synergists and Additives from Botanical Medicines: A Case Study with *Hydrastis Canadensis* (Goldenseal). *J. Nat. Prod.* **2018**, *81* (3), 484–493. <https://doi.org/10.1021/acs.jnatprod.7b00654>.
- (187) Lineweaver, H.; Burk, D. The Determination of Enzyme Dissociation Constants. *J. Am. Chem. Soc.* **1934**, *56* (3), 658–666.  
<https://doi.org/10.1021/ja01318a036>.
- (188) Whiteley, C. G. Enzyme Kinetics: Partial and Complete Non-Competitive Inhibition. *Biochem. Educ.* **1999**, *27*, 15–18.
- (189) Segel, I. H. *Enzyme Kinetics, Behavior and Analysis of Rapid Equilibrium and Steady-State Enzyme Systems*, 1st Editio.; John Wiley & Sons, Ltd.: New York, 1975.
- (190) Ha, C.-E.; Bhagavan, N. V. *Essentials of Medical Biochemistry: With Clinical Cases*, Second Edi.; Elsevier: London, 2015.
- (191) Elsbaey, M.; Mwakalukwa, R.; Shimizu, K.; Miyamoto, T. Pentacyclic Triterpenes from *Lavandula Coronopifolia*: Structure Related Inhibitory Activity on  $\alpha$ -Glucosidase. *Nat. Prod. Res.* **2019**, *0* (0), 1–9.  
<https://doi.org/10.1080/14786419.2019.1655017>.



- (192) Yan, J.; Zhang, G.; Pan, J.; Wang, Y.  *$\alpha$ -Glucosidase Inhibition by Luteolin: Kinetics, Interaction and Molecular Docking*; Elsevier B.V., 2014; Vol. 64. <https://doi.org/10.1016/j.ijbiomac.2013.12.007>.
- (193) Berg, J. M.; Tymoczko, J. L.; Stryer, L.; Gatto, G. J. *Biochemistry*, Seventh Ed.; W. H. Freeman and Company: New York, 2012.
- (194) Hou, W.; Li, Y.; Zhang, Q.; Wei, X.; Peng, A.; Chen, L.; Wei, Y. Triterpene Acids Isolated from Lagerstroemia Speciosa Leaves as  $\alpha$ -Glucosidase Inhibitors. *Phyther. Res.* **2009**, 23, 614–618. <https://doi.org/10.1002/ptr.2661>.
- (195) Ye, X. P.; Song, C. Q.; Yuan, P.; Mao, R. G.  $\alpha$ -Glucosidase and  $\alpha$ -Amylase Inhibitory Activity of Common Constituents from Traditional Chinese Medicine Used for Diabetes Mellitus. *Chin. J. Nat. Med.* **2010**, 8 (5), 349–352. [https://doi.org/10.1016/S1875-5364\(10\)60041-6](https://doi.org/10.1016/S1875-5364(10)60041-6).
- (196) Bogani, P.; Galli, C.; Villa, M.; Visioli, F. Postprandial Anti-Inflammatory and Antioxidant Effects of Extra Virgin Olive Oil. *Atherosclerosis* **2007**, 190 (1), 181–186. <https://doi.org/10.1016/j.atherosclerosis.2006.01.011>.
- (197) Schaffer, S. W.; Azuma, J.; Mozaffari, M. Role of Antioxidant Activity of Taurine in Diabetes. *Can. J. Physiol. Pharmacol.* **2009**, 87, 91–99. <https://doi.org/10.1139/Y08-110>.
- (198) Montonen, J.; Knekt, P.; Järvinen, R.; Reunanen, A. Dietary Antioxidant

Intake and Risk of Type 2 Diabetes. *Diabetes Care* **2004**, 27 (2), 362–366.

<https://doi.org/10.2337/diacare.27.2.362>.

(199) Teng, H.; Chen, L.  $\alpha$ -Glucosidase and  $\alpha$ -Amylase Inhibitors from Seed Oil: A Review of Liposoluble Substance to Treat Diabetes. *Crit. Rev. Food Sci. Nutr.* **2017**, 57 (16), 3438–3448.

*Nutr.* **2017**, 57 (16), 3438–3448.

<https://doi.org/10.1080/10408398.2015.1129309>.

(200) Antónia Nunes, M.; Costa, A. S. G.; Bessada, S.; Santos, J.; Puga, H.; Alves, R. C.; Freitas, V.; Oliveira, M. B. P. P. Olive Pomace as a Valuable Source of Bioactive Compounds: A Study Regarding Its Lipid- and Water-Soluble Components. *Sci. Total Environ.* **2018**, 644, 229–236.

<https://doi.org/10.1016/j.scitotenv.2018.06.350>.

(201) Teng, H.; Yuan, B.; Gothai, S.; Arulselvan, P.; Song, X.; Chen, L. Dietary Triterpenes in the Treatment of Type 2 Diabetes: To Date. *Trends Food Sci. Technol.* **2018**, 72 (June 2017), 34–44.

*Technol.* **2018**, 72 (June 2017), 34–44.

<https://doi.org/10.1016/j.tifs.2017.11.012>.

(202) Gao, D.; Li, Q.; Li, Y.; Liu, Z.; Fan, Y.; Liu, Z.; Zhao, H.; Li, J.; Han, Z.

Antidiabetic and Antioxidant Effects of Oleanolic Acid from *Ligustrum*

*Lucidum* Ait in Alloxan-Induced Diabetic Rats. *Phyther. Res.* **2009**, 23 (1),

1257–1262. <https://doi.org/10.1002/ptr.2603>.

(203) Ngubane, P. S.; Masola, B.; Musabayane, C. T. The Effects of *Syzygium*

Aromaticum-Derived Oleanolic Acid on Glycogenic Enzymes in Streptozotocin-Induced Diabetic Rats. *Ren. Fail.* **2011**, 33 (4), 434–439. <https://doi.org/10.3109/0886022X.2011.568147>.

- (204) Guan, T.; Qian, Y.; Tang, X.; Huang, M.; Huang, L.; Li, Y.; Sun, H. Maslinic Acid, a Natural Inhibitor of Glycogen Phosphorylase, Reduces Cerebral Ischemic Injury in Hyperglycemic Rats by GLT-1 up-Regulation. *J. Neurosci. Res.* **2011**, 89 (11), 1829–1839. <https://doi.org/10.1002/jnr.22671>.
- (205) Fukushima, M.; Matsuyama, F.; Ueda, N.; Egawa, K.; Takemoto, J.; Kajimoto, Y.; Yonaha, N.; Miura, T.; Kaneko, T.; Nishi, Y.; et al. Effect of Corosolic Acid on Postchallenge Plasma Glucose Levels. *Diabetes Res. Clin. Pract.* **2006**, 73 (2), 174–177. <https://doi.org/10.1016/j.diabres.2006.01.010>.
- (206) Supasuteekul, C.; Nonthitipong, W.; Tadtong, S.; Likhitwitayawuid, K.; Tengamnuay, P.; Sritularak, B. Antioxidant, DNA Damage Protective, Neuroprotective, and  $\alpha$ -Glucosidase Inhibitory Activities of a Flavonoid Glycoside from Leaves of *Garcinia Gracilis*. *Brazilian J. Pharmacogn.* **2016**, 26 (3), 312–320. <https://doi.org/10.1016/j.bjp.2016.01.007>.
- (207) Lin, Y. S.; Lee, S. S. Flavonol Glycosides with  $\alpha$ -Glucosidase Inhibitory Activities and New Flavone C-Diosides from the Leaves of *Machilus Konishii*. *Helv. Chim. Acta* **2014**, 97 (12), 1672–1682.

<https://doi.org/10.1002/hlca.201400081>.

- (208) Kim, J.-S.; Kwon, C.-S.; Son, K. H. Inhibition of Alpha-Glucosidase and Amylase by Luteolin, a Flavonoid. *Biosci. Biotechnol. Biochem.* **2000**, *63* (11), 2458–2461. <https://doi.org/10.1271/bbb.64.2458>.
- (209) Loizzo, M. R.; Lecce, G. Di; Boselli, E.; Menichini, F.; Frega, N. G. Inhibitory Activity of Phenolic Compounds from Extra Virgin Olive Oils on the Enzymes Involved in Diabetes, Obesity and Hypertension. *J. Food Biochem.* **2011**, *35* (2), 381–399. <https://doi.org/10.1111/j.1745-4514.2010.00390.x>.
- (210) Alzheimer's Disease International. *The Global Impact of Dementia 2013 – 2050*; Alzheimer's Disease International: London, 2013.
- (211) Scarpini, E.; Scheltens, P.; Feldman, H. Treatment of Alzheimer's Disease: Current Status and New Perspectives. *Lancet Neurol.* **2003**, *2* (9), 539–547. [https://doi.org/10.1016/S1474-4422\(03\)00502-7](https://doi.org/10.1016/S1474-4422(03)00502-7).
- (212) Parihar, M. S.; Hemnani, T. Alzheimer's Disease Pathogenesis and Therapeutic Interventions. *J. Clin. Neurosci.* **2004**, *11* (5), 456–467. <https://doi.org/10.1016/j.jocn.2003.12.007>.
- (213) Craig, L. A.; Hong, N. S.; McDonald, R. J. Revisiting the Cholinergic Hypothesis in the Development of Alzheimer's Disease. *Neurosci. Biobehav. Rev.* **2011**, *35* (6), 1397–1409.

<https://doi.org/10.1016/j.neubiorev.2011.03.001>.

- (214) Fargo, K.; Aisen, P.; Albert, M.; Au, R.; Corrada, M.; DeKosky, S.; Drachman, D.; Fillit, H.; Gitlin, L.; Haas, M.; et al. Alzheimer's Association National Plan Milestone Workgroup. 2014 Report on the Milestones for the US National Plan to Address Alzheimer's Disease. 2014;10:S430-452. In *Alzheimers Dement. J.*; Alzheimers Assoc., 2014; Vol. 10, pp S430-452. <https://doi.org/10.3390/molecules22101663>.
- (215) E Mintzer, J.; F Mirski, D.; S Hoernig, K. Behavioral and Psychological Signs and Symptoms of Dementia: A Practicing Psychiatrist's Viewpoint. *Dialogues Clin. Neurosci.* **2000**, 2 (2), 139–155.
- (216) Francis, P. T.; Palmer, A. M.; Snape, M.; Wilcock, G. K. The Cholinergic Hypothesis of Alzheimer's Disease: A Review of Progress. *J. Neurol. Neurosurg. Psychiatry* **1999**, 66 (2), 137–147. <https://doi.org/10.1136/jnnp.66.2.137>.
- (217) Nugroho, A.; Choi, J. S.; Hong, J. P.; Park, H. J. Anti-Acetylcholinesterase Activity of the Aglycones of Phenolic Glycosides Isolated from *Leonurus Japonicus*. *Asian Pac. J. Trop. Biomed.* **2017**, 7 (10), 849–854. <https://doi.org/10.1016/j.apjtb.2017.08.013>.
- (218) Liu, P.-P.; Xie, Y.; Meng, X.-Y.; Kang, J.-S. History and Progress of Hypotheses and Clinical Trials for Alzheimer's Disease. *Signal Transduct.*

*Target. Ther.* **2019**, 4 (1). <https://doi.org/10.1038/s41392-019-0063-8>.

- (219) Hampel, H.; Mesulam, M. M.; Cuello, A. C.; Farlow, M. R.; Giacobini, E.; Grossberg, G. T.; Khachaturian, A. S.; Vergallo, A.; Cavedo, E.; Snyder, P. J.; et al. The Cholinergic System in the Pathophysiology and Treatment of Alzheimer's Disease. *Brain* **2018**, 141 (7), 1917–1933.  
<https://doi.org/10.1093/brain/awy132>.
- (220) St-Laurent-Thibault, C.; Arseneault, M.; Longpre, F.; Ramassamy, C. Tyrosol and Hydroxytyrosol Two Main Components of Olive Oil, Protect N2a Cells Against Amyloid- $\beta$ -Induced Toxicity. Involvement of the NF- $\kappa$ B Signaling. *Curr. Alzheimer Res.* **2011**, 8 (5), 543–551.  
<https://doi.org/10.2174/156720511796391845>.
- (221) Dunn, W. B.; Overy, S.; Quick, W. P. Evaluation of Automated Electrospray-TOF Mass Spectrometry for Metabolic Fingerprinting of the Plant Metabolome. *Metabolomics* **2005**, 1 (2), 137–148.  
<https://doi.org/10.1007/s11306-005-4433-6>.
- (222) Luthria, D. L.; Lin, L. Z.; Robbins, R. J.; Finley, J. W.; Banuelos, G. S.; Harnly, J. M. Discriminating between Cultivars and Treatments of Broccoli Using Mass Spectral Fingerprinting and Analysis of Variance-Principal Component Analysis. *J. Agric. Food Chem.* **2008**, 56 (21), 9819–9827.  
<https://doi.org/10.1021/jf801606x>.

- (223) Dudzik, D.; Barbas-Bernardos, C.; García, A.; Barbas, C. Quality Assurance Procedures for Mass Spectrometry Untargeted Metabolomics. a Review. *J. Pharm. Biomed. Anal.* **2018**, *147*, 149–173.  
<https://doi.org/10.1016/j.jpba.2017.07.044>.
- (224) Frédérick, M.; Pirotte, B.; Fillet, M.; De Tullio, P. Metabolomics as a Challenging Approach for Medicinal Chemistry and Personalized Medicine. *J. Med. Chem.* **2016**, *59* (19), 8649–8666.  
<https://doi.org/10.1021/acs.jmedchem.5b01335>.
- (225) Dudzik, D.; Revello, R.; Barbas, C.; Bartha, J. L. LC - MS-Based Metabolomics Identification of Novel Biomarkers of Chorioamnionitis and Its Associated Perinatal Neurological Damage. *J. Proteome Res.* **2015**, *14* (3), 1432–1444. <https://doi.org/10.1021/pr501087x>.
- (226) Wasai, M.; Fujimura, Y.; Nonaka, H.; Kitamura, R.; Murata, M.; Tachibana, H. Postprandial Glycaemia-Lowering Effect of a Green Tea Cultivar Sunrouge and Cultivar-Specific Metabolic Profiling for Determining Bioactivity-Related Ingredients. *Sci. Rep.* **2018**, *8* (1), 1–9.  
<https://doi.org/10.1038/s41598-018-34316-8>.
- (227) Bujak, R.; Dagher-Wojtkowiak, E.; Kaliszan, R.; Markuszewski, M. J. PLS-Based and Regularization-Based Methods for the Selection of Relevant Variables in Non-Targeted Metabolomics Data. *Front. Mol. Biosci.* **2016**, *3*

(JUL), 1–10. <https://doi.org/10.3389/fmolb.2016.00035>.

- (228) Goodacre, R.; York, E. V.; Heald, J. K.; Scott, I. M. Chemometric Discrimination of Unfractionated Plant Extracts Analyzed by Electrospray Mass Spectrometry. *Phytochemistry* **2003**, *62* (6), 859–863. [https://doi.org/10.1016/S0031-9422\(02\)00718-5](https://doi.org/10.1016/S0031-9422(02)00718-5).
- (229) Mukherjee, P. K.; Kumar, V.; Houghton, P. J. Screening of Indian Medicinal Plants for Acetylcholinesterase Inhibitory Activity. *Phyther. Res.* **2008**, *22* (4), 544–549. <https://doi.org/10.1002/ptr>.
- (230) Ellman, G. L.; Courtney, K. D.; Andres, V.; Featherstone, R. M. A New and Rapid Colorimetric Determination of Acetylcholinesterase Activity. *Biochem. Pharmacol.* **1961**, *7* (2), 88–95. [https://doi.org/10.1016/0006-2952\(61\)90145-9](https://doi.org/10.1016/0006-2952(61)90145-9).
- (231) Wang, H. P.; Liu, Y.; Chen, C.; Xiao, H. Bin. Screening Specific Biomarkers of Herbs Using a Metabolomics Approach: A Case Study of Panax Ginseng. *Sci. Rep.* **2017**, *7* (1), 1–9. <https://doi.org/10.1038/s41598-017-04712-7>.
- (232) Dias, D. A.; Jones, O. A. H.; Beale, D. J.; Boughton, B. A.; Benheim, D.; Kouremenos, K. A.; Wolfender, J. L.; Wishart, D. S. Current and Future Perspectives on the Structural Identification of Small Molecules in Biological Systems. *Metabolites* **2016**, *6* (4). <https://doi.org/10.3390/metabo6040046>.



- (233) Allard, P. M.; Genta-Jouve, G.; Wolfender, J. L. Deep Metabolome Annotation in Natural Products Research: Towards a Virtuous Cycle in Metabolite Identification. *Curr. Opin. Chem. Biol.* **2017**, *36*, 40–49. <https://doi.org/10.1016/j.cbpa.2016.12.022>.
- (234) Viant, M. R.; Kurland, I. J.; Jones, M. R.; Dunn, W. B. How Close Are We to Complete Annotation of Metabolomes? *Curr. Opin. Chem. Biol.* **2017**, *36*, 64–69. <https://doi.org/10.1016/j.cbpa.2017.01.001>.
- (235) Naz, S.; Gallart-Ayala, H.; Reinke, S. N.; Mathon, C.; Blankley, R.; Chaleckis, R.; Wheelock, C. E. Development of a Liquid Chromatography-High Resolution Mass Spectrometry Metabolomics Method with High Specificity for Metabolite Identification Using All Ion Fragmentation Acquisition. *Anal. Chem.* **2017**, *89* (15), 7933–7942. <https://doi.org/10.1021/acs.analchem.7b00925>.
- (236) Berrueta, L. A.; Alonso-Salces, R. M.; Héberger, K. Supervised Pattern Recognition in Food Analysis. *J. Chromatogr. A* **2007**, *1158* (1–2), 196–214. <https://doi.org/10.1016/j.chroma.2007.05.024>.
- (237) Vaclavik, L.; Lacina, O.; Hajslova, J.; Zweigenbaum, J. The Use of High Performance Liquid Chromatography-Quadrupole Time-of-Flight Mass Spectrometry Coupled to Advanced Data Mining and Chemometric Tools for Discrimination and Classification of Red Wines According to Their Variety.

*Anal. Chim. Acta* **2011**, *685* (1), 45–51.

<https://doi.org/10.1016/j.aca.2010.11.018>.

- (238) Satria, D.; Tamrakar, S.; Suhara, H.; Kaneko, S.; Shimizu, K. Mass Spectrometry-Based Untargeted Metabolomics and  $\alpha$ -Glucosidase Inhibitory Activity of Lingzhi (*Ganoderma Lingzhi*) during the Developmental Stages. *Molecules* **2019**, *24* (11), 1–14. <https://doi.org/10.3390/molecules24112044>.